



*University of Basrah
College of Science
Department of Chemistry*



**Study of Programmed Cell Death 1
(PD-1) Gene Polymorphism and Some
Valid Predictors of Systemic Lupus
Erythematosus Female Patients in
Basrah Province - Iraq**

A Thesis

*Submitted to the Council of the College of Science -
University of Basrah in Partial Fulfillment of the
Requirements for the Degree of Doctor of Philosophy
in Chemistry – Clinical Biochemistry*

By

Sadoun Abbas Eidan Alsalimi

B.Sc. 2011

M.Sc. 2020

Prof. Dr. Adnan J. M. Al-Fartosy

The Supervisor

2024 A.D

1445 A.H

بِسْمِ اللَّهِ الرَّحْمَنِ الرَّحِيمِ

قَالُوا سُبْحَانَكَ لَا عِلْمَ لَنَا إِلَّا مَا
عَلَّمْتَنَا إِنَّكَ أَنْتَ الْعَلِيمُ الْحَكِيمُ

صَدَقَ اللَّهُ الْعَلِيُّ الْعَظِيمُ

سورة البقرة – آية (٣٢)

Supervisor Certification

I certify that this thesis entitles "**Study of Programmed Cell Death 1 (PD-1) Gene Polymorphism and Some Valid Predictors of Systemic Lupus Erythematosus Female Patients in Basrah Province – Iraq**" was prepared by "**Sadoun Abbas Eidan Alsalimi**" under my supervision at the Department of Chemistry - College of Science - University of Basrah as a partial requirement for the degree of Doctor of Philosophy in Chemistry – Clinical Biochemistry.

Signature:



Name: **Prof. Dr. Adnan J. M. Al-Fartosy**

Address: **Department of Chemistry - College of Science - University of Basrah**

Title: **The Supervisor**

Date: **12 / 06 / 2024**

In the view of the available recommendation, I forward this thesis for debate by the examining committee.

Signature:



Name: **Prof. Dr. Hadi Z. Al-Sawaad**


Address: **Department of Chemistry, College of Science, University of Basrah**

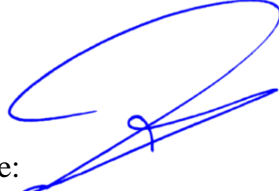
Title: **Head of Department of Chemistry**


Date: **12 / 06 / 2024**


The Examining Committee Certification


We, the examining committee, certify that we read this thesis entitled "**Study of Programmed Cell Death 1 (PD-1) Gene Polymorphism and Some Valid Predictors of Systemic Lupus Erythematosus Female Patients in Basrah Province – Iraq**" and we have examined the student "**Sadoun Abbas Eidan Alsalimi**", and that in our opinion, it is accepted as a thesis for the degree of Doctor of Philosophy in Chemistry – Clinical Biochemistry.


Signature: 
Name: **Dr. Raid M. H. Al-Salih**
Title: **Prof. in Biochemistry**
Address: **University of Thi Qar,
College of Science**
Chairman
Date: **12 / 06 / 2024**

Signature: 
Name: **Dr. Falah H. Shari**
Title: **Prof. in Biochemistry**
Address: **University of Basrah,
College of Pharmacy**
Member
Date: **12 / 06 / 2024**


Signature: 
Name: **Dr. Arwa H. Mahmood**
Title: **Assist. Prof. in Biochemistry**
Address: **University of Basrah,
College of Science**
Member
Date: **12 / 06 / 2024**

Signature: 
Name: **Dr. Bushra A. Abdul Azeez**
Title: **Assist. Prof. in Biochemistry**
Address: **University of Basrah,
College of Science**
Member
Date: **12 / 06 / 2024**

Signature: 
Name: **Dr. Hala S. Nejim**
Title: **Assist. Prof. in Biochemistry**
Address: **University of Basrah,
College of Science**
Member
Date: **12 / 06 / 2024**

Signature: 
Name: **Dr. Adnan J. M. Al-Fartosy**
Title: **Prof. in Clinical Biochemistry**
Address: **University of Basrah,
College of Science**
Member & Supervisor
Date: **12 / 06 / 2024**

Approved by the College Committee of Postgraduate Studies

Signature: 
Name: **Assist. Prof. Dr. Majid N. Humoud**
Address: **The Dean of College of Science - University of Basrah**
Date: **12 / 06 / 2024**



Dedication

To who guided me in my whole life

To who made all my dreams real

To who never let me down

To who gave me everything

To the darling Imam Hussein

(Allah blesses him and his

household)

I dedicate this work with my unending

and deepest love and thankfulness...

Yours Sincerely...

Sadoun...

Acknowledgements

All Praise is to Allah by all of His praiseworthy acts; for all of His gifts, bounties, blessings, and enabling me to achieve this thesis. I'm deeply grateful to the Prophet Mohammed (Allah blessing him and his Household) and his Household (Allah blessing them) for their support, guidance, and kindness to me.

I would like to express my deep thanks and gratitude to my supervisor Prof. Dr. Adnan J. M. Al-Fartosy for his excellent supervision and scientific support throughout this study.

Great appreciation is offered to the Dean of College of Science – University of Basrah Assist. Prof. Dr. Majid N. Humoud, the Dean Vice for scientific affairs and postgraduate studies Prof. Dr. Alaa A. Hassan, the head of postgraduate unit Dr. Mufeed D. Alasadi and his staff, the head of Chemistry Department Prof. Dr. Hadi Z. Al-Sawaad and the previous heads of the department, and the postgraduate guider of Chemistry Department Prof. Dr. Ali A. Abdulwahid for providing me with the necessary facilities. Special appreciation and gratitude are extended to all staff members of the Chemistry Department at the College of Science - University of Basrah and all my colleagues for their support and cooperation.

In addition, sincere thanks and gratefulness are offered to the deanship and departments of College of Nursing – University of Basrah and all the staff members in the College for their continuous assistance and support to complete this thesis.

Furthermore, I would also like to thank all the staff in Al-Basrah, Al-Fayhaa, Al-Sadr and Al-Mawany teaching hospitals for their help and continuous cooperation to complete the thesis.

Finally, I am deeply indebted to all my family members: my mother, my father, my wife, my kids, my brother, my sisters, my uncles, my aunts, all of my relatives for their love, helpfulness, moral support, and encouragement that they gave me throughout this study.

Sadoun

Summary

Systemic lupus erythematosus (SLE) is a combinatorial autoimmune disease (AID) of a complicated nature, distinguished by the generation of diverse autoantibodies. The dysregulation of T-cell-dependent mechanisms that induce autoreactive B-cells is widely acknowledged as a pivotal factor in the pathogenesis of SLE. The presence of these autoantibodies has been observed to result in tissue damage in multiple organs, such as the skin, kidneys, central nervous system (CNS), and joints. Hence, the aim of the present study is to investigate the content and particularities of change of programmed cell death 1 (PD-1) levels as a marker of SLE patients of the population of Basrah Province (southern of Iraq). In this study, 43 SLE patients (females) were participated and 53 apparently healthy controls (females) were followed up for 11 months, till end the study.

The two groups were matched for their body mass index (BMI), complement component 3 (C3), complement component 4 (C4), complement hemolytic 50 (CH50), malondialdehyde (MDA), total antioxidant capacity (TAC), C-reactive protein (CRP), antinuclear antibodies (ANA), anti-double strand DNA (Anti-dsDNA), urea, creatinine, glomerular filtration rate (GFR), interleulin-18 (IL-18), interleukin -37 (IL-37), and PD-1 biomarkers. Compared with normal controls, the results indicated that SLE patients had high significantly ($p < 0.01$) increased levels of MDA, CRP, ANA, Anti-dsDNA, urea, creatinine, IL-18, IL-37, and PD-1. On the other hand, our data reported that C3, C4, CH50, TAC, and GFR were decreased significantly ($p < 0.01$) in SLE patients compared to controls. Moreover, the results obtained indicated that there was a no significant ($p > 0.05$) in BMI level in SLE patients as compared to control group.

Furthermore, for the receiver operating characteristics (ROC), the area under curve (AUC) indicated that C3, C4, CH50, MDA, TAC, CRP, ANA, Anti-dsDNA, urea, creatinine, GFR, IL-18, IL-37, and PD-1 could potentially serve as more precise predictive biomarkers in subjects with SLE (AUC = 0.08, 0.22, 0.091, 0.922, 0.07, 0.894, 0.915, 0.922, 0.919, 0.922, 0.06, 0.985, 0.968, and 0.940 respectively).

The data presented in the study revealed a positive correlation between IL-18 and IL-37 with PD-1. Additionally, IL-18, IL-37, and PD-1 exhibited significantly positive correlations with MDA, CRP, ANA, Anti-dsDNA, urea, and creatinine. Conversely, IL-18, IL-37, and PD-1 had significantly negative correlations with C3, C4, CH50, TAC, and GFR.

In this study, we conducted an investigation into the PD-1 gene polymorphisms located within intron-4 among SLE subjects and a control group of healthy participants at some Basrah teaching hospitals, also studied the effect on serum level PD-1. The polymorphic loci were identified by the utilization of PCR-sequencing, resulting in the recognition of two different loci, namely rs6705653 and rs41386349. In relation to the allelic frequencies and genotype distributions of PD-1 +7499 (G/A), it was shown that the AA genotype exhibited a statistically significant increase among SLE subjects. Consistent with prior research, the homozygous AA and heterozygous GA genotypes exhibited a higher frequency among SLE subjects, while the GG genotype was more commonly observed among individuals without the disease. Therefore, the heightened risk of SLE can be related to the presence of the A allele and, subsequently, the AA genotype at this location. Additionally, it has been observed that the presence of the G allele and GG genotype at the +7499 region of the PD-1 gene may confer protective effects against SLE. The examination of the allelic frequencies of PD-1 +7209 (C/T) polymorphisms in individuals with SLE in comparison to individuals without the condition revealed no statistically significant disparity. The current investigation findings signify the T allele could get considered a potential risk allele for SLE, while the C allele may have a protective effect. Genotypes frequencies polymorphism were found to be consistent with Hardy-Weinberg equilibrium (HWE).

Glossary of Abbreviations

AIDs	Autoimmune Diseases
ACR	American College of Rheumatology
ANA	Antinuclear Antibodies
Anti-dsDNA	Anti-double strand DNA
Anti-RNP	Anti-Ribonucleoprotein
APCs	Antigen Presentation Cells
ARA	American Rheumatism Association
AUC	Area Under Curve
BCR	B-Cells Receptors
BLAST	Basic Local Alignment Search Tool
BMI	Body Mass Index
C3	Complement Component 3
C4	Complement Component 4
CD28	Cluster of Differentiation 28
CDR3	Complementarity-Determining Region 3
CH50	Complement Hemolytic 50
CI	Confidence Interval
CKD	Chronic Kidney Disease
CNS	Central Nervous System
Con A	Concanavalin
CPK	Creatine Phosphokinase
CR1	Complement Receptor 1
CRP	C-Reactive Protein
CTAB	Cetyltrimethylammonium Bromide
CTLA-4	Cytotoxic T-Lymphocyte Antigen-4
CVD	Cardiovascular Disease
DCs	Dendritic Cells
DNA	Deoxyribonucleic Acid
DW	Distilled Water
EC	Extracellular
EDTA	Ethylene Diamine Tetra Acetate
ELISA	Enzyme-Linked Immunosorbent Assay
EMG	Electromyography
FAS	Factor Apoptosis Superfamily
FcγR	Fragment crystallization Gamma Receptor
GFR	Glomerular Filtration Rate
HIV	Human Immunodeficiency Virus
HLA	Human Leukocyte Antigens

HRP	Horseradish Peroxidase
HWE	Hardy-Weinberg Equilibrium
ICOS	Inducible T-Cell Co-Stimulator
ICs	Immunological Complexes
IDT	Integrated DNA Technologies
IFN	Interferon
Ig	Immunoglobulin
IL	Interleukin
IL-18BP	IL-18 Binding Protein
ITIM	Immune-Receptor Tyrosine-Based Inhibitory Motif
ITSM	Immune-Receptor Tyrosine-Based Switch Motif
kDa	Kilo Dalton
LAI	Lupus Activity Index
LN	Lupus Nephritis
LODs	Logarithm of Odds
LPS	Lipopolysaccharide
MBL	Mannose Binding Lectin
MDA	Malondialdehyde
MDRD	Modification of Diet in Renal Disease
NCBI	National Centre for Biotechnology Information
NHANES	National Health and Nutrition Examination Survey
NICEM	National Instrumentation Centre for Environmental Management
NK	Natural Killer
NLRP3	Nucleotide-Binding Oligomerization Domain, Leucine Rich Repeat and Pyrin Domain Containing 3
NO	Nitric Oxide
NSAIDs	Non-Steroidal Anti-Inflammatory Drugs
OD	Optical Density
OR	Odds Ratio
PBMC	Peripheral Blood Mononuclear Cell
PBS	Phosphate Buffered Saline
PCR	Polymerase Chain Reaction
PD-1	Programmed Cell Death 1
PD-L	Programmed Cell Death Ligand
PEW	Protein-Energy Wasting
PHA	Phytohemagglutinin
RAPD	Random Amplification of Polymorphic DNA
RBCs	Red Blood Cells
RNA	Ribonucleic Acid
ROC	Receiver Operating Characteristics
ROS	Reactive Oxygen Species

RPM	Revolutions per Minute
RNPs	Ribonucleoproteins
SD	Standard Deviation
SE	Standard Error
SHP-2	Src Homology 2-Domain-Containing Tyrosine Phosphatase 2
SLAM	Systemic Lupus Activity Measure
SLE	Systemic Lupus Erythematosus
SLEDAI	Systemic Lupus Erythematosus Disease Activity Index
SNPs	Single Nucleotide Polymorphisms
SPSS	Statistical Package for the Social Sciences
TAC	Total Antioxidant Capacity
TBA	Thiobarbituric Acid
TBARS	Thiobarbituric Acid Reactive Substances
TBE	Tris-Borate-Edta
TBS	Tris-HCl Buffered Saline
TCA	Trichloro Acetic Acid
TCR	T-Cell Receptor
Th	T Helper
TLRs	Toll-Like Receptors
TMB	Tetramethyl Benzidine
TNF	Tumor Necrosis Factor
USA	United States of America
UTR	Untranslated Region
UV	Ultraviolet
WBCs	White Blood Cells

Contents

No.	Title	Page
	Acknowledgments	
	Summary	I-II
	Glossary of Abbreviation	III-V
	Contents	VI-VIII
	List of Tables	IX-X
	List of Figures	XI-XII
Chapter One: Introduction		
1.1	Preface about Systemic Lupus Erythematosus (SLE)	1
1.1.1	Environmental Factors of SLE	4
1.1.2	Genetic Factors for SLE	6
1.2	Impaired Regulation of T- and B-cells	7
1.2.1	Tissues Damage: Importance of Autoantibodies and Accumulation of Immune Complexes	8
1.3	Genetic Susceptibility of SLE	9
1.3.1	Linkage Studies in Humans	9
1.3.2	Genes and SLE	10
1.4	Programmed Cell Death-1 (PD-1)	10
1.4.1	PD-1 Protein, Gene and Expression	11
1.4.2	Biological Activity of PD-1	13
1.4.3	Ligands of PD-1	15
1.4.4	PD-1 Signaling	16
1.5	Inflammation and Cytokines	18
1.5.1	Classification of Cytokines	24
1.5.2	Pro-Inflammatory Cytokines	25
1.5.2.1	Interleukin-18 (IL-18)	25
1.5.3	Anti-Inflammatory Cytokines	26
1.5.3.1	Interleukin-37 (IL-37)	26
1.6	The Aims of the Study	28
Chapter Two: Materials and Methods		
2.1	Chemicals and Instruments	29
2.2	Place of Work	32
2.3	Study Design	32
2.3.1	Subjects	32
2.3.1.1	Inclusion Criteria	33
2.3.1.2	Exclusion Criteria	34
2.3.2	Sample Size Calculation	34
2.3.3	Samples	34

2.4	Methods	35
2.4.1	Body Mass Index (BMI)	35
2.4.2	Systemic Lupus Erythematosus Disease Activity Index – 2000 (SLEDAI-2K)	35
2.4.3	Biochemical Estimation	39
2.4.3.1	Immunological Parameters	39
2.4.3.1.1	Levels of Complement Component 3 (C3)	39
2.4.3.1.2	Levels of Complement Component 4 (C4)	41
2.4.3.1.3	Levels of Complement Hemolytic 50 (CH50)	43
2.4.3.1.4	Levels of Antinuclear Antibodies (ANA)	46
2.4.3.1.5	Levels of Anti-double strand DNA (Anti-dsDNA)	51
2.4.3.2	Oxidant/Antioxidant Parameters	55
2.4.3.2.1	Levels of Malondialdehyde (MDA)	55
2.4.3.2.2	Levels of Total Antioxidant Capacity (TAC)	58
2.4.3.3	Kidney Function Parameters	61
2.4.3.3.1	Levels of Urea	61
2.4.3.3.2	Levels of Creatinine	63
2.4.3.3.3	Levels of Glomerular Filtration Rate (GFR)	64
2.4.3.4	Inflammation and Cytokines Parameters	64
2.4.3.4.1	Levels of C-Reactive Protein (CRP)	64
2.4.3.4.2	Levels of Interleukin-18 (IL-18)	68
2.4.3.4.3	Levels of Interleukin-37 (IL-37)	72
2.4.3.4.4	Levels of Programmed Cell Death 1 (PD-1)	76
2.4.4	Genetic Study	80
2.4.4.1	DNA Extraction	80
2.4.4.2	Agarose Gel Electrophoresis of DNA	82
2.4.4.2.1	Preparation of the Agarose Gel	82
2.4.4.2.2	Preparation of the Sample	83
2.4.4.3	Measurement of DNA Concentration and Purity	83
2.4.4.4	The Primers Used in the Interaction	84
2.4.4.5	Maxime PCR PreMix Kit (i-Taq) 20 μ lrxn	84
2.4.4.6	Diagnosis of PD-1 Gene	85
2.5	Statistical Analysis	86
Chapter Three: Results and Discussion		
3.1	Basic Characteristics of Individuals in the Present Study	88
3.2	Total Parameters in this Study	89
3.3	Levels of Body Mass Index (BMI)	90
3.4	Biochemical Parameters	92
3.4.1	Levels of Complement Components	92
3.4.2	Levels of Malondialdehyde (MDA)	95
3.4.3	Levels of Total Antioxidant Capacity (TAC)	98

3.4.4	Levels of C-Reactive Protein (CRP)	100
3.4.5	Levels of Anti-Nuclear Antibody (ANA)	102
3.4.6	Levels of Anti-double strand DNA (Anti-dsDNA)	104
3.4.7	Levels of Urea	106
3.4.8	Levels of Creatinine	109
3.4.9	Levels of Glomerular Filtration Rate (GFR)	111
3.4.10	Levels of Interleukin-18 (IL-18)	114
3.4.11	Levels of Interleukin-37 (IL-37)	116
3.4.12	Levels of Programmed Cell Death-1 (PD-1)	119
3.5	Correlation Analysis	121
3.5.1	Correlation between Serum IL-18 Levels with Biochemical Parameters in SLE Patients	121
3.5.2	Correlation between Serum IL-37 Levels with Biochemical Parameters in SLE Patients	134
3.5.3	Correlation between Serum PD-1 Levels with Biochemical Parameters in SLE Patients	146
3.6	Receiver Operating Characteristic (ROC) Study	157
3.7	Genetic Study for PD-1 Gene	167
3.7.1	DNA Extraction and Polymerase Chain Reaction Technique (PCR)	167
3.7.2	Detection for PD-1 Gene in the Studied Group	169
3.7.3	Purification the Samples from Gel	170
3.7.4	Examination of Hardy-Weinberg Equilibrium for PD-1 Gene Polymorphism	171
3.7.4.1	Genotyping and Allele Frequency of PD-1 SNP +7499	171
3.7.4.2	Genotyping and Allele Frequency of PD-1 SNP +7209	172
3.7.5	Comparison of Genotype and Allele Frequencies of the Two Polymorphism PD-1 Gene (+7499 and +7209)	174
3.7.6	Biochemical Characteristics of SLE and Healthy Control in Relevance to the Distribution of the Genotypes of PD-1 Gene Polymorphism	177
3.7.7	Association of +7499 G/A and +7209 C/T Polymorphism with Serum PD-1 Levels	178
	Conclusion	181
	Recommendations	182
	References	183
Appendices	(1) Biochemical Characteristics of SLE and Healthy Control in Relevance to the Distribution of the Genotypes of PD-1 Gene Polymorphism	205
	(2) Books facilitating the task (Ethical Approval)	209
	(3) Published Researches	211

List of Tables

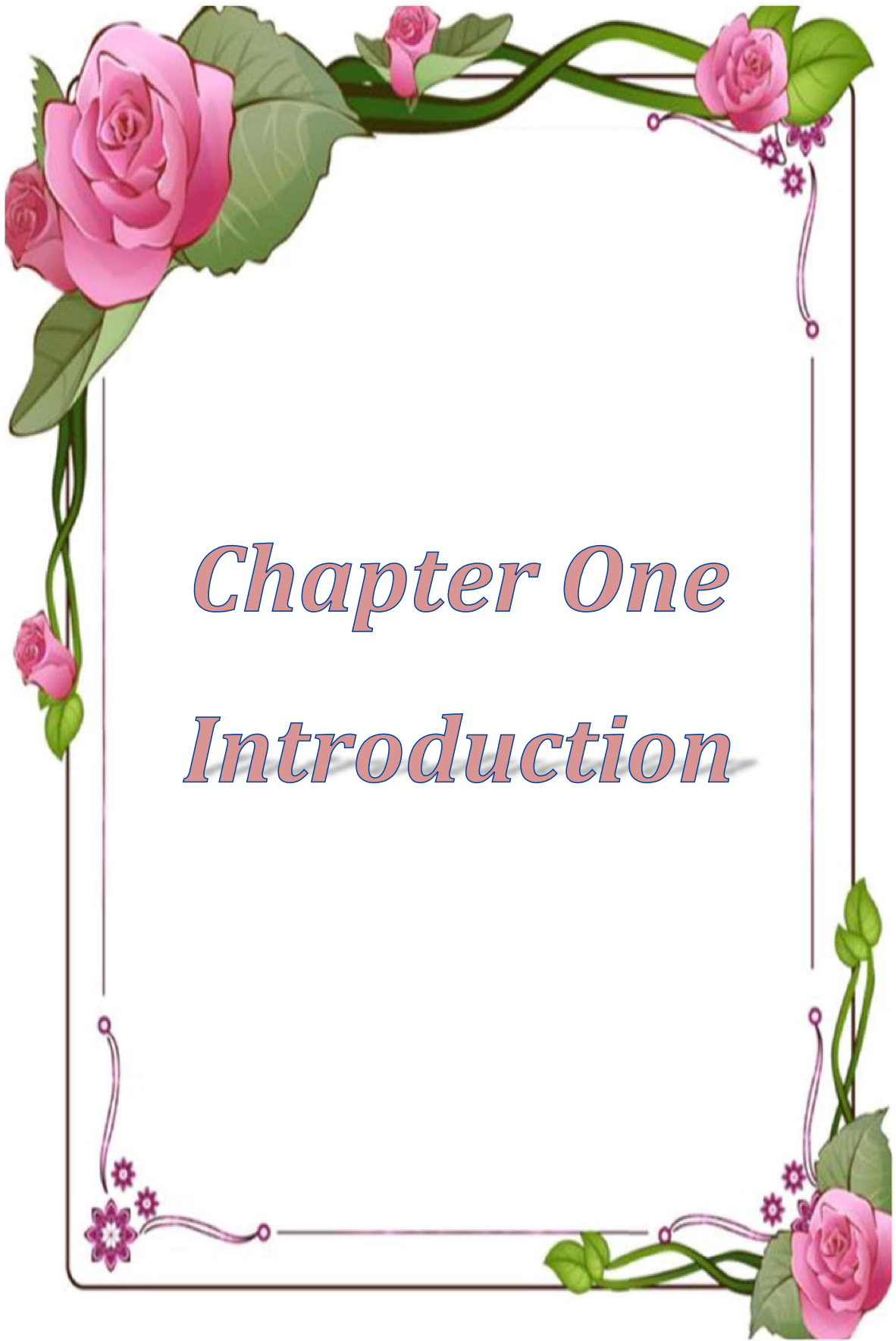
No.	Title	Page
1.1	Environmental factors that may be relevant in the etiology of SLE	5
1.2	Characteristics of PD-1	14
1.3	Cytokine profiles in SLE patients	23
2.1	Chemical compounds with their manufacturer and origins	29
2.2	Diagnostic kits with their catalogue No., manufactures and origins	30
2.3	Instruments with their manufactures and origins	30
2.4	Questionnaire paper form used in this study	33
2.5	SLEDAI-2K variables and points	36
2.6	Plasma protein calibrator dilution for C3 estimation	39
2.7	Sets of tubes with their solutions and additives in C3 estimation	40
2.8	Plasma protein calibrator dilution for C4 estimation	41
2.9	Sets of tubes with their solutions and additives in C4 estimation	42
2.10	Materials of CH50 ELISA kit	44
2.11	Components of ANA ELISA kit	47
2.12	Standards dilution of ANA	48
2.13	Components of Anti-dsDNA ELISA kit	51
2.14	Standards dilution of Anti-dsDNA	52
2.15	Standards dilution of MDA	57
2.16	Standards dilution of TAC	59
2.17	Sets of tubes with their solutions and additives in urea determination	62
2.18	Sets of tubes with their solutions and additives in creatinine determination	63
2.19	Materials of CRP ELISA kit	65
2.20	Standards dilution of CRP	66
2.21	Components of IL-18 ELISA kit	69
2.22	Standards dilution of IL-18	70
2.23	Components of IL-37 ELISA kit	73
2.24	Standards dilution of IL-37	74
2.25	Components of PD-1 ELISA kit	77
2.26	Standards dilution of PD-1	78
2.27	Components of G-spin DNA extraction kit	80
2.28	The specific primer PD-1 gene	84
2.29	The Components of the Maxime PCR PreMix kit (i-Taq)	85
2.30	Mixture of the specific interaction for detection PD-1 gene	85
2.31	The optimum condition of detection PD-1 gene	85
3.1	The demographic characteristics of the present study	88

3.2	Levels of total parameters measured in the present study for SLE patients and the apparently control group	89
3.3	Levels of BMI in SLE patients and control group	90
3.4	Levels of C3, C4 and CH50 in SLE patients and control group	92
3.5	Levels of MDA in SLE patients and control group	96
3.6	Levels of TAC in SLE patients and control group	98
3.7	Levels of CRP in SLE patients and control group	100
3.8	Levels of ANA in SLE subjects and control group	102
3.9	Levels of Anti-dsDNA in SLE patients and control group	104
3.10	Levels of Urea in SLE patients and control group	107
3.11	Levels of Creatinine in SLE patients and control group	109
3.12	Levels of GFR in SLE patients and control group	112
3.13	Levels of IL-18 in SLE patients and control group	114
3.14	Levels of IL-37 in SLE patients and control group	116
3.15	Levels of PD-1 in SLE patients and control group	119
3.16	Correlation between serum IL-18 levels with biochemical parameters in SLE patients group	121
3.17	Correlation between serum IL-37 levels with biochemical parameters in SLE patients group	135
3.18	Correlation between serum PD-1 levels with biochemical parameters in SLE patients group	146
3.19	ROC and AUC analysis of the measured biomarkers for the diagnosis of SLE	157
3.20	The purity and concentration of the extracted DNA	167
3.21	Genotype frequency and allele frequency of SLE subjects (SNP +7499)	171
3.22	Genotype frequency and allele frequency of control (SNP +7499)	172
3.23	Genotype frequency and allele frequency of SLE subjects (SNP +7209)	173
3.24	Genotype frequency and allele frequency of control (SNP +7209)	173
3.25	Allelic and genotypic of SNP +7499 G/A polymorphism in SLE and control groups	175
3.26	Allelic and genotypic of SNP +7209 C/T polymorphism in SLE and control groups	176

List of Figures

No.	Title	Page
1.1	The main etiologies of SLE	2
1.2	A simple overview of the SLE etiology	3
1.3	The main symptoms of AIDs	4
1.4	B7-CD28 family members' schematic structures	11
1.5	Mouse PD-1 structure	12
1.6	PD-1 gene map on chromosome 2q37.3	13
1.7	A theoretical framework for the potential modulation of peripheral tolerance through the interaction between PD-1 and its ligand	15
1.8	Induction of the tyrosine phosphorylation of the ITSM of PD-1	17
1.9	The influence of ILs on the advancement of chronic inflammation and consequent renal dysfunction	20
1.10	Cytokine network	22
1.11	The categorization of ILs according to their impact on biological inflammatory response	24
1.12	IL-18 biological functions	26
1.13	IL-37 immunity regulation role	27
2.1	Standard curve of C3	40
2.2	Standard curve of C4	42
2.3	Standard curve of CH50	46
2.4	Standards solutions preparation of ANA	48
2.5	Standard curve of ANA	50
2.6	Standards solutions preparation of Anti-dsDNA	53
2.7	Standard curve of Anti-dsDNA	55
2.8	Standard curve of MDA	58
2.9	Standard curve of TAC	61
2.10	Standards solutions preparation of CRP	66
2.11	Standard curve of CRP	68
2.12	Standards solutions preparation of IL-18	70
2.13	Standard curve of IL-18	72
2.14	Standards solutions preparation of IL-37	74
2.15	Standard curve of IL-37	76
2.16	Standards solutions preparation of PD-1	78
2.17	Standard curve of PD-1	80
2.18	Working of the electrophoresis system	83
3.1	Comparison of BMI level between SLE patients and healthy control group	90
3.2	Comparison of complement components levels between SLE patients and healthy control group	93

3.3	Comparison of MDA levels between SLE patients and healthy control group	96
3.4	Comparison of TAC levels between SLE patients and healthy control group	98
3.5	Comparison of CRP levels between SLE patients and healthy control group	100
3.6	Comparison of ANA levels between SLE patients and healthy control group	102
3.7	Comparison of Anti-dsDNA levels between SLE patients and healthy control group	105
3.8	Comparison of Urea levels between SLE patients and healthy control group	107
3.9	Comparison of Creatinine levels between SLE patients and healthy control group	110
3.10	Comparison of GFR levels between SLE patients and healthy control group	112
3.11	Comparison of IL-18 levels between SLE patients and healthy control group	114
3.12	Comparison of IL-37 levels between SLE patients and healthy control group	117
3.13	Comparison of PD-1 levels between SLE patients and healthy control group	119
3.14	Linear regression analysis between serum level of IL-18 with the following parameters	129
3.15	Linear regression analysis between serum level of IL-37 with the following parameters	142
3.16	Linear regression analysis between serum level of PD-1 with the following parameters	154
3.17	ROC curve for (A) C3, (B) C4, (C) CH50, (D) ANA, (E) Anti-dsDNA, (F) IL-18, (G) IL-37, (H) PD-1 in SLE patients and control group	161
3.18	ROC curve for (A) BMI, (B) MDA, (C) TAC, (D) CRP, (E) Urea, (F) Creatinine, (G) GFR in SLE patients and control group	165
3.19	Gel electrophoresis of extracted genomic DNA	168
3.20	Agarose gel electrophoresis of PCR amplification products of PD-1 gene in the samples	170
3.21	Association of the (A) PD-1 +7499 G/A and (B) PD-1 +7209 C/T polymorphism with serum PD-1 levels	179



Chapter One
Introduction

Chapter One

1.1. Preface about Systemic Lupus Erythematosus (SLE)

Systemic lupus erythematosus (SLE) is a combinatorial autoimmune disease (AID) of a complicated nature, distinguished by the generation of diverse autoantibodies. The dysregulation of T-cell-dependent mechanisms that induce autoreactive B-cells is widely acknowledged as a pivotal factor in the pathogenesis of SLE (Wang *et al.*, 2021). The presence of these autoantibodies has been observed to result in tissue damage in multiple organs, such as the skin, kidneys, central nervous system (CNS), and joints (Nakanishi, 2018). Due to the intricate nature of the disease and its encompassing array of clinical manifestations, the American Rheumatism Association (ARA) has issued preliminary criteria for the categorization of SLE in 1971. These criteria underwent subsequent revisions from 1982 to 1987 and were further updated in 1997 (Wu *et al.*, 2021). Furthermore, additional indicators are employed to assess the severity of SLE, such as the Systemic Lupus Erythematosus Disease Activity Index (SLEDAI), the Systemic Lupus Activity Measure (SLAM), and the Lupus Activity Index (LAI) (Al-Anazi *et al.*, 2019).

The incidence rate of SLE exhibits variation among distinct ethnic communities. The observed disparity may be attributed to variations in genetics as well as environmental variables. The average incidence rate in the United States of America (USA) is 122 per 100,000 individuals. The incidence rates of the condition in question vary among European Caucasians, with England reporting a rate of 12.5 per 100,000 and Sweden reporting a rate of 39 per 100,000 (Jaing *et al.*, 2021). Individuals of African and Asian descent exhibit higher levels of prevalence and incidence of the condition. The African-Caribbean population exhibits the highest prevalence rate (124.7 per 100,000), followed by the Asian population (48.8 per 100,000), and finally the Caucasian population (20.3 per 100,000) (Bassiouni *et al.*, 2021). A prevalence odds ratio of 2.4 has been recorded for individuals of Chinese

descent compared to individuals of Caucasian descent in the population of Hawaii. From the other hand, the prevalence of SLE was estimated to be 19.28 per 100,000 populations in Saudi Arabia, 6.1 per 100,000 populations (1.2/100,000 males and 11.3/100,000 females) in Egypt, and 40 per 100,000 persons in Iran (Belmokhtar *et al.*, 2022). These findings indicate that both hereditary and environmental variables may contribute to the predisposition to SLE in various populations (Ayoub *et al.*, 2019).

The pathogenesis of SLE entails the perturbation of T- and B-cell function, the generation of autoantibodies, the buildup of immunological complexes (ICs), and the interplay between hereditary and environmental variables (Al-Fartosy *et al.*, 2017a). Figure (1.1) illustrates the main etiologies of SLE and its effect on the body organs.

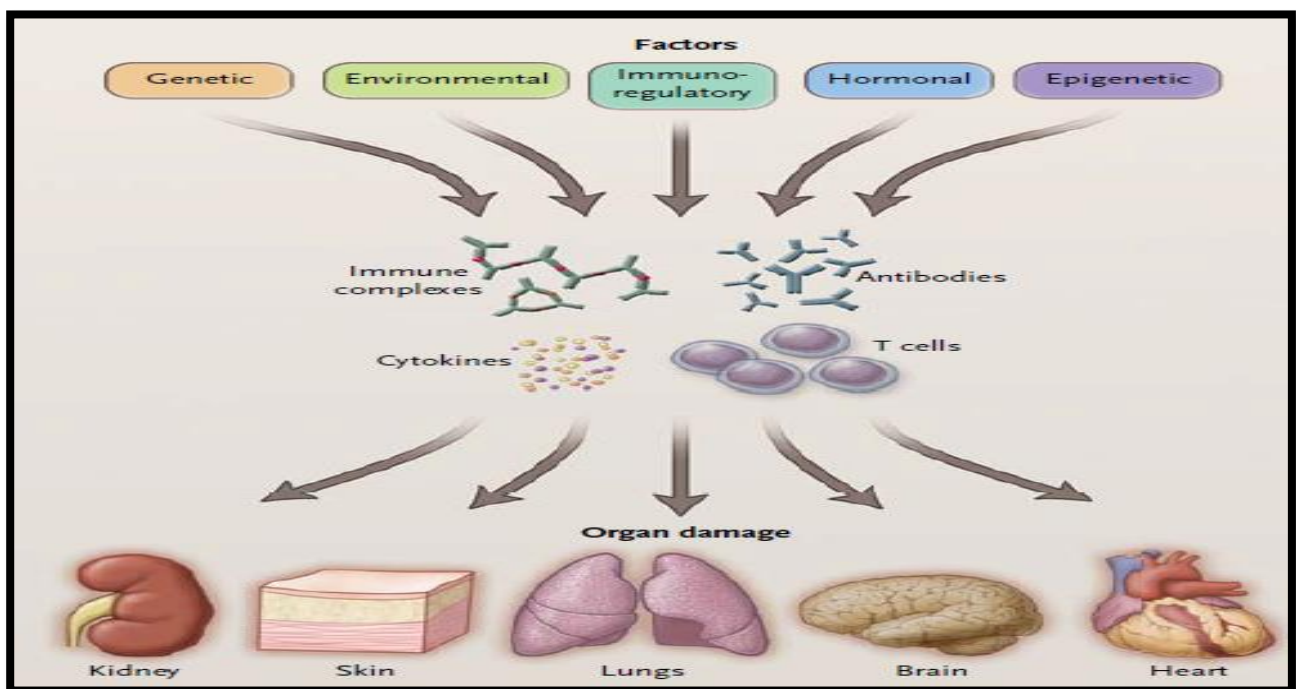


Figure (1.1): The main etiologies of SLE (Zhang *et al.*, 2021b).

The interplay among hereditary and environmental variables contributes to the development of diminished tolerance and deregulation of the immune system. Figure (1.2) provides a concise depiction of the hereditary and environmental variables contribution in SLE etiology. The T-cells that have been stimulated stimulate the

activation of B-cells. The existence of dysregulated active B-cells might elicit a positive feedback response from T-cells, resulting in increased activation of the T-cells (Davaranah *et al.*, 2020). The unregulated interplay between T-cells and B-cells serves to enhance and broaden the autoimmune signaling. Autoantibodies are generated by overactive B-cells, with a portion of them originating from ICs. Both of these substances are deposited within different tissues and organs, resulting in the development of inflammation and tissue damage, which are distinctive features of SLE (Alaanzy *et al.*, 2020).

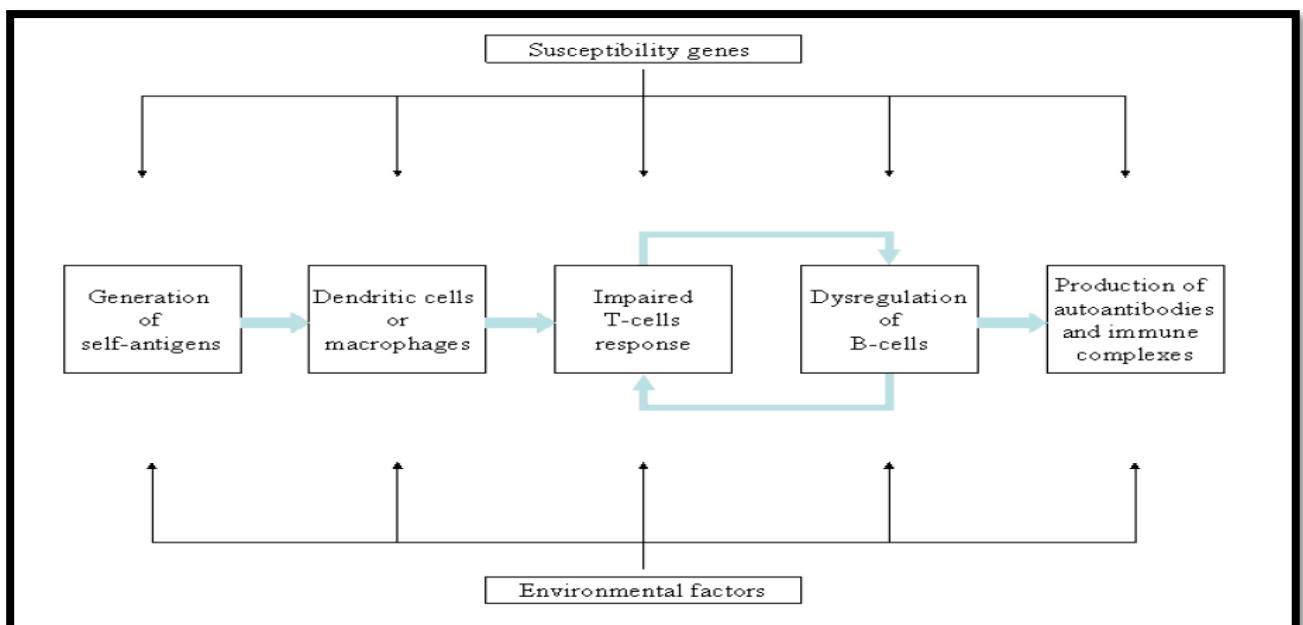


Figure (1.2): A simple overview of the SLE etiology (Kholis *et al.*, 2023).

The manifestation of symptoms associated with SLE can vary significantly among individuals, ranging from severe presentations in certain cases to more moderate manifestations in others. There exist varying degrees of SLE, and the manifestation of symptoms in individuals is likely influenced by a multitude of elements, including genetic predisposition, environmental conditions, and personal well-being (Sam *et al.*, 2021). Despite the existence of different kinds of AIDs, numerous similarities can be observed among their respective symptoms. Typical manifestations of AIDs encompass symptoms such as weariness, joint pain

accompanied by edema, dermatological complications, abdominal pain or gastrointestinal disturbances, recurrent fever, and lymphadenopathy (Kono *et al.*, 2021), as demonstrated in Figure (1.3).

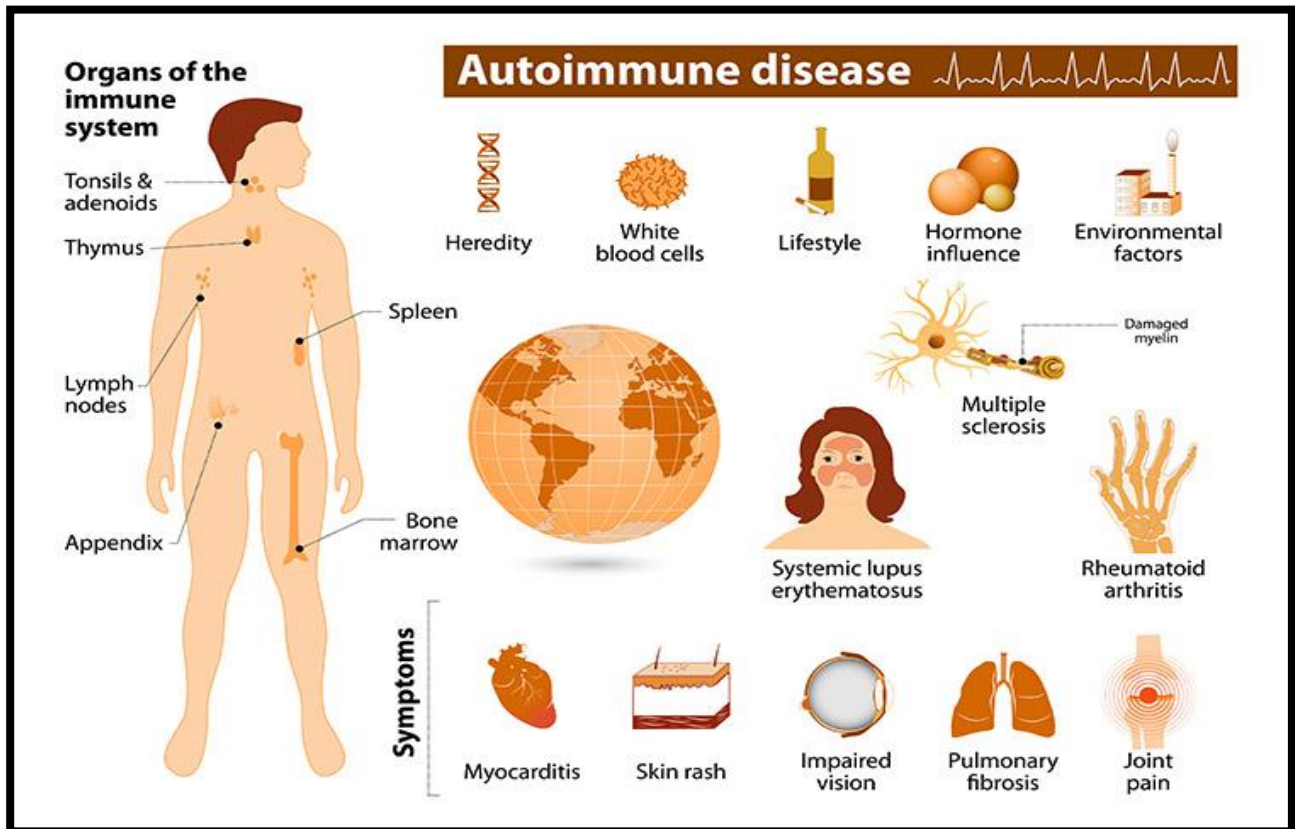


Figure (1.3): The main symptoms of AIDs (Lee and Song, 2020).

1.1.1. Environmental Factors of SLE

The onset of SLE is likely attributed to environmental triggers and external variables, as outlined in Table (1.1).

Table (1.1): Environmental factors that may be relevant in the etiology of SLE (Wasen *et al.*, 2018).

Factor	Example
Chemical/Physical	Aromatic amines. Hydrazine. Drugs (procainamide, hydralazine, isoniazid, phenytoin, penicillamine, chlorpromazine). Tobacco smoke. Hair dyes. UV light.
Dietary	L-canavnine (alfalfa sprouts). High intake of saturated fats.
Infectious	Bacterial DNA/endotoxins. Retroviruses.

Numerous environmental variables that elicit immune response irritation have been documented to be implicated in the initiation of SLE. The factors contributing to this phenomenon encompass bacterial and viral infections, chemical agents, prolonged exposure to sunlight and UV radiation, as well as dietary choices (Uciechowski and Dempke, 2020). Bacterial or viral infections have the potential to elicit distinct reactions, including the activation of B-cells and the occurrence of tissue damage. Additionally, these infections can disrupt immune-regulation, so triggering the onset of SLE. Indeed, there is evidence to show a potential association between human immunodeficiency virus (HIV) infection and SLE. Chemical substances possess the capacity to induce significant irritation, hence serving as catalysts for the onset of SLE (Chen *et al.*, 2018a). Various pharmaceuticals, including procainamide, hydralazine, and isoniazid, which fall within the categories of aromatic amines or hydrazines, have the potential to elicit a lupus-like condition. This is especially true for persons who

possess a genetic predisposition for delayed acetylation. The aforementioned substances and their derivatives are frequently encountered in the compounds utilized in the fields of agriculture, industrial, and commercial applications (Al-Fartosy and Mohammed, 2017c). There is evidence suggesting a potential association between the use of tobacco and hair dyes and the occurrence of SLE. The induction of SLE is widely recognized to be influenced by exposure to sunshine and UV radiation. The prolonged contact of skin to UV radiation results in changes to the positioning and/or composition of DNA, as well as Ro and nRNP antigens. These alterations likely contribute to an increased immunogenic response (Gao *et al.*, 2017b). In addition, UV radiation has been observed to induce the programmed cell death, known as apoptosis, in human keratinocytes. This apoptotic process might potentially stimulate the generation of autoantibodies and result in the formation of skin lesions, thereby serving as a triggering factor in the progression of SLE (Yap *et al.*, 2018). The investigation of dietary elements, such as antioxidants, in SLE has revealed a notable reduction in blood levels of α -tocopherol, β -carotene, and retinol. Current study endeavors are being conducted to ascertain additional potential environmental elements and their respective contributions to SLE (Bommarito *et al.*, 2017).

1.1.2. Genetic Factors for SLE

The role of genetic factors has been identified as being significant in the pathogenesis of SLE. The heredity of SLE is substantiated by the available evidence. The observation of higher concordance rates in monozygotic twins (>20%) compared to dizygotic twins and other full siblings (2-5%) is seen in the context of SLE (Saha *et al.*, 2021). The prevalence of SLE in first-degree relatives is as follows: definite SLE is observed in 3.9% of relatives of individuals with SLE, 2.6% of relatives with discoid lupus, and merely 0.3% of control subjects. Additionally, the heightened risk of SLE in siblings of SLE patients further substantiates the genetic association with SLE (Khan *et al.*, 2018).

1.2. Impaired Regulation of T- and B-cells

The improper stimulation and reproduction of T- and B-cells can be attributed to the loss of tolerance in these cells. The disruption in tolerance may necessitate the utilization of distinct antigens to stimulate T- and B-cells. These antigens may be produced via several mechanisms, which includes as viral or bacterial infection, contact with irritating chemicals, and ultraviolet (UV) radiation (Leonardi *et al.*, 2018). Antigen presentation cells (APCs) are responsible for delivering antigens to T-cells. The process described involves the activation of T-cells, which then prompts the stimulation of B-cells. As a result, a diverse range of autoantibodies is produced. Autoantibody synthesis from T-cell-stimulated B-cells can also be triggered by self-antigens, including DNA-protein and RNA-protein complexes (El-Sayed *et al.*, 2018). Several investigations have provided evidence of T-cell abnormalities in SLE, including a reduction in the quantity of T-cells in the peripheral blood. A diminished proliferative reaction of SLE T-cells to mitogenic lectins, such as phytohemagglutinin (PHA), concanavalin A (Con A), and pokeweed mitogen, as well as lower generation of interleukin-2 (IL-2), have also been observed (Shi *et al.*, 2017; Italiani *et al.*, 2018). SLE is characterized by overactive production of B-cells, leading to an increased presence of autoantibodies, particularly anti-DNA antibodies, in the peripheral blood of individuals with active SLE (Durcan and Petri, 2020). The manifestation of atypical initial transmission of signals occurrences, such as the heightened intracellular calcium responses following the cross-linked state of B-cell receptors, as well as the amplified phosphorylation of protein tyrosine residues mediated by antigen-receptors, serves as additional evidence of the irregularities observed in B-cells within the context of SLE. B-cells in individuals with SLE exhibit heightened sensitivity to the stimulatory effects of cytokines compared to B-cells in individuals without SLE (Al-Fartosy *et al.*, 2019). Furthermore, it has been observed that SLE is characterized by epitope spreading, which refers to the capacity of T- and B-cell immune responses to expand in terms of specificity. This expansion occurs not only at the level of

recognizing a single determinant, but also extends to many places on an autoantigen (Zappulo *et al.*, 2022). Additionally, the diversification of V gene usage in B-cells has also been identified in individuals with SLE. These findings suggest that B-cells in SLE exhibit a heightened capacity for activation in response to diverse stimuli (Zhang *et al.*, 2022).

1.2.1. Tissues Damage: Importance of Autoantibodies and Accumulation of Immune Complexes

The generation of autoantibodies from B-cells is a defining characteristic of the pathophysiology of SLE. Antinuclear antibodies (ANA) have the highest degree of specificity in individuals diagnosed with SLE, while anti-double stranded DNA (Anti-dsDNA) is exclusively seen in patients with SLE (Han *et al.*, 2019). The induction of glomerulonephritis is a notable characteristic associated with anti-DNA antibodies. It is probable that many autoantibodies, including antiphospholipid, antineuronal, anti-ribonucleoprotein (anti-RNP or anti-Ro), antierythrocyte, antilymphocyte, and antiplatelet antibodies, play a direct role in causing tissue damage. This can occur through their direct binding to tissue or by promoting the buildup of ICs (Liao *et al.*, 2017).

The impaired elimination of ICs is evident in SLE. There are multiple variations that may possibly lead to this disability (Lin *et al.*, 2021):

- 1- The diminished quantities of complement receptor 1 (CR1) for the complement system.
- 2- The functioning deficiencies exhibited by the receptors located on the surfaces of cells.
- 3- The insufficient process of phagocytosis of complexes comprising immunoglobulin (Ig) G2 and G3 is attributed to allelic polymorphisms of the Fc gamma receptor gene (FcγR), which result in reduced affinity for binding between the Fc sections of IgG2 and IgG3 (Al-Fartosy *et al.*, 2020a).

Furthermore, a diminished level of C1q, C2, and C4 was observed, indicating impaired elimination of ICs. The aggregation of immune cells has the potential to initiate an inflammatory response, resulting in the impairment of tissues (Smeets *et al.*, 2023).

1.3. Genetic Susceptibility of SLE

The genetic basis of SLE is characterized by a high degree of complexity. The etiology of SLE is postulated to arise from the interplay between genetic predisposition and environmental influences (Rezaieyazdi *et al.*, 2020). To ascertain the genes implicated in a complicated disease, researchers employ a novel conventional method known as genetic linkage. Several chromosomal regions in humans have been demonstrated to be associated with SLE (Al-Fartosy *et al.*, 2017b). Furthermore, a multitude of susceptibility genes have been documented to exhibit an association with SLE. Nevertheless, the impact of susceptibility genes on the occurrence of SLE may vary across various ethnic communities due to the distinct interplay of environmental and genetic variables (Mohamed *et al.*, 2019).

1.3.1. Linkage Studies in Humans

Genetic linkage examination refers to the identification of alleles located inside a certain chromosomal area that exhibit co-segregation with an illness phenotype across multiple generations of a family. This analysis involves the utilization of various genetic indicators as points of references (Mohammed *et al.*, 2018). There is a positive correlation between the proximity of indicators and illness loci, leading to a higher likelihood of their co-segregation. In alternative terms, they exhibit a state of connection. Therefore, according to this approach, illness loci can be found through the examination of biomarkers that are expected to be inherited alongside the illness (Abdalla *et al.*, 2017).

In order to ensure a false positive linkage signal likelihood of less than 5%, it is necessary to establish statistical significance for a susceptibility zone by setting a threshold of a logarithm of odds (LODs) score equal to or greater than 3.3 (Wang *et*

al., 2023). A region is deemed to exhibit suggestive connection if its LOD score is equal to or greater than 1.9. In studies that exclusively involve affected sibling pairs, it is recommended to increase the criteria to a LOD score of > 3.6 (Xu *et al.*, 2021).

1.3.2. Genes and SLE

Numerous genetic factors have been discovered as being correlated with SLE among diverse ethnic populations. The genes encompassed under this set consist of the human leukocyte antigens (HLA), complement components (C1q, C2, and C4), Fc γ R, FAS and FAS ligand, mannose binding lectin (MBL), interleukin-10 (IL-10), cytotoxic T-lymphocyte antigen-4 (CTLA-4), and programmed cell death 1 gene (PDCD1 or PD-1) (Laurent *et al.*, 2017; Topfer *et al.*, 2022).

1.4. Programmed Cell Death-1 (PD-1)

The protein known as Programmed cell death-1 (PDCD1 or PD-1) was initially discovered to play a role in the programmed cell death pathway. However, subsequent research has shown that its production is actually stimulated by the induction of T- and B-cells (Hassel *et al.*, 2017). Furthermore, it has been found to function as an inhibitory molecule, suppressing the activating of lymphocytes, instead of promoting apoptosis. The PD-1 gene is a member of the immunoglobulin receptor superfamily and functions as a co-stimulatory protein involved in programmed cell death (Faris *et al.*, 2022a). This family encompasses multiple members, namely the cluster of differentiation 28 (CD28) receptor, CTLA-4, inducible T-cell co-stimulator (ICOS), and PD-1. Each member of this family possesses both the immunoglobulin (Ig)-V-like and Ig-C-like domains, as depicted in Figure (1.6). Like CTLA-4, this molecule is mostly found on activated T- and B-cells and functions as a negative modulator for both cell types. It serves a critical role in preserving peripheral tolerance (Mohammed and Al-Fartosy, 2022).

The interactions between ligands and receptors are denoted by arrows as shown in Figure (1.4). The abbreviations V and C are used to denote immunoglobulin V-like and C-like domains, respectively. The variable "aa" represents the quantity of amino

acid residues present in the cytoplasmic tail. The symbol Y is used to denote a tyrosine residue. The symbols "+" and "-" are used to represent costimulatory and co-inhibitory signaling, respectively. The molecular weights considered in this context are those associated with the glycosylated form. CD28, CTLA-4, and ICOS are known to exist as homodimers. Homology refers to the process of comparing the homologous genes between mice and humans at the amino acid level. Antigen presentation cells (APCs) play a crucial role in the immune response by presenting antigens to T cells. The inductive phase (ind) of the immune response involves the activation and differentiation of immune cells. Monocytes (M) are a kind of white blood cell that can differentiate into APCs. The extracellular domain (EC) refers to the region of a protein that is located outside of the cell membrane (Fujita, 2017).

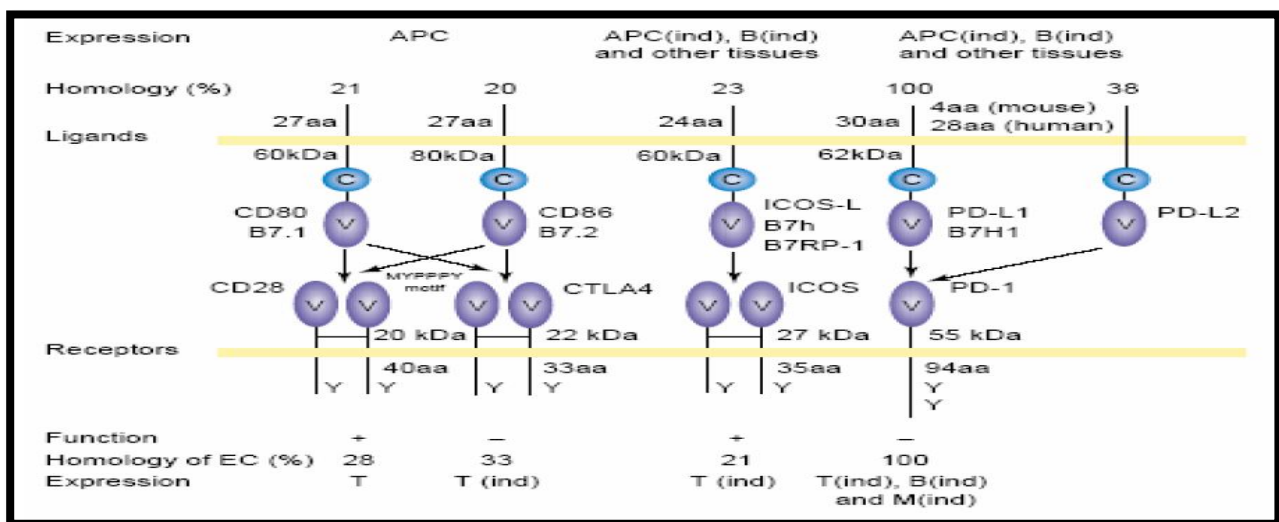


Figure (1.4): B7-CD28 family members' schematic structures (Diaz-Rizo *et al.*, 2017).

1.4.1. PD-1 Protein, Gene and Expression

The human PD-1 (hPD-1) was obtained from the cDNA library of T-cells by the process of hybridization using a mouse (mPD-1) probe. The complete hPD-1 cDNA sequence spans a length of 2,106 nucleotides and is responsible for encoding a protein consisting of 288 amino acids. The hPD-1 and mPD-1 genes exhibit a 70%

degree of similarity at the nucleotide level and a 60% degree of similarity at the amino acid level (Tu *et al.*, 2019).

The PD-1 receptor is a transmembrane protein of type I, weighing approximately 55 kDa. It possesses an extracellular region that consists of a single V-like domain. The cytoplasmic tail of the protein comprises two tyrosine residues, with the N-terminal tyrosine situated within an immune-receptor tyrosine-based inhibitory motif (ITIM) (Abdualhay and Al-Fartosy, 2022). The crystal structure with a resolution of 2.0 Å has been determined and is depicted in Figure (1.5). Both CTLA-4 and PD-1, despite belonging to the same family and exerting inhibitory effects on T-cell activation, have distinct structural variations in regions that are functionally significant. These discrepancies may be attributed to the specific ligands that each molecule binds to (Vincent *et al.*, 2018).

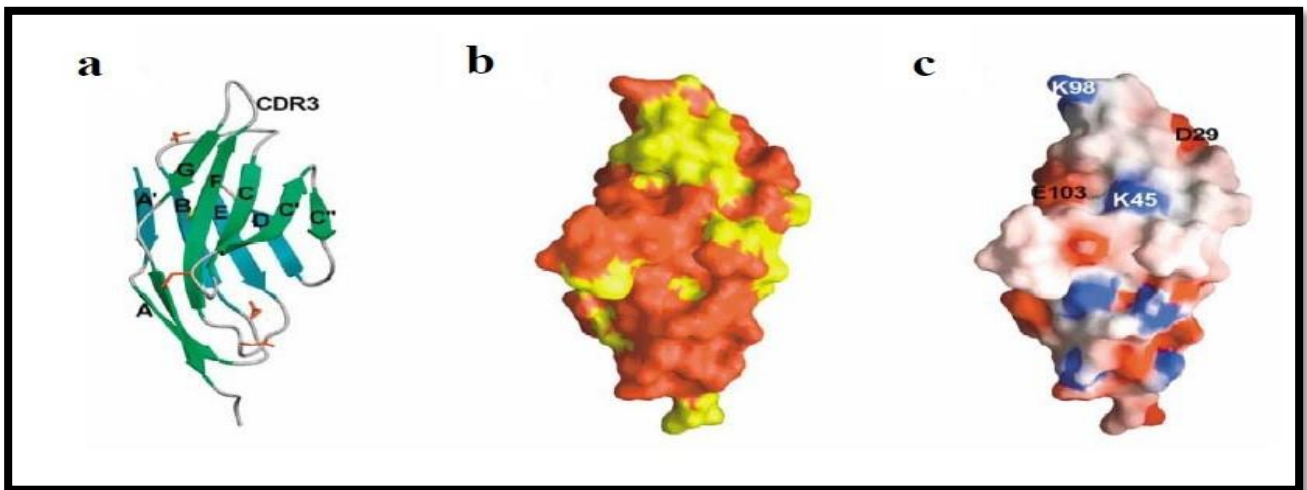


Figure (1.5): Mouse PD-1 structure (Page *et al.*, 2021).

Figure (1.5) explains: a) The ribbon diagram depicted illustrates the structure of the immunoglobulin variable (Ig V) domain. The front sheets, colored green, consist of A'GFCC'C" strands, while the back sheets, colored aqua, are composed of ABED strands. The complementarity-determining region 3 (CDR3) loop has been appropriately designated. The four putative glycosylation sites are indicated in the color red.; b) The hydrophobic nature of the molecular surface. The hydrophobic residues are denoted by the color yellow, whereas the hydrophilic residues are

represented by the color red.; and c) The electrostatic molecular surface refers to the distribution of electric charges on the surface of a molecule. Red and blue colors are used to represent negative and positive potentials, respectively. The orientations of a), b) and c) are similar (Sam *et al.*, 2021).

The PD-1 gene is located in the chromosomal region 2q37.3, which has been identified as a susceptibility locus (SLEB2) for SLE. The genomic region under consideration encompasses a total of five exons, spanning a length of 9.6 kilobases (Lindblom *et al.*, 2022a), as depicted in Figure (1.6). The expression of PD-1 can be observed on thymocytes during and after the process of T-cell receptor (TCR) β -selection. This expression occurs throughout the transition from the CD4-CD8- stage to the CD4+CD8+ stage. Additionally, mature T- and B-cells exhibit PD-1 expression subsequent to activation. Furthermore, it is shown that activated myeloid lineage cells, such as macrophages, also exhibit this expression (Schwartz *et al.*, 2019).

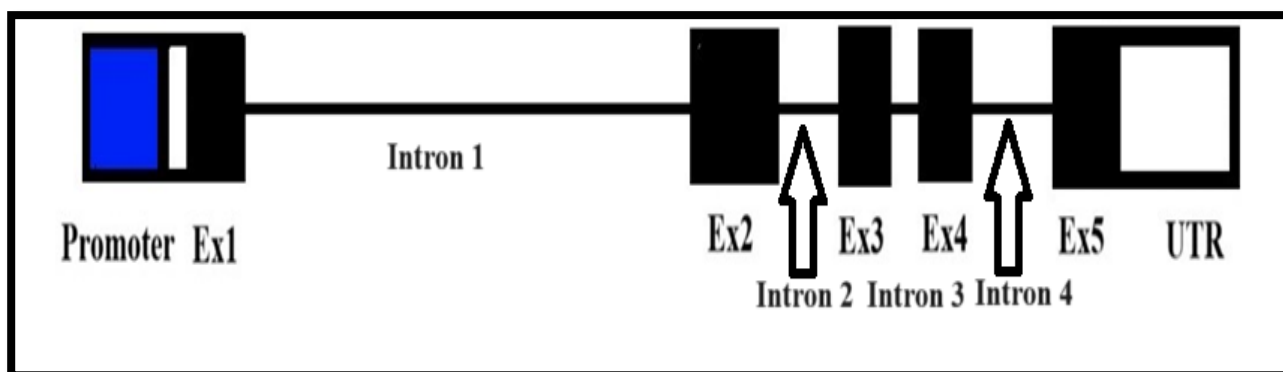


Figure (1.6): PD-1 gene map on chromosome 2q37.3 (Zhang *et al.*, 2021a).

Multiple single nucleotide polymorphisms (SNPs) have been detected within the PD-1 gene, specifically at positions -538, +6438, +7146, +7209, +7499, +7625, +7785, and +8738 (Kitagori *et al.*, 2019; Huang *et al.*, 2020).

1.4.2. Biological Activity of PD-1

As previously stated, PD-1 serves as an inhibitory receptor on T- and B-cells, playing a crucial role in the regulation of their stimulation and, consequently, the maintenance of peripheral tolerance (Ali *et al.*, 2021b). The interaction between the

PD-1 receptor and its ligands, PD-L1 and PD-L2, triggers the expression of PD-1 and then initiates a cascade of downstream molecules that generate an inhibitory signal against the activating of T- and B-cells (Al-Fartosy *et al.*, 2023). The attributes of PD-1 are succinctly outlined in Table (1.2), which will be further upon in the subsequent discussion.

Table (1.2): Characteristics of PD-1 (Aibara *et al.*, 2018; Ichinose *et al.*, 2018; Sun *et al.*, 2019; Galli *et al.*, 2019).

Property		Characteristic
Ligands		PD-L1 and PD-L2
Receptor Expression	T-cells	Rapidly upregulated after activation.
	B-cells	Upregulated after activation.
	Myeloid cells	Upregulated after activation.
Ligand expression in lymphoid tissues	Location	PD-L1 expressed on T-cells, B-cells, monocytes and DCs; PD-L2 expressed on DCs; PD-L1 and PD-L2 expressed on thymic epithelial cells; in the spleen and in lymph nodes.
	Kinetics and regulation of expression	PD-L1 and PD-L2 induced by activation of IFN- γ treatment of monocytes and DCs.
Ligands expression in non-lymphoid tissues	Location	PD-L1 and PD-L2 expressed on placenta and heart (PD-L1 on placental syncytiotrophoblasts at high levels and cardiac myocytes and endothelium). PDL1 also expressed on pancreas, lung, liver and foetal liver and expressed in a variety of tumor cell lines including breast and ovarian tumors.
	Kinetics and regulation of expression	PD-L1 induced on endothelial cells by IFN- α , - β and - γ .
Function	Proliferation and IL-2 production	Inhibits.
	Effector cytokine production	Inhibits.
	Cell cycle	Block G1 to S phase progression.
	Tolerance	Small role in central T-cell tolerance. Role in peripheral T- and B-cell tolerance. Late onset of phenotype (weeks to months after birth). Late lethality associated with glomerulonephritis.
	Defects in gene knockout mice	arthritis and cardiomyopathy Defects in the regulation of: T-cell proliferation (mild) B-cell & Myeloid-cell proliferation.

1.4.3. Ligands of PD-1

As demonstrated in Figure (1.7), the ligands associated with PD-1 include PD-L1 (also known as B7H1), and PD-L2 (also known as B7-DC). The aforementioned ligands belong to the B7 receptor family. The expression of PD-L1 is observed on splenic T-cells, B-cells, macrophages, and dendritic cells (DCs) in their newly separated state (Mike *et al.*, 2019). Following stimulation, there is an increase of PD-L1 on T-cells, macrophages, and DCs. Conversely, the production of PD-L2 is only observed on macrophages and DCs following activation with cytokines. The regulation of PD-L1 and PD-L2 expression is known to vary depending on the presence of T helper1 (Th1) and T helper 2 (Th2) cytokines (Lindblom *et al.*, 2022b). The expression of PD-L1 is significantly elevated on inflammatory macrophages and can be further enhanced through contact with lipopolysaccharide (LPS) and interferon-gamma (IFN- γ). In contrast, PD-L2 is not typically present on inflammatory macrophages but can be induced through alternate stimulation mediated by interleukin-4 (IL-4) (Klein *et al.*, 2019).

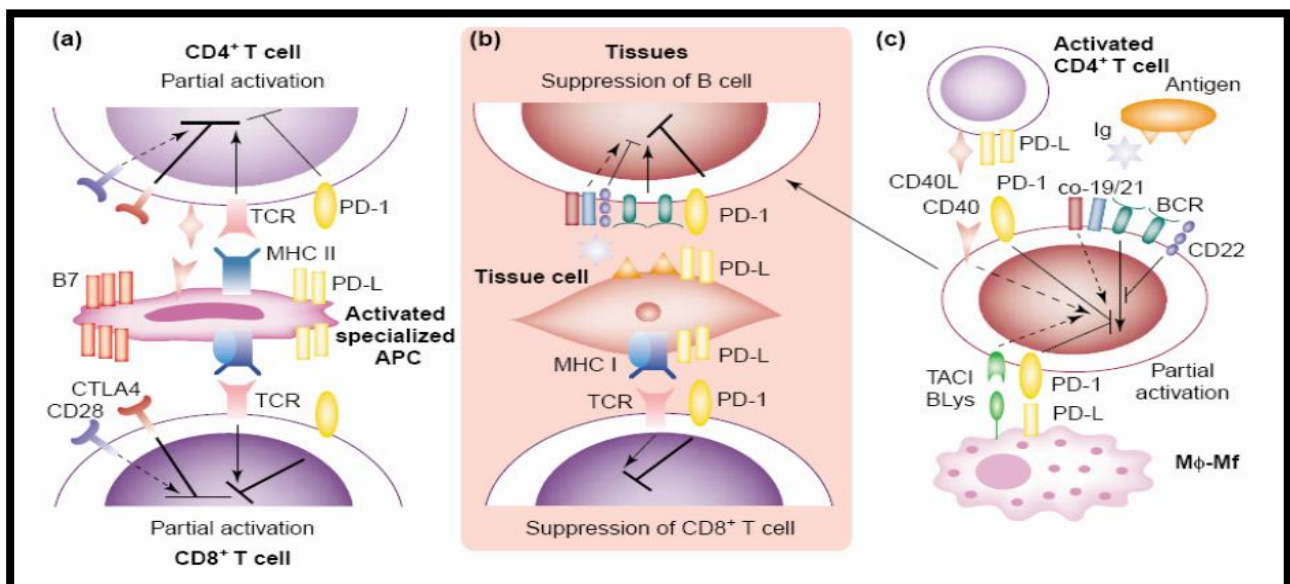


Figure (1.7): A theoretical framework for the potential modulation of peripheral tolerance through the interaction between PD-1 and its ligand (Davaranpanah *et al.*, 2020).

Figure (1.7) shows: a) Autoreactive CD4⁺ and autoreactive CD8⁺ T-cells have the potential to undergo inadequate activation when interacting with antigen presented cells (APCs) through various surface chemicals, as shown.; b) Certain autoreactive B-cells and autoreactive CD8⁺ T-cells have the ability to travel towards specific tissues. Once they reach these tissues, they can be controlled in a negative manner by parenchymal tissue cells through their association of PD-1 and PD-L. Activating signals are represented by black arrows, while probable activating signals are denoted by black dashed arrows. On the other hand, inhibitory signals are indicated by black bars.; and c) Autoreactive B-cells have the potential to undergo partial activation through their interaction with either activated autoreactive CD4⁺ T-cells or monocytes/macrophages (M ϕ -Mf). (Sharaf-Eldin et al., 2020).

1.4.4. PD-1 Signaling

The interaction of PD-L1 with PD-1 on T-cells inhibits the stimulation of human T-cells by anti-CD3. The production of PD-1 on active T-cells reaches its peak when there is a weak signal from the T-cell receptor (TCR), indicating that T-cells with weak activation are most susceptible to downregulation through interaction with PDL (Faris *et al.*, 2022b). Furthermore, the interaction between PD-1 and PD-L2 also hinders the development of T-cells and the creation of cytokines by CD4⁺ cells that are controlled by the TCR. When subjected to a small amount of antigens, the connection between PD-L2 and PD-1 hinders the transmission of robust B7-CD28 signals (Arpaci *et al.*, 2021). Conversely, this relationship decreases the generation of cytokines but does not affect the expansion of T-cells when exposed to an elevated level of antigens (Al-Fartosy *et al.*, 2020c).

Recent research studies have indicated that PD-L has the ability to enhance T-cell proliferation and promote the production of cytokines in a beneficial manner. The precise mechanism underlying this phenomenon remains ambiguous; however, it introduces the potential that PD-1 signaling may elicit both positive and negative signals (Engel *et al.*, 2021; Lu *et al.*, 2021a). Previous research has indicated that the

inhibitory function of PD-1 is initiated through the immune-receptor tyrosine-based switch motif (ITSM) rather than the immune-receptor tyrosine-based inhibitory motif (ITIM) (ITSM is a component ITIM) (Chauhan *et al.*, 2021). The inhibitory function of PD-1 relies on the interaction between Src homology 2-domain-containing tyrosine phosphatase 2 (SHP-2) and ITSM, as depicted in Figure (1.8). The precise mechanism underlying the ITSM in PD-1 remains uncertain (Noris-García *et al.*, 2018). However, the ITSM exhibited by CD150, an immune-receptor belonging to the CD150 receptor subfamily, has been characterized as capable of interacting with different downstream targets. This interaction can subsequently trigger either positive or negative signaling pathways in T- and B-cells (Ramirez *et al.*, 2018).

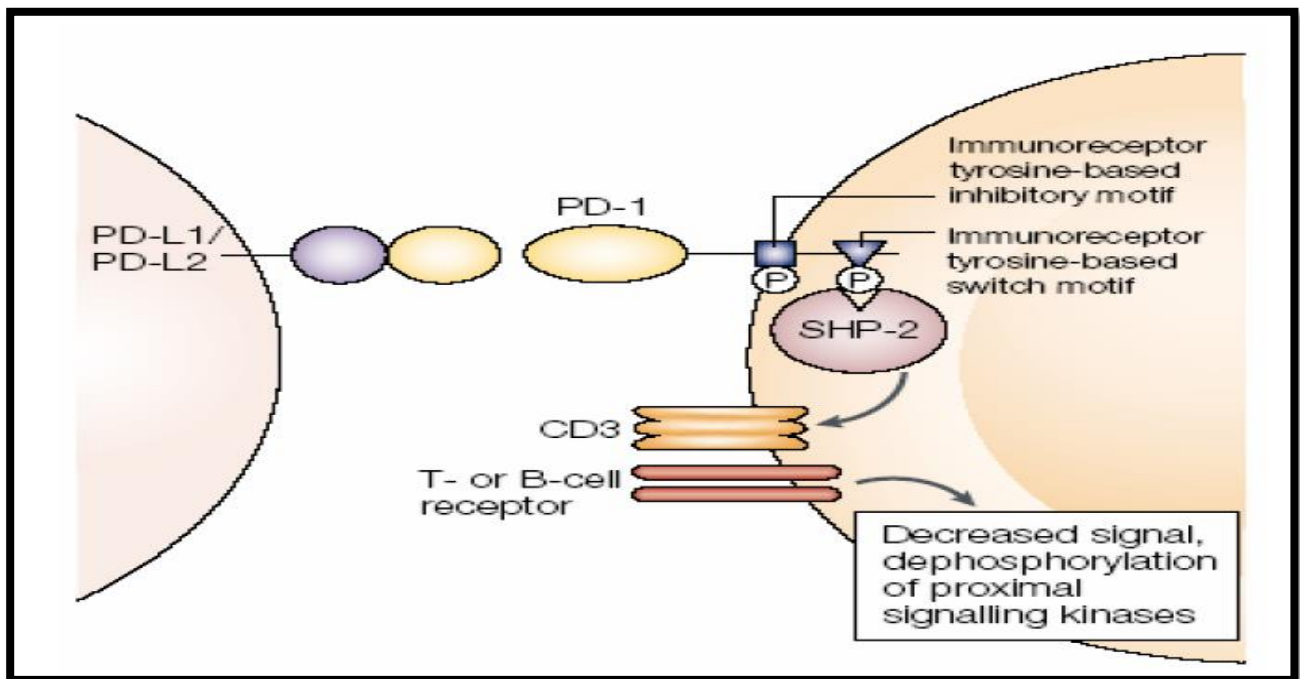


Figure (1.8): Induction of the tyrosine phosphorylation of the ITSM of PD-1 (Furie *et al.*, 2019).

As per Figure (1.8), the inhibitory signal mediated by PD-1:PD-L is abolished by mutation of the ITSM tyrosine residues, but not the ITIM tyrosine residues. The interaction between TCR and PD-1 can result in the phosphorylation of tyrosine residues and subsequent activation of SHP-2, leading to the dephosphorylation of signaling molecules and a decrease in the synthesis of cytokine mRNA. The

simultaneous binding of both PD-1 and the B-cells receptors (BCR) has the ability to impede the process of tyrosine phosphorylation in effector signaling molecules (Lu *et al.*, 2021b).

The interaction between SHP-2 and PD-1 results in the de-phosphorylation of downstream signaling molecules and subsequent activation of the Ras/Raf/MEK/Erk pathway. This stimulation can induce either G0/G1 cell cycle arrest or active growth, contingent upon the strength and period of the signal (Al-Fartosy and Ati, 2021). At low concentrations of antigen, both PD-1 ligands have the ability to cause cell cycle arrest. Nevertheless, when exposed to elevated concentrations of antigen, these ligands do not limit T-cell proliferation (Postal *et al.*, 2020).

1.5. Inflammation and Cytokines

Cytokines are a diverse set of tiny proteins that are synthesized by immune cells upon activation, as well as by stromal cells. These proteins play a crucial role in modulating the biological immune inflammatory response and are implicated in the etiology of systemic disorders in humans (Pan *et al.*, 2020). The term "lymphokines" was used to specifically refer to the cytokines produced by lymphocytes. The official designation of cytokines as interleukins (ILs) was established during the second International Lymphokine Conference held in Interlaken, Switzerland, in 1979 (Reid *et al.*, 2020). Subsequently, there has been a substantial increase in the quantity of ILs. By the conclusion of the 21st century, the collective assemblage of interleukins had expanded to encompass a total of 30 distinct entities (Hinterleitner *et al.*, 2021). Subsequently, this number continued to rise, resulting in the current designation of 40 identified ILs. It is evident that there exists a limited body of research pertaining to the biological implications of the recently identified ILs (Khanjari *et al.*, 2020).

Furthermore, it is worth noting that the most recent IL to have its entire structure elucidated was IL-40 in 2017. From a synthetic and symbolic perspective, one may hypothesize that the total number of ILs may be 40 (Shruthi *et al.*, 2021). Certain ILs have garnered significant attention from immunologists, whilst others

have gotten comparatively less scrutiny due to their perceived lesser significance in human biology (Coronel-Restrepo *et al.*, 2017).

ILs are a class of protein molecules categorized as cytokines, which are synthesized by many cells within the human body, including those of the immune system. They play a crucial role in multiple significant cellular processes, encompassing proliferation, maturation, migration, and adhesion (Al-Fartosy and Mohammed, 2017a). Additionally, they contribute to the activation and differentiation of cells within the immune system. Furthermore, previous research has demonstrated that ILs, which are a component of the cytokine network, exert an influence on several physiological processes within the human body. These processes encompass metabolic activity, as well as the cardiovascular and neuroendocrine systems, thereby facilitating the regulation of homeostasis (Mende *et al.*, 2018; Cappelli *et al.* 2017). Nevertheless, the intricate and extensive range of activities and impact exerted by these cells can potentially result in their excessive suppression and the subsequent onset of pathological conditions. This pertains to AIDs, diabetes, neoplastic and neurological problems, as well as kidney diseases (Aarslev *et al.*, 2017).

The clearance of several cytokines occurs mostly in the kidney, making it a crucial site for this process, as illustrated in Figure (1.9). In individuals with CKD, there is a significant disruption in the delicate balance between pro-inflammatory cytokines and their inhibitors (Fukasawa *et al.*, 2017). The dialysis technique enhances the activation of circulating nuclear cells, leading to an increased generation of cytokines, hence intensifying their response to the presence of endotoxins (Shi *et al.*, 2017). The altered immune response in uremia gives rise to a condition of continuous inflammation, which is widely observed in individuals with CKD and is associated with comorbidities including the occurrence of protein-energy wasting (PEW) and atherosclerotic vascular disease (Al-Fartosy and Mohammed, 2017b). The coexistence of inflammation, PEW, and atherosclerosis is frequently observed in

individuals with CKD. Notably, each of these risk variables has been found to independently predict outcomes in this patient population (Jiang *et al.*, 2021).

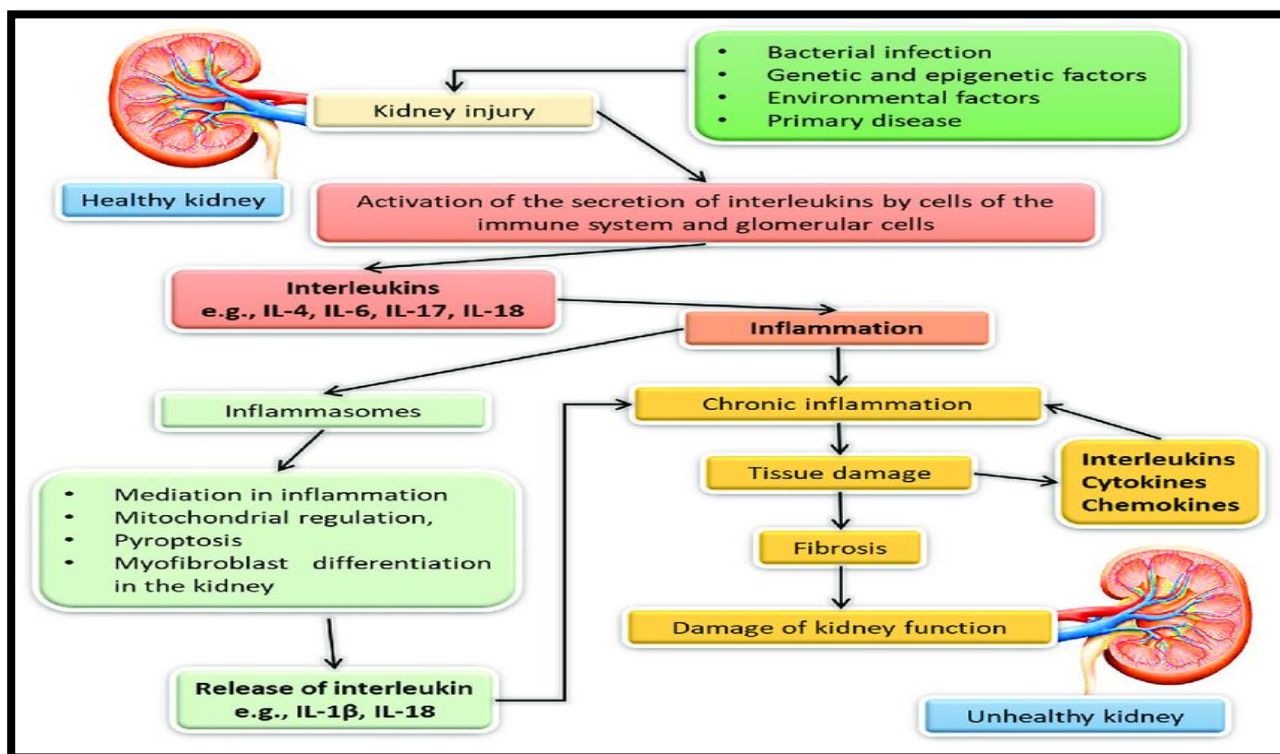


Figure (1.9): The influence of ILs on the advancement of chronic inflammation and consequent renal dysfunction (Kwon *et al.*, 2019).

Cytokines, which are soluble proteins characterized by a relatively small molecular weight, are synthesized in response to an antigen and other stimuli. They serve as chemical mediators, exerting regulatory control over diverse facets of both the innate and humoral immune systems (Lin *et al.*, 2018). Cytokines are synthesized by a wide range of cells that participate in both innate and humoral immune responses, with a particular emphasis on Th lymphocytes. CD4 Th cells can be categorized into two main categories. Th1 cells are responsible for the production of various pro-inflammatory cytokines, including IFN- γ , IL-12, and tumor necrosis factor- α (TNF- α). These cytokines play a crucial role in enhancing cellular immunity (Singla *et al.*, 2017). On the other hand, Th2 cells secrete a distinct group of cytokines, principally IL-4, IL-5, IL-10, and IL-6, which are involved in promoting humoral immunity. A T-regulatory cell, characterized by the presence of CD4+ and CD25 markers, has the

ability to secrete IL-10 and exert regulatory effects on both Th1 and Th2 immune responses (Bae and Lee, 2017).

Th1 cytokines have the ability to induce the production of nitric oxide (NO) and other inflammatory mediators. Additionally, they enhance the functional activity of T cytotoxic cells, natural killer (NK) cells, and activated macrophages (Al-Fartosy *et al.*, 2021). As a result, these cytokines collectively have a pro-inflammatory effect. In contrast, Th2 cytokines serve to impede the activation of macrophages, suppress T cell proliferation, and hinder the synthesis of pro-inflammatory cytokines, thus playing a role in promoting anti-inflammatory mechanisms (Nagafuchi *et al.*, 2019). The Th1 and Th2 immune responses exhibit reciprocal inhibition. Therefore, the activities of Th2 cells are inhibited by IL-12 and IFN- γ , whereas the activities of Th1 cells are inhibited by IL-4 and IL-10, as demonstrated in Figure (1.10). The relative proportion of pro- and anti-inflammatory cytokines, rather than their total quantity, may play a critical role in the advancement of the atherosclerotic plaque (Deng and Tsao, 2017). In order to gain a comprehensive understanding of the cytokine dysregulation observed in patients with SLE, it is necessary to take into account numerous factors. These factors include the dynamic nature of cytokines, which are subject to constant changes, as well as their regulation by inhibitors or other cytokines that exert opposing effects (Tarr *et al.*, 2017; Islam *et al.*, 2020). Cytokines seldom function in isolation since they induce a diverse array of cell types to generate and release other cytokines in a sequential manner. The increase in the level of a single cytokine promptly triggers the upregulation or downregulation of multiple other cytokines. The detection of paracrine effects of cytokines might be challenging due to their predominantly local rather than systemic nature (Teh *et al.*, 2019).

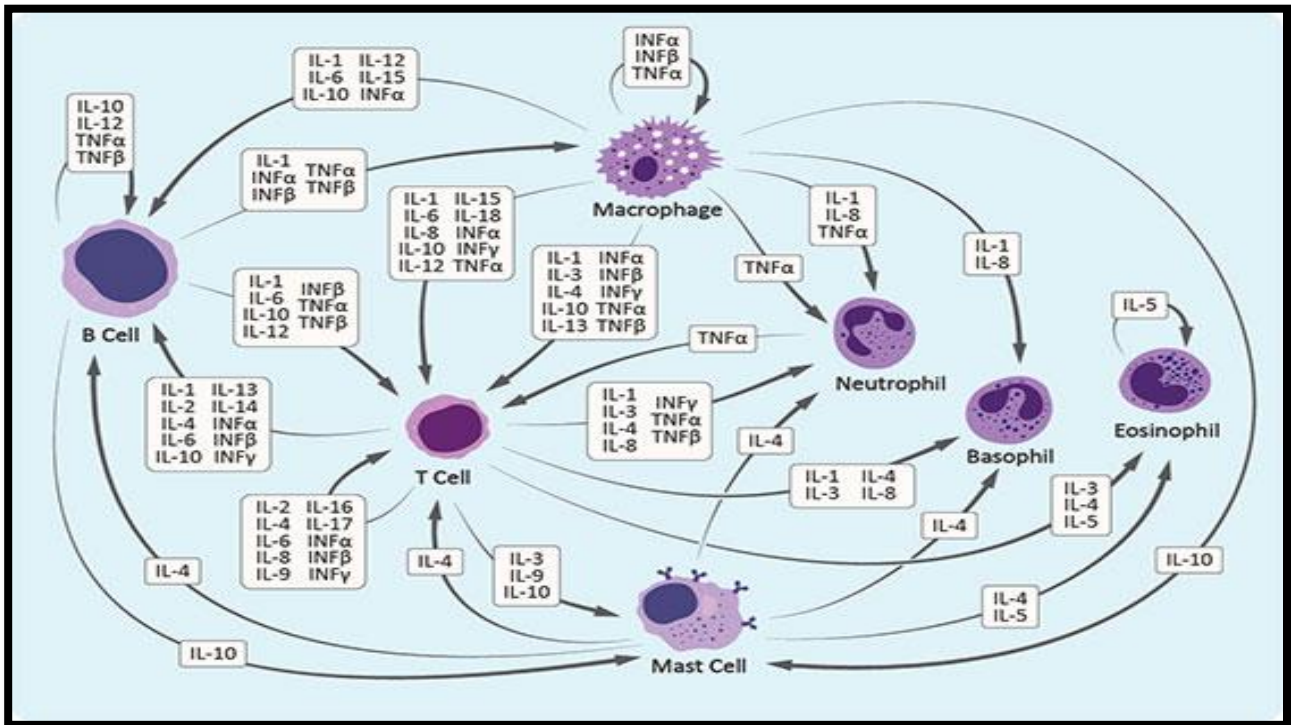


Figure (1.10): Cytokine network (Takeshima *et al.*, 2019).

Extensive research has been conducted on the cytokine profiles observed in patients with SLE. The profiles have been succinctly summarized and are presented in Table (1.3).

Table (1.3): Cytokine profiles in SLE patients (Lambring *et al.*, 2019; van der Meulen *et al.*, 2019; Zhang *et al.*, 2020; Belmokhtar *et al.*, 2022)

Cytokine	Profiles
IL-2	<ul style="list-style-type: none"> ↑ IL-2 expression in PBMCs. ↑ IL-2 mRNA expression in lymphocytes. ↑ Serum sIL-2 receptor expression. ↓ IL-2 production to antigenic and mitogenic stimulation in T-cells.
IL-6	<ul style="list-style-type: none"> ↑ IL-6 mRNA expression in PBMCs. ↑ IL-6 production in stimulated whole blood culture. ↑ Serum IL-6 concentration.
IL-10	<ul style="list-style-type: none"> ↑ Spontaneous IL-10 production in PBMCs. ↑ Ratio of IL-10: IFN-γ secreting cells in PBMCs. ↑ IL-10 mRNA expression in PBMCs. ↑ IL-10 concentration and correlates with disease activity.
IL-12	<ul style="list-style-type: none"> Impaired production of IL-12 by stimulated PBMCs. IL-12 supplementation inhibits Ig and anti-DNA antibody production by PBMCs. IL-12 inhibits the action of IL-10 on PBMCs.
Other Cytokines	<ul style="list-style-type: none"> ↑ Serum IL-5, IL-16 and IL-18 concentration. ↑IFN-γ mRNA expression in PBMCs. ↑ Serum IFN-γ concentration. ↑IFN-α mRNA expression in PBMCs. ↑ Serum IFN-α concentration.

The expression of IL-2 is reduced in T-cells that have been stimulated in individuals with SLE compared to those in controls (Chen *et al.*, 2018b). Furthermore, these SLE T-cells exhibit diminished responsiveness to IL-2 stimulation when compared to T-cells from individuals without SLE. Nevertheless, the levels of IL-2

expression in newly isolated peripheral blood mononuclear cells (PBMCs) from individuals with SLE are shown to be higher in comparison to those from healthy controls (He *et al.*, 2020). It has been observed that T-cells in SLE patients are able to generate a normal quantity of IL-2 when optimally stimulated with phytohemagglutinin (PHA) in combination with phorbol esters or anti-CD28 antibodies (Moon *et al.*, 2020).

1.5.1. Classification of Cytokines

The classification of ILs can be based on their impact on the inflammatory state. ILs can be categorized as pro-inflammatory, anti-inflammatory ILs, and those with mixed inflammatory effects, as depicted in Figure (1.11).

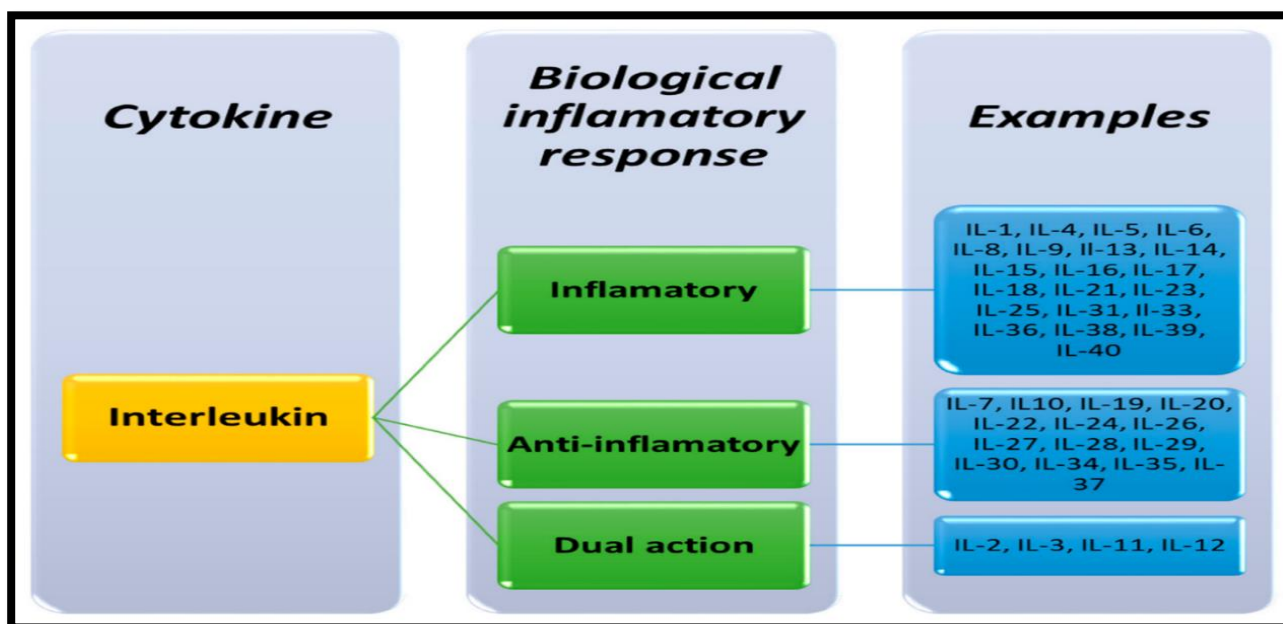


Figure (1.11): The categorization of ILs according to their impact on biological inflammatory response (Silverman, 2019).

1.5.2. Pro-Inflammatory Cytokines

1.5.2.1. Interleukin-18 (IL-18)

Interleukin-18 (IL-18) is a multifunctional signaling molecule that is synthesized by several cell types, such as macrophages, hematopoietic cells, and endothelial cells. The molecule in question plays a role in the modulation of both innate and acquired immune responses, as well as IL-12, but with varying outcomes (Fujita, 2017). In addition to IL-12 and IL-15, IL-18 is a highly effective stimulator of IFN- γ synthesis by both NK cells and Th1 lymphocytes. Consequently, IL-18 is likely to have a role in the development of AIDs. Indeed, AIDs frequently exhibit a simultaneous elevation in the quantities of both IL-18 and IFN- γ in the bloodstream (Al-Fartosy *et al.*, 2020b). In contrast, allergic diseases are commonly distinguished by elevated levels of IL-18 in conjunction with diminished levels of IFN- γ . Additionally, IL-18 has been observed to exert an angiogenic effect. Additionally, it has been demonstrated that IL-18 possesses the ability to enhance hunger and contribute to the pathogenesis of obesity (Dini *et al.*, 2017).

The available body of research has provided clarification that IL-18 may possess a significant association with the symptoms of SLE and may contribute to its fundamental mechanisms (Diaz-Rizo *et al.*, 2017). In the MRL/lpr mice model, the introduction of foreign IL-18 resulted in an exacerbation of disease extent, while the administration of anti-IL-18 had a mitigating effect on lupus in the mice (Islam *et al.*, 2019). Figure (1.12) illustrates the biological functions of IL-18.

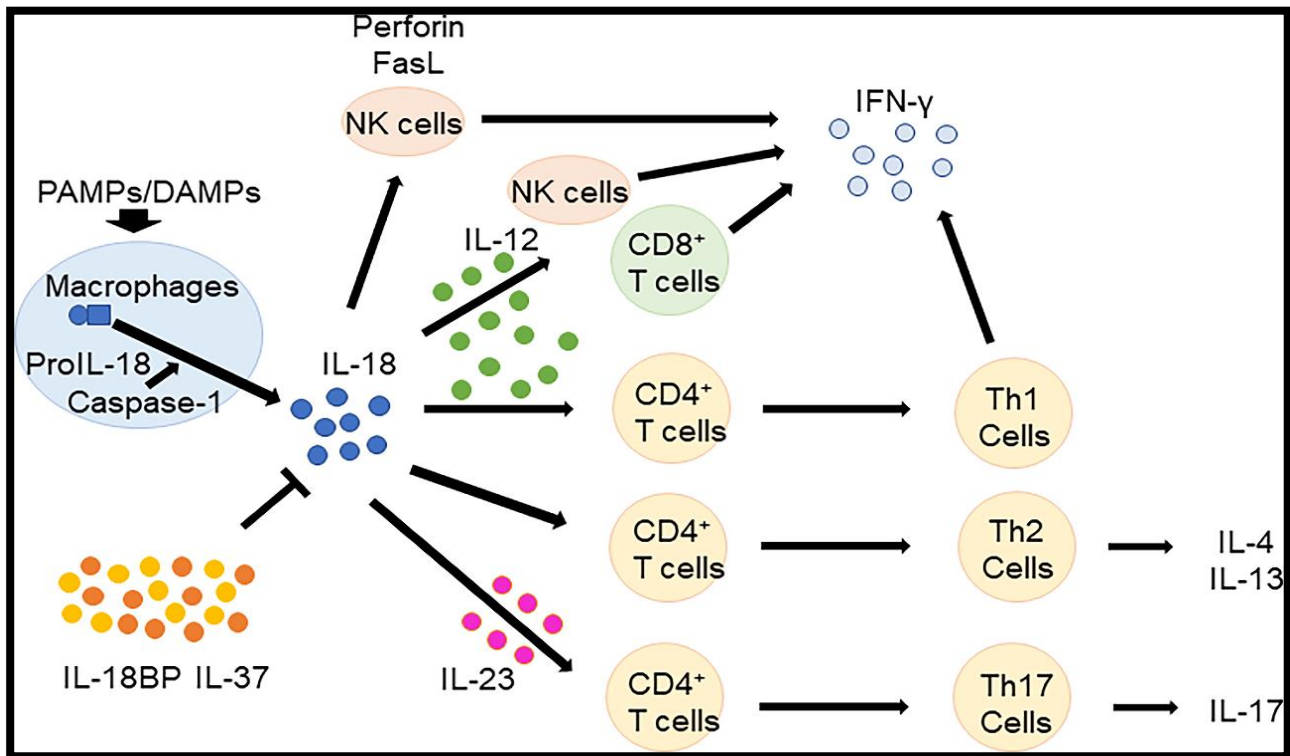


Figure (1.12): IL-18 biological functions (Bellan *et al.*, 2020).

1.5.3. Anti-Inflammatory Cytokines

1.5.3.1. Interleukin-37 (IL-37)

Interleukin-37 (IL-37) is a recently identified constituent of the IL-1 family. There have been reports on the existence of five different splice variants of IL-37, which are referred to as IL-37a, IL-37b, IL-37c, IL-37d, and IL-37e. The longest splice variation of the gene encoding IL-37 is IL-37b, which consists of five out of the six exons (Yin *et al.*, 2020). The isoform NM014439 has recently been officially recognized as IL-37. The elucidation of the mechanism of action and biological activities of IL-37 is now in its early stages. IL-37 has amino acid sequences that are similar to those found in IL-18 (Dall'Ara *et al.*, 2018). Additionally, IL-37 has the capability to interact with both IL-18 receptors and IL-18 binding protein (IL-18BP). Despite its low affinity for the IL-18 Ra chain, IL-37 has the ability to form a trimeric complex through sequential binding to IL-18BP and subsequently to IL-18 RB

(Fanouriakis *et al.*, 2019). The trimeric complex potentially hinders the involvement of IL-18 RB in IL-18 signal transduction, serving as an inhibitory mechanism. However, a recent study has proposed that IL-37 might also attenuate innate immunity by means of an intracellular process that necessitates NLRP3 and inflammasomes (Hanna Kazazian *et al.*, 2019).

IL-37 is a significant cytokine belonging to the IL-1 family. It shares structural resemblances with IL-18, but interestingly exhibits an anti-inflammatory function. Experimental evidence has demonstrated that IL-37 effectively inhibits the release of key pro-inflammatory cytokines such as TNF- α , IL-6, and IL-1 β , as well as various chemokines (Ahmad *et al.*, 2022). IL-37 holds significant importance as a cytokine involved in maintaining immune homeostasis and functioning as an immune regulator as demonstrated in Figure (1.13). It exhibits potential therapeutic advantages in cancer immunotherapy by inhibiting the immunosuppressive effects of IL-6, IL-1 β , and TNF- α (Ali *et al.*, 2021a). Additionally, IL-37 shows promise in mitigating autoimmune pathologies by counteracting tissue damage induced by inflammatory cytokines (Beberashvili *et al.*, 2023).

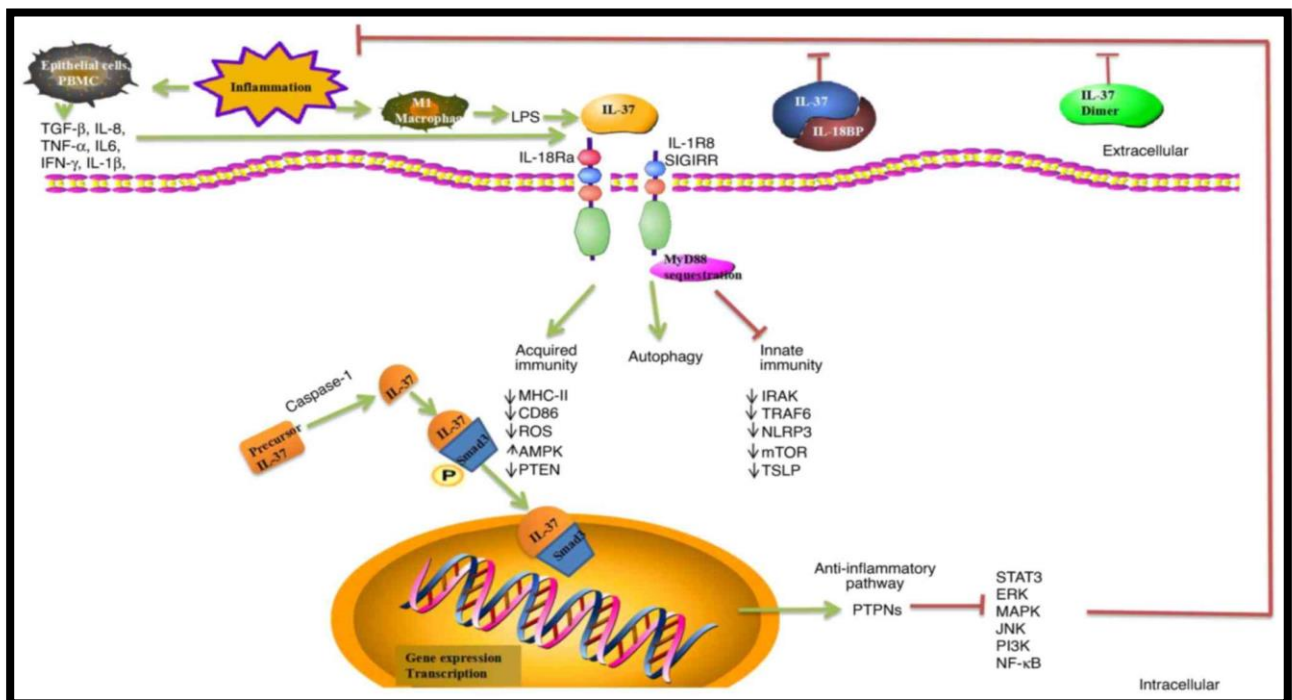
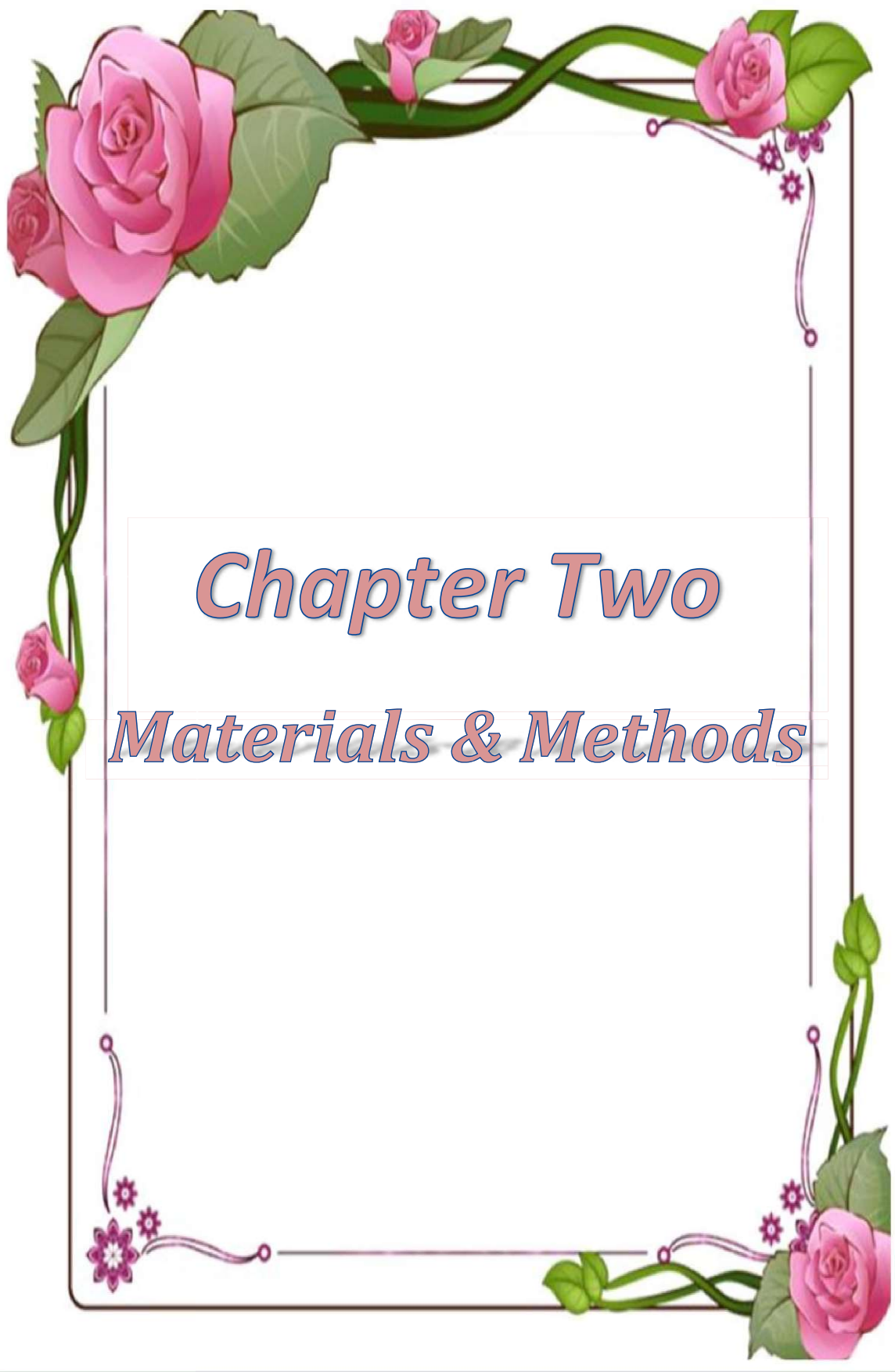


Figure (1.13): IL-37 immunity regulation role (Brookes and Power, 2022).

1.6. The Aims of the Study

Systemic Lupus Erythematosus (SLE) is considered one of the most serious forms of autoimmune disorders (AIDs). Despite the significant advancements in the field of healthcare, the mortality rate among SLE patients remains at an unsatisfactory level. Elevated levels of pro-inflammatory cytokines have been linked to heightened mortality rates among SLE patients on a global scale. Nevertheless, there has been a lack of research conducted in the Province of Basrah - Iraq, regarding the examination of inflammation biomarkers and their impact on SLE patients. Therefore, this study endeavors to investigate the following objectives:

- 1- To study the effect of SLE on the level of some serum parameters (C3, C4, CH50, MDA, TAC, ANA, Anti-dsDNA, urea, creatinine, GFR, and PD-1), and some cytokines (such as IL-18, IL-37) for SLE patients compared with a healthy control.
- 2- To investigate the effect of SLE on the level of oxidant/antioxidant status for SLE patients in comparison to healthy controls.
- 3- To verify the genetic association between gene PD-1 (SNPs: +7499 G/A and +7209 C/T) in SLE patients in comparison to healthy controls.
- 4- To elucidate the genetic role of PD-1 polymorphisms as a predisposing factor for progression level. The distribution of each genotype in SLE patients and control subjects was compared after the polymorphism of the PD-1 gene was identified.
- 5- To evaluate the associations between PD-1 polymorphism and serum levels in identifying the functional polymorphism that may influence PD-1 levels.
- 6- To analyze the correlation between PD-1 level and biochemical parameters in the current study and its association with SLE patients.
- 7- To study the receiver operating characteristic (ROC) between biochemical parameters in the current study and its association with SLE patients and control.
- 8- To assess the clinical features, disease severity, and manifestations of SLE patients.
- 9- To provide recommendations for improving the diagnosis, treatment, and support of SLE patients.



Chapter Two

Materials & Methods

Chapter Two

2.1. Chemicals and Instruments

The chemicals, kits and instruments used in this work listed in Tables (2.1), (2.2) and (2.3).

Table (2.1): Chemical compounds with their manufacturer and origins

Chemicals	Manufacturer / Origin
Absolute Ethanol	Fluka / Switzerland
Agarose	Conda / USA
Deionize Sterile Distilled Water	Bioneer / South Korea
Distilled Water	Naturel / Turkey
Ethidium bromide	Intron / Korea
Ladder 100bp	Kapa / USA
Loading dye (6X)	Intron / Korea
Primers of PD-1 gene	Integrated DNA technologies / USA
Red safe staining solution	Intron / Korea
Sodium chloride (NaCl)	Fluka / Switzerland
Sodium hydroxide (NaOH)	Fluka / Switzerland
Sodium phosphate acidic	Fluka / Switzerland
Sodium phosphate basic	Fluka / Switzerland
Thiobarabituric acid (TBA)	BDH / England
Trichloro acetic acid (TCA)	BDH / England
TBE buffer (10X)	Conda / USA

Table (2.2): Diagnostic kits with their catalogue No., manufactures and origins.

Biomarkers	Catalogue No.	Manufacture/Origin
ANA kit	LS-F67388	LS Bio / USA
Anti-dsDNA kit	MBS269122	MyBioSource / USA
C3 kit	3170005	Linear / Spain
C4 kit	3171005	Linear / Spain
CH50 kit	AMS.E01C0237	AMSBIO / UK
Creatinine kit	1123010	Linear / Spain
CRP kit	BPE193	BT-Lab / China
Genomic DNA extraction kit	17045	Intron / Korea
IL-18 kit	E0147Hu	BT-Lab / China
IL-37 kit	E1947Hu	BT-Lab / China
MDA kit	DTBA-100	Bioassay Systems / USA
PD-1 kit	E3331Hu	BT-Lab / China
Pre-mix PCR kit	25025	Intron / Korea
TAC kit	STA-360	Cell Biolabs / USA
Urea kit	1156015	Linear / Spain

Table (2.3): Instruments with their manufactures and origins.

Instrument	Manufacturer / Origin
AURA TM PCR Cabinet	Biosan / Italy
Centrifuge	Heraeus – Christ / Germany
Combi-spin	Biosan / Lativa
Deep freezer	Nikai / Japan

Document system	Labnet / USA
EDTA Tubes	Compoblast / UAE
Electrophoreses	CBS Scientific / USA
ELISA Reader	Human / Germany
ELISA Washer	FLX-50 / USA
Incubator	Memmert / Germany
Micropipette (100-1000) μL	Gilson / France
Micropipette (10-100) μL	Gilson / France
Microplate reader	Biotech / USA
Microspin	Biosan / Lativa
Microspin 12, High-speed Mini-centrifuge	Biosan / Lativa
Microwave	Memmert / Germany
Multi Gene OptiMax Gradient Thermal Cycler	Labnet / USA
Nanodrop	Quawell / Hong kong
Power Supply	Labnet / USA
Sensitive balance	Jrad / Germany
Stop Watch	Fisher Scientific / USA
UV transmission	Vilber Lourmat / France
UV-Vis Spectrophotometer (Double Beam)	V - 1200 / UV- EMC - LAB / Germany
V-1 plus Vortex (for tubes)	Digsystem / Germany
Vortex	Digsystem / Germany
Water bath	Memmert / Germany

2.2. Place of Work

This study was conducted in Department of Chemistry - College of Science - University of Basrah, Department of Basic Sciences - College of Nursing - University of Basrah, and Al-Mawany, Al-Sadr, Al-Fayhaa, and Al-Basrah teaching hospitals in the Province of Basrah – Iraq.

2.3. Study Design

This section provides a comprehensive discussion of the study design, encompassing various aspects such as the selection of subjects, target population, collection of samples, the criteria used for inclusion and exclusion of cases and controls, with the studied parameters: body mass index (BMI), complement component 3 (C3), complement component 4 (C4), complement hemolytic 50 (CH50), malondialdehyde (MDA), total antioxidant capacity (TAC), C-reactive protein (CRP), antinuclear antibodies (ANA), anti-double strand DNA (Anti-dsDNA), urea, creatinine, glomerular filtration rate (GFR), interleulin-18 (IL-18), interleukin -37 (IL-37), and programmed cell death 1 (PD-1).

2.3.1. Subjects

The current investigation is a case-control clinical trial. The study involved the collection of samples from four teaching hospitals located in the Basrah Province, Iraq. These hospitals are Al-Mawany, Al-Sadr, Al-Fayhaa, and Al-Basrah. The sampling period spanned from September 2022 to October 2023. Forty-three female volunteers who diagnosed with SLE were chosen as participants for this study, ranging in age from 27 to 45 years old. A comparison was conducted between these subjects and an apparently healthy control group of 53 women. The clinicians utilized the ACR 1997 criteria, as recommended by the American College of Rheumatology, to diagnose individuals with SLE (Hu *et al.*, 2022). The duration of SLE was defined as the period starting from the patient's initial diagnosis of SLE. All of the volunteers hailed from Basrah Province. Prior to participating in the study, all subjects were provided with an informed written agreement. All enrolled patients provided consent for participation in

the trial. Demographic data were obtained through a structured questionnaire conducted during the visit. The age, duration of SLE, health behaviors (smoking, alcohol use, and exercise), medical history, and current medications are defined using a standard self-administered questionnaire paper (Lee *et al.*, 2019), as shown in Table (2.4).

Table (2.4): Questionnaire paper form used in this study.

No.		Mobile	
Patient's name		Age	
Sex	Man	Height	
	Woman	Weight	
Full Address			
Age at SLE Diagnosis			
Duration of SLE			
Smoking Habits	Yes		Drinking
	No		Alcohol
Food Habits	Vegetarian		Demographic
	Non-Vegetarian		Area
Educational Status	Learned		Employment
	Illiterate		Status
Medicines	Regular		
	Irregular		
Any other remarks			

2.3.1.1. Inclusion Criteria

The patients with SLE, who were chosen for inclusion in their respective groups, were diagnosed by doctors according to the guidelines outlined in the ACR 1997 criteria. The control group consisted of persons who were in good health and did not have SLE, a family history of SLE, acute or chronic AIDs, or were taking any medications known to affect immunity. Each of the volunteers experienced a consistent

and unchanging clinical progression for a minimum duration of three months (Kwon *et al.*, 2019; Kubick *et al.*, 2021).

2.3.1.2. Exclusion Criteria

Individuals who were excluded from the study included those who had concomitant blood-borne contagious infectious diseases such as hepatitis A, B, or C, or HIV, as well as those with cirrhosis, end-stage renal disease, pregnancy, other connective tissue diseases, bacterial infection, diabetes mellitus, uncontrolled hypertension, overlap syndrome, malignant tumors, chronic infections, drug-induced lupus, smoking, alcohol consumption, rheumatic diseases, genetic syndromes, receiving any steroid or immunosuppressant treatments, and liver disease. These exclusions were made because the physiology of complement is altered and not well understood in these specific cohorts (Shahrokhi *et al.*, 2017; Gergianaki *et al.*, 2018; Qi *et al.*, 2018; Aringer *et al.*, 2019).

2.3.2. Sample Size Calculation

The appropriate number of samples was established through a calculation of the proportion of the population, taking into account the following assumptions: a prevalence of SLE of 1.81%, a confidence level of 95%, and a margin of error of 4% (representing absolute precision) (Shruthi *et al.*, 2021):

$$n = [(Z_{\alpha/2})^2 \times P (1-P) / d^2] = [(1.96)^2 \times 0.0181 (1-0.0181) / (0.04)^2] = 43$$

Let n represent the required sample size, P denote the prevalence rate of SLE at 1.81%, $Z_{\alpha/2}$ represent the standardized normal distribution value at the 95% confidence interval (1.96), and d represent the margin of error at 4% (Mohammed *et al.*, 2023).

2.3.3. Samples

The blood samples were obtained during the early hours, specifically between 09:00 and 10:00 am, following a period of 30 minutes of rest in the supine posture. A total of 10 mL of fresh venous blood was obtained from both patients and healthy volunteers using a vein punch technique. The collected blood was then divided into two portions. The first portion, consisting of 3 mL, was transferred into polypropylene tubes

containing EDTA. The tubes were gently shaken to facilitate the detection of the (PD-1) gene. DNA extraction from peripheral blood leukocytes was performed using a Genomic DNA Purification Kit (AL-hameedawi and Al-Shawi, 2023). The second portion, consisting of 7 mL, was transferred to a standard tube that lacked any anticoagulant. This allowed for the natural process of clotting to occur for a duration of 20 minutes at ambient room temperature. Following the coagulation of the blood, it was subjected to centrifugation with a force of 402 times the acceleration due to gravity (402 x g) for a duration of 20 minutes, resulting in the separation of the serum. The blood that was obtained was promptly employed for the measurement of variables in this investigation, while the remaining serum was maintained at a temperature of -80°C till it was utilized (Yuan *et al.*, 2020).

2.4. Methods

2.4.1. Body Mass Index (BMI)

The calculation of body mass index (BMI) involved dividing the weight in kilograms by the square of the height in meters, as per the given formula:

$$\text{BMI (kg/m}^2\text{)} = \text{Weight (Kg)} / \text{Height (m}^2\text{)}$$

The measurement of height and weight was conducted using a stadiometer and balance-beam scale that were periodically calibrated. Participants were instructed to wear light clothing and remove their shoes throughout the measurement process (Al-Fartosy *et al.*, 2020a).

2.4.2. Systemic Lupus Erythematosus Disease Activity Index – 2000 (SLEDAI-2K)

Principle:

The Systemic Lupus Erythematosus Disease Activity Index (SLEDAI) is a comprehensive measure that was originally created and introduced in 1985 as a clinical tool for evaluating the overall activity of the disease (Rees *et al.*, 2017). The physicians developed a revised version of SLEDAI, known as SLEDAI-2000 (SLEDAI-2K),

which enables the assessment of persistent disease activity in several aspects such as skin rash, alopecia, mucosal ulcers, and proteinuria, as illustrated in Table (2.5). This updated version was validated against the original SLEDAI (Fike *et al.*, 2019). The SLEDAI and SLEDAI-2K are tools used to assess disease activity in SLE. These indices document the presence or absence of specific descriptors of disease activity throughout a 30-day period. While SLEDAI-2K has been utilized for the purpose of determining the reduction in disease activity, it is crucial to emphasize that SLEDAI-2K specifically measures improvement in the descriptors that fully resolve (Chen *et al.*, 2020a).

Table (2.5): SLEDAI-2K variables and points (Gao *et al.*, 2017a; Yang *et al.*, 2020; Samuels *et al.*, 2022; Schell *et al.*, 2022).

No.	Variable	Status	Points
1	Recent onset seizure	No	0
		Yes	8
2	Psychosis: Altered ability to function in normal activity due to severe disturbance in the perception of reality (include hallucinations, incoherence, marked loose associations, impoverished thought content, marked illogical thinking, and bizarre, disorganized, or catatonic behavior); exclude uremia and drug causes.	No	0
		Yes	8
3	Organic brain syndrome: Altered mental function with impaired orientation, memory, or other intellectual function (with rapid onset and fluctuating clinical features), inability to sustain attention to environment, and ≥ 2 of the following: perceptual disturbance, incoherent speech, insomnia or daytime drowsiness, and increased or decreased psychomotor activity; exclude metabolic, infectious, or drug causes	No	0
		Yes	8
4	Visual disturbance: Retinal changes of SLE (include cytoid bodies, retinal hemorrhages, serous exudates or hemorrhages in	No	0
		Yes	8

	choroid, and optic neuritis); exclude hypertensive, infectious, or drug causes		
5	New onset sensory or motor neuropathy involving cranial nerves	No	0
		Yes	8
6	Lupus headache: Severe, persistent headache (may be migrainous but must be nonresponsive to narcotic analgesia)	No	0
		Yes	8
7	New onset stroke: Exclude arteriosclerosis	No	0
		Yes	8
8	Vasculitis: Ulceration, gangrene, tender finger nodules, periungual infarction, splinter hemorrhages or biopsy, and angiogram proof of vasculitis	No	0
		Yes	8
9	Arthritis: ≥ 2 joints with pain and signs of inflammation (i.e., tenderness, swelling, or effusion)	No	0
		Yes	4
10	Myositis: Proximal muscle aching/weakness associated with elevated CPK/aldolase, EMG changes, or a biopsy showing myositis	No	0
		Yes	4
11	Heme-granular or RBC urinary casts	No	0
		Yes	4
12	Hematuria: >5 RBC/high-power field; exclude stone, infection, or other cause	No	0
		Yes	4
13	Proteinuria: >0.5 g/24 hours	No	0
		Yes	4
14	Pyuria: >5 WBC/high-power field; exclude infection	No	0
		Yes	4
15	Inflammatory-type rash	No	0
		Yes	2

16	Alopecia	No	0
		Yes	2
17	Oral or nasal mucosal ulcers	No	0
		Yes	2
18	Pleuritic chest pain with pleural rub/effusion or pleural thickening	No	0
		Yes	2
19	Pericarditis: Pericardial pain with ≥ 1 of the following: rub, effusion, or EKG/echocardiogram confirmation	No	0
		Yes	2
20	Low complement: CH50, C3, or C4 decreased below lower limit of normal for lab	No	0
		Yes	2
21	High DNA binding: Increased above normal range for lab	No	0
		Yes	2
22	Temp $>100.4^{\circ}\text{F}$ (38°C): Exclude infectious causes	No	0
		Yes	1
23	Platelets $<100 \times 10^9/\text{L}$: Exclude drug causes	No	0
		Yes	1
24	WBC $<3 \times 10^9/\text{L}$: Exclude drug causes	No	0
		Yes	1
Total Points of SLEDAI-2K			X

2.4.3. Biochemical Estimation

In order to assess the concentrations of biochemical parameters in the blood of individuals diagnosed with SLE and those who are considered apparently healthy control subjects, a series of biochemical analyses were conducted using established protocols, as follows:

2.4.3.1. Immunological Parameters

2.4.3.1.1. Levels of Complement Component 3 (C3)

Principle:

The complement component 3 (C3) test is a turbidimetric quantitative method used to determine the concentration of the C3 in human serum or plasma. Insoluble complexes are formed when samples containing C3 are combined with anti-human C3 antibodies. The degree of light scattering exhibited by the immunocomplexes is contingent upon the concentration of C3 present in the patient sample. This can be measured by comparing it to a calibrator with a known C3 concentration (Narani, 2019).

Reagents:

- 1- R1a Vial: C3 at. (Goat antibodies anti-human C3, tris buffer 20 mmol/L, pH 8.2. Sodium azide 0.95 g/L.).
- 2- Plasma Protein Multicalibrator: Protein Calibrator.

Reagent Preparation:

Ready to use.

Calibration Curve:

Plasma Protein Calibrator was diluted in NaCl 9 g/L as shown in Table (2.6):

Table (2.6): Plasma protein calibrator dilution for C3 estimation

Dilution	1	2	3	4	5	6
Calibrator	-	10 µL	25 µL	50 µL	75 µL	100 µL
NaCl 9 g/L	100 µL	90 µL	75 µL	50 µL	25 µL	-
Factor	0	0.1	0.25	0.5	0.75	1

The concentration of C3 in each dilution was determined by multiplying the concentration of the C3 Protein Calibrator by the relevant factor.

Procedures:

- 1- The reagent, samples, calibrator, and distilled water were pre-warmed to 37°C.
- 2- Three sets of tubes were prepared as shown in Table (2.7):

Table (2.7): Sets of tubes with their solutions and additives in C3 estimation

Solution/Tube	Sample	Calibrator	Blank
Sample	10 μ L	-	-
Calibrator	-	10 μ L	-
Distilled Water	-	-	10 μ L
Reagent (R1)	1 mL	1 mL	1 mL

- 3- All tubes were mixed well by vortex.
- 4- The absorbance (A) of the serum samples and calibrator were measured after 2 minutes of the sample or calibrator addition against the blank at wave length 340nm by using cuvette of 1 cm light path of Spectrophotometer.

Calculations:

The different absorbance values (A) against the C3 concentration of each calibrator dilution was plotted. C3 concentration in the sample was calculated by interpolation of its (A) value in the calibration curve as shown in Figure (2.1).

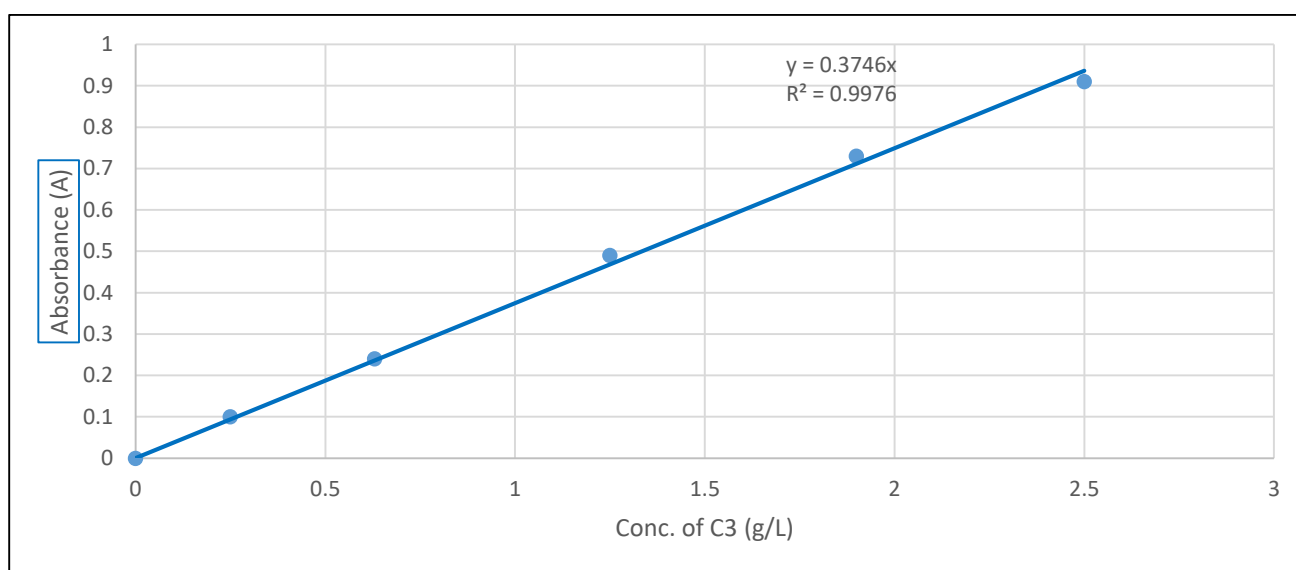


Figure (2.1): Standard curve of C3

2.4.3.1.2. Levels of Complement Component 4 (C4)

Principle:

The complement component 4 (C4) test is a quantitative turbidimetric method used to determine the concentration of the C4 in human serum or plasma. Insoluble complexes are observed when samples containing C4 are combined with anti-human C4 antibodies. The quantification of the scattering light of immunocomplexes is contingent upon the concentration of C4 in the patient sample. This can be accomplished by comparing it to a calibrator with a known C4 content (Fava and Petri, 2019).

Reagents:

1- R1a Vial: C4 at. (Goat antibodies anti-human C4, tris buffer 20 mmol/L, pH 8.2. Sodium azide 0.95 g/L).

2- Plasma Protein Multicalibrator: Protein Calibrator.

Reagent Preparation:

Ready to use.

Calibration Curve:

Plasma Protein Calibrator was diluted in NaCl 9 g/L as shown in Table (2.8):

Table (2.8): Plasma protein calibrator dilution for C4 estimation

Dilution	1	2	3	4	5	6
Calibrator	-	10 µL	25 µL	50 µL	75 µL	100 µL
NaCl 9 g/L	100 µL	90 µL	75 µL	50 µL	25 µL	-
Factor	0	0.1	0.25	0.5	0.75	1

The C4 concentration of each dilution was obtained by multiplying the concentration of the C4 Protein Calibrator by the corresponding factor.

Procedures:

- 1- The reagent, samples, calibrator, and distilled water were pre-warmed to 37°C.
- 2- Three sets of tubes were prepared as shown in Table (2.9):

Table (2.9): Sets of tubes with their solutions and additives in C4 estimation

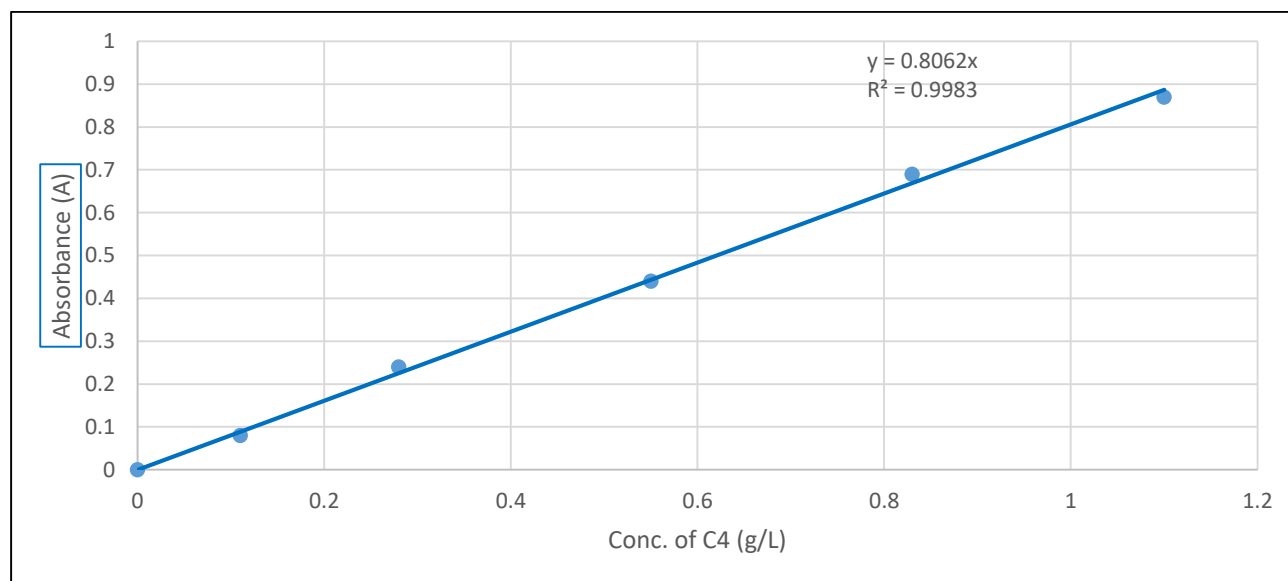
Solution/Tube	Sample	Calibrator	Blank
Sample	25 μ L	-	-
Calibrator	-	25 μ L	-
Distilled Water	-	-	25 μ L
Reagent (R1)	1 mL	1 mL	1 mL

3- All tubes were mixed well by vortex.

4- The absorbance (A) of the serum samples and calibrator were measured after 2 minutes of the sample or calibrator addition against the blank at wave length 340nm by using cuvette of 1 cm light path of Spectrophotometer.

Calculations:

The different absorbance values (A) against the C4 concentration of each calibrator dilution was plotted. C4 concentration in the sample was calculated by interpolation of its (A) value in the calibration curve as shown in Figure (2.2).

**Figure (2.2): Standard curve of C4**

2.4.3.1.3. Levels of Complement Hemolytic 50 (CH50)**Principle:**

The measurement of complement hemolytic 50 (CH50) level is conducted using the enzyme-linked immunosorbent assay (ELISA) technique. The CH50 ELISA kit utilizes the quantitative sandwich enzyme immunoassay technique. The microtiter plate has been pre-coated with a monoclonal antibody that exhibits specificity towards CH50. Subsequently, standards or samples are introduced into the wells of the microtiter plate, where, if present, CH50 will adhere to the wells that have been pre-coated with antibodies. To quantitatively ascertain the quantity of CH50 in the sample, a standardized preparation of horseradish peroxidase (HRP)-conjugated polyclonal antibody, which is specifically designed for CH50, is introduced into each well to create a "sandwich" formation with the immobilized CH50 on the plate. After the microtiter plate is subjected to incubation, the wells are meticulously rinsed in order to eliminate any remaining unattached components. Subsequently, solutions containing substrates are introduced into individual wells. The enzyme horseradish peroxidase (HRP) and its corresponding substrate undergo a brief incubation period to initiate the reaction. Color change will only occur in wells that contain both CH50 and enzyme-conjugated antibody. The enzyme-substrate reaction is concluded by introducing a solution of sulphuric acid, and the resulting alteration in color is quantitatively assessed using spectrophotometry at a specific wavelength of 450 nm. A standard curve is constructed to establish a correlation between the optical density (O.D.) of color and the concentration of standard samples. The concentration of CH50 in each sample is determined by interpolation from the standard curve (Mitratza *et al.*, 2021).

Materials:

CH50 ELISA kit materials were shown in Table (2.10).

Table (2.10): Materials of CH50 ELISA kit

No.	Material	Specification	Quantity
1	Microtiter Plate	96 wells	Strip-well
2	Enzyme Conjugate	10 mL	1 vial
3	Standard A	0 U/mL	1 vial
4	Standard B	50 U/mL	1 vial
5	Standard C	100 U/mL	1 vial
6	Standard D	250 U/mL	1 vial
7	Standard E	500 U/mL	1 vial
8	Standard F	1000 U/mL	1 vial
9	Substrate A	6 mL	1 vial
10	Substrate B	6 mL	1 vial
11	Stop Solution	6 mL	1 vial
12	Wash Solution (100 X)	10 mL	1 vial
13	Balance Solution	3 mL	1 vial
14	Instruction	1	1

Reagent Preparation:

1- Wash Solution: A 10 mL of wash solution concentrate (100×) was diluted with 990 mL of distilled water to prepare 1000 mL of Wash Solution (1×).

Procedures:

1- Prior to usage, all kit components and samples were equilibrated to room temperature, namely within the range of 20-25 °C.

2- The wells that had been coated were carefully placed and fastened within the holder. Subsequently, a volume of 50 µL containing both standards and samples was introduced into the corresponding well of the micro-titer plate that had been pre-coated with antibodies. Subsequently, a volume of 50 µL of PBS with a pH range of 7.0-7.2 was introduced into the well designated as the blank control.

3- A volume of 100 μL of conjugate was introduced into each well, excluding the blank control well, and thoroughly mixed. The plate was securely sealed and placed in an incubator set at a temperature of 37°C for a duration of 1 hour.

4- The incubation mixture was removed by aspirating the contents of the plate into a washbasin. Every well was entirely filled with a $1\times$ wash solution. Subsequently, the contents of the dish were aspirated into a washbasin. The aforementioned technique was iterated on five separate occasions, resulting in a cumulative total of five washes. Following the cleaning process, the plate was inverted and dried by gently striking it against absorbent paper until all traces of moisture were eliminated.

5- A volume of 50 μL of Substrate A and 50 μL of Substrate B were added to each well, including the blank control well, in a sequential manner. The wells were securely sealed and subjected to incubation for a duration of 10 to 15 minutes at a temperature range of 20°C to 25°C .

6- A volume of 50 μL of Stop Solution was added to each well, including the blank control well, and thoroughly mixed.

7- The Optical Density (OD) was measured at a wavelength of 450 nm using a microplate reader without delay.

Calculations:

The standard curve was constructed as shown in Figure (2.3):

- 1- CH50 standard value on each standard vial was determined.
- 2- The standard curve was constructed by plotting the absorbance for the CH50 standards (vertical axis) versus the CH50 standard concentrations in IU/mL (horizontal axis) on a linear graph paper.
- 3- The absorbance for standards and each unknown sample from the curve was read.

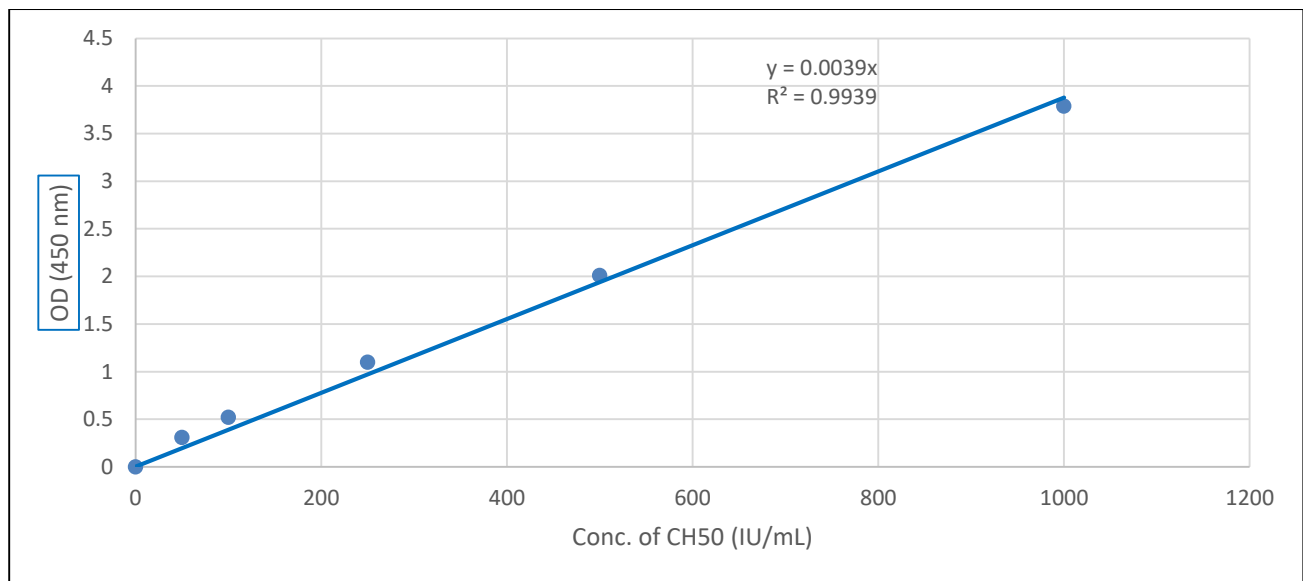


Figure (2.3): Standard curve of CH50

2.4.3.1.4. Levels of Antinuclear Antibodies (ANA)

Principle:

The methodology employed in this assay is founded upon the sandwich enzyme-linked immunosorbent assay (ELISA) premise. The microtiter plate provided for the experiment has been pre-coated with a capture antibody that is specific to the target of interest. Standards or samples are introduced into the wells, where the target antigen subsequently forms a binding interaction with the capture antibody. The Unbound Standard or sample has been wiped away. Subsequently, a detection antibody conjugated with biotin is introduced, facilitating its binding to the antigen that has been immobilized. The unbound detecting antibody is subsequently removed using a washing process. Subsequently, the Streptavidin-Horseradish Peroxidase (HRP) conjugate is introduced, facilitating its binding to the biotin moiety. The Unbound Streptavidin-HRP conjugate is removed through the process of washing. Subsequently, a TMB substrate is introduced into the system, initiating a reaction with the HRP enzyme, hence leading to the manifestation of color. To conclude the colour development reaction, a solution containing sulfuric acid is introduced. Subsequently, the optical density (OD) of the well is assessed at a specific wavelength of $450\text{nm} \pm 2$

nm. A standard curve for OD is created by utilizing known concentrations of antigens. By comparing the OD of an unknown sample to the standard curve, it becomes possible to ascertain the concentration of antigens present in the sample (Nakanishi, 2018).

Reagents:

ANA ELISA kit materials were shown in Table (2.11).

Table (2.11): Components of ANA ELISA kit

No.	Component	Specification
1	Coated 96-well Strip Plate	1
2	Standard (Lyophilized)	2 vials
3	Sample Diluent	1 vial x 20mL
4	Biotinylated Detection Antibody (100x)	1 vial x 120 μ L
5	Detection Antibody Diluent	1 vial x 10mL
6	HRP-Streptavidin Conjugate (100x)	1 vial x 120 μ L
7	HRP-Streptavidin Conjugate Diluent	1 vial x 10mL
8	Wash Buffer (25x)	1 vial x 30mL
9	TMB Substrate	1 vial x 10mL
10	Stop Solution	1 vial x 10mL
11	Adhesive Plate Sealers	4
12	Instruction Manual	1

Reagent Preparation:

1- Standard Stock Solution (1000 ng/mL): The standard vial underwent a brief centrifugation process in order to assure the complete collection of all lyophilized material at the bottom of the vial. One tube of Standard was re-suspended with 1 mL of Sample Diluent and incubated at room temperature for 10 minutes with moderate agitation. The suggested method for diluting standard solutions is as shown in Table (2.12) and Figure (2.4):

Table (2.12): Standards dilution of ANA

Concentration	Standard No.	Dilution Steps
100 ng/mL	D1	10 μ L of Stock Standard into 90 μ L of Sample Diluent
50 ng/mL	D2	300 μ L of D1 into 300 μ L of Sample Diluent
25 ng/mL	D3	300 μ L of D2 into 300 μ L of Sample Diluent
12.5 ng/mL	D4	300 μ L of D3 into 300 μ L of Sample Diluent
6.25 ng/mL	D5	300 μ L of D4 into 300 μ L of Sample Diluent
3.125 ng/mL	D6	300 μ L of D5 into 300 μ L of Sample Diluent
1.563 ng/mL	D7	300 μ L of D6 into 300 μ L of Sample Diluent
0 ng/mL	Zero	250 μ L Dilution Buffer

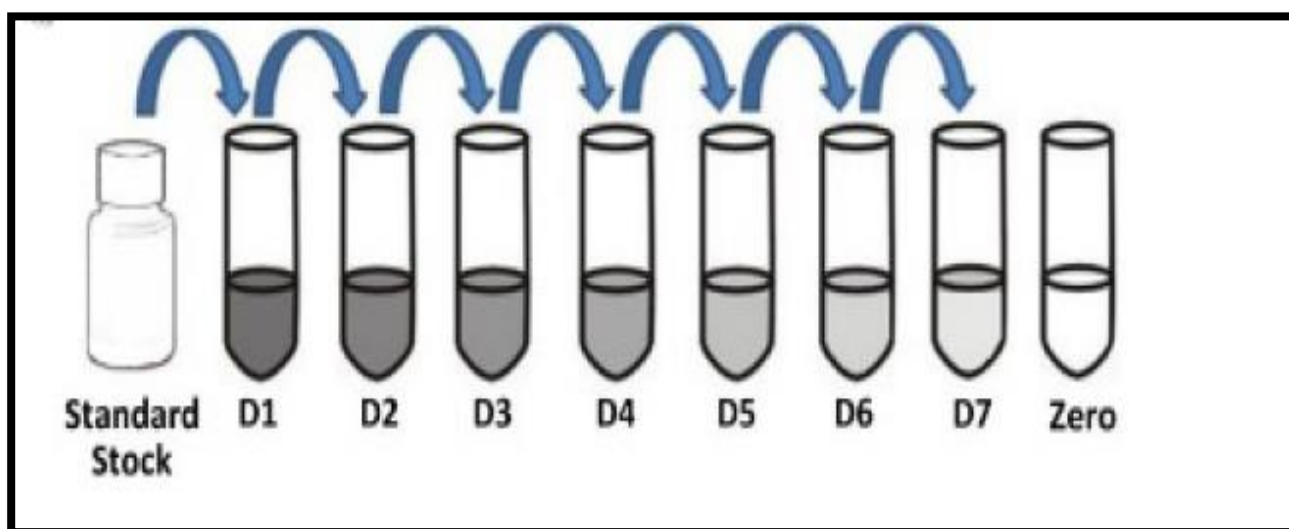


Figure (2.4): Standards solutions preparation of ANA

2- 1x Wash Buffer: A volume of 750 mL of Working Wash Buffer was generated through the process of dilution. This involved combining 30 mL of a concentrated solution known as 25x Wash Buffer Concentrate with 720 mL of distilled water.

3- 1x Biotinylated Detection Antibody: The concentrated Biotinylated Detection Antibody was diluted to the appropriate working concentration by utilizing the

Detection Antibody Diluent at a ratio of 1:100. The resulting mixture was properly mixed.

4- 1x HRP-Streptavidin Conjugate: The HRP-Streptavidin Conjugate, which was in a concentrated form, was diluted to the desired working concentration by employing the HRP-Streptavidin Conjugate Diluent at a ratio of 1:100. The resulting mixture was then thoroughly mixed.

Procedures:

1- Prior to usage, all components of the kit, including standards and samples, were equilibrated to room temperature, namely within the range of 20-25 °C. The TMB Substrate was heated to a temperature of 37°C and maintained at this temperature for a duration of 30 minutes.

2- A volume of 100 µL of Standard, Blank, and Sample solutions were introduced into each well of a plate, which was subsequently sealed with a plate sealer. The plate was then incubated at a temperature of 37°C for a duration of 90 minutes.

3- The liquid was removed from the plate through aspiration. Subsequently, the object was reversed and gently tapped upon a pristine sheet of absorbent paper. Each well underwent two washes.

4- Each well was supplemented with 100µL of a working solution containing 1x Biotinylated Detection Antibody. The wells were then sealed with a plate sealer and gently shaken to facilitate proper mixing. Subsequently, the plate was incubated at a temperature of 37°C for a duration of 60 minutes.

5- The liquid was extracted from each well and subjected to three rounds of washing, whereby about 350 µL of 1x Wash Buffer was added at each washing step. Each wash was permitted to remain undisturbed for a duration of 1-2 minutes prior to complete aspiration. Following the previous washing step, aspiration was performed once again in order to eliminate any residual Wash Buffer. Subsequently, the plate was inverted and gently tapped against a sheet of clean absorbent paper.

6- Each well was supplemented with 100 µL of a working solution containing HRP-Streptavidin Conjugate at a concentration of 1x. The wells were then sealed with a fresh

plate sealer and subjected to an incubation period of 30 minutes at a temperature of 37°C.

7- The liquid was extracted from each well and subsequently rinsed five times, following the procedure described in step 5.

8- Each well was supplemented with 90 µL of TMB Substrate solution, followed by the placement of a fresh plate sealer. The samples were then incubated at a temperature of 37°C for a duration of 10-20 minutes.

9- Each well was supplemented with 50 µL of Stop Solution. The color blue underwent an instantaneous transformation to yellow.

10- The optical density (OD) of each well was promptly measured using a microplate reader configured to operate at a wavelength of 450 nm.

Calculations:

The standard curve was constructed as shown in Figure (2.5):

1- The construction of the standard curve involved the plotting of the OD values for the ANA standards on the vertical axis, while the concentrations of the ANA standards in ng/mL were plotted on the horizontal axis.

2- The average absorbance for each standard and sample was computed and then adjusted by subtracting the average OD of the zero standard.

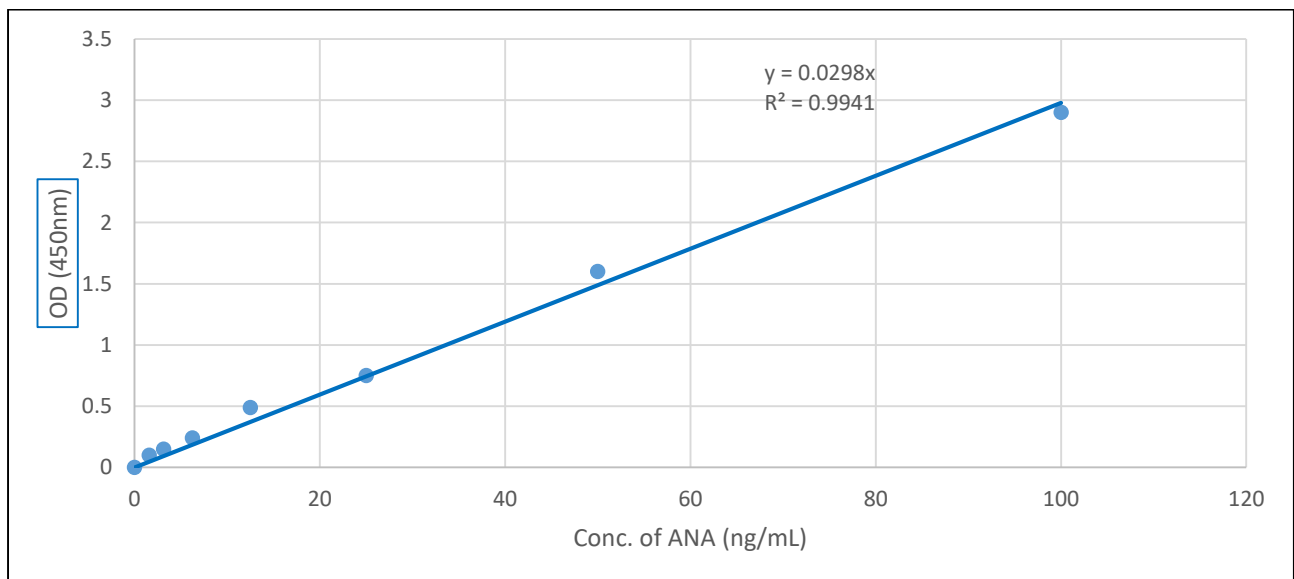


Figure (2.5): Standard curve of ANA

2.4.3.1.5. Levels of Anti-double strand DNA (Anti-dsDNA)

Principle:

The kit uses the Double Antigen Sandwich Enzyme-Linked Immunosorbent Assay (ELISA) technique. The pre-coated antigen utilized in this study is a Related-Human Anti-dsDNA antigen, but the detection antigen employed is a distinct antigen. The ELISA plate wells are loaded with samples, which are subsequently rinsed with either PBS or TBS following their respective introductions into the wells. Subsequently, Avidin-peroxidase conjugates are introduced into the wells. The TMB substrate is employed for chromogenic detection subsequent to the complete removal of the enzyme conjugate from the wells using PBS or TBS washing. The reaction of TMB results in the formation of a blue product through the peroxidase activity, which subsequently transitions to a yellow color upon the introduction of the stop solution (Color Reagent C). There exists a positive correlation between the color intensity and quantity of the target analyte present in the sample (Wu *et al.*, 2021).

Reagents:

Anti-dsDNA ELISA kit components were demonstrated in Table (2.13)

Table (2.13): Components of Anti-dsDNA ELISA kit

No.	Component	Specification
1	Antigen pre-coated plate	8 x 12
2	Human Anti-dsDNA Standards	2 vial
3	Antigen (1:100)	1 vial
4	Enzyme conjugate (1:100)	1 vial
5	Enzyme diluent	1 vial
6	Antigen diluent	1 vial
7	Standard diluent	1 vial
8	Sample diluent	1 vial
9	Washing buffer (1:25)	1 vial
10	Color Reagent A	1 vial

11	Color Reagent B	1 vial
12	Color Reagent C	1 vial
13	Manual	1 set

Reagent Preparation:

1- Standard Solution (400 IU/mL): A volume of 1 mL of Standard Diluent was introduced to the lyophilized standard vial, and subsequently left undisturbed for a duration of 30 minutes. Once the standard solution had fully dissolved, it was gently agitated and subsequently labelled on the tube. A total of seven sterile tubes were selected and appropriately marked with their respective anticipated concentrations, namely 200, 100, 50, 25, 12.5, 6.25, and 0 IU/mL. Each tube was supplemented with 300 μ L of Standard Diluent. A volume of 300 μ L of diluent was extracted from the reconstituted standard and thereafter introduced into the tube labelled as 200 IU/mL. The contents were thoroughly mixed. A volume of 300 μ L of diluent was extracted from the tube containing a concentration of 200 IU/mL and thereafter combined with the tube containing a concentration of 100 IU/mL. The resulting mixture was thoroughly mixed. The aforementioned processes were iterated for each instance of the 6.25 IU/mL standard. The negative control in the 0IU/mL tube was the standard diluent. The suggested approach for diluting standard solutions is as shown in Table (2.14) and Figure (2.6):

Table (2.14): Standards dilution of Anti-dsDNA

Concentration	Standard No.	Dilution Steps
400 IU/mL	Tube # 1	Standard vial into 1 mL of Standard Diluent
200 IU/mL	Tube # 2	300 μ L of Tube#1 into 300 μ L of Standard Diluent
100 IU/mL	Tube # 3	300 μ L of Tube#2 into 300 μ L of Standard Diluent
50 IU/mL	Tube # 4	300 μ L of Tube#3 into 300 μ L of Standard Diluent
25 IU/mL	Tube # 5	300 μ L of Tube#4 into 300 μ L of Standard Diluent

12.5 IU/mL	Tube # 6	300 μ L of Tube#5 into 300 μ L of Standard Diluent
6.25 IU/mL	Tube # 7	300 μ L of Tube#6 into 300 μ L of Standard Diluent
0 IU/mL	Tube # 8 (Zero)	100 μ L Standard Diluent

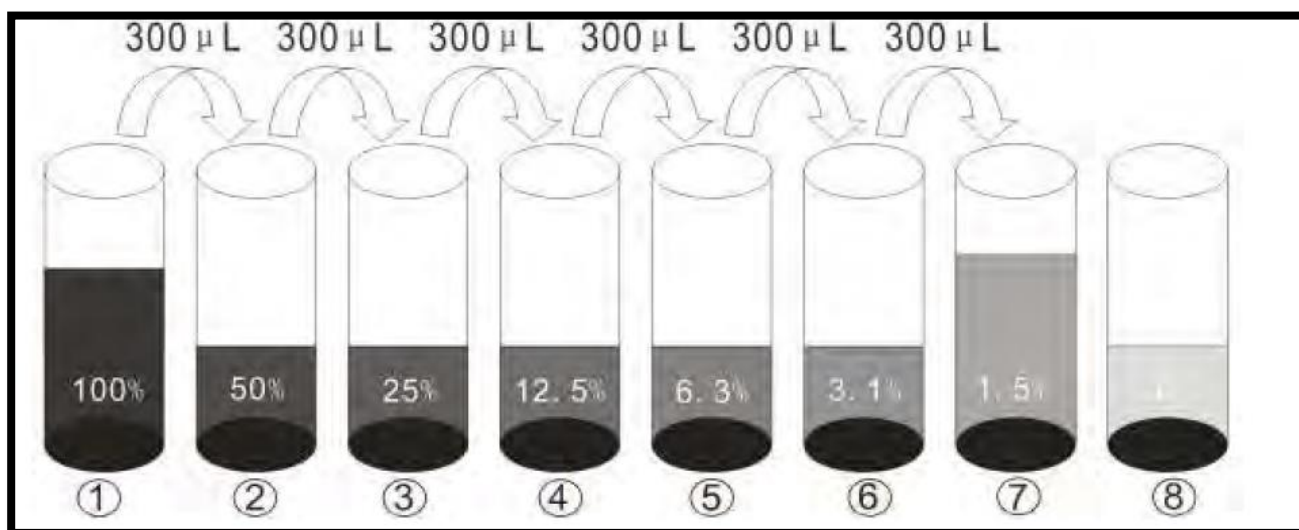


Figure (2.6): Standards solutions preparation of Anti-dsDNA

- 2- Antigen: The antigen solution was diluted with antigen diluent at a ratio of 1:100.
- 3- Enzyme Conjugate: The Enzyme Conjugate solution was diluted with the Enzyme Diluent at a ratio of 1:100.
- 4- Color Reagent: The Color Reagent solution was made by combining Color Reagent A and Color Reagent B in a ratio of 9:1.
- 5- Washing Buffer: The concentrated washing buffer was diluted by adding distilled water in a ratio of 1:25.

Procedures:

- 1- Prior to use, all components of the kit, including standards and samples, were equilibrated to room temperature, namely within the range of 20-25 °C.
- 2- A volume of 100 μ L of both standards and samples was added to each well of the plate, which was then sealed with a plate sealer. The plate was thereafter incubated for a duration of 90 minutes at a temperature of 37°C.

3- The liquid was removed by aspiration of the plate. Subsequently, the sample was inverted and gently tapped onto a sheet of pristine absorbent paper. Each well underwent two rounds of washing.

4- Each well was supplemented with 100 μ L of Antigen, followed by the application of a plate sealer. The mixture was gently stirred to promote proper homogenization and subsequently incubated for a duration of 60 minutes at a temperature of 37°C.

5- The liquid was extracted from each well and subjected to a triple wash procedure, involving the addition of approximately 350 μ L of 1x Wash Buffer during each wash. Each wash was permitted to remain undisturbed for a duration of 1-2 minutes prior to complete aspiration. Following the previous washing step, aspiration was performed once again in order to eliminate any residual Wash Buffer. Subsequently, the plate was inverted and gently tapped against a sheet of clean absorbent paper.

6- A volume of 100 μ L of Enzyme Conjugate was introduced into each well, followed by the placement of a fresh plate sealer. The samples were then subjected to incubation at a temperature of 37°C for a duration of 30 minutes.

7- The liquid was extracted from each well and subsequently subjected to a series of five washes, following the protocol described in step 5.

8- A volume of 100 μ L of the Color Reagent that had been produced in advance was introduced into each well, followed by incubation at a temperature of 37°C for a duration of 30 minutes, while ensuring the absence of light.

9- A volume of 100 μ L of Color Reagent C was added to each well and thoroughly mixed.

10- The optical density (OD) of each well was measured using a microplate reader set to 450 nm after a duration of 10 minutes.

Calculations:

The standard curve was constructed as shown in Figure (2.7):

1- The construction of the standard curve involved the plotting of the OD values for the Anti-dsDNA standards on the vertical axis, while the concentrations of the Anti-dsDNA standards in IU/mL were represented on the horizontal axis.

2- The average absorbance values for each standard and sample were computed and then adjusted by subtracting the average OD of the zero standard.

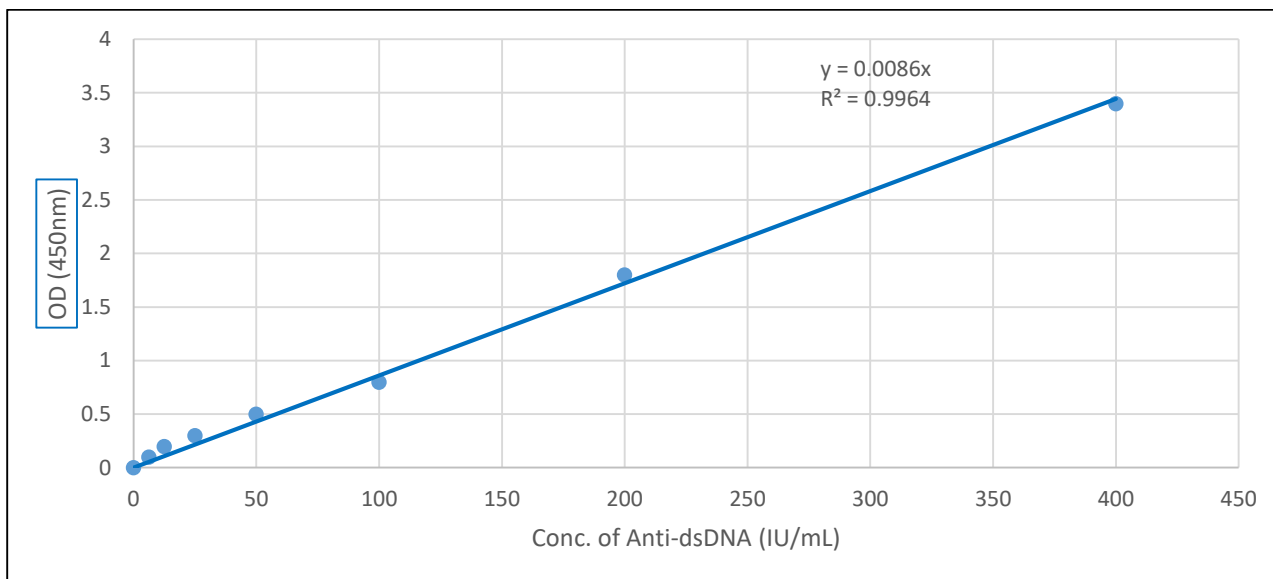


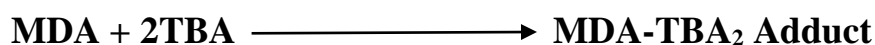
Figure (2.7): Standard curve of Anti-dsDNA

2.4.3.2. Oxidant/Antioxidant Parameters

2.4.3.2.1. Levels of Malondialdehyde (MDA)

Principle:

Thiobarbituric acid reactive substances (TBARS) refer to a class of low-molecular-weight end products, primarily malondialdehyde (MDA), which are generated as a result of the breakdown of lipid peroxidation products. Elevated concentrations of TBARS have been observed in various pathological conditions, including SLE. Assays for the measurement of TBARS are widely utilized in both research and drug development due to their simplicity, straightforwardness, and high level of accuracy. The TBARS assay developed by BioAssay Systems relies on the chemical reaction between TBARS and thiobarbituric acid (TBA), resulting in the formation of a visually detectable pink colored product. The concentration of TBARS in the sample exhibits a direct proportionality to the color intensity observed at a wavelength of 535 nm (Lu *et al.*, 2021a).



Reagents:

- 1- Thiobarbituric acid (TBA) Reagent: 25 mL.
- 2- Malondialdehyde (MDA) standard solution: 50 μ L 6 M.
- 3- 10% Trichloroacetic acid (TCA): 25 mL.

Reagent Preparation:

Ready to use.

Sample Preparation:

- 1- In the context of serum samples, a volume of 100 μ L from each sample was carefully transferred into a properly labelled 1.5 mL tube.
- 2- A volume of 200 μ L of ice-cold solution. Each sample was treated with a 10% TCA solution and incubated on ice for a duration of 5 minutes.
- 3- The samples underwent centrifugation for a duration of 5 minutes at a rotational speed of 14,000 revolutions per minute (rpm) using an Eppendorf Centrifuge. Subsequently, 200 μ L of every transparent supernatant were carefully transferred into a freshly labelled tube. The dilution factor employed for the pretreated samples is denoted as $n = 3$.

Procedures:

- 1- All components were brought to a state of thermal equilibrium with the ambient room temperature. Furthermore, a water bath was established and the temperature was calibrated to 100°C.
- 2- The conventional tube underwent centrifugation in order to precipitate any MDA that could have adhered to the cap or inner walls of the tube.
- 3- A total of 4 μ L of a 6 M concentration solution of MDA were combined with 2396 microliters of deionized water, resulting in a final concentration of 10 mM MDA.
- 4- A solution of 30 μ M MDA was generated by combining 3 μ L (μ L) of a 10 mM MDA solution with 997 μ L of deionized water. The dilution of standards is shown in Table (2.15).

Table (2.15): Standards dilution of MDA

No.	30 μM MDA + H ₂ O	Vol (μL)	MDA (μM)
1	300 μL + 0 μL	300	30
2	180 μL + 120 μL	300	18
3	90 μL + 210 μL	300	9
4	0 μL + 300 μL	300	0

5- A volume of 200 μL was aliquoted from each standard and subsequently put into individual 1.5 mL screw cap tubes, which were appropriately labelled.

6- A volume of 200 μL of TBA Reagent was introduced into each of the tubes containing both the standards and samples. The tubes were subjected to vortexing in order to facilitate mixing, followed by incubation at a temperature of 100°C for a duration of 60 minutes.

7- The tubes were subjected to cooling until they reached the ambient temperature, followed by vortexing and a brief centrifugation.

8- A volume of 100 μL was taken from each tube and transferred into separate tubes.

9- The measurement of absorbance (A) for both the serum samples and standards was conducted at a wavelength of 535nm using a cuvette with a light path of 1 cm in a Spectrophotometer. The blank was used as a reference.

Calculations:

The absorbance value (A) for the blank (#4) was subtracted from the absorbance values of all the standard and sample measurements. The change in absorbance at 535nm was graphed against the concentrations of the standards, and the gradient of the standard curve was calculated as shown in Figure (2.8). The concentration of TBARS in the samples was determined using the following calculation method:

$$\text{MDA } (\mu\text{mol/L}) = (A_{\text{sample}} - A_{\text{blank}}) \times n / \text{Slope } (\mu\text{M}^{-1})$$

Where: n = sample dilution factor = 3 μM MDA equivalents

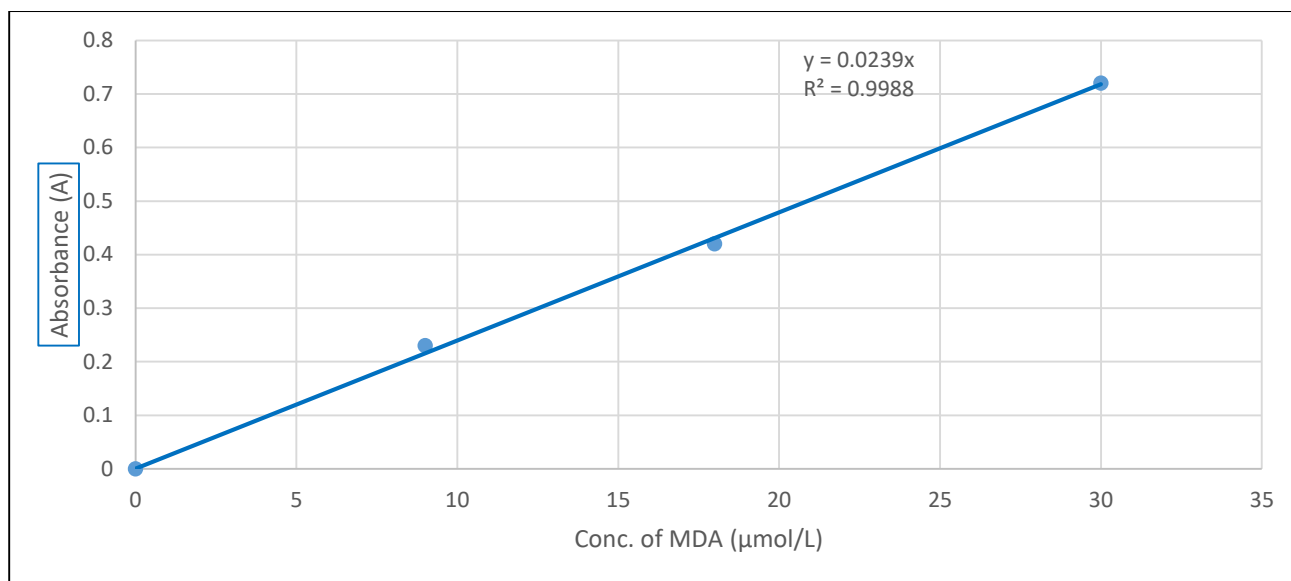


Figure (2.8): Standard curve of MDA

2.4.3.2.2. Levels of Total Antioxidant Capacity (TAC)

Principle:

The total antioxidant capacity (TAC) test kit is utilized to quantify the TAC present in a given sample. The samples are subjected to comparison with a predetermined concentration of a uric acid standard. The samples and standards undergo dilution using a reaction reagent. Following the introduction of copper, the reaction progresses over a brief duration. The reaction is halted and subsequently analyzed using a spectrophotometer set to a wavelength of 490 nm. The determination of TAC is conducted by the process of comparing it with established uric acid criteria (Al-Gahtani, 2021).

Reagents:

- 1- Uric Acid Standard: One 100 mg tube of powder.
- 2- Reaction Buffer (100X): One 400 µL amber tube.
- 3- Copper Ion Reagent (100X): One 1.0 mL tube.
- 4- Stop Solution (10X): One 1.5 mL tube.

Reagent Preparation:

1- 1X Reaction Buffer: The reaction buffer was diluted at a ratio of 1:100 using 1X PBS and thoroughly mixed to achieve uniformity.

2- 1X Copper Ion Reagent: The reagent containing copper ions was diluted at a ratio of 1:100 with deionized water and well mixed until a uniform mixture was obtained.

3- 1X Stop Solution: The stop solution was diluted at a ratio of 1:10 with deionized water and thoroughly mixed until a homogeneous mixture was achieved.

Preparation of Uric Acid Standard Curve:

1- Fresh standards of uric acid were generated by accurately measuring the quantity of uric acid (UA) powder required to obtain a solution with a concentration of 10 mg/mL in 1N NaOH. The concentration of the solution, which is 10 mg/mL, can be converted to a concentration of 60 mM. A 60 mM solution of uric acid was utilized in the process of creating a 2 mM solution of uric acid. This was achieved by adding 100 μ L of the 60 mM uric acid standard to 2.9 mL of deionized water (DW).

2- A set of uric acid standards that were not used previously were made in deionized water, following the instructions provided in Table (2.16).

Table (2.16): Standards dilution of TAC

Tubes	2 mM UA standard (μ L)	DW (μ L)	Resulting UA (mM)
1	500	500	1
2	500 of tube #1	500	0.5
3	500 of tube #2	500	0.25
4	500 of tube #3	500	0.125
5	500 of tube #4	500	0.0625
6	500 of tube #5	500	0.03125
7	500 of tube #6	500	0.0156
8	500 of tube #7	500	0.0078
9	500 of tube #8	500	0.0039
10	0	500	0

Procedures:

- 1- All components were allowed to reach thermal equilibrium with the ambient room temperature.
- 2- Tubes were supplemented with 20 μL of the diluted uric acid standards or samples.
- 3- Each tube was supplemented with 180 μL of the 1X reaction buffer using a micropipette, ensuring thorough mixing.
- 4- The absorbance (A) of the serum samples and standards was initially measured at a wavelength of 490nm using a cuvette with a light path of 1 cm in a Spectrophotometer.
- 5- A volume of 50 μL of the 1X copper ion reagent was introduced into each tube in order to commence the reaction, which was thereafter incubated for a duration of 5 minutes at a temperature of 37°C.
- 6- To halt the reaction, 50 μL of a 1X stop solution was introduced into each tube.
- 7- The final absorbance (A) of the serum samples and standards was measured at a wavelength of 490nm using a cuvette with a light path of 1 cm in a Spectrophotometer.

Calculations:

- 1- The net absorbance (A) was determined by subtracting the initial absorbance measurements of both samples and standards (Step#4) from the final measurements obtained for each (Step#7).
- 2- The plot of net absorbance was generated by correlating it with the concentration of uric acid for the purpose of constructing the uric acid standard curve as shown in Figure (2.9).
- 3- The determination of the antioxidant capacity of unidentified samples was performed by comparing the net absorbance values of the samples with the uric acid reference curve.

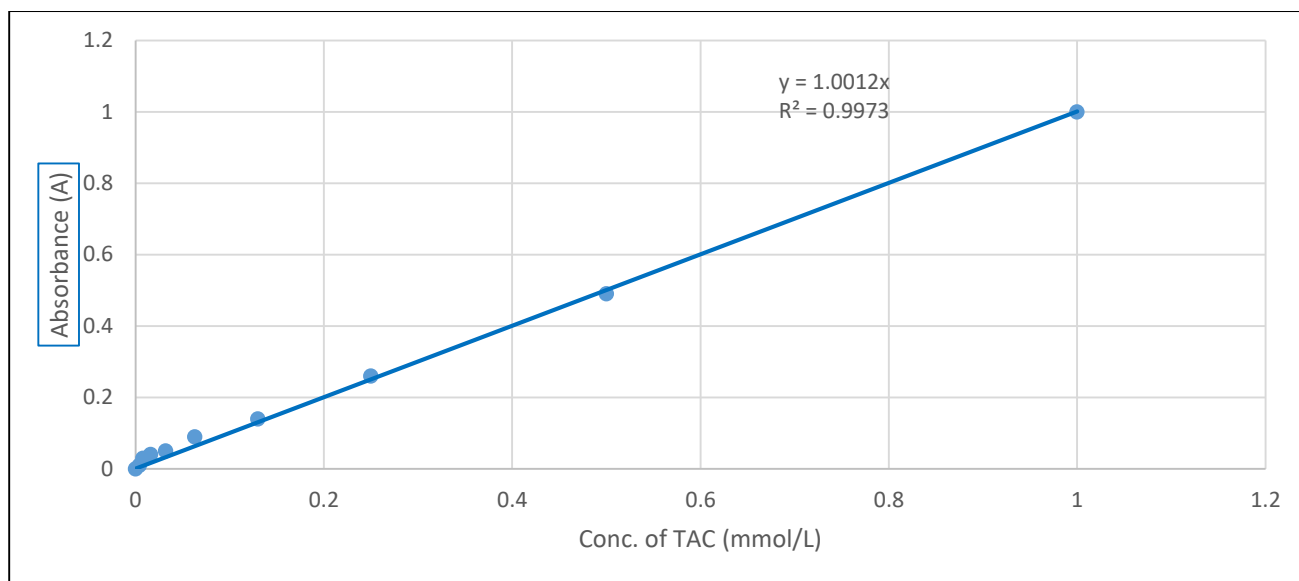


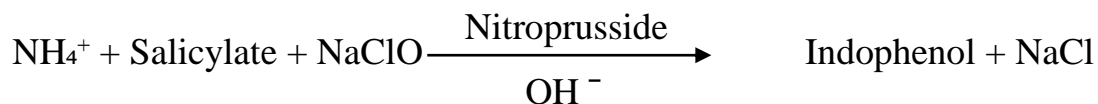
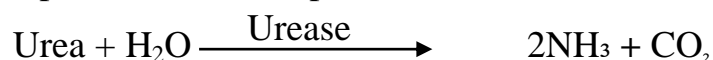
Figure (2.9): Standard curve of TAC

2.4.3.3. Kidney Function Parameters

2.4.3.3.1. Levels of Urea

Principle:

The process of urea hydrolysis involves the enzymatic action of urease, resulting in the conversion of urea into ammonia and carbon dioxide. The ammonia produced undergoes a reaction with alkaline hypochlorite and sodium salicylate in the presence of sodium nitroprusside as a coupling agent, resulting in the formation of a green chromophore. The magnitude of the color produced is directly related to the concentration of urea present in the sample (Al-Anazi *et al.*, 2019).



Reagents:

- 1- R1 Vial: Enzyme Reagent (Urease > 500 U/mL).
- 2- R2 Vial: Buffered Chromogen (Phosphate Buffer 20mmol/L with PH=6.9, EDTA 2mmol/L, Sodium salicylate 60mmol/L & Sodium nitroprusside 3.4mmol/L).

3- R3 Vial: Alkaline Hypochlorite (Sodium hypochlorite 10 mmol/L & Sodium hydroxide 150mmol/L).

4- Standard Concentration Solution of Urea (50 mg/dL).

Reagent Preparation:

1- The Working Reagent Solution was created by combining the contents of the R1 vial with the contents of the R2 vial.

Procedures:

1- Three sets of tubes were constructed as per Table (2.17):

Table (2.17): Sets of tubes with their solutions and additives in urea determination

Solution/Tube	Sample	Standard	Blank
Working Reagent	1 mL	1 mL	1 mL
Standard	-	10 μ L	-
Sample	-	-	10 μ L

2- The tubes were well combined using a vortex and thereafter incubated at a temperature of 37°C for a duration of 5 minutes.

3- A volume of 1 mL of R3 vial solution was uniformly dispensed into each tube, well mixed using a vortex mixer, and thereafter subjected to an incubation period of 5 minutes at a temperature of 37 °C.

4- The measurement of absorbance (A) was conducted for both the sample and standard, relative to the blank, using a spectrophotometer with a cuvette of 1 cm light path at a wavelength of 600 nm.

Calculations:

$$\text{Level of urea (mg/dL)} = (A_{\text{sample}} / A_{\text{standard}}) \times n$$

Where: n = Concentration of urea in standard solution = 50 mg/dL.

2.4.3.3.2. Levels of Creatinine

Principle:

The methodology employed in this approach is derived from a modified version of the original picrate reaction as described by Jaffe. The reaction between creatinine and picrate ions under alkaline circumstances results in the formation of a crimson complex. The rate at which the complex is formed, as determined by the rise in absorbance over a defined time interval, is directly proportional to the concentration of creatinine present in the sample (Jaing *et al.*, 2021).

Reagents:

- 1- R1 Vial: Picric acid 25mmol/L.
- 2- R2 Vial (Alkaline buffer): Phosphate buffer 300 mmol/L pH 12.7, SDS 2.0 g/L (w/v).
- 3- Standard Concentration Solution of Creatinine (2 mg/dL).

Reagent Preparation:

- 1- The Working Reagent Solution was created by combining the contents of the R1 vial with the contents of the R2 vial.

Procedures:

- 1- The working reagent, samples, and standard were pre-incubated at a temperature of 37°C in preparation for the reaction.
- 2- Three sets of tubes were constructed as per Table (2.18):

Table (2.18): Sets of tubes with their solutions and additives in creatinine determination

Solution/Tube	Blank	Standard	Sample
Distilled Water	100 μ L	-	-
Standard	-	100 μ L	-
Sample	-	-	100 μ L
Working Reagent	1 mL	1 mL	1 mL

- 3- The tubes were thoroughly combined using a vortex.

4- The absorbance of the samples and standard at two time points, 30 seconds (A₁) and 90 seconds (A₂), was measured at a wavelength of 510nm using a cuvette with a light path of 1 cm in a Spectrophotometer. The measurements were compared against a blank.

Calculations:

$$\text{Level of creatinine (mg/dL)} = [(A_2 - A_1)_{\text{sample}} / (A_2 - A_1)_{\text{standard}}] \times n$$

Where: n = Concentration of creatinine in standard solution = 2 mg/dL.

2.4.3.3.3. Levels of Glomerular Filtration Rate (GFR)

Glomerular filtration rate (GFR) levels were calculated by the Modification of Diet in Renal Disease Study (MDRD) equation (Bassiouni *et al.*, 2021):

$$\text{GFR (mL/min/1.73 m}^2\text{)} = 186 \times \text{Serum Cr}^{-1.154} \times \text{age}^{-0.203} \times 1.212 \text{ (if subject is black)} \\ \times 0.742 \text{ (if subject is woman)}$$

2.4.3.4. Inflammation and Cytokines Parameters

2.4.3.4.1. Levels of C-Reactive Protein (CRP)

Principle:

The present product is a commercially available Sandwich Enzyme-Linked Immunosorbent Assay (ELISA) kit specifically developed for the purpose of detecting Human C-Reactive Protein (CRP). The assay plate was pre-coated with a monoclonal antibody specific to mouse anti-Human CRP. Upon the introduction of the sample containing CRP into the plate, a binding interaction occurs between the protein and the antibodies that are immobilized on the surface of the wells. Subsequently, a mouse anti-Human CRP Antibody coupled with horseradish peroxidase is introduced into the wells, where it selectively attaches to the CRP present in the sample. Following the process of well washing, the addition of substrate solutions ensues, whereby the observed color intensity is shown to exhibit a direct proportionality to the quantity of Human CRP that is present. The reaction is terminated by the addition of an acidic stop solution, followed by the measurement of absorbance at a wavelength of 450 nm (Wang *et al.*, 2021).

Reagents:

CRP ELISA kit components were shown in Table (2.19).

Table (2.19): Materials of CRP ELISA kit

No.	Material	Specification
1	Pre-coated ELISA Plate	12 × 8 well strips × 1
2	Standard Solution	0.2mL × 1 vail
3	Dilution Buffer	20mL × 1 vail
4	Stop Solution	6mL × 1 vail
5	Substrate Solution A	12mL × 1 vail
6	Substrate Solution B	12mL × 1 vail
7	Wash Buffer Concentrate (25x)	20mL × 1 vail
8	Detection Antibody Concentrate	0.6mL × 1 vail
9	User manual	1
10	Plate Sealers	2pcs
11	Zipper bag	1pcs

Reagent Preparation:

1- Standard Solution: A stock standard solution of 1 ng/mL (Standard No.7) was prepared by reconstituting 50 μ L of the standard solution (10 ng/mL) with 450 μ L of Dilution Buffer. Prior to dilution, the standard was allowed to rest for a duration of 15 minutes while being gently agitated. The standard points were generated using a sequential dilution process using the standard stock solution (1ng/mL) and Dilution Buffer. The dilution factor of 1:2 was applied to produce solutions with concentrations of 0.5ng/mL, 0.25ng/mL, 0.125ng/mL, 0.0625ng/mL, 0.03125ng/mL, and 0.015625ng/mL. The Dilution Buffer functions as the reference standard with a concentration of 0 pg/ μ L. The recommended approach for diluting standard solutions is as shown in Table (2.20) and Figure (2.10):

Table (2.20): Standards dilution of CRP

Concentration	Standard No.	Dilution Steps
1ng/mL	Standard No.1	50uL Original Standard + 450uL Dilution Buffer
0.5ng/mL	Standard No.2	250µL Standard No.1 + 250µL Dilution Buffer
0.25ng/mL	Standard No.3	250µL Standard No.2 + 250µL Dilution Buffer
0.125ng/mL	Standard No.4	250µL Standard No.3 + 250µL Dilution Buffer
0.0625ng/mL	Standard No.5	250µL Standard No.4 + 250µL Dilution Buffer
0.03125ng/mL	Standard No.6	250µL Standard No.5 + 250µL Dilution Buffer
0.015625ng/mL	Standard No.7	250µL Standard No.6 + 250µL Dilution Buffer
0ng/mL	Standard No.0	250µL Dilution Buffer

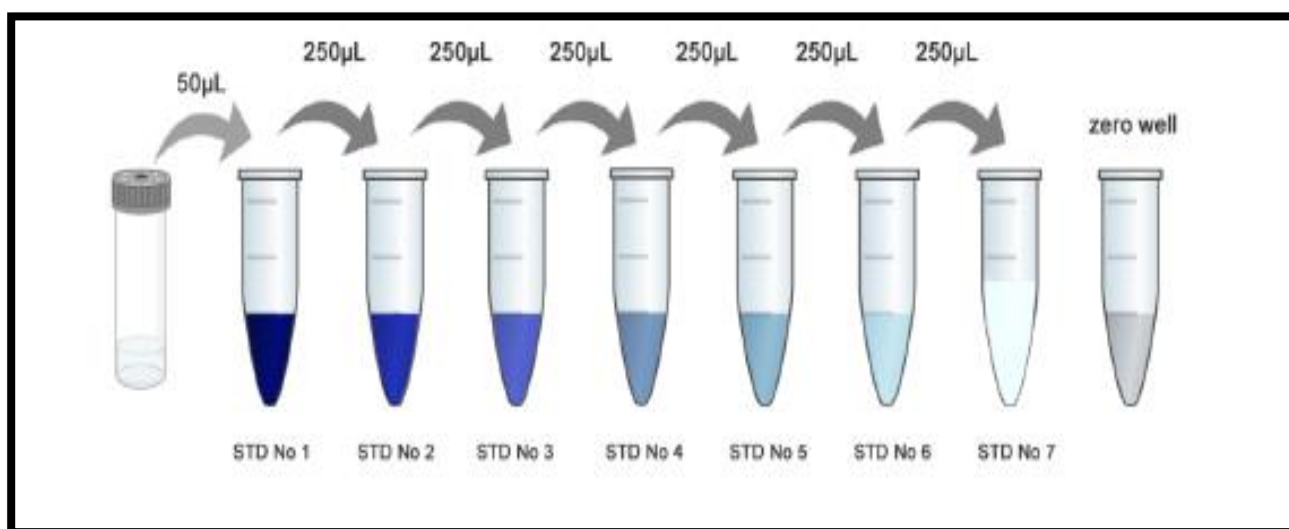


Figure (2.10): Standards solutions preparation of CRP

2- Wash Buffer: To make a 500 µL solution of 1× Wash Buffer, 20 µL of Wash Buffer Concentrate were combined with 480 µL of distilled water.

3- Solution Substrate: Equal quantities of Solution A and Solution B were combined within a duration of 10 minutes, while ensuring protection from light.

4- To create a 12 mL Detection Antibody Solution, 0.6 mL of Detection Antibody Concentrate was combined with 11.4 mL of Dilution Buffer.

Procedures:

- 1- Prior to use, all kit components, standards, and samples were equilibrated to room temperature, namely within the range of 20-25 °C.
- 2- The quantity of strips required for the test was ascertained and subsequently placed into the designated frames.
- 3- A volume of 100 μL of standards and samples was introduced into each well, followed by the application of a plate sealer. The plate was then incubated at room temperature for a duration of 2 hours.
- 4- The contents of the plate were disposed of. Each well was treated with 300 μL of 1 \times Wash Buffer and allowed to incubate for a duration of 1 minute. Subsequently, the liquid was aspirated and the wells were gently dried using clean paper towels. The procedure was replicated on two occasions, resulting in a cumulative total of three washes. A thorough extraction of liquid was ensured during each stage.
- 5- A volume of 100 μL of the Detection Antibody Solution was introduced into each well. The plate was securely sealed and subjected to incubation for a duration of one hour at ambient temperature.
- 6- The aspiration/wash procedure was reiterated, following the same steps as outlined in Step 4.
- 7- A volume of 200 μL of Substrate Solution, which had been pre-mixed during the reagent preparation phase, was introduced into each well. The samples were then incubated for a duration of 20 minutes at room temperature, ensuring they were kept away from any sources of light.
- 8- A volume of 50 μL of Stop Solution was applied to each well in order to halt the reaction. The color of the solution in the wells underwent a transition from blue to yellow.
- 9- The optical density (OD) of each well was promptly measured using a microplate reader set to 450 nm within a time frame of 10 minutes subsequent to the addition of the stop solution.

Calculations:

The standard curve was constructed as shown in Figure (2.11):

- 1- The construction of the standard curve involved the plotting of the OD values for the CRP standards on the vertical axis, while the concentrations of the CRP standards in pg/mL were plotted on the horizontal axis.
- 2- The mean absorbance values for both the standard and sample were computed and then adjusted by subtracting the average OD of the zero standard.

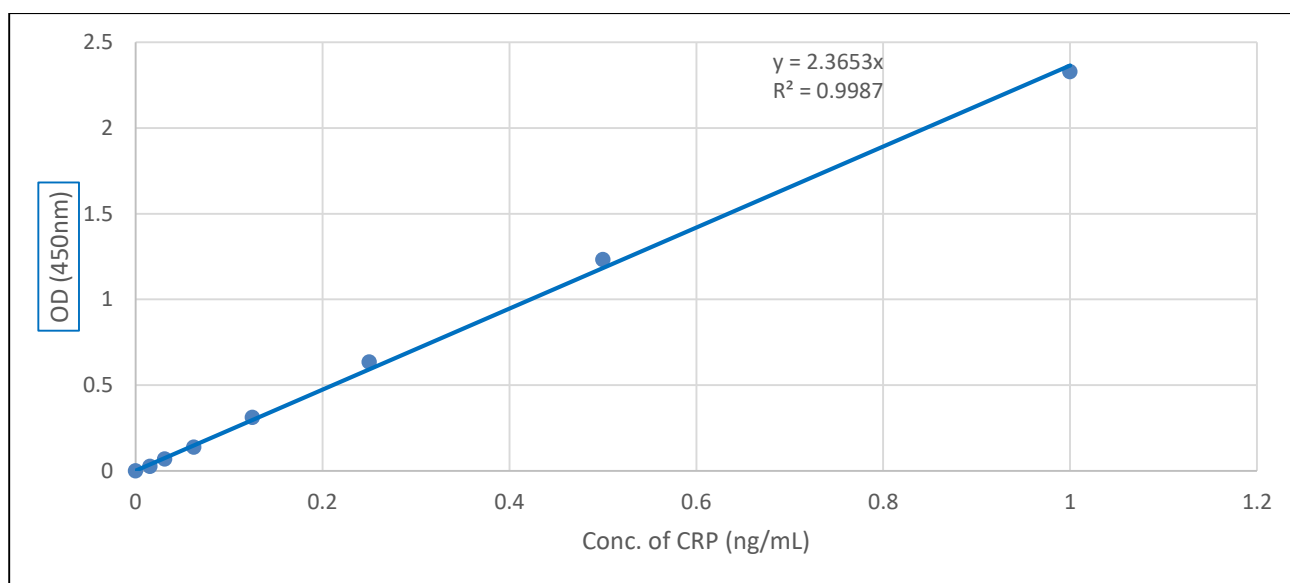


Figure (2.11): Standard curve of CRP assay

2.4.3.4.2. Levels of Interleukin-18 (IL-18)**Principle:**

The provided kit is a Sandwich Enzyme-Linked Immunosorbent Assay (ELISA). The plate has been pre-coated with an antibody specific to Human IL18. The addition of IL18, which is present in the sample, results in its binding to the antibodies that are coated on the wells. Subsequently, the biotinylated Human IL18 Antibody is introduced into the sample and forms a binding interaction with IL18. Subsequently, the Streptavidin-HRP conjugate is introduced into the system and forms a complex with the Biotinylated IL18 antibody. Following the incubation period, any unbound Streptavidin-HRP is eliminated with a further washing procedure. Next, the substrate solution is introduced, resulting in the development of color that is directly proportional

to the quantity of Human IL18 present. The reaction is concluded by introducing an acidic stop solution, and the absorbance is then quantified at a wavelength of 450 nm (Ayoub *et al.*, 2019).

Reagents:

IL-18 ELISA kit components were listed in Table (2.21).

Table (2.21): Components of IL-18 ELISA kit

No.	Components	Quantity
1	Pre-coated ELISA Plate	12 x 8 well strips x 1
2	Standard Solution (128ng/mL)	0.5mL x 1
3	Standard diluent	3mL x 1
4	Streptavidin-HRP	6mL x 1
5	Stop solution	6mL x 1
6	Substrate solution A	6mL x 1
7	Substrate solution B	6mL x 1
8	Wash buffer Concentrate (25x)	20mL x 1
9	Biotinylated Human IL18 antibody	1mL x 1
10	Plate Sealers	2 pics
11	User instruction	1

Reagent Preparation:

1- Standard Solution: The 120 μ L of the standard solution with a concentration of 128ng/mL were mixed with an equal volume (120 μ L) of standard diluent to produce a standard stock solution with a concentration of 64ng/mL. Prior to creating dilutions, the standard was permitted to rest for a duration of 15 minutes while being gently agitated. The standard points were generated by a sequential dilution process, whereby the standard stock solution (64ng/mL) was diluted 1:2 with a standard diluent. This resulted in the creation of solutions with concentrations of 32ng/mL, 16ng/mL, 8ng/mL, and

4ng/mL. The recommended approach for diluting standard solutions is shown in Table (2.22) and Figure (2.12):

Table (2.22): Standards dilution of IL-18

Concentration	Standard No.	Dilution Steps
64 ng/mL	Standard No.5	120 μ L Original standard + 120 μ L Standard diluent
32 ng/mL	Standard No.4	120 μ L Standard No.5 + 120 μ L Standard diluent
16 ng/mL	Standard No.3	120 μ L Standard No.4 + 120 μ L Standard diluent
8 ng/mL	Standard No.2	120 μ L Standard No.3 + 120 μ L Standard diluent
4 ng/mL	Standard No.1	120 μ L Standard No.2 + 120 μ L Standard diluent
0 ng/mL	Standard No.0	120 μ L Standard diluent

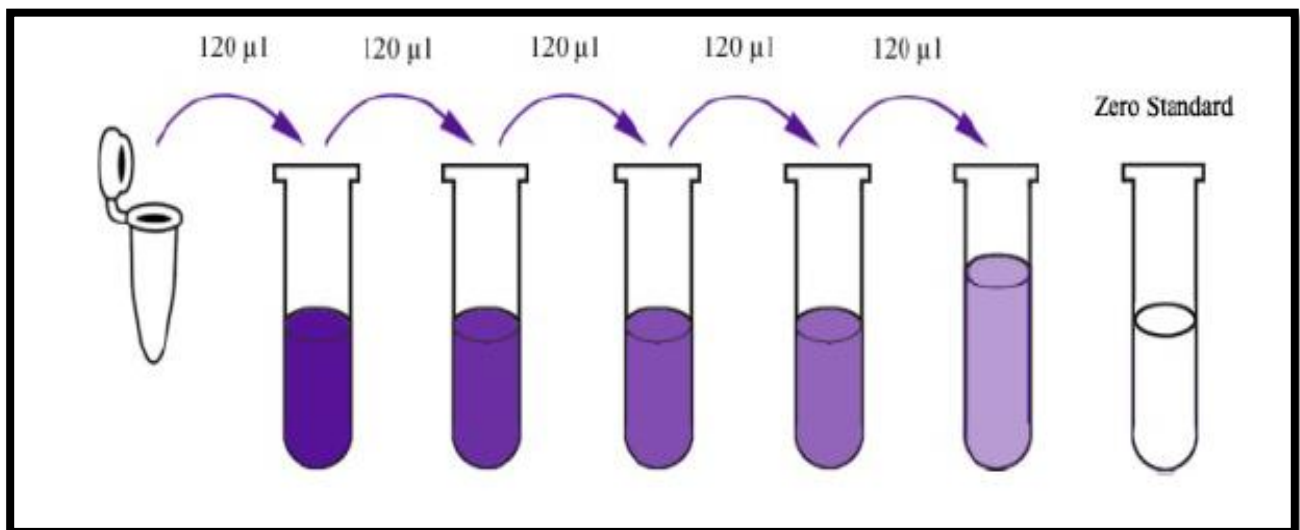


Figure (2.12): Standards solutions preparation of IL-18

2- Wash Buffer: A volume of 20 mL of wash buffer was used. A solution of Concentrate 25x was diluted with distilled water in order to obtain a final volume of 500 mL, resulting in a 1x concentration of Wash Buffer.

Procedures:

- 1- Prior to use, all kit components, standards, and samples were equilibrated to room temperature, namely within the range of 20-25 °C.
- 2- The quantity of strips required for the test was ascertained and subsequently placed into the designated frames.
- 3- A volume of 50 µL of standard solution was introduced into the designated wells for standards. The omission of antibody addition to the standard wells was due to the presence of biotinylated antibody in the standard solution.
- 4- Samples of 40 µL were introduced into the designated wells for analysis. Next, a volume of 10µL of Human IL18 antibody was introduced into the sample wells.
- 5- A volume of 50 µL of streptavidin-HRP was introduced into the wells containing the samples and standards, excluding the blank control well. The plate was coated with a sealing agent and subjected to incubation for a duration of one hour at a temperature of 37°C.
- 6- The sealer was detached, and thereafter, the plate underwent a total of five washes with wash buffer. The wells were immersed in 300 µL of wash buffer for a duration ranging from 30 seconds to 1 minute for each washing step. The plate was transferred onto paper towels.
- 7- A volume of 50 µL of substrate solution A was added to each well. Subsequently, 50 µL of substrate solution B was introduced into each well. The plate was subjected to incubation at a temperature of 37°C in a light-restricted environment for a duration of 10 minutes. Additionally, a fresh sealer was applied to cover the plate throughout this process.
- 8- A volume of 50 µL of Stop Solution was introduced into each well, resulting in an instantaneous transformation of the blue color to yellow.
- 9- The optical density (OD) of each well was promptly measured using a microplate reader set to 450 nm within a time frame of 10 minutes subsequent to the addition of the stop solution.

Calculations:

The standard curve was constructed as per Figure (2.13):

- 1- The construction of the standard curve involved the plotting of the OD values for the IL-18 standards on the vertical axis, while the horizontal axis represented the concentrations of the IL-18 standards in ng/mL.
- 2- The average absorbance for each standard and sample was computed and then adjusted by subtracting the average optical density of the zero standard.

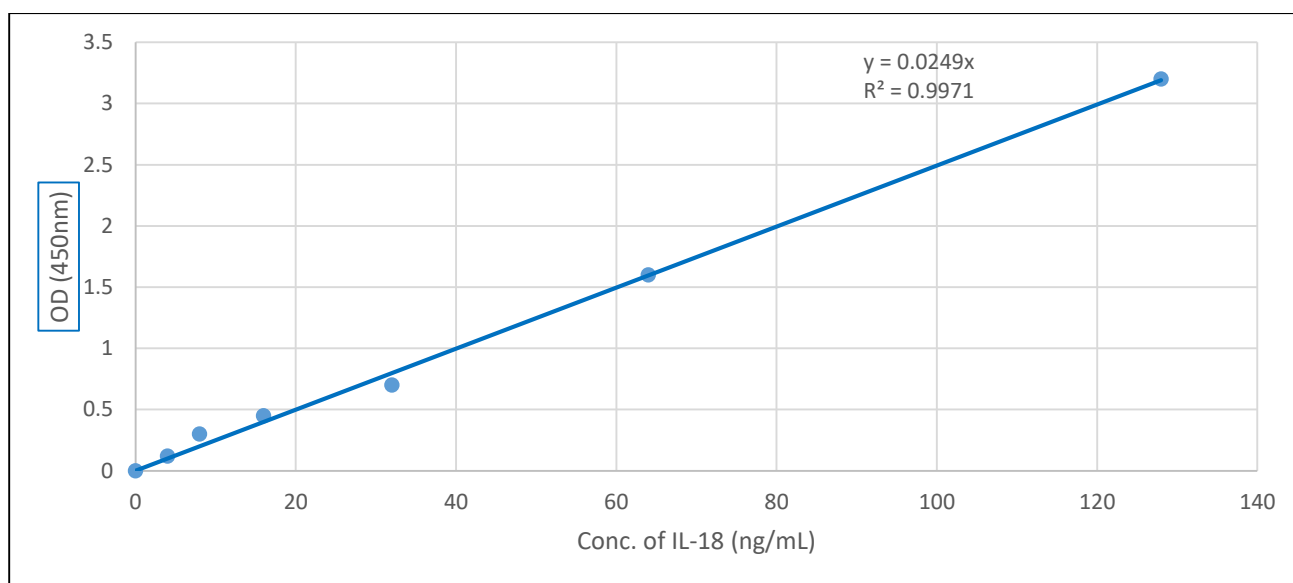


Figure (2.13): Standard curve of IL-18

2.4.3.4.3. Levels of Interleukin-37 (IL-37)**Principle:**

The provided kit is a Sandwich Enzyme-Linked Immunosorbent Assay (ELISA). The plate has been pre-coated with an antibody specific to Human IL37. The addition of IL37, which is present in the sample, results in its binding to the antibodies that are coated on the wells. Subsequently, the biotinylated Human IL37 Antibody is introduced into the sample, where it selectively interacts with IL37, forming a binding complex. Subsequently, the Streptavidin-HRP conjugate is introduced into the system, facilitating its binding to the Biotinylated IL37 antibody. Following the incubation period, any unbound Streptavidin-HRP is eliminated with a further washing procedure. Next, the

substrate solution is introduced, resulting in the development of color that is directly proportional to the quantity of Human IL37 present. The reaction is concluded by introducing an acidic stop solution, and the absorbance is then quantified at a wavelength of 450 nm (Al-Fartosy *et al.*, 2017a).

Reagents:

IL-37 ELISA kit components were listed in Table (2.23).

Table (2.23): Components of IL-37 ELISA kit

No.	Components	Quantity
1	Pre-coated ELISA Plate	12 x 8 well strips x 1
2	Standard Solution (480ng/mL)	0.5mL x 1
3	Standard diluent	3mL x 1
4	Streptavidin-HRP	6mL x 1
5	Stop solution	6mL x 1
6	Substrate solution A	6mL x 1
7	Substrate solution B	6mL x 1
8	Wash buffer Concentrate (25x)	20mL x 1
9	Biotinylated Human IL37 antibody	1mL x 1
10	Plate Sealers	2 pics
11	User instruction	1

Reagent Preparation:

1- Standard Solution: The 120 μ L of the standard solution with a concentration of 480ng/mL were mixed with 120 μ L of a standard diluent to create a standard stock solution with a concentration of 240ng/mL. Before making dilutions, the standard was given a 15-minute period of rest with mild agitation. The standard points were generated by sequentially diluting the standard stock solution (240ng/mL) at a 1:2 ratios with the standard diluent, resulting in solutions with concentrations of 120ng/mL, 60ng/mL,

30ng/mL, and 15ng/mL. The recommended procedure for diluting standard solutions is as shown in Table (2.24) and Figure (2.14):

Table (2.24): Standards dilution of IL-37

Concentration	Standard No.	Dilution Steps
240 ng/mL	Standard No.5	120 μ L Original standard + 120 μ L Standard diluent
120 ng/mL	Standard No.4	120 μ L Standard No.5 + 120 μ L Standard diluent
60 ng/mL	Standard No.3	120 μ L Standard No.4 + 120 μ L Standard diluent
30 ng/mL	Standard No.2	120 μ L Standard No.3 + 120 μ L Standard diluent
15 ng/mL	Standard No.1	120 μ L Standard No.2 + 120 μ L Standard diluent
0 ng/mL	Standard No.0	120 μ L Standard diluent

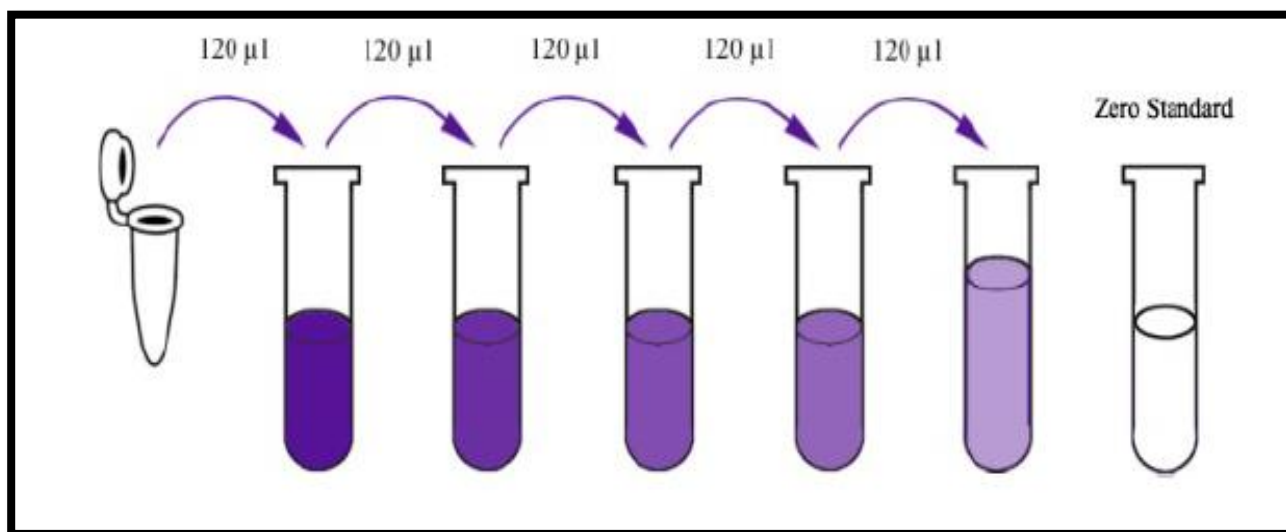


Figure (2.14): Standards solutions preparation of IL-37

2- Wash Buffer: A volume of 20 mL of wash buffer was used. A 25-fold dilution of Concentrate 25x was performed using distilled water, resulting in the production of 500 mL of 1x Wash Buffer.

Procedures:

- 1- Prior to usage, all components of the kit, including standards and samples, were equilibrated to room temperature, namely within the range of 20-25 °C.
- 2- The quantity of strips required for the test was ascertained and subsequently placed into the designated frames.
- 3- A volume of 50 µL of standard solution was introduced into the designated wells for the standards. The omission of antibody addition to the standard wells was due to the presence of biotinylated antibody within the standard solution.
- 4- Samples of 40 µL were introduced into the designated wells for analysis. Next, a volume of 10µL of Human IL37 antibody was introduced into the sample wells.
- 5- A volume of 50 µL of streptavidin-HRP was introduced into the wells containing the samples and standards, excluding the blank control well. The plate was coated with a sealing agent and subjected to incubation at a temperature of 37°C for a duration of 1 hour.
- 6- The sealer was detached, and thereafter, the plate underwent a series of five washes using wash buffer. The wells were immersed in 300 µL of wash buffer for a duration of 30 seconds to 1 minute for each washing step. The plate was transferred onto paper towels.
- 7- Each well was supplemented with 50 µL of substrate solution A. Subsequently, 50 µL of substrate solution B was introduced into each well. The plate was subjected to incubation at a temperature of 37°C in the absence of light, and subsequently sealed with a fresh sealer for a duration of 10 minutes.
- 8- A volume of 50 µL of Stop Solution was introduced into each well, resulting in an immediate color change from blue to yellow.
- 9- The optical density (OD) of each well was promptly measured using a microplate reader set to a wavelength of 450 nm within a time frame of 10 minutes subsequent to the addition of the stop solution.

Calculations:

The standard curve was constructed as per Figure (2.15):

1- The construction of the standard curve involved the plotting of the OD values for the IL-37 standards on the vertical axis, while the horizontal axis represented the concentrations of the IL-37 standards in ng/mL.

2- The mean absorbance values for both the standard and sample were computed and subsequently adjusted by subtracting the average OD of the zero standard.

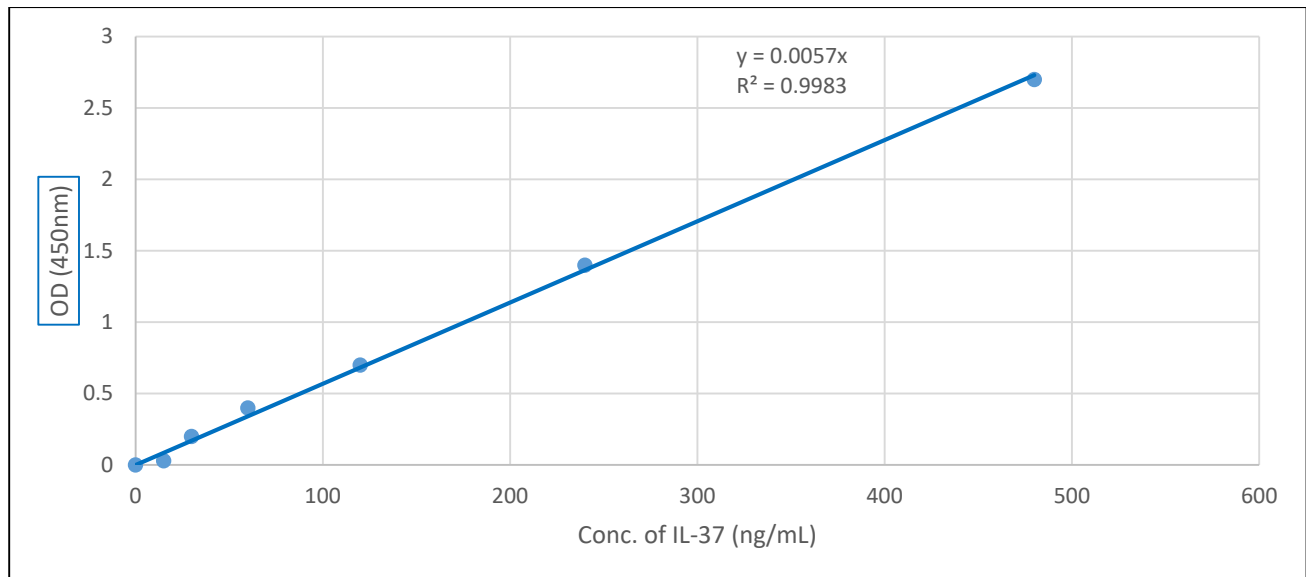


Figure (2.15): Standard curve of IL-37

2.4.3.4.4. Levels of Programmed Cell Death 1 (PD-1)

Principle:

The aforementioned kit is a Sandwich Enzyme-Linked Immunosorbent Assay (ELISA). The plate has been pre-coated with an antibody specific to Human PDCD1. The addition of PDCD1 in the sample results in its binding to the antibodies that are coated on the wells. Subsequently, the biotinylated Human PDCD1 Antibody is introduced into the sample, where it selectively associates with PDCD1. Subsequently, the Streptavidin-HRP conjugate is introduced and forms a complex with the Biotinylated PDCD1 antibody. Following the incubation period, any unbound Streptavidin-HRP is eliminated with a further washing procedure. Next, the substrate solution is introduced, resulting in the development of color that is directly proportional to the quantity of Human PDCD1 present. The reaction is concluded by the introduction

of an acidic stop solution, and the measurement of absorbance is performed at a wavelength of 450 nm (Zhang *et al.*, 2021a).

Reagents:

PD-1 ELISA kit components were listed in Table (2.25).

Table (2.25): Components of PD-1 ELISA kit

No.	Components	Quantity
1	Pre-coated ELISA Plate	12 x 8 well strips x 1
2	Standard Solution (64ng/mL)	0.5mL x 1
3	Standard diluent	3mL x 1
4	Streptavidin-HRP	6mL x 1
5	Stop solution	6mL x 1
6	Substrate solution A	6mL x 1
7	Substrate solution B	6mL x 1
8	Wash buffer Concentrate (25x)	20mL x 1
9	Biotinylated Human PD-1 antibody	1mL x 1
10	Plate Sealers	2 pics
11	User instruction	1

Reagent Preparation:

1- Standard Solution: The standard solution, consisting of 120 μ L, with a concentration of 64ng/mL, was mixed with an equal volume of standard diluent, resulting in a standard stock solution with a concentration of 32ng/mL. Prior to creating dilutions, the standard was allowed to rest for a duration of 15 minutes with gentle agitation. The standard points were generated by a sequential dilution process, whereby the standard stock solution (32ng/mL) was diluted at a ratio of 1:2 with a standard diluent. This resulted in the production of solutions with concentrations of 16ng/mL, 8ng/mL, 4ng/mL, and 2ng/mL. The suggested procedure for diluting standard solutions is as shown in Table (2.26) and Figure (2.16):

Table (2.26): Standards dilution of PD-1

Concentration	Standard No.	Dilution Steps
32 ng/mL	Standard No.5	120 μ L Original standard + 120 μ L Standard diluent
16 ng/mL	Standard No.4	120 μ L Standard No.5 + 120 μ L Standard diluent
8 ng/mL	Standard No.3	120 μ L Standard No.4 + 120 μ L Standard diluent
4 ng/mL	Standard No.2	120 μ L Standard No.3 + 120 μ L Standard diluent
2 ng/mL	Standard No.1	120 μ L Standard No.2 + 120 μ L Standard diluent
0 ng/mL	Standard No.0	120 μ L Standard diluent

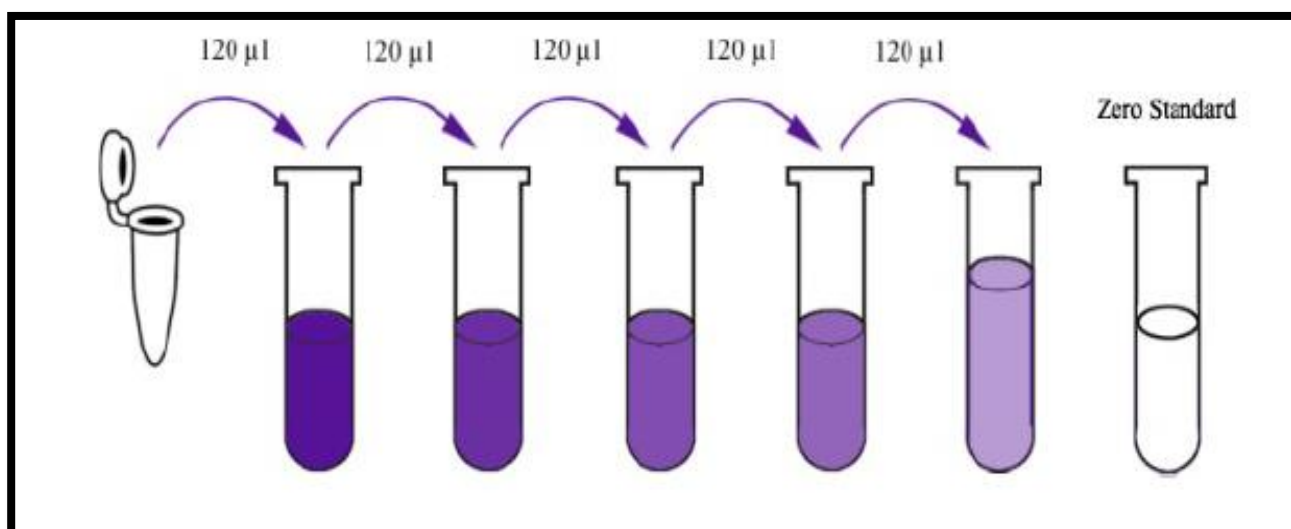


Figure (2.16): Standards solutions preparation of PD-1

2- Wash Buffer: A volume of 20 mL of wash buffer was used. A solution of Concentrate 25x was diluted with distilled water in order to produce a 1x Wash Buffer with a final volume of 500 mL.

Procedures:

1- Prior to use, all components of the kit, including standards and samples, were equilibrated to room temperature, namely within the range of 20-25 °C.

- 2- The quantity of strips required for the test was ascertained and subsequently placed into the designated frames.
- 3- A volume of 50 μL of standard solution was introduced into the designated wells for standards. The omission of antibody addition to the standard wells was due to the presence of biotinylated antibody within the standard solution.
- 4- Sample wells were supplemented with 40 μL samples. Next, a volume of 10 μL of Human PD-1 antibody was introduced into the sample wells.
- 5- A volume of 50 μL of streptavidin-HRP was introduced into the wells containing the samples and standards, excluding the blank control well. The plate was coated with a sealing agent and subjected to incubation for a duration of 1 hour at a temperature of 37°C.
- 6- The sealer was subsequently detached, and the plate underwent a total of five washes with wash buffer. The wells were immersed in 300 μL of wash buffer for a duration of 30 seconds to 1 minute for each washing step. The plate was transferred onto absorbent paper towels.
- 7- Each well was supplemented with 50 μL of substrate solution A. Subsequently, 50 μL of substrate solution B was introduced into each well. The plate was subjected to incubation at a temperature of 37°C in a dark environment, and subsequently, a fresh sealer was applied, with a duration of 10 minutes.
- 8- A volume of 50 μL of Stop Solution was introduced into each well, resulting in an immediate color change from blue to yellow.
- 9- The optical density (OD) of each well was promptly measured using a microplate reader set to 450 nm within a time frame of 10 minutes subsequent to the addition of the stop solution.

Calculations:

The standard curve was constructed as per Figure (2.17):

- 1- The construction of the standard curve involved the plotting of the OD values for the PD-1 standards on the vertical axis, while the concentrations of the PD-1 standards in ng/mL were plotted on the horizontal axis.

2- The mean absorbance values for both the standard and sample were computed and then adjusted by subtracting the average OD of the zero standard.

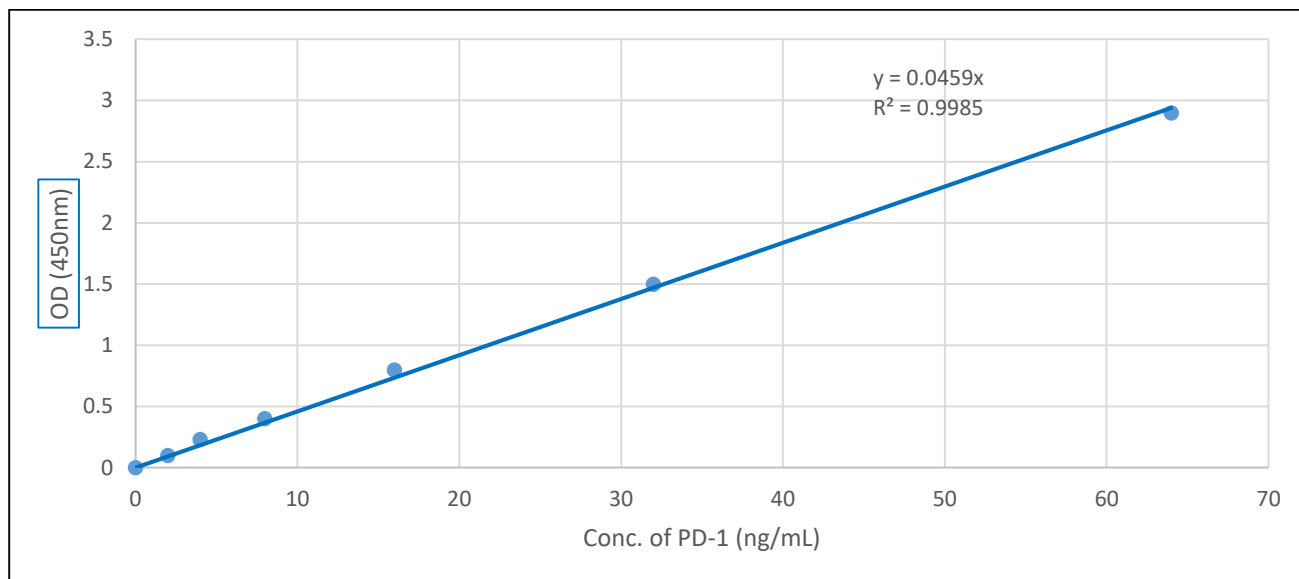


Figure (2.17): Standard curve of PD-1

2.4.4. Genetic Study

2.4.4.1. DNA Extraction

The DNA extraction procedure was carried out following the protocol provided by the G-spin DNA extraction kit as shown in Table (2.27) (Davarpناه *et al.*, 2020).

Table (2.27): Components of G-spin DNA extraction kit

No.	Label	Contents 50 Columns
1	Buffer CL	25 mL
2	Buffer BL	25 mL
3	Buffer WA	40 mL
4	Buffer WB	10 mL
5	Buffer CE	10 mL
6	Spin Column / Collection Tube	50 ea
7	RNase A (Lyophilized powder)	3 mg x 1 vial
8	Proteinase K (Lyophilized powder)	22 g x 1 vial

The DNA extraction process involved the isolation of DNA from whole blood, following the procedure outlined below (Alaanzy *et al.*, 2020; Sam *et al.*, 2021; Kholis *et al.*, 2023):

- 1- A volume of 200 μL of blood culture was transferred using a pipette into a micro-centrifuge tube with a capacity of 1.5 mL.
- 2- A volume of 20 μL of Proteinase K and 5 μL of Ribonuclease RNase A Solution were introduced into the sample tube and thereafter mixed with care.
- 3- A volume of 200 μL of Buffer BL was introduced into the upper sample tube and subsequently mixed in a thorough manner. To prevent potential genomic DNA damage, any intense vortexing was deliberately avoided. The lysate underwent incubation at a temperature of 56°C for a duration of 10 minutes. To achieve full lysis, it is recommended to mix the contents of the tube by inverting it three to four times throughout the incubation period. The 1.5 mL tube was subjected to centrifugation in order to eliminate any residual liquid adhering to the inner surface of the tube's rim.
- 4- A volume of 200 μL of 100% ethanol was introduced into the lysate and well mixed with gentle inversion for 5-6 repetitions or by pipetting without vortexing. Following the mixing process, the 1.5 mL tube was subjected to a brief centrifugation step in order to eliminate any residual droplets present on the inside surface of the lid.
- 5- The mixture from step 4 was meticulously transferred to the Spin Column using a 2 mL Collection Tube, ensuring that the rim remained dry. Subsequently, the cap was securely secured, and the sample was subjected to centrifugation at a speed of 13,000 RPM for a duration of 1 minute. The filtrate and the Spin Column, which were both situated within a 2 mL Collection Tube, were disposed of.
- 6- A volume of 700 μL of Buffer WA was introduced into the Spin Column, ensuring that the rim was not wetted, followed by centrifugation at a speed of 13,000 RPM for a duration of 1 minute. The flow-through and reuse of the Collection Tube were deemed as not viable and were subsequently discarded.
- 7- A volume of 700 μL of Buffer WB was introduced into the Spin Column, ensuring that the rim remained dry, followed by centrifugation at a speed of 13,000 RPM for a

duration of 1 minute. The flow-through was discarded and the Column was transferred into a 2 mL Collection Tube (for reuse). Subsequently, the sample was centrifuged for an additional 1 minute to remove any remaining moisture from the membrane. Both the flow-through and collection tube were completely discarded. A volume of 40 (160) mL of 100% ethanol was added to Buffer IWB.

8- The Spin Column was inserted into a novel 1.5 mL tube (not included), and a volume ranging from 30 to 100 μ L of Buffer CE was applied directly onto the membrane. The sample was incubated at room temperature for a duration of 1 minute, followed by centrifugation at a speed of 13,000 RPM for 1 minute in order to elute.

2.4.4.2. Agarose Gel Electrophoresis of DNA

Electrophoresis is commonly employed for the purpose of identifying DNA fragments subsequent to the extraction process, or to ascertain the conclusion of polymerase chain reaction (PCR) interaction in the presence of standard DNA, hence enabling the differentiation of bundle sizes in the resulting PCR interaction products on the agarose gel (Kono *et al.*, 2021).

2.4.4.2.1. Preparation of the Agarose Gel

According to multiple studies, the agarose gel was prepared with a 0.8 % concentration by dissolving 0.8 g of agarose in 100 ml of TBE buffer that had been prepared beforehand (Leonardi *et al.*, 2018; Lee and Song, 2020). The agarose solution was subjected to boiling followed by gradual cooling to a temperature range of 45-50°C. The gel was carefully poured into the pour plate, which had been previously prepared with an agarose support. Prior to pouring, a comb was fixed onto the plate to create wells that would accommodate the samples (El-Sayed *et al.*, 2018). The gel was carefully poured in order to minimize the formation of air bubbles and subsequently allowed to cool for a duration of 30 minutes. The comb was delicately extracted from the solid agarose (Shi *et al.*, 2017). The plate was affixed to its stand within the horizontal electrophoresis unit, which was comprised of the tank employed in the electrophoresis process. The tank has been filled with Tris-Borate-EDTA (TBE) buffer, which has been used to completely cover the surface of the gel (Italiani *et al.*, 2018).

2.4.4.2.2. Preparation of the Sample

A volume of 3 μL of the processor loading buffer (Intron / Korea) was combined with 5 μL of the DNA sample intended for electrophoresis (loading dye). Following the mixing step, the resulting mixture was loaded into the wells of the gel (Durcan and Petri, 2020). An electric current with a voltage of 5 V was applied for a duration of 1 hour until the migration of the tincture was observed to have occurred over the gel. The gel was subjected to UV irradiation at a wavelength of 336 nm after being immersed in a pool containing 30 μL of Red Safe Nucleic Acid Staining Solution and 500 mL of distilled water (Al-Fartosy *et al.*, 2019).

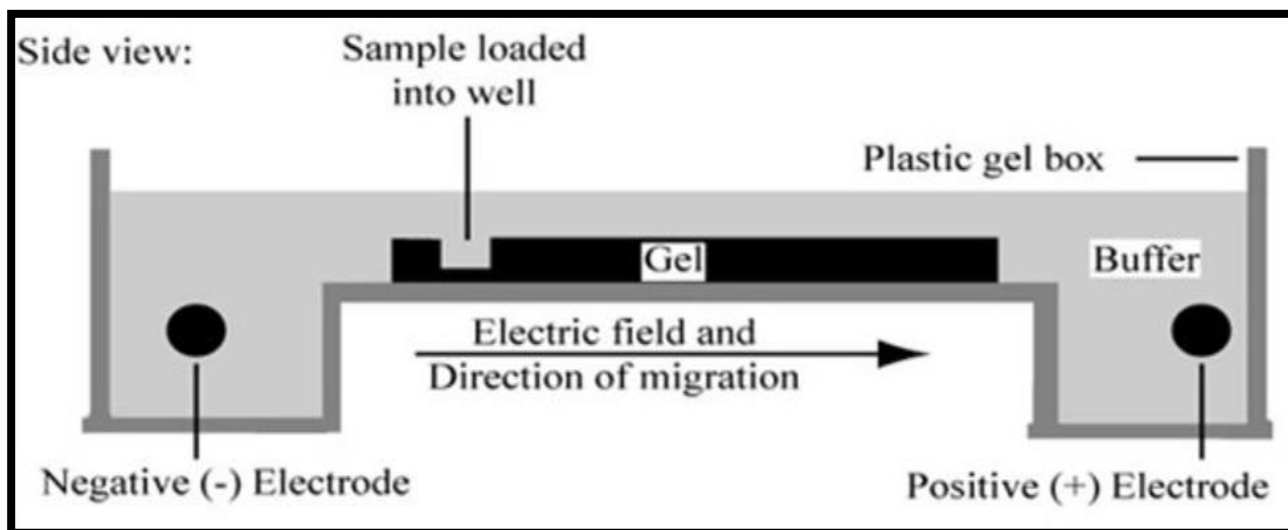


Figure (2.18): Working of the electrophoresis system (Zappulo *et al.*, 2022).

2.4.4.3. Measurement of DNA Concentration and Purity

The concentration and purity of the extracted DNA were assessed using a nanodrop spectrophotometer (Quawell/Hong Kong). A volume of 2 μL of DNA was applied to the spectrophotometer lens and measured at a wavelength of 260/280 nm (Zhang *et al.*, 2022). The resulting data was displayed on a laptop screen connected to the nanodrop instrument. The nanodrop lens was cleansed using distilled water (DW) and a cotton swab after each sample, while the remaining samples were subsequently quantified (Han *et al.*, 2019).

2.4.4.4. The Primers Used in the Interaction

The primers underwent lyophilization and were subsequently reconstituted in deionized water to achieve a final concentration of 100 pmol/ μ L as a stock solution, as shown in Table (2.28). This stock solution was stored at -20°C . To prepare a working primer suspension with a concentration of 10 pmol/ μ L, 10 μ L of the stock solution was combined with 90 μ L of deionized water, resulting in a final volume of 100 μ L (Liao *et al.*, 2017). The primer quality was assessed by IDT (Integrated DNA Technologies company, USA).

Table (2.28): The specific primer PD-1gene (Lin *et al.*, 2021)

Primer	Sequence	Tm ($^{\circ}\text{C}$)	GC (%)	Product Size
Forward	5'-ACAATAGGAGCCAGGCGCA-3'	61	58	695 bp
Reverse	5'-GGGTCCTCCTTCTTTGAGG-3'	60.7	58	

2.4.4.5. Maxime PCR PreMix Kit (i-Taq) 20 μ lrxn

The Maxime PCR PreMix Kit offered by Intron includes a range of PreMix kits designed for different experimental purposes, as well as a 2X Master mix solution as demonstrated in Table (2.29). The Maxime PCR Pre Mix Kit (i-Taq) is a product that combines all necessary components, including i-Taq DNA polymerase, dNTP mixture, reaction buffer, and others, into a single tube for performing one reaction of PCR. This particular device has been designed to yield optimal outcomes while providing the utmost convenience with its integrated system (Al-Fartosy *et al.*, 2020b). One primary rationale is because it encompasses all essential elements required for PCR, namely a template DNA, a primer set, and distilled water. One additional factor is the inclusion of a gel loading buffer for the purpose of conducting electrophoresis. This feature renders it appropriate for a wide range of sample experiments, owing to its expedient and straightforward utilization technique (Smeets *et al.*, 2023).

Table (2.29): The Components of the Maxime PCR PreMix kit (i-Taq)

Material	Volume
i-Taq DNA Polymerase	5 U/ μ L
dNTPs	2.5 mM
Reaction buffer (10X)	1X
Gel loading buffer	1X

2.4.4.6. Diagnosis of PD-1 Gene

Tables (2.30) and (2.31) explain the mixture of the specific interaction for detection PD-1 gene and the optimum condition of detection PD-1 gene, respectively.

Table (2.30): Mixture of the specific interaction for detection PD-1 gene

Components	Volume
Taq PCR Pre Mix	5 μ L
Forward primer	10 picomols / μ L (1 μ L)
Reverse primer	10 picomols / μ L (1 μ L)
DNA	1.5 μ L
Distill water	16.5 μ L
Final volume	25 μ L

Table (2.31): The optimum condition of detection PD-1 gene (Saha *et al.*, 2021)

No.	Step	Tm ($^{\circ}$ C)	Time	No. of Cycles
1	Initial Denaturation	95	5 min	1
2	Denaturation-2	95	30 sec	35
3	Annealing	61	40 sec	
4	Extension-1	72	40 sec	
5	Extension-2	72	5 min	1

2.5. Statistical Analysis

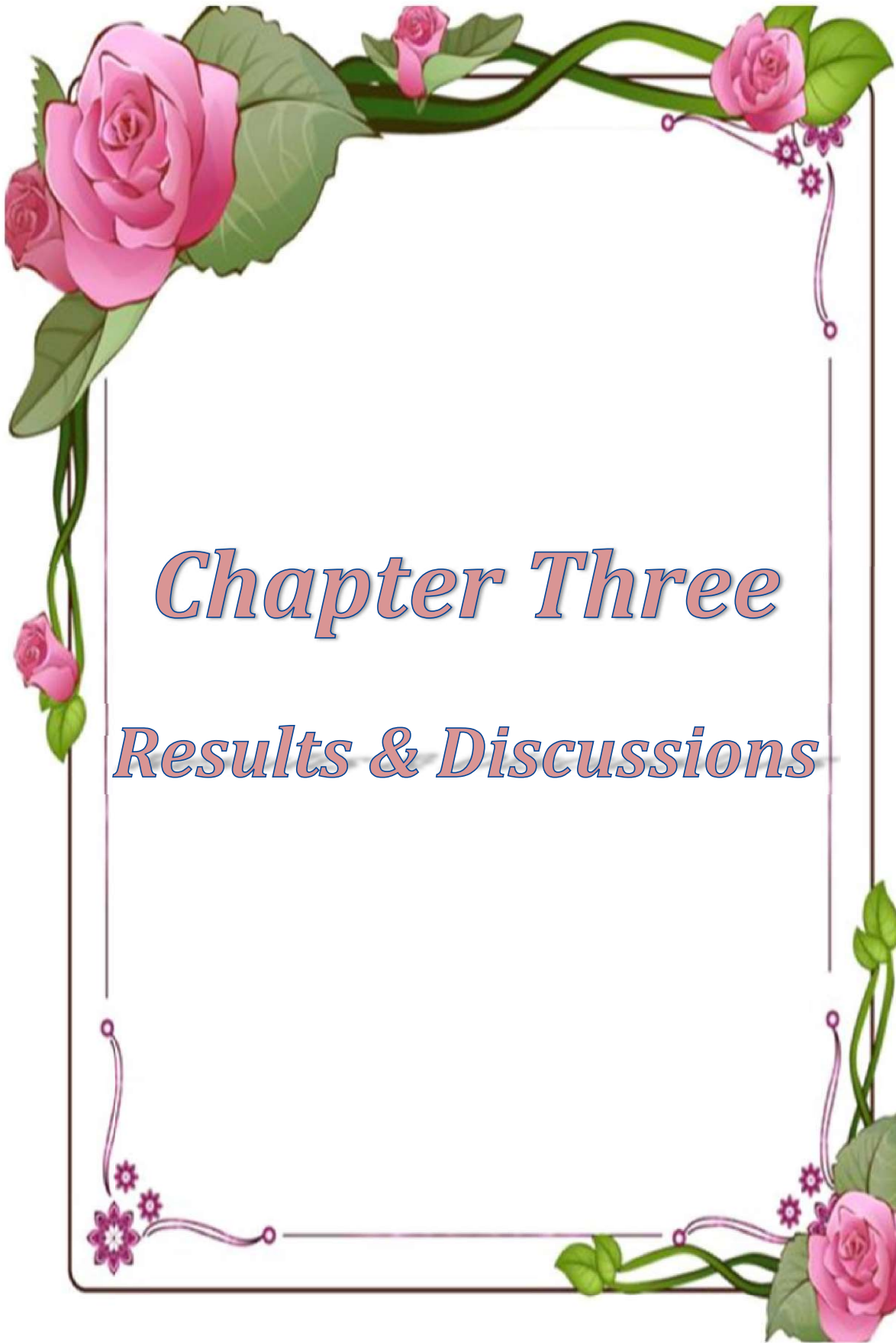
The statistical analysis was conducted using version 26 of the Statistical Package for the Social Sciences (SPSS) developed by IBM Corporation, located in Armonk, NY, USA. The data was distributed in a typical manner, and the analysis of variances was employed to compare the groups prior to conducting Dunnett's t-test in order to ascertain the statistical significance (Uciechowski and Dempke, 2020). The sensitivities and specificities, together with the corresponding 95% confidence interval (CI), were computed using the receiver operating characteristics (ROC) curve. This curve was generated by graphing sensitivity on the y-axis versus 1-specificity on the x-axis, and the area under the ROC curve (AUC) was determined (Chen *et al.*, 2018b). The Pearson correlation method was employed to establish the correlations. The values of one group frequently exhibited greater (or lesser) magnitudes in compared to the values of the reference group. A significance level of $p < 0.05$ was considered to be statistically significant, while a significance level of $p < 0.01$ was considered to be very significant. Additionally, AUC value that is close to 0 or 1 indicates a strong diagnostic value (Al-Fartosy and Mohammed, 2017c).

The frequencies of categorical data, specifically genotypes and alleles, were determined and analyzed for adherence to the Hardy-Weinberg equilibrium (HWE). The genotyping and allele frequencies of the PD-1 gene were assessed and compared among different groups using a chi-square test. The present study examines the odds ratio (OR) and corresponding 95%CI. The HWE is a mathematical formula utilized for the estimation of genotypes and allele frequencies (Gao *et al.*, 2017b). The mathematical explanation is provided by the following equation:

$$p^2 + 2pq + q^2 = 1$$

The variable p denotes the frequency of the major allele, while the variable q represents the frequency of the minor allele. The HWE is a statistical model that allows for the estimation of genotype and allele frequencies within a population. It also provides a means to analyze the degree to which a population deviates from HWE (Yap *et al.*,

2018). This assessment is often conducted by comparing the observed genotypes with the expected genotypes using a chi-square test. If the calculated p-value is less than 0.05, it indicates a significant divergence from the HWE. If the calculated p-value is greater than 0.05, it indicates that there is no significant deviation from the HWE for the mean (Wasen *et al.*, 2018).



Chapter Three

Results & Discussions

Chapter Three

3.1. Basic Characteristics of Individuals in the Present Study

A total of 43 female patients diagnosed with SLE were chosen as participants for this research investigation. A total of 53 apparently healthy female controls were selected to match with the patients. Table (3.1) presents the overall characteristics of the subjects that participated in the current investigation.

Table (3.1): The demographic characteristics of the present study

The Characteristics		SLE Patients	Healthy Control Group
Total Subjects No.		43	53
Age (Years) (Mean±SD)		35.44 ± 4.85	34.29 ± 5.19
BMI (Kg/m ²)		23.92 ± 0.13	23.99 ± 0.86
SLE Duration (Years) (Mean±SD)		0.99 ± 0.24	0
SLEDAI		2.75 ± 1.22	0
Demographic Area	Urban	34	45
	Rural	9	8
Educational Background	Learned	37	41
	Illiterate	6	12
Smoking Habits	Positive	0	0
	Negative	43	53
Food Habits	Vegetarian	32	43
	Non-Vegetarian	11	10
Employment Status	Employed	29	37
	Not Employed	14	16

Data are presented as mean ± SD, SD: Standard Deviation, BMI: Body Mass Index, SLEDAI: Systemic Lupus Erythematosus Disease Activity Index.

The data given in the current study indicated that both the sick group and the healthy control group consisted exclusively of individuals who did not smoke. Moreover, the majority of the participants, including both sick and healthy controls, resided in urban areas. Additionally, all participants possessed a high level of education and were employed in favourable work environments. There exist significant disparities between urban and rural places, primarily characterised by discrepancies in

environmental conditions, pollution levels, social dynamics, psychological factors, genetic factors, dietary patterns, and other factors. These gaps are notably escalating in urban regions (Brookes and Power, 2022). Additionally, it can be shown from Table (3.1) that the majority of the participants in both the SLE group and the healthy control group were residents of the Basrah Province. Hence, the findings of our study may not accurately reflect the overall condition of patient groups in Iraq, primarily due to the limited participation of patients from Al-Basrah, Al-Sadr, Al-Mawany, and Al-Fayhaa teaching hospitals. This limitation is attributed to the relatively low number of patients attending these hospitals and their willingness to actively participate in our research.

3.2. Total Parameters in this Study

Table (3.2) shows the levels of all parameters were measured in this work.

Table (3.2): Levels of total parameters measured in the present study for SLE patients and the apparently control group

The Characteristics	SLE Patients	Healthy Control	P-Value
	N = 43 (Women)	N = 53 (Women)	
	Mean ± SD	Mean ± SD	
C3 (g/L)	0.85 ± 0.39 **	1.63 ± 0.20	<0.01
C4 (g/L)	0.29 ± 0.12 **	0.44 ± 0.17	<0.01
CH50 (IU/mL)	51.46 ± 15.24 **	81.69 ± 8.99	<0.01
MDA (µmol/L)	2.49 ± 0.75 **	0.87 ± 0.15	<0.01
TAC (pg/mL)	1.62 ± 0.40 **	2.19 ± 0.46	<0.01
CRP (mg/dL)	10.77 ± 4.83 **	0.17 ± 0.04	<0.01
ANA (IU/mL)	2.39 ± 0.73 **	0.98 ± 0.31	<0.01
Anti-dsDNA (IU/mL)	28.22 ± 6.38 **	15.63 ± 2.47	<0.01
Urea (mg/dL)	54.98 ± 12.60 **	28.27 ± 7.40	<0.01
Creatinine (mg/dL)	1.07 ± 0.18 **	0.70 ± 0.10	<0.01
GFR (mL/min/1.73 m²)	61.89 ± 18.66 **	99.53 ± 18.77	<0.01
IL-18 (pg/mL)	301.61 ± 72.51 **	92.83 ± 23.78	<0.01
IL-37 (pg/mL)	209.42 ± 59.50 **	51.28 ± 6.95	<0.01
PD-1 (pg/mL)	779.14 ± 346.89 **	127.68 ± 24.56	<0.01

Data are presented as mean ± SD; SD: standard deviation; N: no. of subjects; C3: complement component 3; C4: complement component 4; CH50: complement hemolytic 50; MDA: malondialdehyde; TAC: total antioxidant capacity; CRP: C-reactive protein; ANA: antinuclear antibodies; Anti-dsDNA: anti-double-stranded DNA; GFR: glomerular filtration rate; IL: interleukin; PD-1: programmed death-1; p-value (Non-Significant [p>0.05], A * indicated Significant [p<0.05], A ** indicated High Significant [p<0.01]) indicated the level of significance in comparison with the corresponding control value.

3.3. Levels of Body Mass Index (BMI)

The current investigation demonstrated a lack of statistically significant alteration ($p > 0.05$) in body mass index (BMI) values among patients with SLE as compared to the control group (23.92 ± 0.13 vs. 23.99 ± 0.86 kg/m²), as depicted in Table (3.3) and Figure (3.1).

Table (3.3): Levels of BMI in SLE patients and control group

		BMI (kg/m ²)	
		SLE Patients (N = 43)	Healthy Control (N = 53)
Mean ± SD		23.92 ± 0.13	23.99 ± 0.86
SE		0.02	0.12
Range		23.71 - 24.13	21.01 - 24.53
95% CI	Lower	23.88	23.76
	Upper	23.96	24.23

Data are presented as mean ± SD, SD: Standard Deviation, SE: Standard Error, Range: is the difference between the highest and lowest values in the set, 95% CI: Confidence Intervals (Lower and Upper), p-value (Non-Significant [$p > 0.05$], A * indicated Significant [$p < 0.05$], A ** indicated High Significant [$p < 0.01$]) indicated the level of significance in comparison with the corresponding control value.

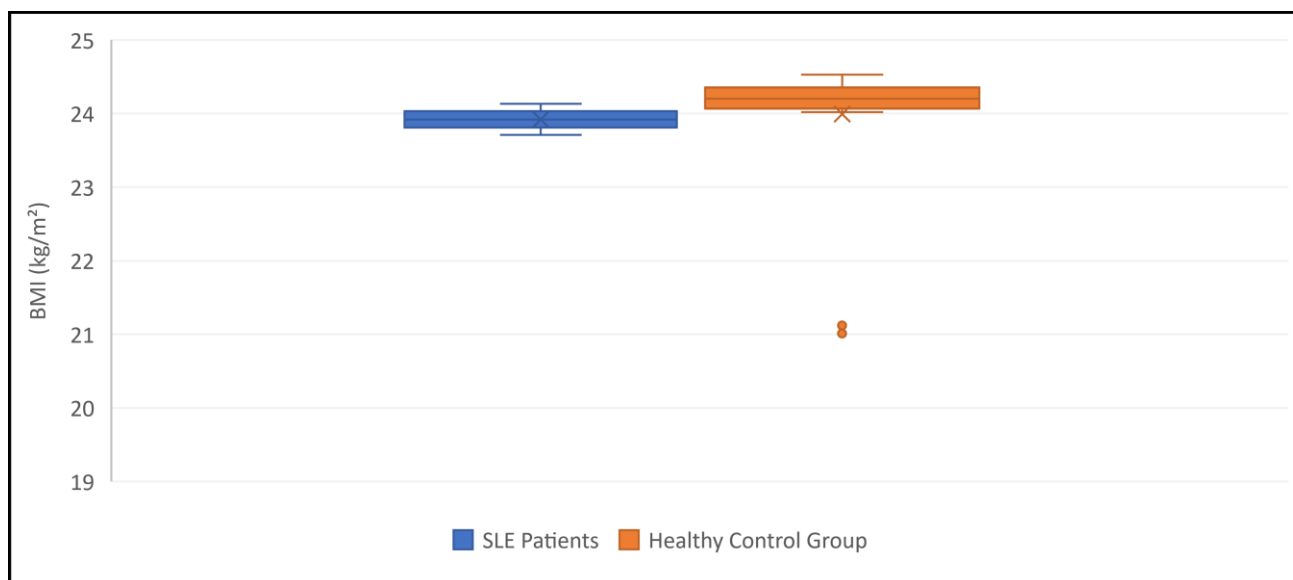


Figure (3.1): Comparison of BMI level between SLE patients and healthy control group.

Obesity, as characterized by a body mass index (BMI) equal to or exceeding 30 kg/m², continues to be a significant health concern in the USA and other Western nations. Based on data from the National Health and Nutrition Examination Survey (NHANES), there has been a persistent upward trend in the prevalence of obesity over the course of several decades. Specifically, the rates of obesity were recorded at 22.5% during the period of 1988-1994, 30.6% during 1999-2002, and 37.9% during 2013-2014 (Beberashvili *et al.*, 2023).

The measurement of obesity is commonly assessed by the utilisation of a straightforward anthropometric indicator known as BMI. This index is computed by dividing an individual's weight (in kilogrammes) by the square of their height (in metres squared, m²). Consequently, BMI can be employed as a tool to ascertain the level of glycaemic control (Ali *et al.*, 2021a). The presence of excess body fat has been widely linked to a condition characterized by modified immune function and persistent low-level inflammation. The identification of adipokines, which are soluble inflammatory mediators synthesized by adipocytes, has provided valuable insights into the underlying mechanisms connecting obesity and autoimmune disorders (Ahmad *et al.*, 2022).

In the context of SLE, it has been observed that the adipokine known as leptin has a role in enhancing the viability of autoreactive T lymphocytes, while concurrently diminishing the population of regulatory T cells (Treg cells) in murine models. Notwithstanding these findings, the association between obesity and SLE continues to be a subject of debate and disagreement among the academic community (Hanna Kazazian *et al.*, 2019). Numerous clinical investigations have shown a correlation between obesity and an increased susceptibility to renal impairment, namely LN (Dall'Ara *et al.*, 2018; Fanouriakis *et al.*, 2019). Additionally, obesity has been associated with an elevated burden of atherosclerosis, impaired neurocognitive function, reduced physical activity, heightened fatigue, and a deterioration in the overall quality of life among individuals diagnosed with SLE. The significance of these findings lies in the fact that obesity is more commonly detected in individuals with SLE,

and cardiovascular disease (CVD) continues to be the primary cause of death in this population (Yin *et al.*, 2020). Nevertheless, research examining the precise correlation between heightened adiposity and disease activity in SLE has revealed no discernible link between the two variables. The study in question had a notable limitation in that it solely relied on a tiny sample size comprising participants from a singular ethnic background (Bellan *et al.*, 2020). The analysis of another study has revealed a significant independent association between a normal BMI level and increased disease activity in individuals with SLE. This discovery holds significant clinical significance, as it indicates that addressing increased adiposity could serve as a possible target or supplementary preventive strategy for enhancing outcomes in individuals with SLE (Islam *et al.*, 2019).

3.4. Biochemical Parameters

3.4.1. Levels of Complement Components

The present study showed a high significant decrease ($p < 0.01$) in complement component 3 (C3), complement component 4 (C4) and complement hemolytic 50 (CH50) levels in SLE patients compared to control group (0.85 ± 0.39 vs. 1.63 ± 0.20 g/L), (0.29 ± 0.12 vs. 0.44 ± 0.17 g/L) and (51.46 ± 15.24 vs. 81.69 ± 8.99 IU/mL) respectively, as illustrated in Table (3.4) and Figure (3.2).

Table (3.4): Levels of C3, C4 and CH50 in SLE patients and control group

Marker	SLE Patients (N = 43)					Healthy Control (N = 53)				
	Mean \pm SD	SE	Range	95% CI		Mean \pm SD	SE	Range	95% CI	
				Lower	Upper				Lower	Upper
C3 (g/L)	$0.85 \pm$ 0.39 **	0.06	0.37 – 1.93	0.73	0.97	$1.63 \pm$ 0.20	0.03	1.30 – 1.98	1.57	1.68
C4 (g/L)	$0.29 \pm$ 0.12 **	0.02	0.11 – 0.63	0.25	0.32	$0.44 \pm$ 0.17	0.02	0.21 – 0.83	0.40	0.49
CH50 (IU/mL)	$51.46 \pm$ 15.24 **	2.32	37.62 – 97.03	46.77	56.15	$81.69 \pm$ 8.99	1.24	65.13 – 97.03	79.21	84.17

Data are presented as mean \pm SD, SD: Standard Deviation, SE: Standard Error, Range: is the difference between the highest and lowest values in the set, 95% CI: Confidence Intervals (Lower and Upper), p-value (Non-Significant [$p > 0.05$], A * indicated Significant [$p < 0.05$], A ** indicated High Significant [$p < 0.01$]) indicated the level of significance in comparison with the corresponding control value.

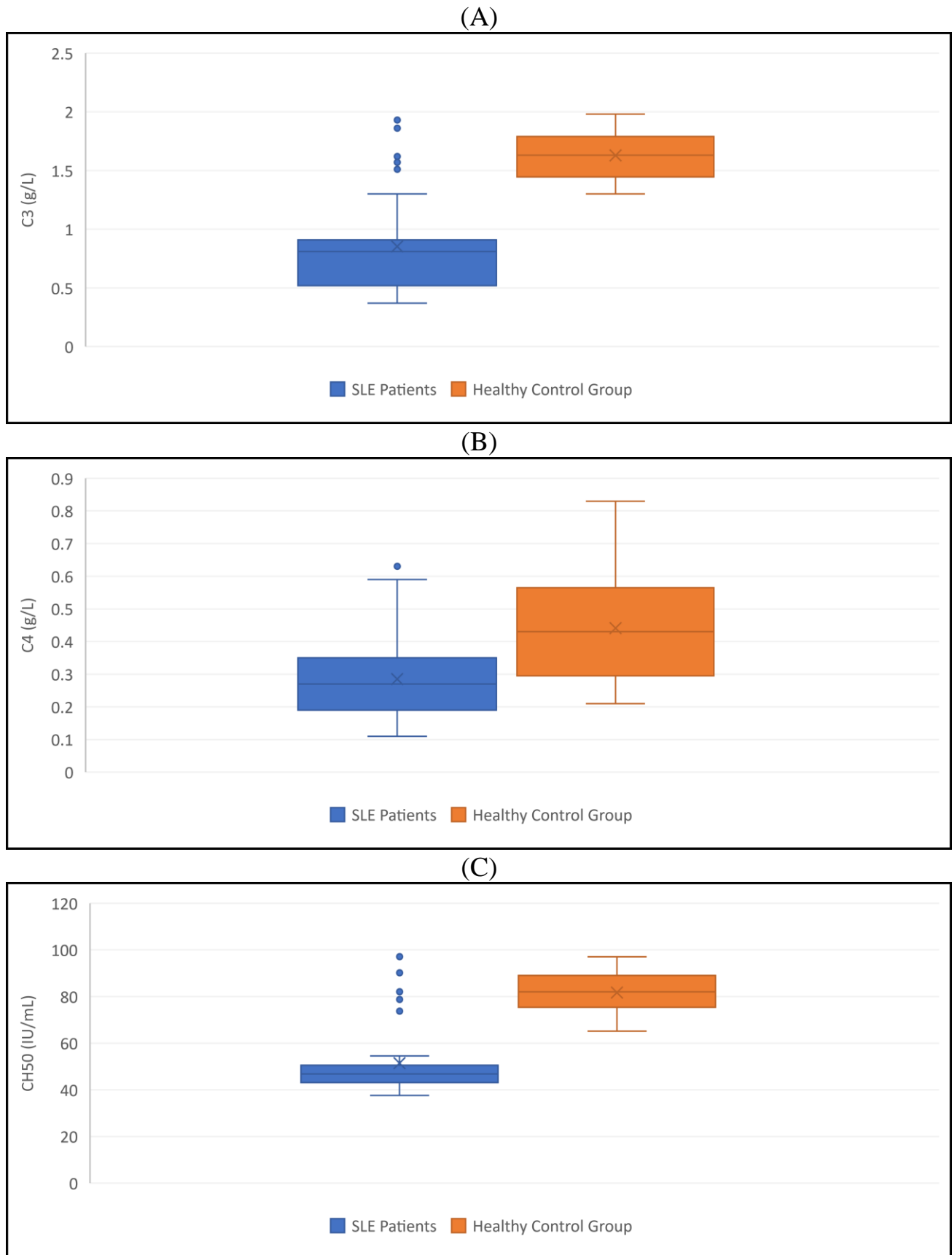


Figure (3.2): Comparison of complement components levels between SLE patients and healthy control group: (A) C3; (B) C4; (C) CH50.

Complement component 3 (C3) and complement component 4 (C4) are proteins that constitute essential components of the immune system and are predominantly present in the bloodstream. The entity in question is widely acknowledged as a fundamental element of the complement system, fulfilling pivotal functions in both immune response and inflammation (Diaz-Rizo *et al.*, 2017). The CH50 (Complement Hemolytic 50) is not a discrete chemical entity or molecule possessing a distinct chemical composition. Instead, it serves as a functional assay or examination employed to quantify the functionality of the complement system, an intricate assemblage of proteins presents in the bloodstream (Al-Fartosy *et al.*, 2020b). CH50 test evaluates the functional efficacy of the classical complement pathway, which encompasses a series of proteins that interact to execute immunological responses and facilitate the death of target cells, such as bacteria or cells coated with antibodies (Dini *et al.*, 2017).

The observed reduction in complement component levels among individuals with SLE in our study may be attributed to heightened activation of the complement system. The activation of the complement cascade can occur through the interaction of ICs, which are produced by the binding of antibodies to self-antigens (Fujita, 2017). These ICs are commonly observed in individuals with SLE. The activation of the complement system results in the depletion of complement components by their cleavage into active fragments. The act of consuming excessive amounts of complement components can result in a decrease in the quantities of these components in circulation (Silverman, 2019).

In addition, under the context of SLE, immune complexes that consist of autoantibodies and self-antigens have the ability to accumulate in different tissues, with a particular affinity for the kidneys and the skin. This phenomenon can lead to the regional activation of the complement system, leading to the attachment and subsequent reduction of complement components in the bloodstream (Moon *et al.*, 2020). Additionally, it has been observed that individuals diagnosed with SLE may experience renal impairment (LN), resulting in the excretion of complement components in the

urine. This phenomenon has the potential to further exacerbate the depletion of complement components inside the circulatory system (He *et al.*, 2020).

Furthermore, SLE has the potential to impact both the generation and functionality of complement proteins. Certain individuals with SLE may have a decrease in the production of complement components. This can occur as a result of autoantibodies specifically targeting complement components or owing to inflammation and tissue damage affecting the liver, which is the site of synthesis for complement proteins (Chen *et al.*, 2018b). Similarly, several patients diagnosed with SLE exhibit the production of autoantibodies that selectively attack complement components. The presence of these autoantibodies can result in the subsequent destruction and depletion of the target, hence causing a further reduction in its concentration within the serum (Belmokhtar *et al.*, 2022).

Moreover, it should be noted that genetic differences in complement proteins or their regulators have the potential to render individuals more vulnerable to SLE and exert an impact on complement activity. Certain genetic variants have the potential to increase an individual's susceptibility to decreased levels of complement components in the context of SLE (Zhang *et al.*, 2020).

The decrease in levels of complement components in our study can potentially contribute to the immunological dysregulation observed in patients with SLE, hence resulting in the emergence of clinical symptoms and organ damage (van der Meulen *et al.*, 2019). SLE has the potential to impact the synthesis and efficacy of complement proteins. In certain instances, autoimmune reactions, inflammation, or liver impairment might lead to a diminished production of complement components, which are synthesized in the liver (Lambring *et al.*, 2019).

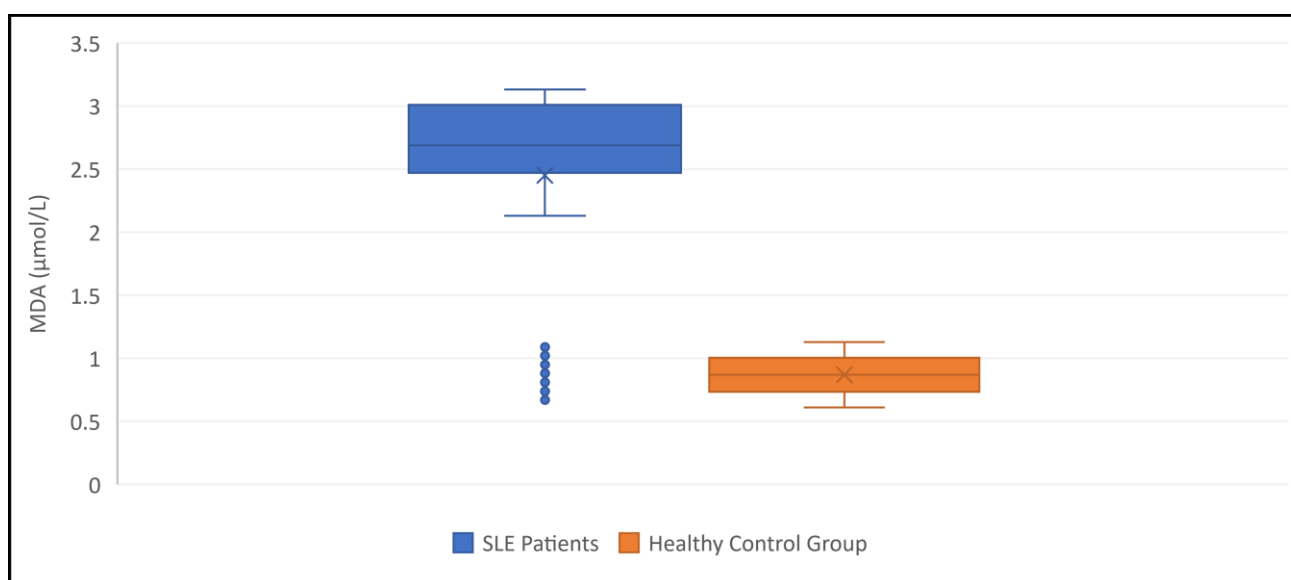
3.4.2. Levels of Malondialdehyde (MDA)

The present study showed a high significant increase ($p < 0.01$) in malondialdehyde (MDA) levels in SLE patients compared to control group (2.49 ± 0.75 vs. 0.87 ± 0.15 $\mu\text{mol/L}$) as illustrated in Table (3.5) and Figure (3.3).

Table (3.5): Levels of MDA in SLE patients and control group

		MDA ($\mu\text{mol/L}$)	
		SLE Patients (N = 43)	Healthy Control (N = 53)
Mean \pm SD		2.49 \pm 0.75 **	0.87 \pm 0.15
SE		0.11	0.02
Range		0.67 – 3.13	0.61 – 1.13
95% CI	Lower	2.22	0.83
	Upper	2.68	0.91

Data are presented as mean \pm SD, SD: Standard Deviation, SE: Standard Error, Range: is the difference between the highest and lowest values in the set, 95% CI: Confidence Intervals (Lower and Upper), p-value (Non-Significant [$p > 0.05$], A * indicated Significant [$p < 0.05$], A ** indicated High Significant [$p < 0.01$]) indicated the level of significance in comparison with the corresponding control value.

**Figure (3.3): Comparison of MDA levels between SLE patients and healthy control group.**

Malondialdehyde (MDA) is an organic molecule that exists as a colourless liquid and has the nominal chemical formula $\text{CH}_2(\text{CHO})_2$. MDA is a molecule with strong reactivity, existing predominantly in the enol form. The phenomenon arises spontaneously and serves as an indicator for the presence of oxidative stress and lipid peroxidation (Takeshima *et al.*, 2019).

The observed increase in MDA levels in patients with SLE in our study, as compared to the healthy control group, may be attributed to the presence of chronic

inflammation and malfunction of the immune system. In individuals with SLE, the immune system exhibits heightened activity, leading to an overproduction of reactive oxygen species (ROS) as a component of the inflammatory reaction (Teh *et al.*, 2019). ROS possess the ability to initiate an assault on cellular membranes' lipid components, hence inducing lipid peroxidation and the subsequent generation of MDA (Islam *et al.*, 2020). Despite the presence of inherent antioxidant defense mechanisms in the body to combat oxidative stress, it is observed that these mechanisms might become overloaded or impaired in individuals with SLE. Consequently, this gives rise to an impaired capacity to efficiently counteract ROS and hinder lipid peroxidation, thereby resulting in elevated levels of MDA (Tarr *et al.*, 2017).

Moreover, it should be noted that in SLE, the autoantibodies have the capability to create ICs when they bind with self-antigens. These complexes then proceed to accumulate in different organs, therefore causing localized inflammation and the induction of oxidative stress. The presence of localized inflammation has the potential to lead to elevated levels of MDA in the tissues that are impacted (Deng and Tsao, 2017).

Additionally, SLE has the potential to induce harm to multiple organs and tissues, encompassing blood vessels, joints, and the kidneys, specifically referred to as LN. The leakage of biological components, such as lipid-rich membranes, into the bloodstream can occur as a result of tissue damage and cell injury. The components that have been produced can potentially serve as targets for ROS, leading to an elevation in the levels of MDA (Nagafuchi *et al.*, 2019).

On the other hand, it is worth noting that genetic variables have the potential to exert an influence on an individual's vulnerability to SLE as well as their response to oxidative stress. Certain genetic variants may potentially increase the susceptibility of specific SLE patients to elevated levels of oxidative stress and generation of MDA (Al-Fartosy *et al.*, 2021).

3.4.3. Levels of Total Antioxidant Capacity (TAC)

The present study showed a high significant decrease ($p < 0.01$) in total antioxidant capacity (TAC) levels in SLE patients compared to control group (1.62 ± 0.40 vs. 2.19 ± 0.46 pg/mL) as illustrated in Table (3.6) and Figure (3.4).

Table (3.6): Levels of TAC in SLE patients and control group

		TAC (pg/mL)	
		SLE Patients (N = 43)	Healthy Control (N = 53)
Mean \pm SD		1.62 \pm 0.40 **	2.19 \pm 0.46
SE		0.06	0.06
Range		0.83 – 2.85	1.41 – 2.97
95% CI	Lower	1.49	2.06
	Upper	1.74	2.32

Data are presented as mean \pm SD, SD: Standard Deviation, SE: Standard Error, Range: is the difference between the highest and lowest values in the set, 95% CI: Confidence Intervals (Lower and Upper), p-value (Non-Significant [$p > 0.05$], A * indicated Significant [$p < 0.05$], A ** indicated High Significant [$p < 0.01$]) indicated the level of significance in comparison with the corresponding control value.

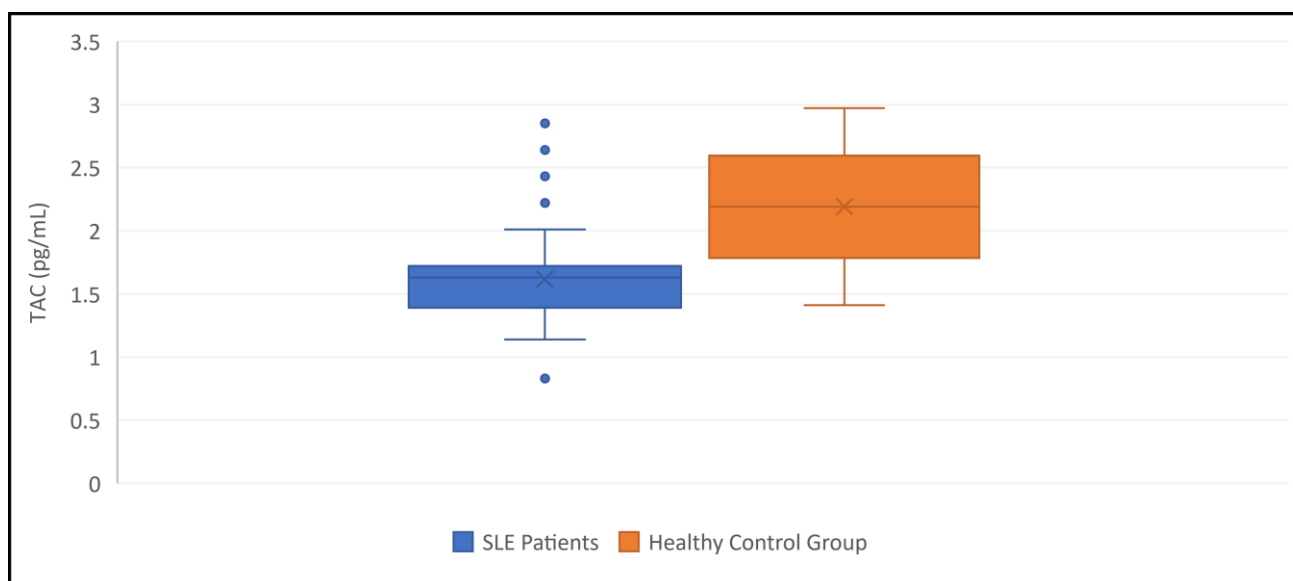


Figure (3.4): Comparison of TAC levels between SLE patients and healthy control group.

The total antioxidant capacity (TAC) refers to the comprehensive ability of an individual's biological system to mitigate the detrimental effects of oxidative stress through the neutralisation of ROS and free radicals (Bae and Lee, 2017).

The observed reduction in TAC among patients with SLE in our study may be attributed to the presence of chronic inflammation and impaired immune system functioning, as compared to the healthy control group. As SLE is characterised by an overactive immunological response, leading to the production of an excessive quantity of ROS and free radicals (Singla *et al.*, 2017). The presence of these very reactive compounds has the potential to overpower the body's antioxidant defence mechanisms, resulting in the occurrence of oxidative stress and the subsequent depletion of antioxidants such as TAC (Lin *et al.*, 2018).

Moreover, the prominent presence of inflammation in SLE has the potential to exacerbate the depletion of antioxidants and thus decrease TAC levels. The production of inflammatory cytokines during SLE exacerbates oxidative stress by promoting the generation of ROS and suppressing the action of antioxidant enzymes (Kwon *et al.*, 2019).

Furthermore, SLE has the potential to impair the body's antioxidant mechanisms, hence reducing their efficacy in counteracting ROS and free radicals. Impaired antioxidant enzyme activity or diminished levels of essential antioxidants, such as vitamins C and E, glutathione, and superoxide dismutase, may be observed in certain individuals with SLE. This phenomenon has the potential to result in a reduction in TAC levels (Jiang *et al.*, 2021).

In addition, people diagnosed with SLE generate autoantibodies that target their own tissues and biological constituents. The interaction between these autoantibodies and antioxidants can lead to a disruption in the functionality of the antioxidants and a subsequent reduction in their levels. An instance of autoantibodies targeting antioxidants such as glutathione has been documented in patients with SLE, resulting in diminished TAC (Shi *et al.*, 2017).

On the contrary, SLE has the potential to cause renal dysfunction, specifically LN. This phenomenon can lead to the depletion of antioxidants and proteins that play a

role in antioxidant defence within the urine, thus resulting in a further reduction of TAC levels (Al-Fartosy and Mohammed, 2017b).

Moreover, the presence of genetic polymorphisms in antioxidant genes has the potential to impact an individual's vulnerability to oxidative stress and might potentially lead to reduced TAC levels in specific SLE patients (Pan *et al.*, 2020).

3.4.4. Levels of C-Reactive Protein (CRP)

The present study showed a high significant increase ($p < 0.01$) in C-reactive protein (CRP) levels in SLE patients compared to control group (10.77 ± 4.83 vs. 0.17 ± 0.04 mg/dL) as illustrated in Table (3.7) and Figure (3.5).

Table (3.7): Levels of CRP in SLE patients and control group

		CRP (mg/dL)	
		SLE Patients (N = 43)	Healthy Control (N = 53)
Mean \pm SD		10.77 ± 4.83 **	0.17 ± 0.04
SE		0.74	0.005
Range		0.11 – 13.69	0.11 – 0.23
95% CI	Lower	9.28	0.16
	Upper	12.25	0.18

Data are presented as mean \pm SD, SD: Standard Deviation, SE: Standard Error, Range: is the difference between the highest and lowest values in the set, 95% CI: Confidence Intervals (Lower and Upper), p-value (Non-Significant [$p > 0.05$], A * indicated Significant [$p < 0.05$], A ** indicated High Significant [$p < 0.01$]) indicated the level of significance in comparison with the corresponding control value.

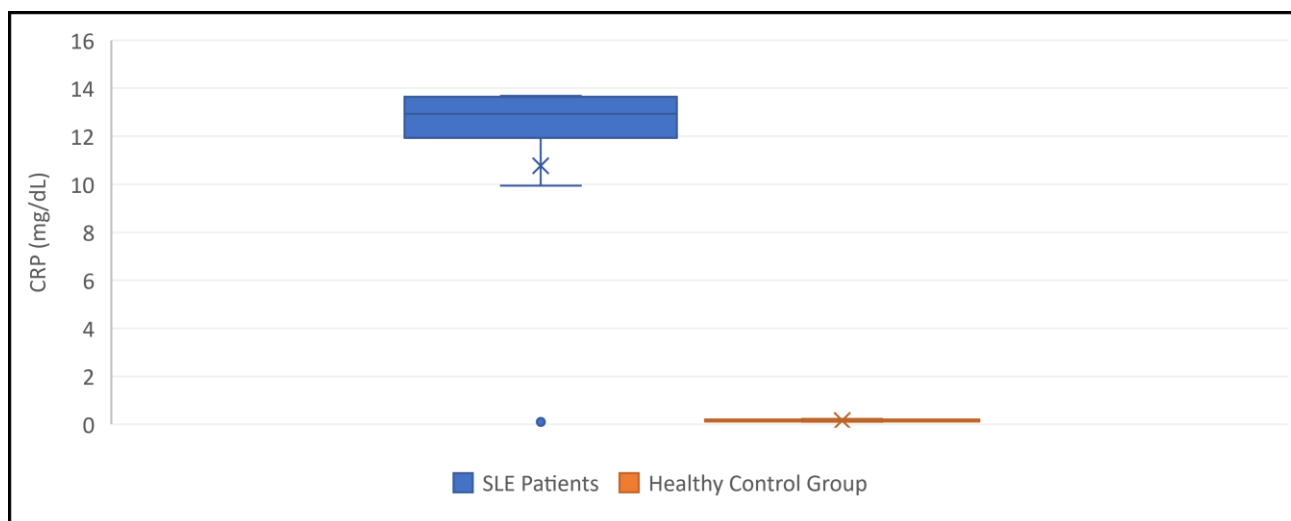


Figure (3.5): Comparison of CRP levels between SLE patients and healthy control group.

C-reactive protein (CRP) is a biomarker synthesised by the liver during the acute-phase response, triggered by inflammation or tissue damage (Fukasawa *et al.*, 2017).

The observed elevated levels of CRP in patients with SLE compared to a control group of healthy individuals in our study may be attributed to an excessive immune response characterised by the production of autoantibodies targeting the body's own tissues. The persistent state of inflammation can induce hepatic synthesis of CRP as a component of the acute-phase reaction (Aarslev *et al.*, 2017). Similarly, SLE is recognised for its characteristic pattern of disease activity, characterised by episodes of heightened symptoms (flares) interspersed with periods of symptom relief (remission) (Mende *et al.*, 2018). During episodes of illness exacerbation, there is an augmentation of the inflammatory response, resulting in heightened synthesis of pro-inflammatory cytokines, notably IL-6. IL-6, in a reciprocal manner, induces hepatic synthesis of CRP, leading to increased concentrations (Cappelli *et al.* 2017).

Furthermore, SLE has the potential to induce harm to multiple organs and tissues, with a particular emphasis on the kidneys (LN), resulting in cellular injury and tissue degeneration. The occurrence of tissue damage can result in the release of various cellular components, such as nuclear material and cellular debris, into the circulatory system (Al-Fartosy and Mohammed, 2017a). The aforementioned components, when released, have the potential to serve as indicators of danger, thereby initiating an inflammatory response and prompting the formation of CRP.

Moreover, in the context of SLE, it is frequently observed that ICs, which consist of antibodies attached to self-antigens, are generated and subsequently deposited in diverse tissues. This process significantly contributes to the initiation and perpetuation of inflammation, ultimately leading to tissue destruction. The ICs have the ability to induce the secretion of inflammatory mediators and CRP (Coronel-Restrepo *et al.*, 2017).

Moreover, individuals diagnosed with SLE exhibit a heightened susceptibility to infections as a result of immune system dysregulation. Infections have the potential to

initiate an acute-phase response, resulting in an increase in levels of CRP (Shruthi *et al.*, 2021).

From the other hand, genetic differences have the potential to impact an individual's vulnerability to inflammation and perhaps have a role in elevating CRP levels in specific SLE patients (Khanjari *et al.*, 2020).

3.4.5. Levels of Anti-Nuclear Antibody (ANA)

The present study showed a high significant increase ($p < 0.01$) in anti-nuclear antibody (ANA) levels in SLE patients compared to control group (2.39 ± 0.73 vs. 0.98 ± 0.31 IU/mL) as illustrated in Table (3.8) and Figure (3.6).

Table (3.8): Levels of ANA in SLE subjects and control group

		ANA (IU/mL)	
		SLE Subjects (N = 43)	Healthy Control (N = 53)
Mean \pm SD		2.39 ± 0.73 **	0.98 ± 0.31
SE		0.11	0.04
Range		0.58 – 2.92	0.46 – 1.50
95% CI	Lower	2.16	0.89
	Upper	2.61	1.07

Data are presented as mean \pm SD, SD: Standard Deviation, SE: Standard Error, Range: is the difference between the highest and lowest values in the set, 95% CI: Confidence Intervals (Lower and Upper), p-value (Non-Significant [$p > 0.05$], A * indicated Significant [$p < 0.05$], A ** indicated High Significant [$p < 0.01$]) indicated the level of significance in comparison with the corresponding control value.

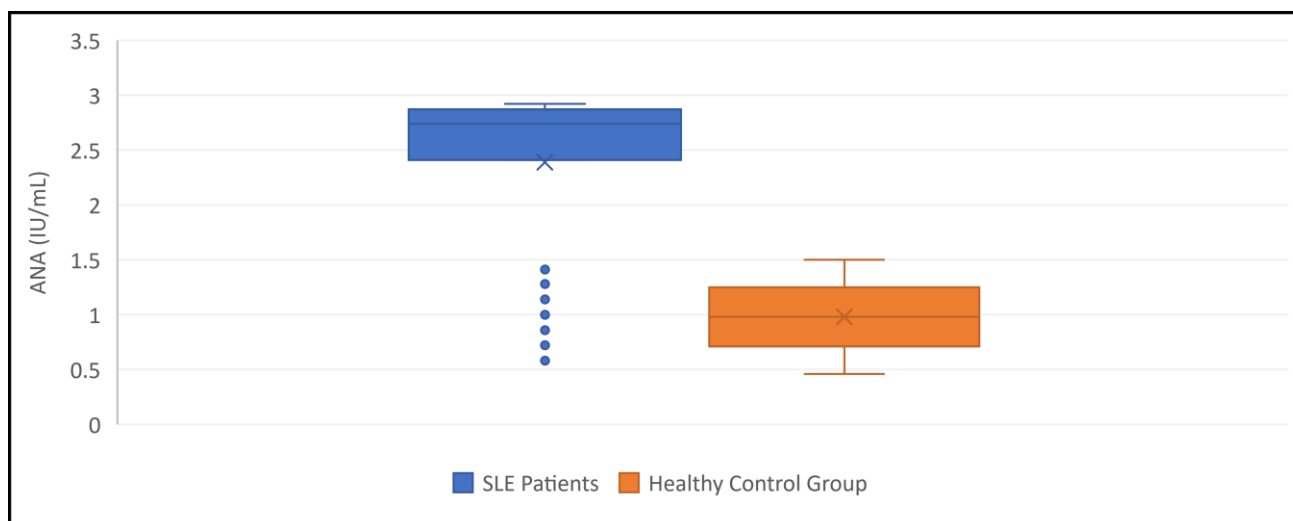


Figure (3.6): Comparison of ANA levels between SLE patients and healthy control group.

Antinuclear antibodies (ANA) are a class of antibodies that specifically recognise and bind to different constituents of the cell nucleus, encompassing DNA, RNA, and nucleoproteins (Hinterleitner *et al.*, 2021).

The observed elevation of ANA in patients with SLE, as opposed to the control group of healthy individuals, may be attributed to dysregulation of the immune system. As SLE is characterised by the production of autoantibodies, such as ANAs, which target the body's own biological components. The deregulation of the immune system results in the excessive production of ANAs (Reid *et al.*, 2020). In individuals who are in a state of good health, the immune system is equipped with mechanisms that provide immunological tolerance, thereby preventing the immune system from mounting an attack against self-antigens. Since SLE is characterised by the breakdown of tolerance mechanisms, which results in the activation of the immune system against nuclear components. This immunological response leads to increased levels of ANA (Pan *et al.*, 2020).

Furthermore, it is worth noting that hereditary variables exert a substantial influence on the pathogenesis of SLE. Specific genetic variants have the potential to augment an individual's vulnerability to autoimmunity and the generation of ANAs. Genetic variables have been identified as potential contributors to the heightened prevalence of ANAs in individuals with SLE (Catalan-Dibene *et al.*, 2018). Moreover, other environmental factors, including infections, exposure to UV radiation, and hormone fluctuations, have the potential to initiate or worsen SLE (Postal *et al.*, 2020). These stimuli have the potential to induce activation of the immune system, resulting in the production of ANAs and other autoantibodies (Al-Fartosy and Ati, 2021).

Moreover, it has been suggested that epigenetic modifications, which have the ability to modify gene expression without modifying the DNA sequence itself, have a role in the pathogenesis of SLE. These alterations have the potential to impact the transcription of genes involved in immune control and the synthesis of autoantibodies, such as ANAs (Furie *et al.*, 2019).

Furthermore, SLE is correlated with an elevated incidence of apoptosis, which refers to the process of programmed cell death, affecting several cell populations, including immune cells. Apoptosis is a biological process wherein nuclear components become exposed and subsequently released, rendering them more readily accessible to the immune system. This phenomenon plays a role in the generation of ANAs (Ramirez *et al.*, 2018). Additionally, ANAs have the ability to generate ICs upon binding to nuclear antigens. The deposition of ICs in several organs, including the kidneys (as observed in LN), skin, and joints, can induce inflammation and worsen the generation of ANA (Chauhan *et al.*, 2021).

3.4.6. Levels of Anti-double strand DNA (Anti-dsDNA)

The present study showed a high significant increase ($p < 0.01$) in anti-double stranded DNA (Anti-dsDNA) levels in SLE patients compared to control group (28.22 ± 6.38 vs. 15.63 ± 2.47 IU/mL) as illustrated in Table (3.9) and Figure (3.7).

Table (3.9): Levels of Anti-dsDNA in SLE patients and control group

		Anti-dsDNA (IU/mL)	
		SLE Patients (N = 43)	Healthy Control (N = 53)
Mean \pm SD		28.22 ± 6.38 **	15.63 ± 2.47
SE		0.97	0.34
Range		12.43 – 33.92	11.47 – 19.79
95% CI	Lower	26.26	14.95
	Upper	30.18	16.31

Data are presented as mean \pm SD, SD: Standard Deviation, SE: Standard Error, Range: is the difference between the highest and lowest values in the set, 95% CI: Confidence Intervals (Lower and Upper), p-value (Non-Significant [$p > 0.05$], A * indicated Significant [$p < 0.05$], A ** indicated High Significant [$p < 0.01$]) indicated the level of significance in comparison with the corresponding control value.

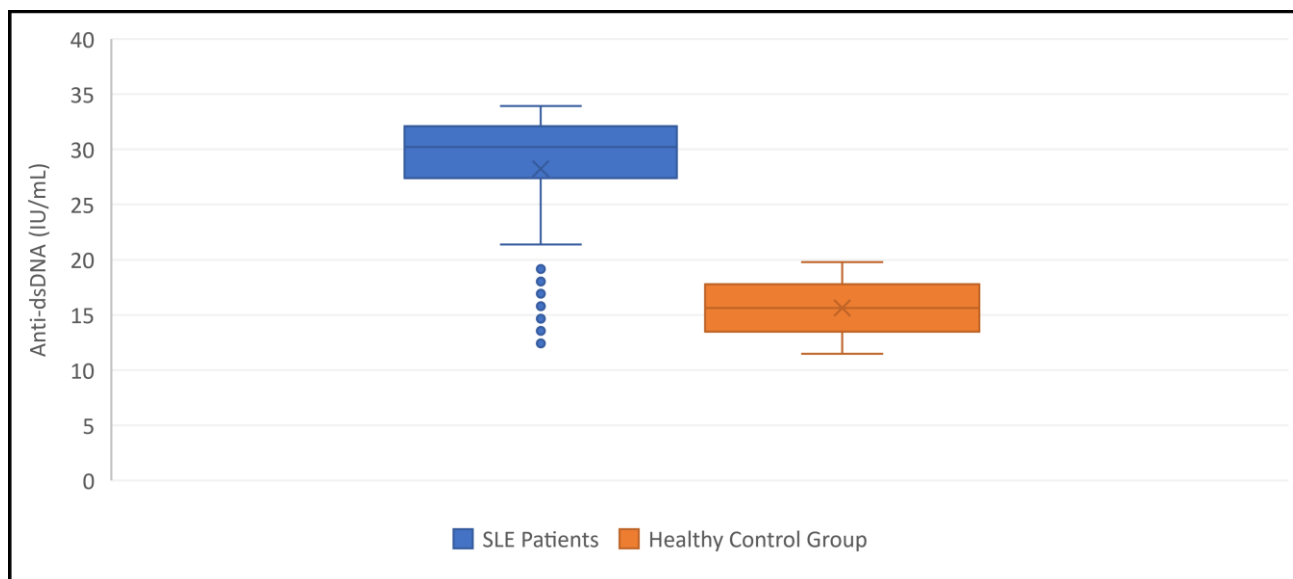


Figure (3.7): Comparison of Anti-dsDNA levels between SLE patients and healthy control group.

Anti-double stranded DNA (Anti-dsDNA) antibodies are a subset of ANA that specifically bind to the target antigen of double stranded DNA. The antibodies in question exhibit specificity towards a particular kind of DNA that is localised within the cellular nucleus (Noris-García *et al.*, 2018).

The observed elevation in Anti-dsDNA levels in patients with SLE relative to a control group of healthy individuals in our study may potentially be attributed to hereditary factors. The development of SLE is heavily influenced by genetic factors. Certain individuals possess a genetic predisposition that renders them more susceptible to the development of AIDs such as SLE (Engel *et al.*, 2021). Certain genetic variations have been found to be linked to a heightened susceptibility to SLE. These variants have the potential to disrupt immune regulatory processes, resulting in the generation of anti-dsDNA antibodies (Lu *et al.*, 2021b). Moreover, other environmental factors, including infections, hormone fluctuations, and UV light exposure, have the potential to initiate or worsen SLE. These stimuli have the potential to induce the synthesis of anti-dsDNA antibodies in persons who are susceptible (Arpaci *et al.*, 2021).

Moreover, B cells are a subset of leukocytes that assume a pivotal function in the immunological response. SLE is characterised by the hyperactivity of B cells, which

leads to the overproduction of antibodies, particularly anti-dsDNA antibodies. The aetiology of this atypical B cell functioning remains incompletely elucidated, but it is probable that a combination of genetic and environmental influences contributes to its manifestation (Al-Fartosy *et al.*, 2020c).

Furthermore, within a robust immune system, the body possesses inherent capabilities to identify and accept its own tissues, so averting any potential immune response directed towards self-tissue. Since SLE is characterised by a disruption in immunological tolerance, resulting in the generation of autoantibodies targeting self-antigens, specifically double-stranded DNA (dsDNA). The factors contributing to this decline in tolerance are multifaceted and encompass several immunological mechanisms (Faris *et al.*, 2022b).

In addition, it should be noted that in individuals with SLE, the production of anti-dsDNA antibodies might result in their binding to DNA fragments that are released from cells that have undergone damage. The process of binding leads to the development of ICs, which have the potential to accumulate in many organs, with a particular affinity for the kidneys (LN) (Sharaf-Eldin *et al.*, 2020). This physiological mechanism has the potential to initiate an inflammatory response and inflict harm upon vital organs, hence exacerbating the autoimmune reaction. The localization of these antibodies within the renal tissue can give rise to an inflammatory response and subsequent harm, leading to an upregulation in the production of anti-dsDNA antibodies as the immune system endeavours to eliminate the ICs (Lindblom *et al.*, 2022b).

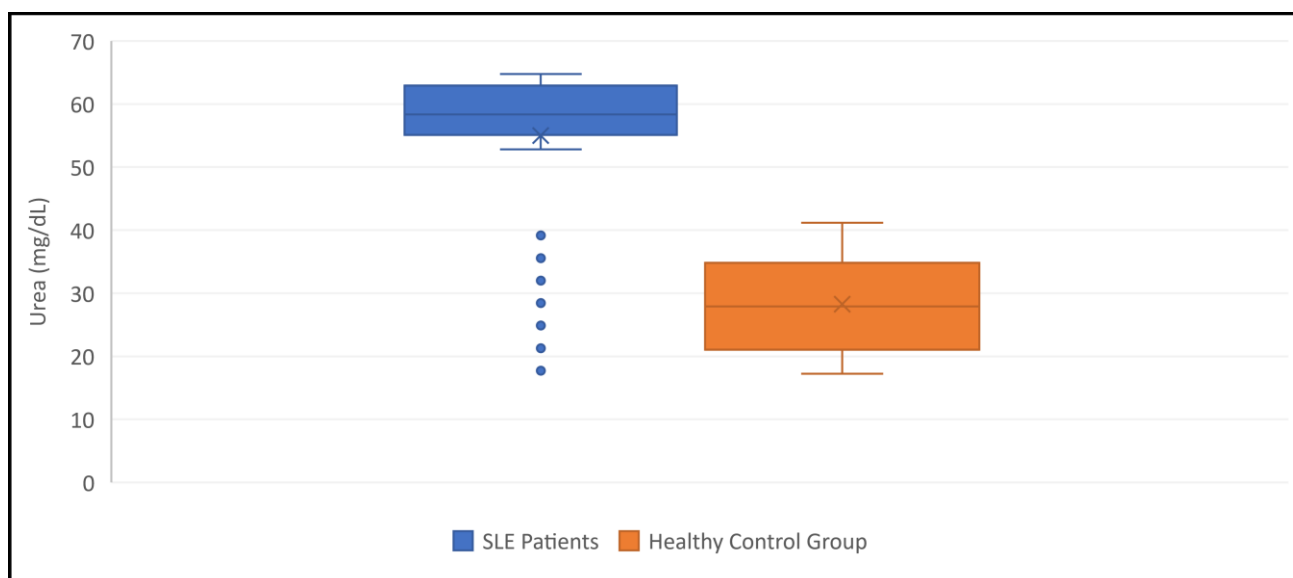
3.4.7. Levels of Urea

The present study showed a high significant increase ($p < 0.01$) in urea levels in SLE patients compared to control group (54.98 ± 12.60 vs. 28.27 ± 7.40 mg/dL) as illustrated in Table (3.10) and Figure (3.8).

Table (3.10): Levels of Urea in SLE patients and control group

		Urea (mg/dL)	
		SLE Patients (N = 43)	Healthy Control (N = 53)
Mean ± SD		54.98 ± 12.60 **	28.27 ± 7.40
SE		1.92	1.02
Range		17.73 – 64.73	17.22 – 41.19
95% CI	Lower	51.10	26.23
	Upper	58.85	30.31

Data are presented as mean ± SD, SD: Standard Deviation, SE: Standard Error, Range: is the difference between the highest and lowest values in the set, 95% CI: Confidence Intervals (Lower and Upper), p-value (Non-Significant [$p > 0.05$], A * indicated Significant [$p < 0.05$], A ** indicated High Significant [$p < 0.01$]) indicated the level of significance in comparison with the corresponding control value.

**Figure (3.8): Comparison of Urea levels between SLE patients and healthy control group.**

Urea is a hydrophilic compound with a molecular mass of 60 g/mol that is synthesised endogenously in humans through the metabolic processes of proteins and nitrogen. The chemical has the highest concentration in the blood of individuals afflicted with renal failure. The glomerulus has a high degree of permeability in filtering the substance, but the tubules lack the capacity to actively secrete it. Nevertheless, an estimated 40-70 percent of the substance is reabsorbed passively from the renal tubules (Klein *et al.*, 2019).

The notable elevation in urea concentration observed in individuals with SLE has the potential to induce renal impairment or renal dysfunction by the induction of irreversible harm to numerous nephrons, which are minuscule filtration units located within each kidney (Mike *et al.*, 2019). Consequently, SLE individuals experience impaired ability of the kidneys to regulate fluid and electrolyte balance, leading to increased concentrations of urea in their bodies. Urea, a by-product of the liver's breakdown of amino acids and other nitrogenous metabolites, is typically eliminated from the body through renal excretion at a pace that matches its production. When there is a decline in renal function, there is a gradual build-up of blood urea concentrations (Sun *et al.*, 2019).

Furthermore, renal involvement in SLE frequently results in proteinuria, a condition characterised by the excessive amount of protein in the urine. Proteinuria can lead to the excretion of serum proteins, such as albumin, so disrupting the equilibrium of fluid within the circulatory system. Insufficient amounts of serum proteins may potentially result in elevated concentrations of urea in the bloodstream (Aibara *et al.*, 2018).

Moreover, it is worth noting that hypertension, also known as high blood pressure, frequently arises as a consequence of LN and can exacerbate renal impairment. Elevated blood pressure has the potential to cause detrimental effects on the renal microvasculature, so compromising the kidneys' capacity to effectively filter waste substances, consequently resulting in increased amounts of urea (Ichinose *et al.*, 2018).

In addition, many drugs employed for the management of SLE may induce adverse effects that impact renal function and contribute to heightened levels of urea. Non-steroidal anti-inflammatory drugs (NSAIDs) are occasionally administered to alleviate pain and inflammation associated with SLE; nevertheless, it is important to note that these medications can potentially impact renal blood flow and function (Galli *et al.*, 2019).

On the contrary, individuals diagnosed with SLE may encounter augmented fluid depletion as a result of factors such as elevated body temperature, profuse perspiration, or the administration of diuretic drugs, which are employed to alleviate symptoms. The condition of dehydration has the potential to result in the concentration of blood and elevated amounts of urea (Al-Fartosy *et al.*, 2023). Moreover, individuals diagnosed with SLE may encounter alterations in their dietary patterns or appetite as a result of the condition itself or the therapies employed to manage it. Insufficient dietary intake or poor hydration can have a detrimental impact on renal function and lead to heightened concentrations of urea (Ali *et al.*, 2021b).

Moreover, individuals diagnosed with SLE face a heightened susceptibility to infections as a result of immune system impairment, which can be attributed to the underlying disease. Infections have the potential to induce fever and heightened metabolic requirements, which may consequently give rise to heightened urea concentrations (Huang *et al.*, 2020).

3.4.8. Levels of Creatinine

The present study showed a high significant increase ($p < 0.01$) in creatinine levels in SLE patients compared to control group (1.07 ± 0.18 vs. 0.70 ± 0.10 mg/dL) as illustrated in Table (3.11) and Figure (3.9).

Table (3.11): Levels of Creatinine in SLE patients and control group

		Creatinine (mg/dL)	
		SLE Patients (N = 43)	Healthy Control (N = 53)
Mean \pm SD		1.07 ± 0.18 **	0.70 ± 0.10
SE		0.03	0.01
Range		0.59 – 1.29	0.57 – 0.91
95% CI	Lower	1.01	0.67
	Upper	1.12	0.72

Data are presented as mean \pm SD, SD: Standard Deviation, SE: Standard Error, Range: is the difference between the highest and lowest values in the set, 95% CI: Confidence Intervals (Lower and Upper), p-value (Non-Significant [$p > 0.05$], A * indicated Significant [$p < 0.05$], A ** indicated High Significant [$p < 0.01$]) indicated the level of significance in comparison with the corresponding control value.

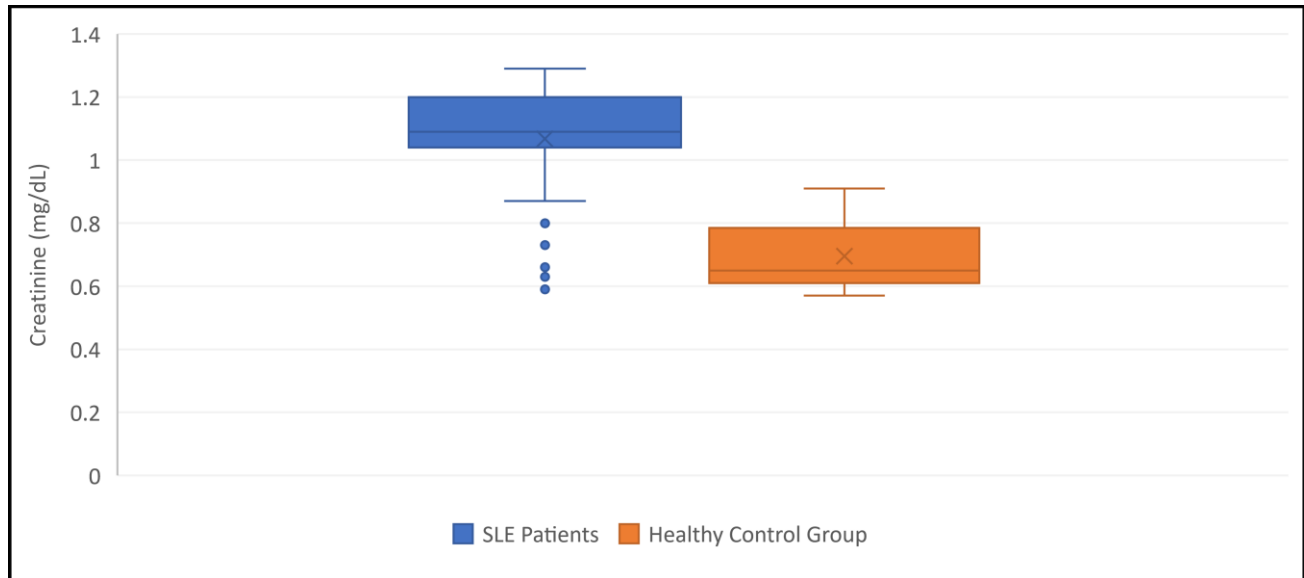


Figure (3.9): Comparison of Creatinine levels between SLE patients and healthy control group.

Creatinine is a metabolic by-product resulting from the breakdown of creatine phosphate during muscle and protein metabolism. The glomerulus is responsible for the filtration of creatinine, whereas the proximal tubule excretes a minor quantity of creatinine into the glomerular filtrate (Chisavu *et al.*, 2023).

The observed elevation in serum creatinine levels in patients with SLE may be attributed to the presence of inflammation. The presence of inflammation can result in detrimental effects on the renal tissue, hence compromising the kidneys' capacity to effectively filter waste substances, such as creatinine. Consequently, increased levels of creatinine serve as a prevalent indicator of renal impairment in individuals with SLE (Kitagori *et al.*, 2019). Moreover, the glomerular filtration rate (GFR) serves as an indicator of the kidneys' efficacy in removing waste substances from the bloodstream. In the context of LN, the physiological response of inflammation, proteinuria, and subsequent tissue damage has been observed to have a negative impact on the GFR. This, in turn, leads to a reduction in the ability of the kidneys to effectively clear creatinine from the bloodstream, ultimately leading in elevated levels of serum creatinine (Zhang *et al.*, 2021b).

Moreover, SLE frequently presents with hypertension, particularly in instances of LN. Hypertension has the potential to cause detrimental effects on the renal microvasculature, resulting in compromised filtration capabilities of the kidneys and subsequent elevation of creatinine levels (Schwartz *et al.*, 2019).

Additionally, several drugs employed in the management of SLE have the potential to impact renal function and lead to elevated levels of creatinine. In certain instances, the administration of NSAIDs may result in adverse effects that impact renal blood flow or induce renal impairment (Page *et al.*, 2021). Patients diagnosed with SLE have a heightened susceptibility to infections owing to the weakened state of their immune system. This compromised immune response can be attributed to the underlying disease process. Infections have the ability to induce fever and heightened metabolic requirements, which may potentially contribute to the elevation of creatinine levels (Lindblom *et al.*, 2022a).

On the contrary, individuals diagnosed with SLE may encounter augmented fluid depletion as a result of factors such as elevated body temperature, profuse perspiration, or the use of diuretic drugs, which are employed for symptom management. The condition of dehydration has the potential to result in the concentration of blood and elevated levels of creatinine (Abdualhay and Al-Fartosy, 2022). Furthermore, alterations in eating patterns or appetite as a consequence of the illness or its therapeutic interventions can impact nutritional status and renal function, potentially resulting in elevated levels of creatinine (Vincent *et al.*, 2018).

3.4.9. Levels of Glomerular Filtration Rate (GFR)

The present study showed a high significant decrease ($p < 0.01$) in glomerular filtration rate (GFR) levels in SLE patients compared to control group (61.89 ± 18.66 vs. 99.53 ± 18.77 mL/min/1.73 m²) as illustrated in Table (3.12) and Figure (3.10).

Table (3.12): Levels of GFR in SLE patients and control group

GFR (mL/min/1.73 m ²)		
	SLE Patients (N = 43)	Healthy Control (N = 53)
Mean ± SD	61.89 ± 18.66 **	99.53 ± 18.77
SE	2.85	2.58
Range	44.70 – 120.50	66.90 – 126.30
95% CI		
Lower	56.14	94.35
Upper	67.63	104.70

Data are presented as mean ± SD, SD: Standard Deviation, SE: Standard Error, Range: is the difference between the highest and lowest values in the set, 95% CI: Confidence Intervals (Lower and Upper), p-value (Non-Significant [p>0.05], A * indicated Significant [p<0.05], A ** indicated High Significant [p<0.01]) indicated the level of significance in comparison with the corresponding control value.

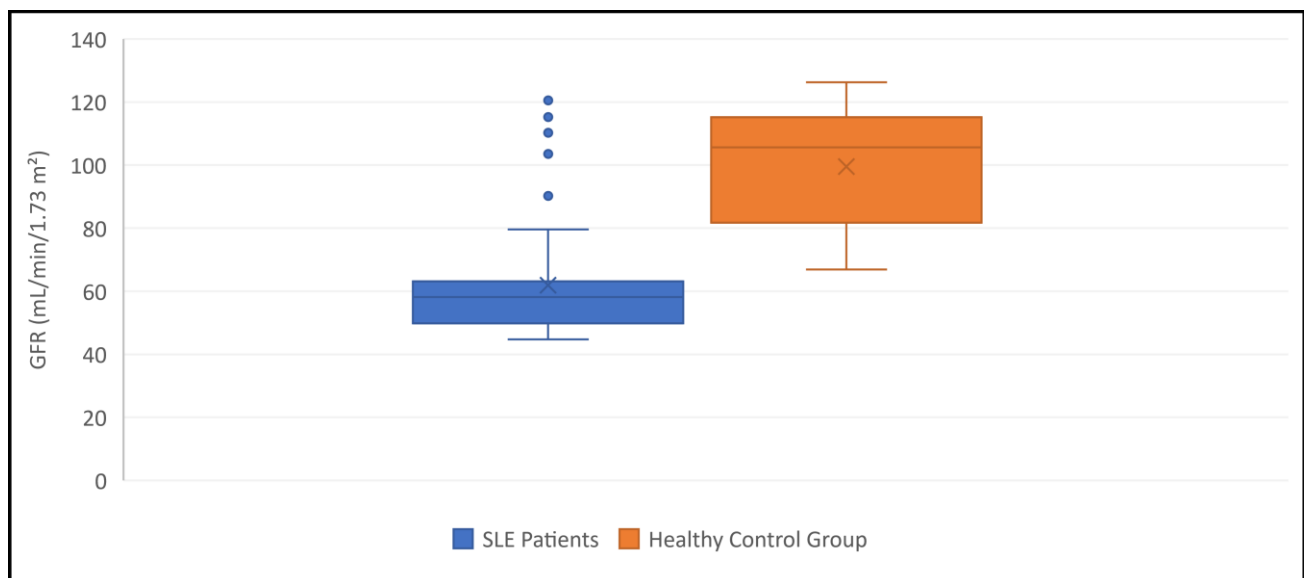


Figure (3.10): Comparison of GFR levels between SLE patients and healthy control group.

The glomerular filtration rate (GFR) is a crucial metric for assessing the renal filtration capability and is widely employed in clinical practise. The estimated GFR (eGFR) holds significant importance in the evaluation of individuals with suspected or diagnosed renal disease in clinical settings (Tu *et al.*, 2019). The measurement of GFR necessitates the utilisation of an optimal filtration marker. This marker should possess certain characteristics, including unhindered filtration by the kidney, absence of plasma protein binding, non-toxicity, and the absence of metabolic alterations, tubular

secretion, or absorption. An example of such a marker is creatinine. GFR refers to the velocity at which the two million glomeruli inside the renal system undertake the process of plasma filtration, facilitating the elimination of waste substances (Diaz-Rizo *et al.*, 2017).

In the present investigation, it is plausible to explain the observed decrease in GFR among individuals with SLE to the presence of inflammation and consequential renal tissue impairment. Inflammation has the potential to impact the glomeruli, which are the small renal units responsible for efficient waste filtration within the kidneys. As a consequence, the capacity of these glomeruli to effectively filter waste products may be diminished. Consequently, a decline in GFR occurs, resulting in compromised renal function (Faris *et al.*, 2022a).

In addition, since SLE is characterised by the production of autoantibodies and ICs. These ICs have the potential to accumulate in the renal tissue. The presence of these deposits has the potential to induce an inflammatory reaction inside the renal system, resulting in subsequent harm and a decrease in GFR (Hassel *et al.*, 2017).

Furthermore, renal involvement in SLE frequently results in proteinuria which may arise as a consequence of glomerular injury, wherein the glomeruli, responsible for the filtration of proteins in the bloodstream, become impaired. The detection of an abundance of proteins in the urine can serve as an indicator of impaired kidney function and might potentially lead to a reduction in GFR (Mohammed and Al-Fartosy, 2022).

Moreover, SLE has the potential to induce vascular inflammation, specifically affecting the renal blood vessels. The occurrence of vasculitis inside the kidneys has the potential to impede the circulation of blood and inflict harm onto the renal tissue, consequently leading to a decrease in GFR (Wang *et al.*, 2022a).

Additionally, SLE frequently presents with hypertension, particularly in instances of LN. Hypertension has the potential to cause detrimental effects on the renal microvasculature, so compromising the kidneys' capacity to effectively filter waste substances and resulting in a decline in GFR (Chao *et al.*, 2021).

On the contrary, SLE is associated with an elevated susceptibility to thrombosis. The occurrence of renal thrombosis, characterised by the presence of blood clots inside the renal veins, can impede the normal circulation of blood to the kidneys. Consequently, this obstruction can induce kidney impairment, ultimately causing a reduction in the GFR (Arab-Zozani *et al.*, 2021).

3.4.10. Levels of Interleukin-18 (IL-18)

The present study showed a high significant increase ($p < 0.01$) in interleukin-18 (IL-18) levels in SLE patients compared to control group (301.61 ± 72.51 vs. 92.83 ± 23.78 pg/mL) as illustrated in Table (3.13) and Figure (3.11).

Table (3.13): Levels of IL-18 in SLE patients and control group

		IL-18 (pg/mL)	
		SLE Patients (N = 43)	Healthy Control (N = 53)
Mean \pm SD		301.61 \pm 72.51 **	92.83 \pm 23.78
SE		11.06	3.27
Range		105.15 – 359.75	52.79 – 132.87
95% CI	Lower	279.29	86.27
	Upper	323.92	99.39

Data are presented as mean \pm SD, SD: Standard Deviation, SE: Standard Error, Range: is the difference between the highest and lowest values in the set, 95% CI: Confidence Intervals (Lower and Upper), p-value (Non-Significant [$p > 0.05$], A * indicated Significant [$p < 0.05$], A ** indicated High Significant [$p < 0.01$]) indicated the level of significance in comparison with the corresponding control value.

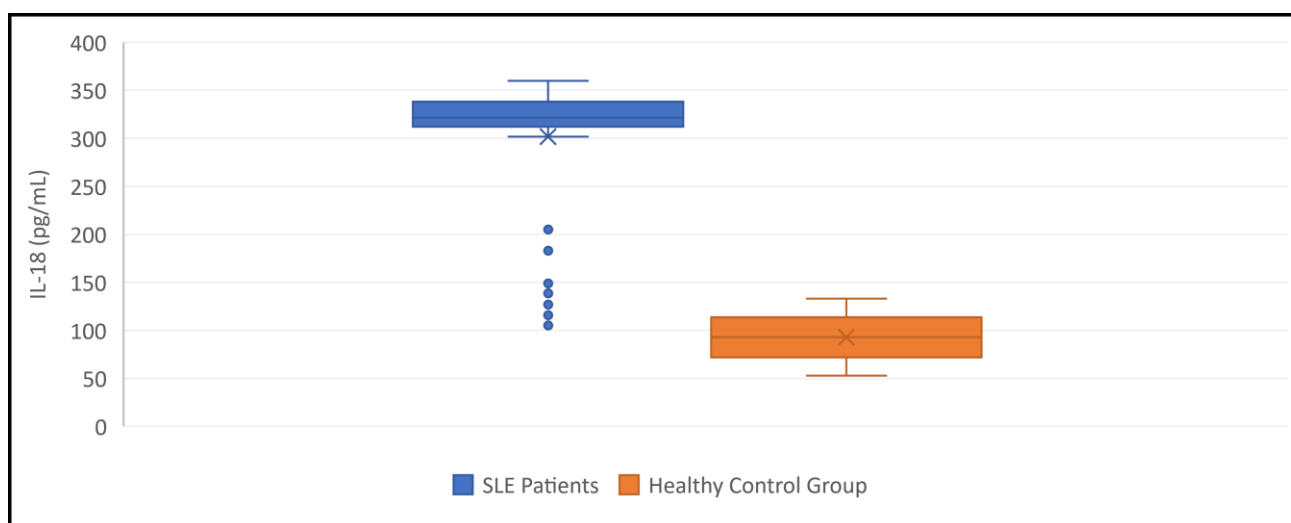


Figure (3.11): Comparison of IL-18 levels between SLE patients and healthy control group.

Interleukin-18 (IL-18) is classified as a member of the IL-1 family of cytokines, a collection of 11 cytokines that facilitate the functioning of the innate immune system. IL-18 is known to have a crucial function as a primary protective factor in the defence mechanisms of the host (Wang *et al.*, 2022b).

The observed elevation of blood IL-18 levels in patients with SLE may be attributed to the presence of inflammation. Elevated levels of IL-18 may arise as a result of the pro-inflammatory condition observed in SLE, given that immune cells secrete IL-18 in reaction to inflammatory stimuli (Mertowska *et al.*, 2022).

Furthermore, individuals diagnosed with SLE may exhibit abnormalities in the synthesis and functioning of several ILs, such as IL-18. The dysregulation of IL-18 production can result in an overabundance of this cytokine, hence playing a role in the development of inflammation and dysfunction within the immune system (Yan *et al.*, 2021). In certain individuals diagnosed with SLE, particularly during episodes of illness exacerbation or the occurrence of severe symptoms, there may be an occurrence of a cytokine storm. This phenomenon involves the release of a multitude of pro-inflammatory cytokines, such as IL-18, at elevated concentrations. This syndrome frequently correlates with significant organ involvement and exacerbation of SLE symptoms (Du *et al.*, 2017).

Moreover, it is worth noting that SLE frequently presents with kidney involvement, which is referred to as LN. Elevated levels of IL-18 may arise as a consequence of inflammation and renal tissue injury, given that the kidneys serve as a site for IL-18 synthesis. The assessment of kidney inflammation in individuals with SLE can be enhanced by the measurement of IL-18 levels in urine (Al-Shawi and Al-Fartosy, 2022).

Furthermore, it is important to note that endothelial cells are responsible for lining the inner walls of blood arteries and possess a significant role in maintaining optimal vascular function. SLE has the potential to induce endothelial dysfunction, resulting in the initiation of an inflammatory response and subsequent impairment of

vascular integrity. This pathological condition has the potential to induce the secretion of IL-18 and various other cytokines (Plachouri *et al.*, 2019). Furthermore, it is worth noting that ICs have the ability to develop and accumulate in diverse tissues, such as blood vessels and organs. The activation of immune cells by ICs can result in the synthesis of IL-18 and various other inflammatory mediators (Zanatta *et al.*, 2020).

On the other hand, it is worth noting that genetic predisposition has the potential to exert an influence on the production and regulation of cytokines, such as IL-18. Certain genetic variations have the potential to enhance the likelihood of heightened IL-18 levels in SLE individuals (Sánchez-Pérez *et al.*, 2017). Exposure to several environmental factors, including UV light, stress, and specific dietary components, has been observed to potentially induce exacerbations of SLE and contribute to IL-18 elevated levels (Dini *et al.*, 2017).

In addition, individuals diagnosed with SLE exhibit increased vulnerability to infections owing to the weakened state of their immune system resulting from the presence of the disease. Specific infections have the capacity to induce the secretion of IL-18 as an integral component of the immune reaction to the infection (Lee and Song, 2018).

3.4.11. Levels of Interleukin-37 (IL-37)

The present study showed a high significant increase ($p < 0.01$) in interleukin-37 (IL-37) levels in SLE patients compared to control group (209.42 ± 59.50 vs. 51.28 ± 6.95 pg/mL) as illustrated in Table (3.14) and Figure (3.12).

Table (3.14): Levels of IL-37 in SLE patients and control group

		IL-37 (pg/mL)	
		SLE Patients (N = 43)	Healthy Control (N = 53)
Mean ± SD		209.42 ± 59.50 **	51.28 ± 6.95
SE		9.07	0.95
Range		48.13 – 252.73	39.58 – 62.98
95% CI	Lower	191.11	49.36
	Upper	227.73	53.20

Data are presented as mean \pm SD, SD: Standard Deviation, SE: Standard Error, Range: is the difference between the highest and lowest values in the set, 95% CI: Confidence Intervals (Lower and Upper), p-value (Non-Significant [$p > 0.05$], A * indicated Significant [$p < 0.05$], A ** indicated High Significant [$p < 0.01$]) indicated the level of significance in comparison with the corresponding control value.

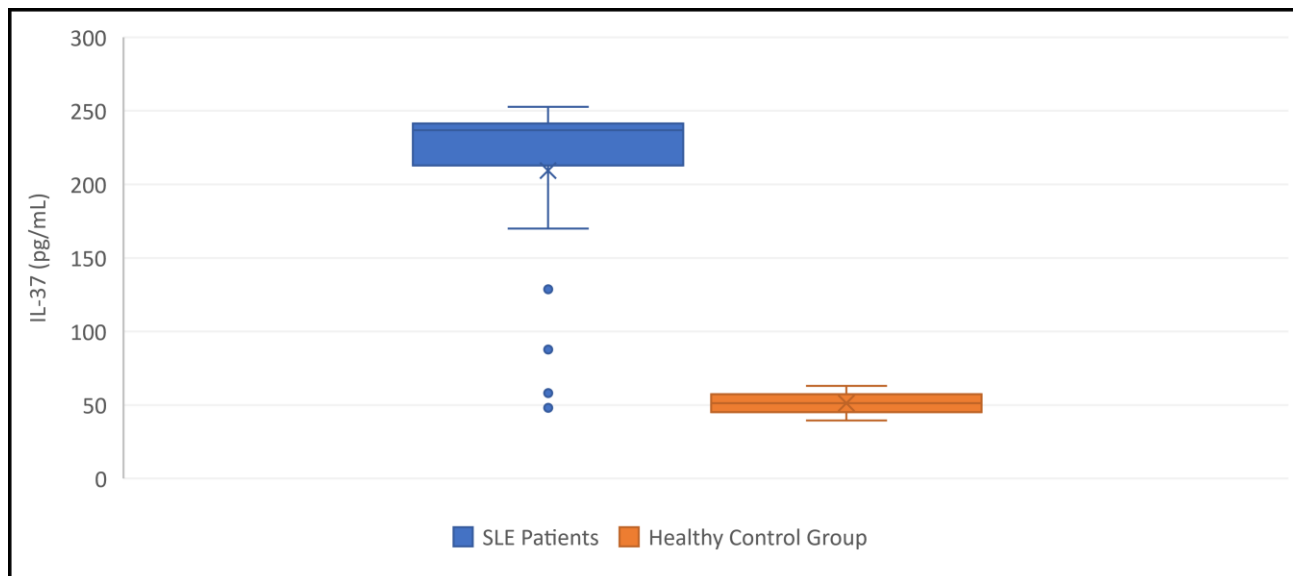


Figure (3.12): Comparison of IL-37 levels between SLE patients and healthy control group.

Interleukin-37 (IL-37) is a cytokine with anti-inflammatory properties, which serves as a regulator of the immune system and aids in the suppression of inflammatory reactions (Jaing *et al.*, 2021).

The observed elevation of serum IL-37 levels in patients with SLE may be attributed to the presence of inflammation. The presence of increased levels of IL-37 in SLE could perhaps indicate a compensatory response initiated by the body to mitigate the excessive inflammation and immunological activity characteristic of the condition (Rashad *et al.*, 2019). IL-37 functions as an endogenous anti-inflammatory mediator, and elevated concentrations of this cytokine may represent an intrinsic regulatory mechanism aimed at modulating the inflammatory reaction. Since SLE is characterised by its autoimmune nature, wherein the immune system initiates an assault on healthy tissues, hence instigating inflammatory responses (Shields *et al.*, 2017). Prior research has demonstrated that the expression of IL-37 is significantly increased in various cell types, including PBMCs, macrophages, epithelial cells, DCs, and T cells, in response

to the activation of pro-inflammatory cytokines such as IL-18, IFN- γ , IL-1 β , and TNF. Conversely, IL-37 expression is either lower or not consistently observed in non-stimulated target cells and healthy human tissues (Xue *et al.*, 2022).

IL-37 is potentially synthesised as a response to the occurrence of autoimmunity, with the aim of alleviating the autoimmune assault on the organism. In addition, IL-37 has the capacity to elicit immunomodulatory responses through the inhibition of several immune cell populations, such as T cells and DCs. Elevated levels of IL-37 may serve as a regulatory mechanism to mitigate immunological dysregulation in SLE (Miyake *et al.*, 2018).

Furthermore, it is plausible that genetic factors contribute to the modulation of IL-37 levels. Certain genetic variations have been found to potentially contribute to an augmented production of IL-37 or a compromised regulatory mechanism, hence rendering specific individuals more susceptible to heightened levels of IL-37 in the context of inflammation or autoimmune (Demir *et al.*, 2018).

Moreover, it is possible for endothelial dysfunction to manifest, resulting in the onset of inflammation and subsequent impairment of blood vessel integrity. IL-37 has the potential to be synthesised as a defensive mechanism in response to endothelial dysfunction (Mok, 2019). The activation of inflammatory reactions in SLE can result in detrimental effects on many tissues, such as the skin, joints, and internal organs such as kidney (LN). IL-37 is potentially secreted in response to tissue damage as a component of the body's innate immune response, aiming to restrict excessive inflammation and facilitate the process of tissue healing (Sun *et al.*, 2017).

Additionally, it is frequently seen that there is dysregulation of several cytokines and chemokines in SLE. The presence of these imbalances can have an impact on the synthesis and functioning of IL-37 and other cytokines, hence leading to an increase in IL-37 levels (Alsalimi *et al.*, 2023).

3.4.12. Levels of Programmed Cell Death-1 (PD-1)

The present study showed a high significant increase ($p < 0.01$) in programmed death-1 (PD-1) levels in SLE patients compared to control group (779.14 ± 346.89 vs. 127.68 ± 24.56 pg/mL) as illustrated in Table (3.15) and Figure (3.13).

Table (3.15): Levels of PD-1 in SLE patients and control group

		PD-1 (pg/mL)	
		SLE Patients (N = 43)	Healthy Control (N = 53)
Mean \pm SD		779.14 ± 346.89 **	127.68 ± 24.56
SE		52.90	3.37
Range		87.53 – 1165.98	86.34 – 169.02
95% CI	Lower	672.38	120.91
	Upper	885.90	134.45

Data are presented as mean \pm SD, SD: Standard Deviation, SE: Standard Error, Range: is the difference between the highest and lowest values in the set, 95% CI: Confidence Intervals (Lower and Upper), p-value (Non-Significant [$p > 0.05$], A * indicated Significant [$p < 0.05$], A ** indicated High Significant [$p < 0.01$]) indicated the level of significance in comparison with the corresponding control value.

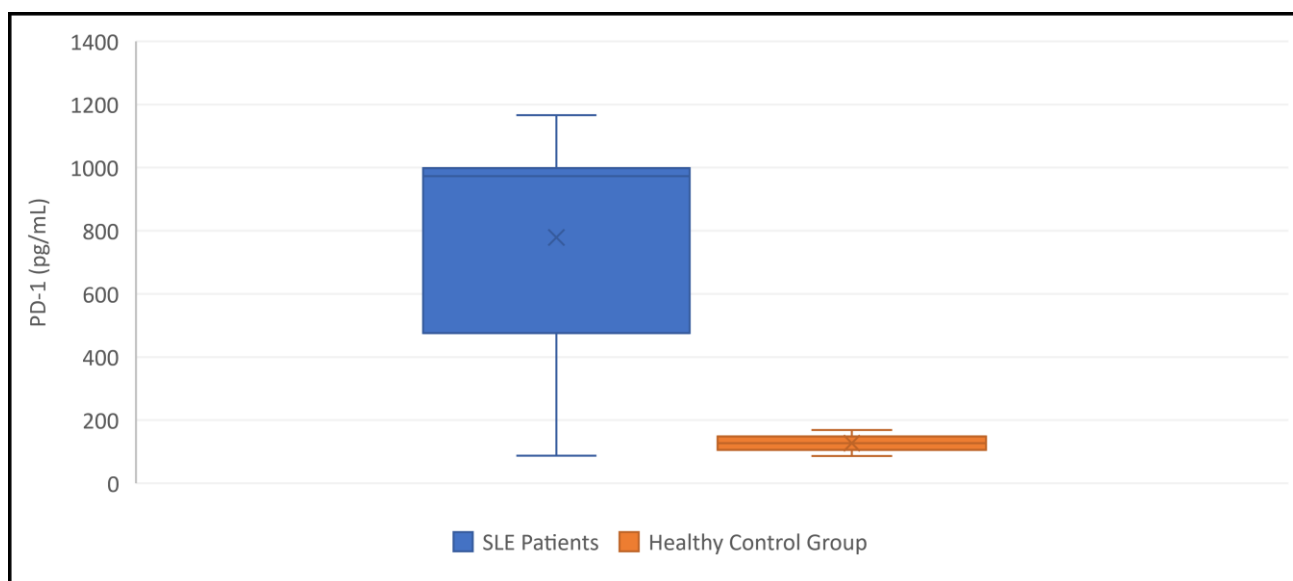


Figure (3.13): Comparison of PD-1 levels between SLE patients and healthy control group.

The protein known as programmed cell death protein 1 (PD-1) is a receptor located on the surface of T cells and B cells. Its primary function is to regulate the immune system, making it an essential component in immune system regulation (Dai

et al., 2019). PD-1 exerts its inhibitory effects on immune responses by binding to its ligands, PD-L1 or PD-L2. This interaction serves to regulate immune activation and mitigate the risk of excessive immunological activity and the development of autoimmune reactions (Morand *et al.*, 2020).

The observed elevation of serum PD-1 levels in individuals with SLE may be attributed to the presence of chronic inflammation and dysregulation of the immune system. The persistent inflammatory condition can result in the activation of immunological checkpoints, such as PD-1, as a regulatory mechanism to suppress exaggerated immune reactions (Dey *et al.*, 2021). Increased levels of PD-1 may serve as a compensatory strategy employed by the immune system to inhibit the autoimmune responses and inflammation that are characteristic of SLE. The human body may upregulate the expression of PD-1 as a mechanism of self-regulation, aiming to mitigate and halt more tissue damage (Topfer *et al.*, 2022).

Moreover, PD-1 serves as an indicator of T cell fatigue, a condition characterised by diminished responsiveness of T cells to antigenic stimulation. SLE can give rise to T cell malfunction and exhaustion, which may result in heightened expression of PD-1 on T cell surfaces due to compromised functionality (Laurent *et al.*, 2017). Moreover, SLE is correlated with the existence of autoantibodies and ICs, which are characterised as self-antigens. Prolonged exposure to these endogenous antigens can induce T cells to upregulate PD-1 as they engage with autoantigens, in an effort to attenuate the immune response directed towards self-antigens (Xu *et al.*, 2021).

In addition, it is plausible that genetic variables have a role in the modulation of PD-1 expression. Specific genetic variations have the potential to confer a predisposition in individuals towards heightened production of PD-1, hence rendering them more vulnerable to SLE (Wang *et al.*, 2023).

Furthermore, individuals diagnosed with SLE exhibit an elevated susceptibility to infections as a result of compromised immune system functioning. Infections have

the ability to elicit immunological responses and induce the development of immune checkpoints, such as PD-1 (Abdalla *et al.*, 2017).

3.5. Correlation Analysis

3.5.1. Correlation between Serum IL-18 Levels with Biochemical Parameters in SLE Patients

Table (3.16) and Figure (3.14) present an investigation into the impact of serum IL-18 on the biochemical analysis of the group of patients diagnosed with SLE. This examination was conducted using linear regression analysis.

A statistically insignificant positive connection was seen between the levels of IL-18 and BMI in patients diagnosed with SLE.

In addition, a strong negative connection was seen between the levels of C3, C4, CH50, TAC, and GFR with the level of IL-18 in the group of patients with SLE.

On the other hand, a strong positive association was seen between the level of IL-18 and many markers including MDA, CRP, ANA, Anti-dsDNA, urea, creatinine, IL-37, and PD-1 in the group of patients diagnosed with SLE.

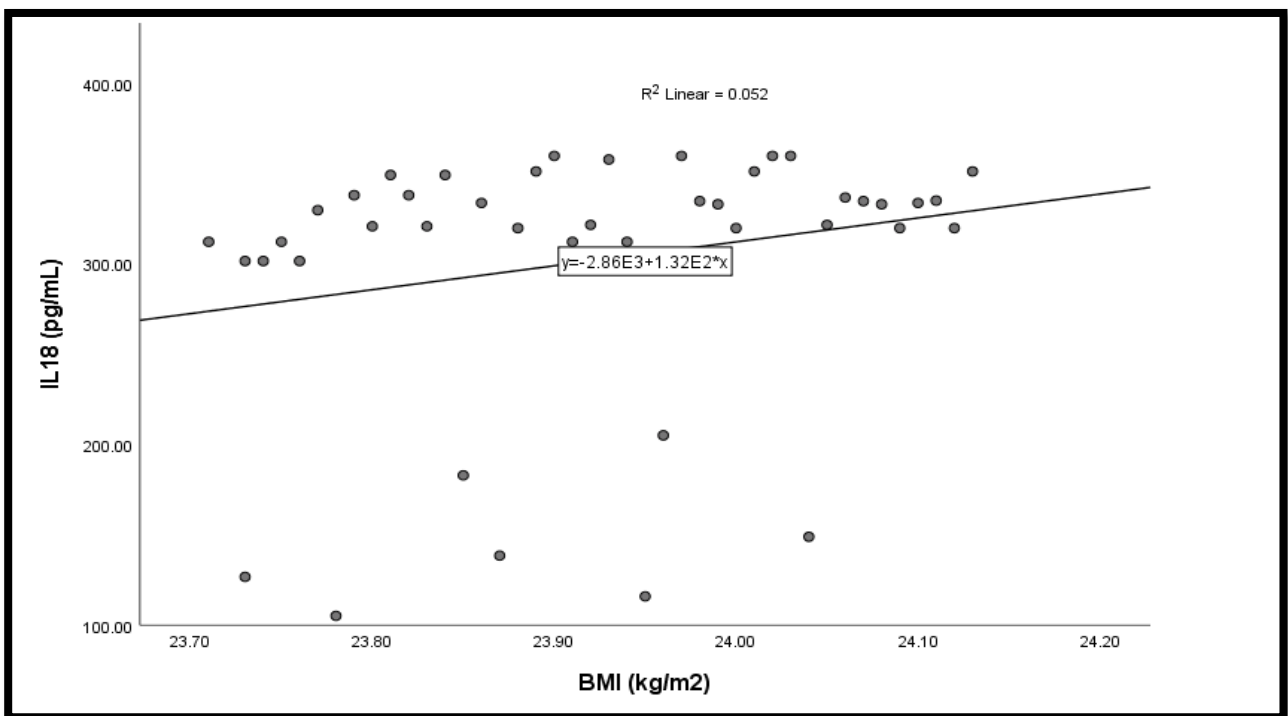
Table (3.16): Correlation between serum IL-18 levels with biochemical parameters in SLE patients group

Parameter	IL-18 (pg/mL)	
	r	P-Value
BMI (kg/m ²)	0.229	0.141
C3 (g/L)	-0.925	<0.01
C4 (g/L)	-0.581	<0.01
CH50 (IU/mL)	-0.983	<0.01
MDA (μmol/L)	0.923	<0.01
TAC (pg/mL)	-0.694	<0.01
CRP (mg/dL)	0.974	<0.01
ANA (IU/mL)	0.871	<0.01

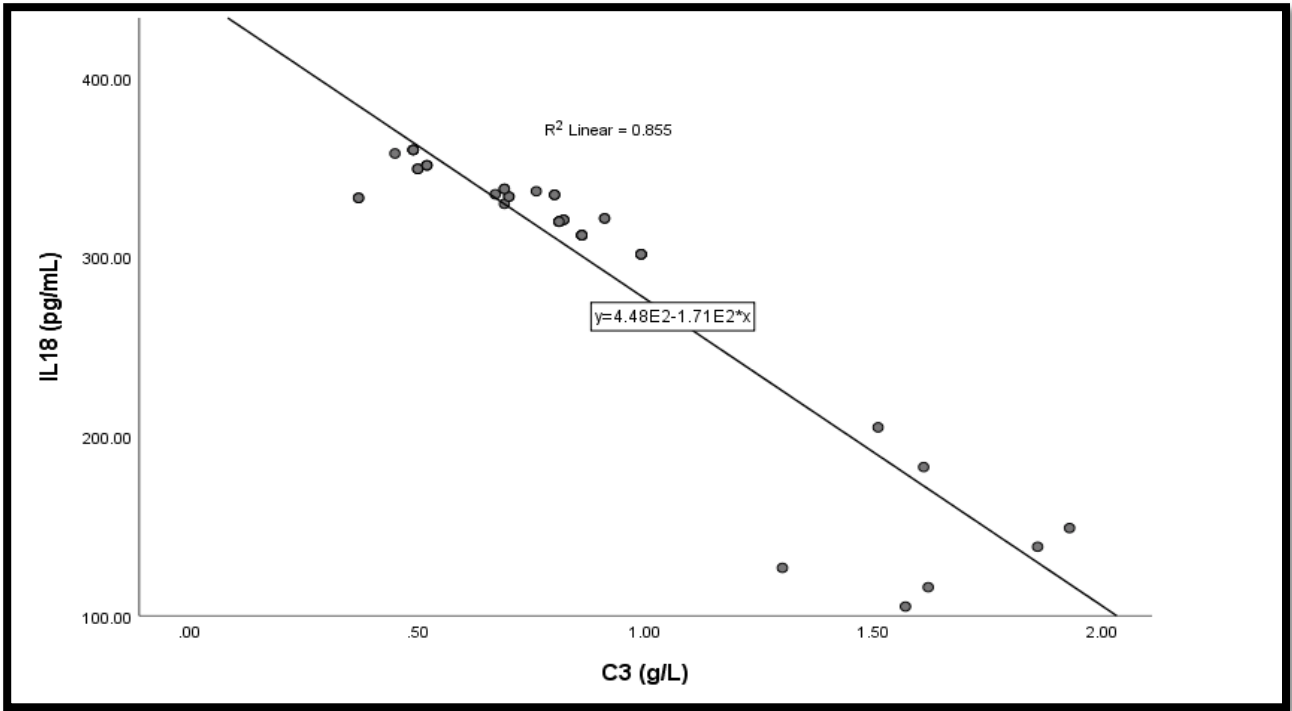
Anti-dsDNA (IU/mL)	0.901	<0.01
Urea (mg/dL)	0.924	<0.01
Creatinine (mg/dL)	0.908	<0.01
GFR (mL/min/1.73 m ²)	-0.843	<0.01
IL-37 (pg/mL)	0.672	<0.01
PD-1 (pg/mL)	0.543	<0.01

r = Pearson correlation coefficient

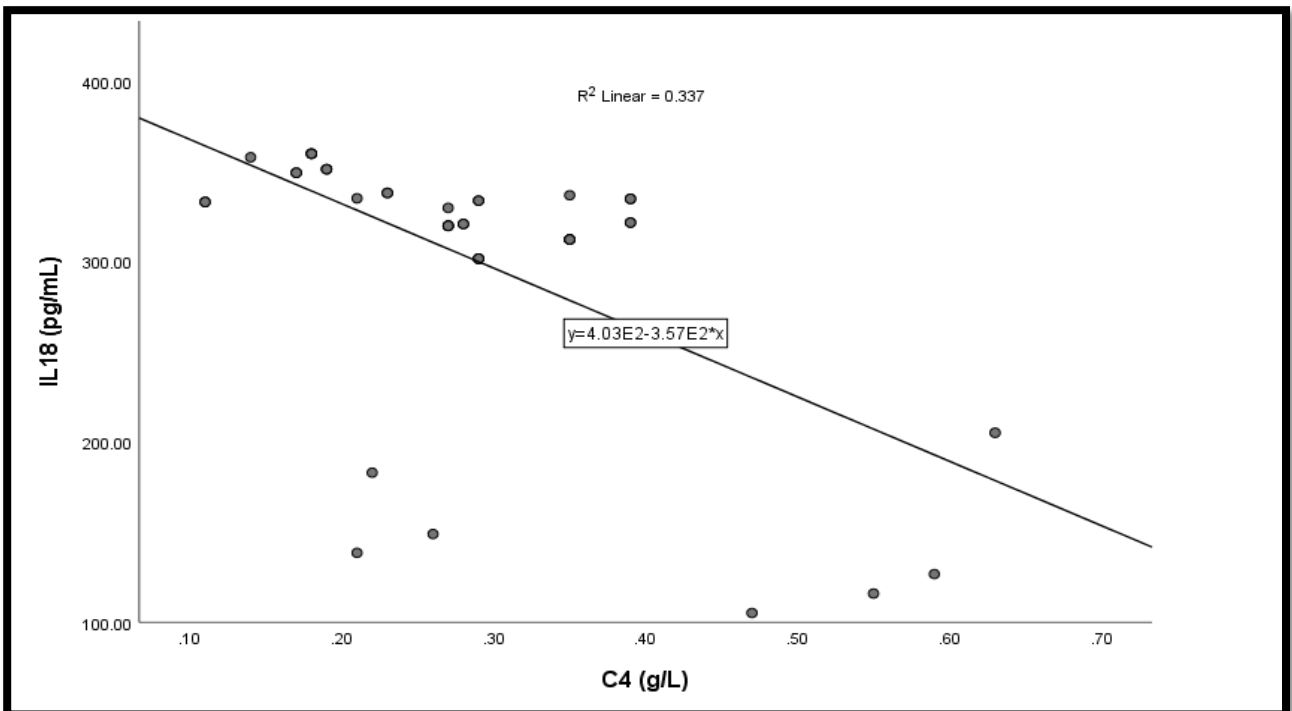
(A)



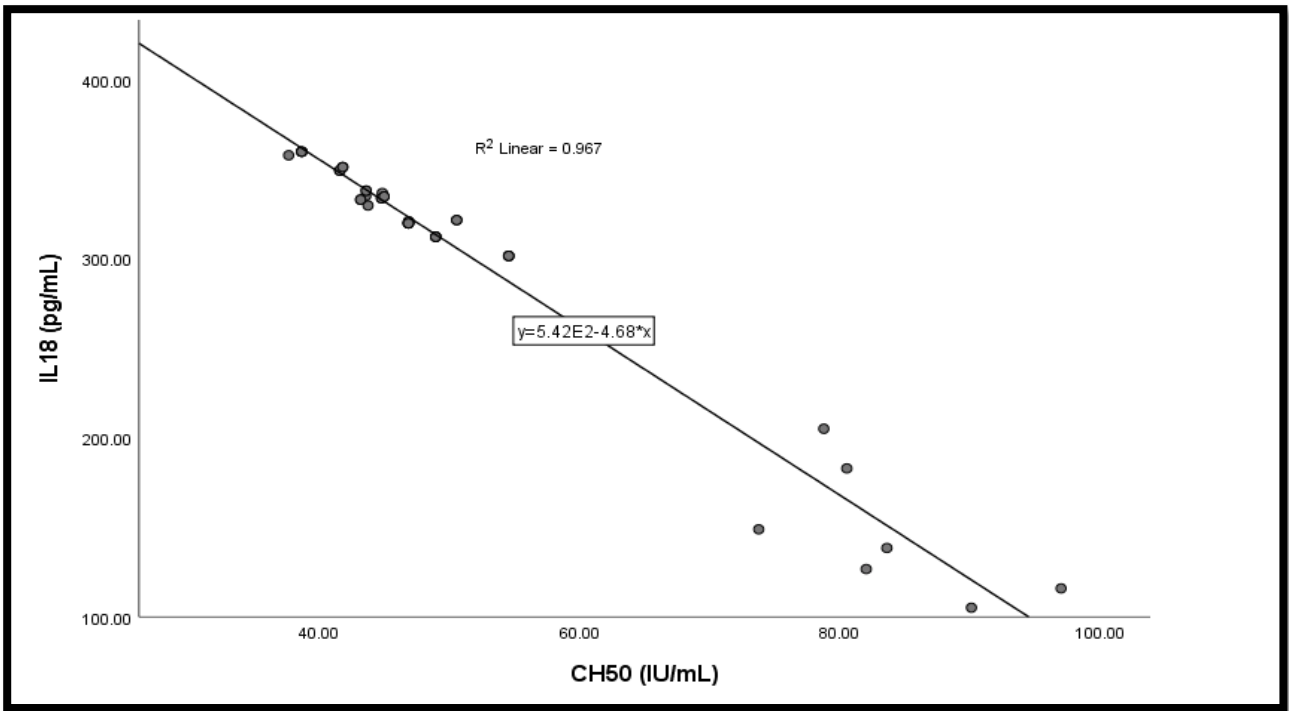
(B)



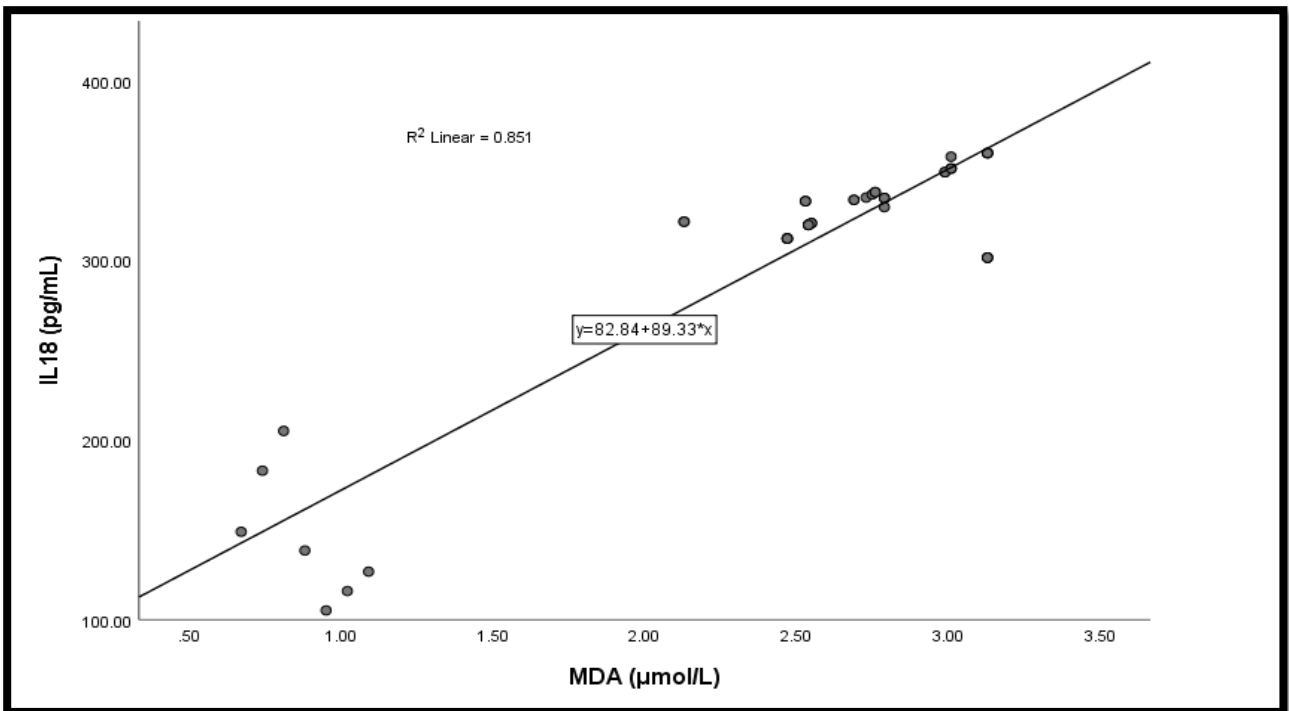
(C)



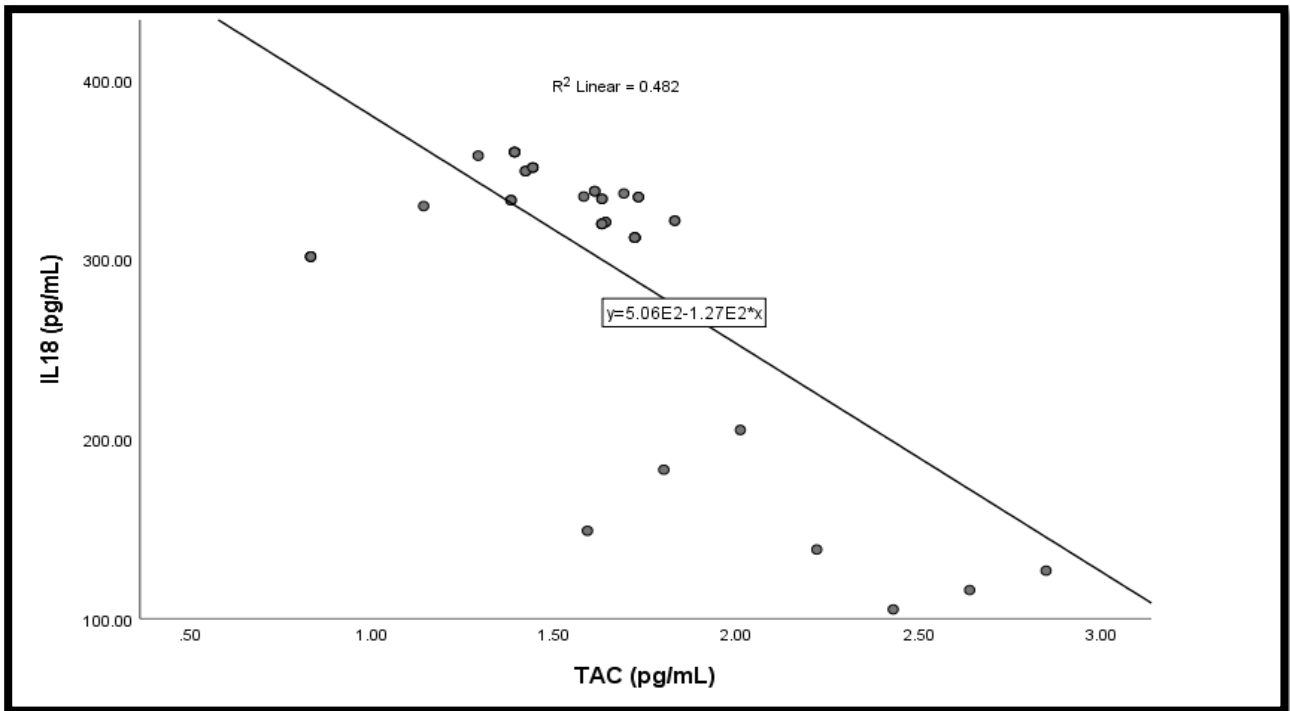
(D)



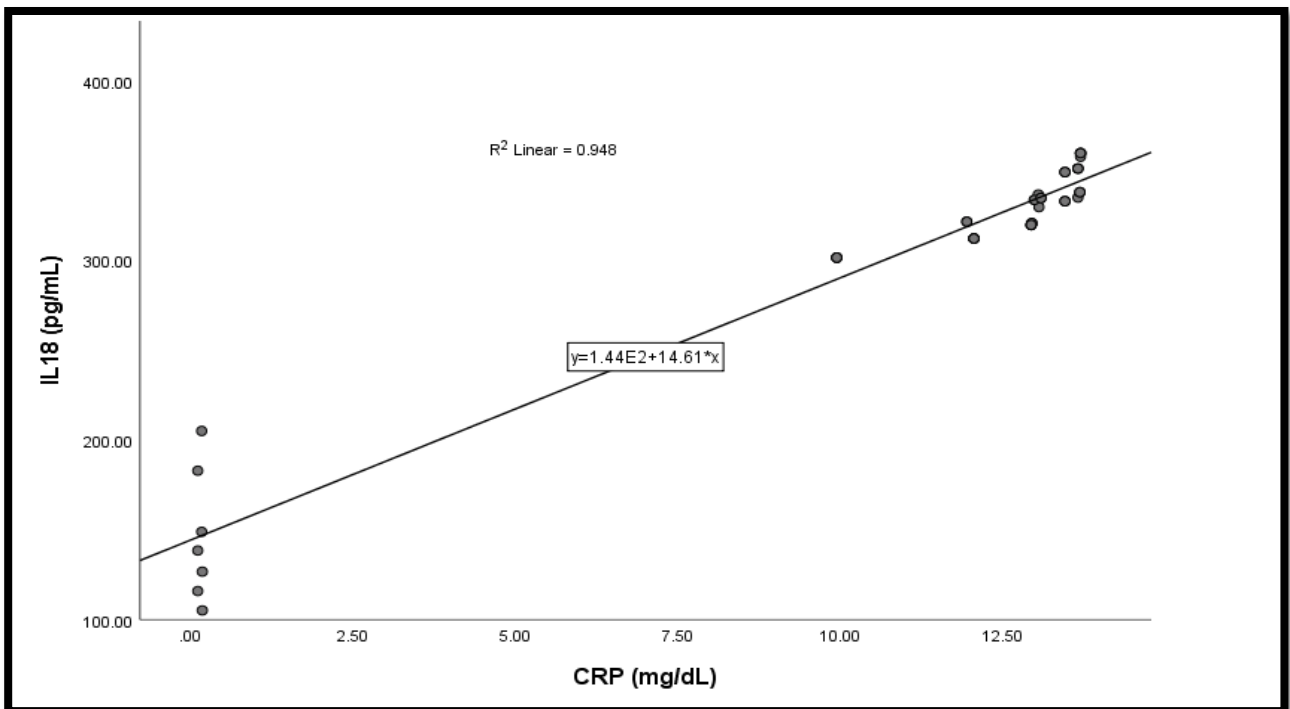
(E)



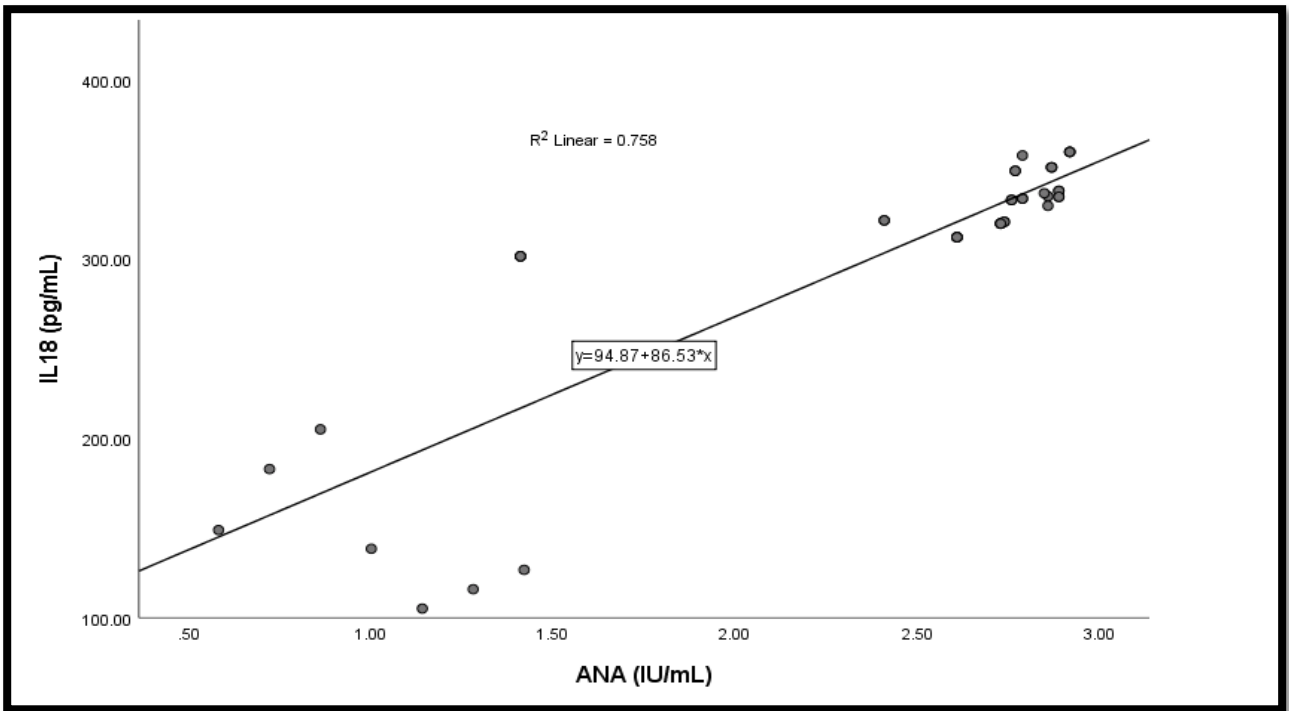
(F)



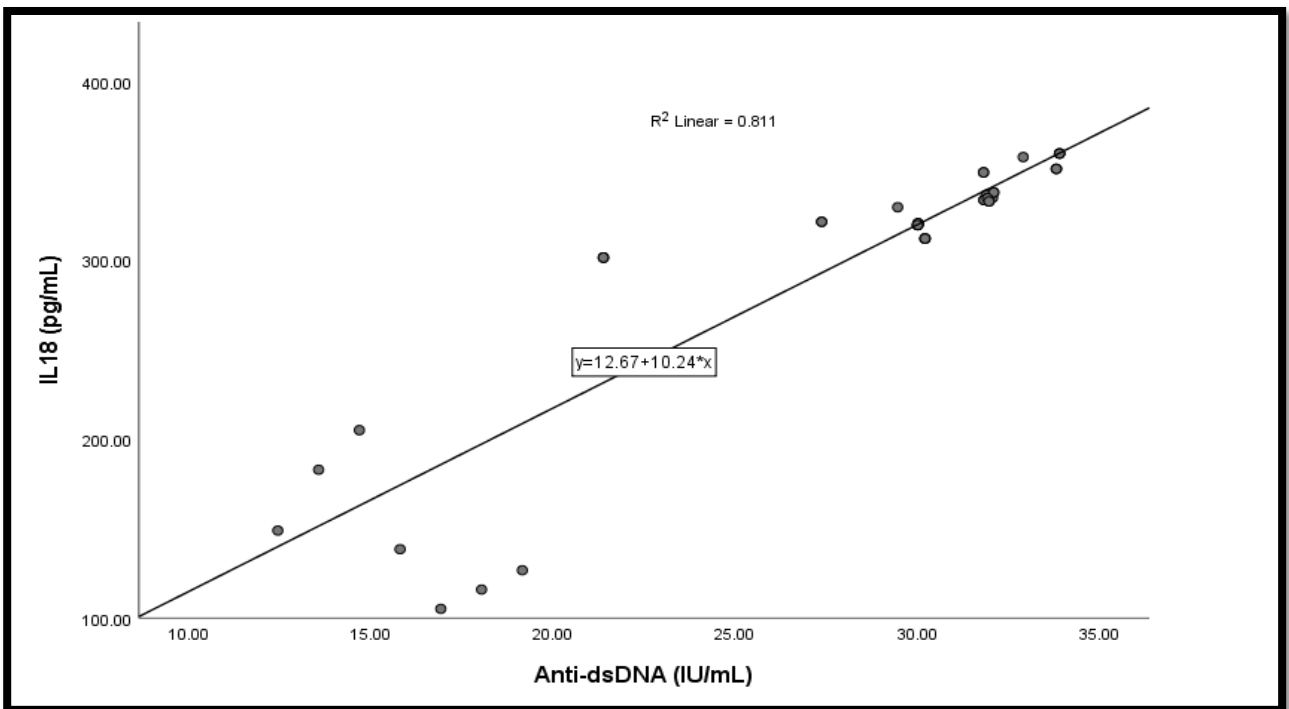
(G)



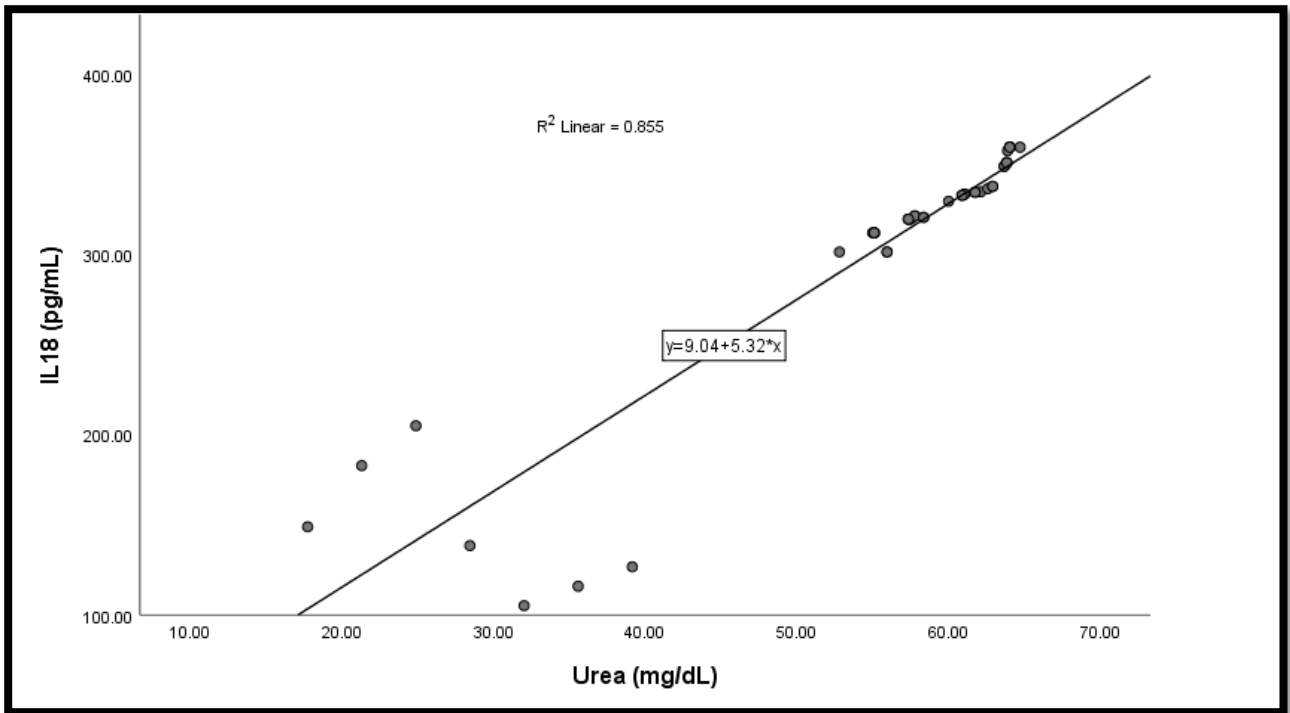
(H)



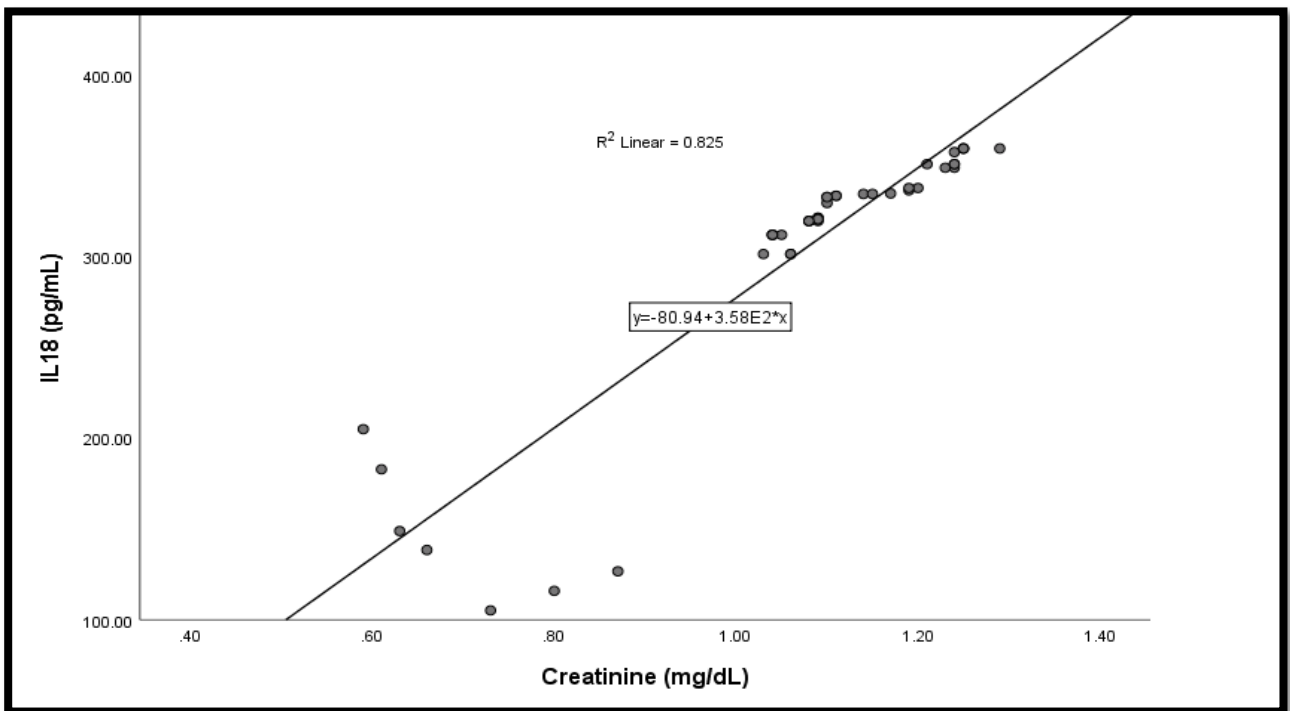
(I)



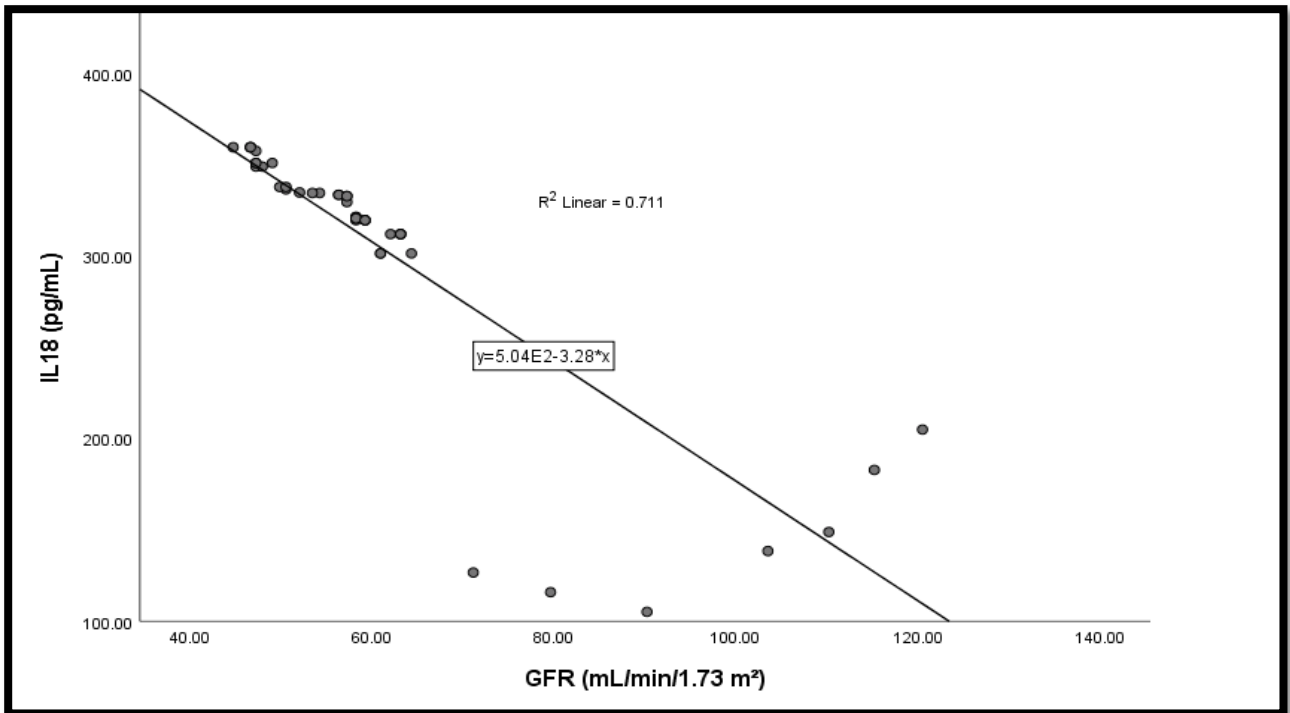
(J)



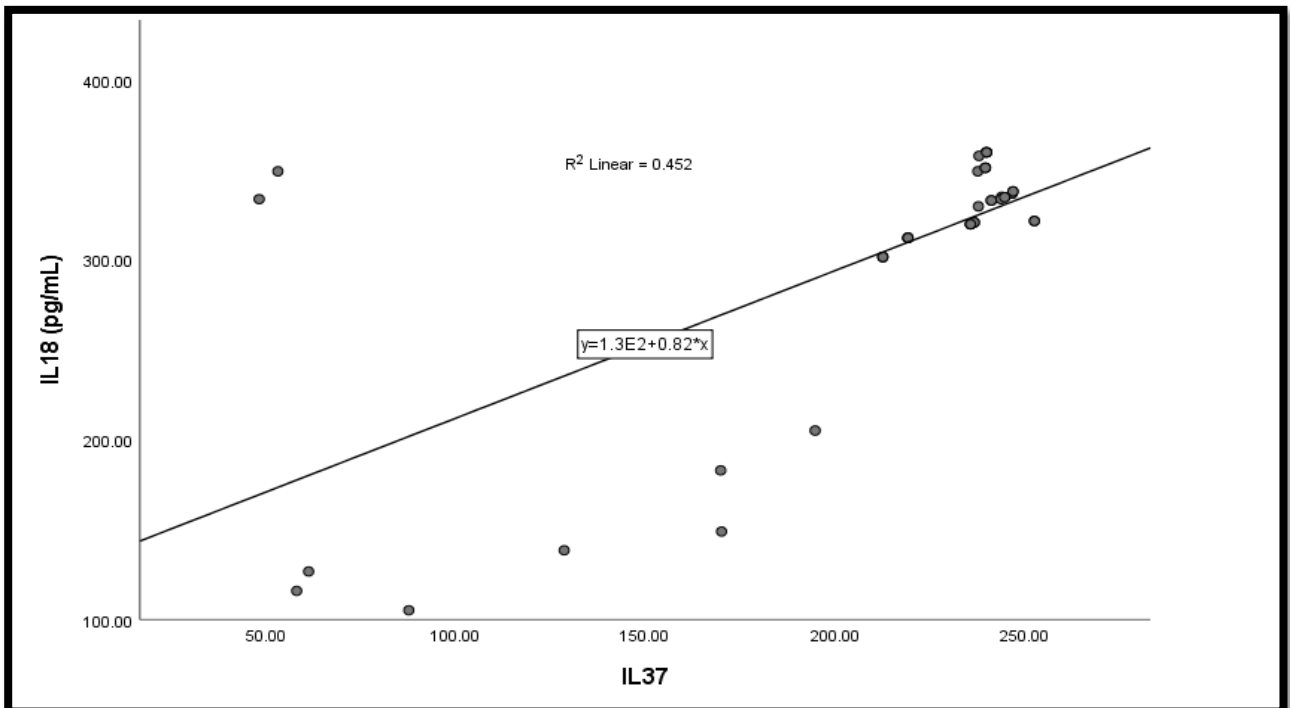
(K)



(L)



(M)



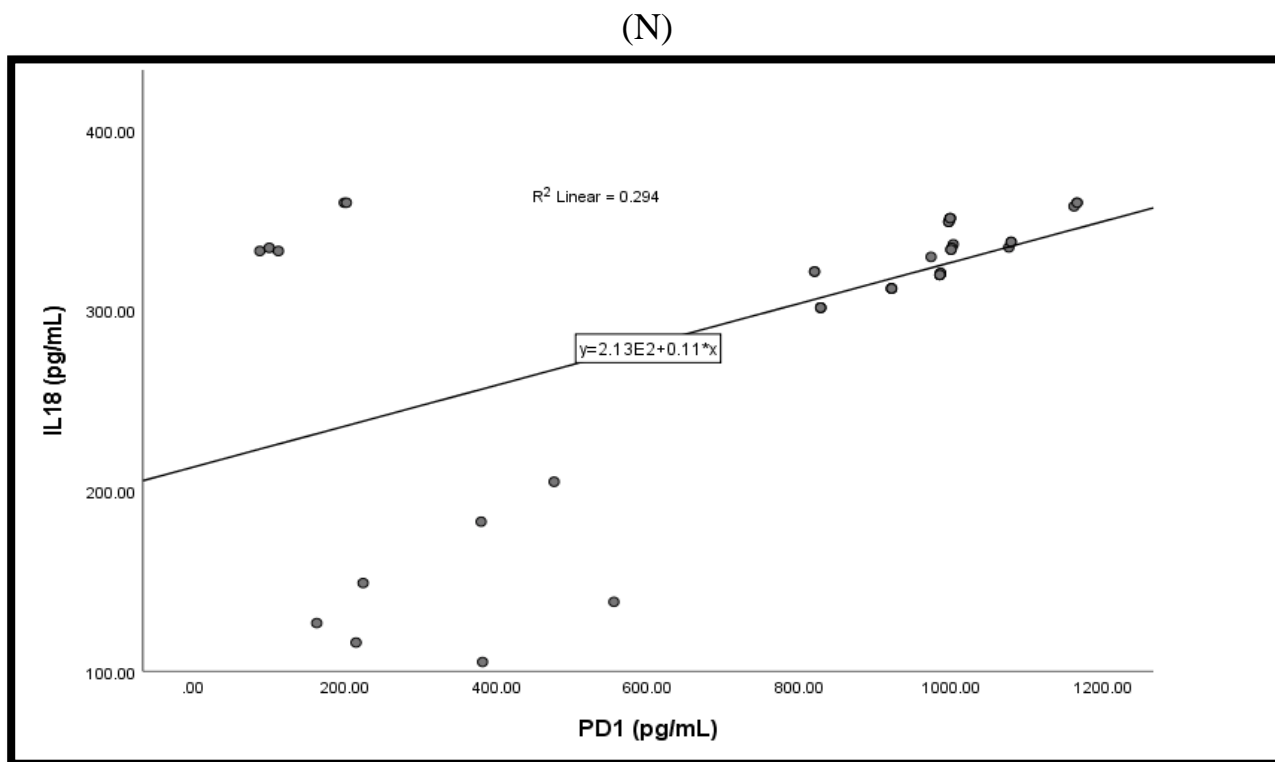


Figure (3.14): Linear regression analysis between serum levels of IL-18 with the following parameters: (A) BMI, (B) C3 (C) C4, (D) CH50, (E) MDA, (F) TAC, (G) CRP, (H) ANA, (I) Anti-dsDNA, (J) Urea, (K) Creatinine, (L) GFR, (M) IL-37, (N) PD-1.

The findings of this investigation indicate a strong and statistically significant inverse relationship between the levels of C3, C4, and CH50, and the levels of IL-18 in patients with SLE. These results imply a potential association between deficiencies in C3, C4, and CH50 and dysregulation of IL-18 in the context of SLE (Mohammed *et al.*, 2018). SLE frequently exhibits dysregulation of the complement system, wherein deficiencies of C3, C4, and CH50 are recognised characteristics of the condition. The reduced immunological capabilities of the complement system can be attributed to decreased levels of C3, C4, and CH50. This phenomenon may result in diminished elimination of ICs, characterised by the aggregation of antibodies and antigens, and heightened inflammatory response (Al-Fartosy *et al.*, 2017b). The formation of ICs may occur as a result of the presence of autoantibodies that specifically recognise and bind to self-antigens. Complement components, such as C3 and C4, typically fulfil a function

in the clearance of ICs. In the event of a deficit in these constituents, the accumulation of ICs may occur, hence initiating an inflammatory response and potentially impacting the generation of IL-18 (Rezaieyazdi *et al.*, 2020). A decrease in complement activity has the potential to result in an augmented inflammatory response. IL-18 has been identified as a key player in the modulation of inflammatory processes. Hence, the increased levels of IL-18 could potentially be attributed to the augmented inflammatory response that arises from defects in the complement system (Mohamed *et al.*, 2019).

Furthermore, it is worth noting that SLE frequently exhibits oxidative stress as a prevailing characteristic. The occurrence of this phenomenon can be attributed to the generation of ROS and the presence of inflammation. Elevation of oxidative stress levels in SLE can induce detrimental effects on cellular and tissue integrity. Specifically, the lipids present in cell membranes are susceptible to impairment, leading to the generation of MDA (Khan *et al.*, 2018). Antioxidants are of paramount importance in the preservation of cellular homeostasis by effectively regulating the equilibrium between free radicals and antioxidants, so safeguarding cells against oxidative harm. Patients diagnosed with SLE frequently encounter oxidative stress as a result of the inflammatory characteristics inherent in the condition (Saha *et al.*, 2021). The observation of diminished TAC implies a potential decline in the body's capacity to mitigate oxidative stress, hence facilitating the accumulation of free radicals and their propensity to induce harm. The presence of persistent inflammation and immune system activation in SLE can give rise to the generation of ROS and subsequent oxidative stress. Oxidative stress has the potential to initiate and intensify the inflammatory response (Bommarito *et al.*, 2017). Elevated levels of MDA can function as an indicator of oxidative stress, signifying the presence of cellular and tissue damage caused by oxidative assault. Lower levels of TAC indicate a potential decline in the body's capacity to mitigate the harmful effects of oxidative stress (Hu *et al.*, 2022). The insufficiency of antioxidants can potentially lead to the accumulation of oxidative damage, hence facilitating the release of pro-inflammatory molecules such as IL-18.

Oxidative stress has the potential to cause harm to several cellular constituents, such as DNA, proteins, and lipids. Lipid peroxidation, resulting in the generation of MDA, serves as an indicator of cellular membrane impairment. The occurrence of cellular damage has the potential to initiate inflammatory responses and induce the secretion of cytokines such as IL-18 (Lee *et al.*, 2019).

Moreover, the production of IL-18 can be triggered by many inflammatory signals, including those originating from CRP. In the context of SLE, it has been observed that immune cells have the potential to upregulate the production of IL-18 when the body is in an inflammatory condition. IL-18 has the ability to enhance inflammatory reactions through its promotion of the synthesis of additional pro-inflammatory cytokines and chemokines (Kwon *et al.*, 2019). This phenomenon has the potential to initiate a positive feedback loop, wherein heightened levels of CRP and IL-18 contribute to the maintenance and intensification of inflammation in SLE. The presence of increased levels of CRP and IL-18 could potentially indicate the persistent immunological dysregulation and tissue damage observed in SLE (Aringer *et al.*, 2019).

Furthermore, the existence of ANA, particularly anti-dsDNA, is a distinctive characteristic of SLE. It is well accepted that these antibodies are pivotal in the pathophysiology of the disease. ICs have the ability to bind with nuclear antigens, resulting in the initiation of inflammatory responses and subsequent tissue damage (Qi *et al.*, 2018). ANA, specifically anti-dsDNA, have the ability to create ICs by binding with nuclear antigens and fragments of DNA. The activation of complement and immune cells can be initiated by these ICs, leading to the induction of an inflammatory response (Gergianaki *et al.*, 2018). Additionally, IL-18 has the potential to be synthesized as a component of the inflammatory cascade that is begun by the deposition of ICs. It has been demonstrated that anti-dsDNA antibodies are capable of interacting with Toll-like receptors (TLRs) present on immune cells, specifically TLR-9. This interaction subsequently triggers the synthesis of pro-inflammatory cytokines, such as IL-18. The interplay between anti-dsDNA and TLRs has the potential to play a role in

immunological dysregulation and the initiation of inflammation in SLE (Shahrokhi *et al.*, 2017). Elevated concentrations of ANA and anti-dsDNA are indicative of persistent immune system activation and the presence of autoimmunity in SLE. The persistent stimulation of the immune system might result in the continuous synthesis of pro-inflammatory cytokines such as IL-18 (AL-hameedawi and Al-Shawi, 2023). The detection of ANA and anti-dsDNA suggests the occurrence of immune system dysregulation, characterized by the immune system erroneously attacking the body's own tissues. The immunological dysfunction can lead to the secretion of pro-inflammatory mediators, such as IL-18 (Yuan *et al.*, 2020).

In addition, it is important to note that renal involvement, referred to as LN, is a prevalent consequence associated with SLE. In the context of LN, the immune system initiates an assault on the kidneys, resulting in the occurrence of inflammation and subsequent impairment. This phenomenon may lead to a decline in renal function, as indicated by elevated concentrations of urea and creatinine in the bloodstream (Al-Fartosy *et al.*, 2020b). A diminished GFR is suggestive of impaired renal function, a common occurrence in individuals with SLE who have LN. This implies that the renal system exhibits decreased efficacy in eliminating waste products from the bloodstream, resulting in the accumulation of toxins and waste materials within the organism (Rees *et al.*, 2017). LN is distinguished by renal inflammation and the secretion of pro-inflammatory cytokines. IL-18 is an example of a cytokine that possesses pro-inflammatory characteristics. The presence of increased IL-18 levels could potentially be attributed to the augmented inflammatory reaction linked to renal impairment (Fike *et al.*, 2019). The occurrence of inflammation and subsequent tissue damage within the renal system can induce cellular stress and trigger the production of danger signals. The aforementioned signals have the capacity to initiate the synthesis of pro-inflammatory cytokines, such as IL-18 (Chen *et al.*, 2020). Impairment of the immune system's regular control can occur as a result of kidney injury. IL-18 is involved in the modulation of

immunological responses, and its aberrant regulation may be implicated in the immune dysfunction observed in SLE patients with renal manifestations (Schell *et al.*, 2022).

On the other hand, IL-37 has been widely recognised for its potent anti-inflammatory characteristics, enabling it to effectively mitigate the detrimental effects induced by pro-inflammatory cytokines, such as IL-18. Within the framework of SLE, the human body may exhibit an upregulation of IL-37 as a regulatory mechanism aimed at modulating the exaggerated inflammatory reaction. The observed increase in concentrations of both IL-37 and IL-18 may be indicative of the intricate and disrupted immunological reactions observed in SLE (Samuels *et al.*, 2022). Although IL-37 exhibits an inclination to mitigate inflammation, its efficacy may not be adequate to effectively counterbalance the impact of IL-18. The observed strong association between IL-37 and IL-18 suggests that the human body may be employing a regulatory mechanism to manage the persistent inflammation observed in SLE (Yang *et al.*, 2020). Nevertheless, it is possible that this particular regulator may not exhibit efficacy in effectively managing the inflammatory processes associated with the disease, resulting in the persistence of elevated levels of cytokines (Gao *et al.*, 2017a).

Conversely, dysregulation of PD-1 expression and signalling on immune cells has been observed in individuals with SLE. This implies that the PD-1 pathway may exhibit reduced efficacy in transmitting inhibitory signals to T cells and other components of the immune system (Narani, 2019). Dysregulated PD-1 signalling has the potential to induce heightened activation of immune cells and subsequent release of cytokines, such as IL-18. The primary expression of PD-1 is observed on T cells, and its signalling plays a crucial role in the regulation of T cell responses. The impairment of PD-1 signalling can lead to the over-activation of T cells and the subsequent secretion of pro-inflammatory cytokines, such as IL-18 (Fava and Petri, 2019). PD-1 and its corresponding ligands have been observed to be expressed on various immune cell types, including B cells and macrophages. The dysregulation of PD-1 signalling has the potential to disturb the equilibrium of interactions among various immune cell

populations, resulting in an inflammatory milieu that facilitates the generation of IL-18 (Mitratza *et al.*, 2021). PD-1 plays a crucial role in the maintenance of immunological tolerance and the prevention of autoimmune reactions. The dysregulation of PD-1 signalling has been implicated in the disruption of immunological tolerance, leading to the recognition and attack of self-antigens by the immune system. This aberrant immune response can subsequently trigger the IL-18 release and several other pro-inflammatory cytokines (Lu *et al.*, 2021a).

3.5.2. Correlation between Serum IL-37 Levels with Biochemical Parameters in SLE Patients

Table (3.17) and Figure (3.15) analyse the impact of serum IL-37 on the biochemical investigation of the group of patients with SLE, using linear regression analysis.

A weak positive connection was found between IL-37 levels and BMI levels in patients with SLE.

Additionally, a strong negative association was found between the levels of C3, C4, CH50, TAC, and GFR with the level of IL-37 in the group of patients with SLE.

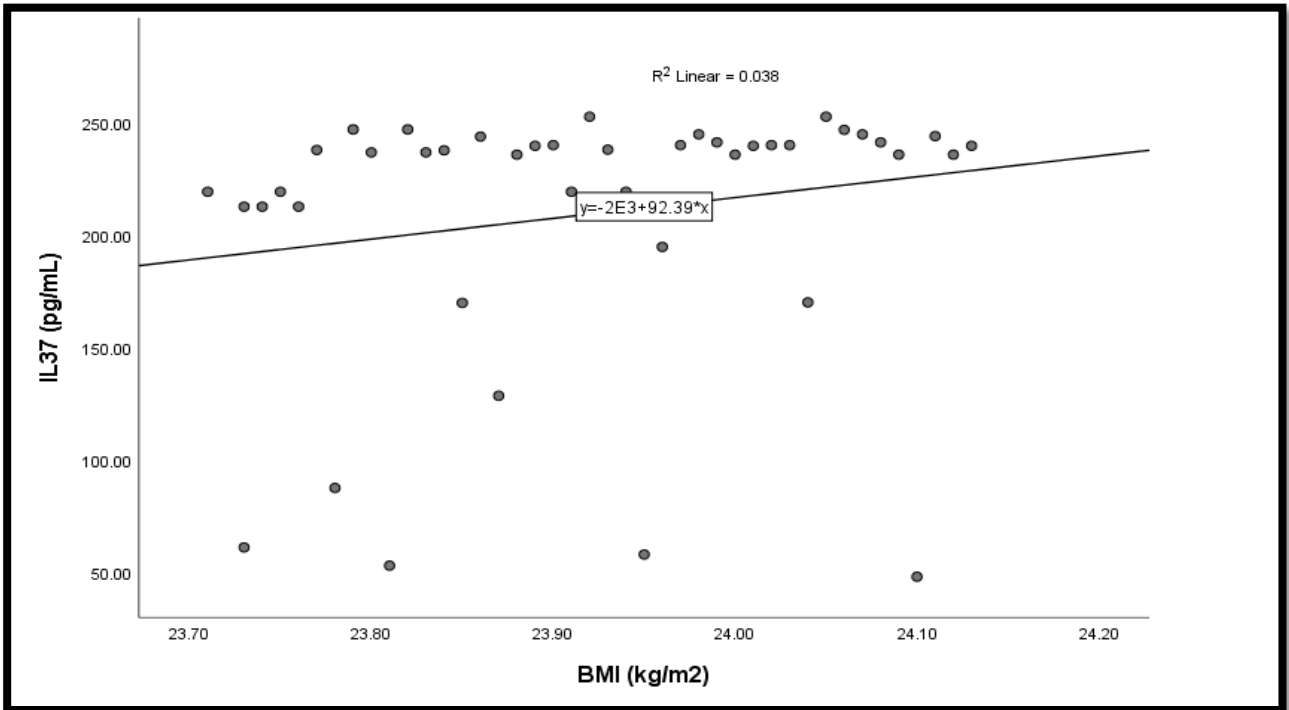
On the other hand, a strong positive association was found between the level of IL-37 and the levels of MDA, CRP, ANA, Anti-dsDNA, urea, creatinine, IL-18, and PD-1 in the group of patients with SLE.

Table (3.17): Correlation between serum IL-37 levels with biochemical parameters in SLE patients group

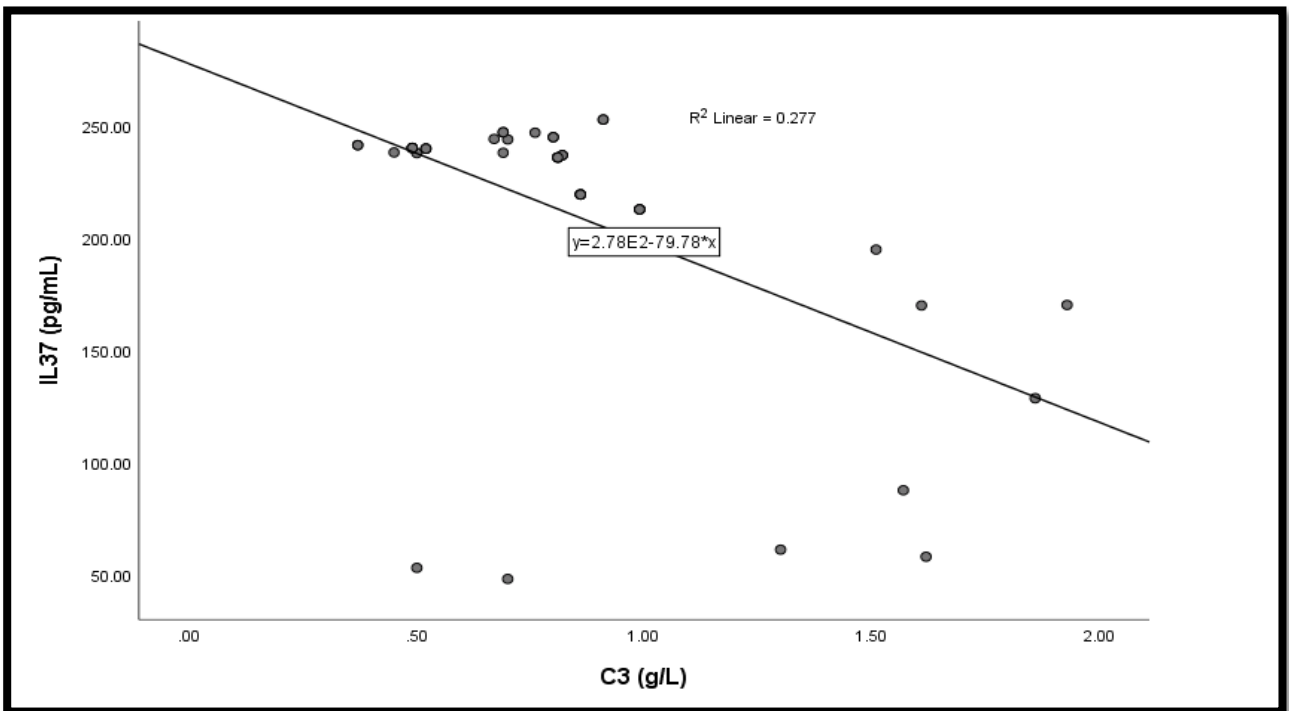
Parameter	IL-37 (pg/mL)	
	r	P-Value
BMI (kg/m ²)	0.194	0.212
C3 (g/L)	-0.526	<0.01
C4 (g/L)	-0.501	<0.01
CH50 (IU/mL)	-0.660	<0.01
MDA (μmol/L)	0.544	<0.01
TAC (pg/mL)	-0.533	<0.01
CRP (mg/dL)	0.638	<0.01
ANA (IU/mL)	0.524	<0.01
Anti-dsDNA (IU/mL)	0.528	<0.01
Urea (mg/dL)	0.527	<0.01
Creatinine (mg/dL)	0.508	<0.01
GFR (mL/min/1.73 m ²)	-0.500	<0.01
IL-18 (pg/mL)	0.672	<0.01
PD-1 (pg/mL)	0.502	<0.01

r = Pearson correlation coefficient

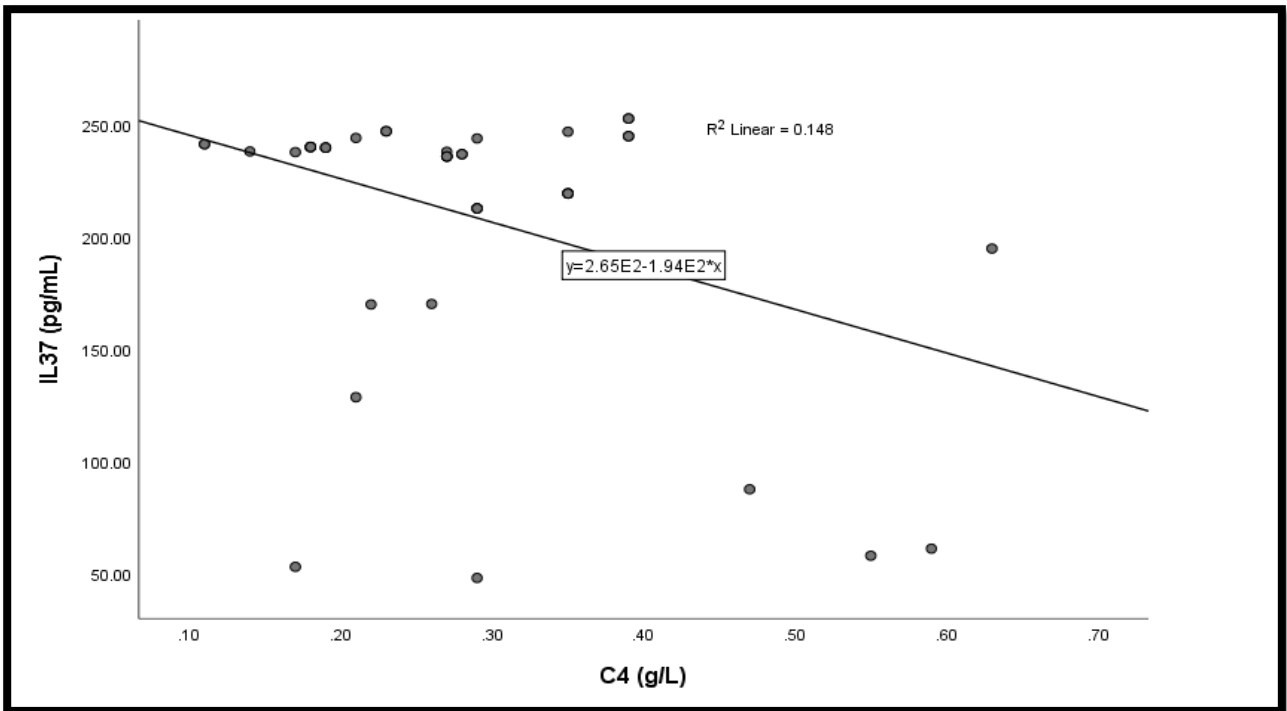
(A)



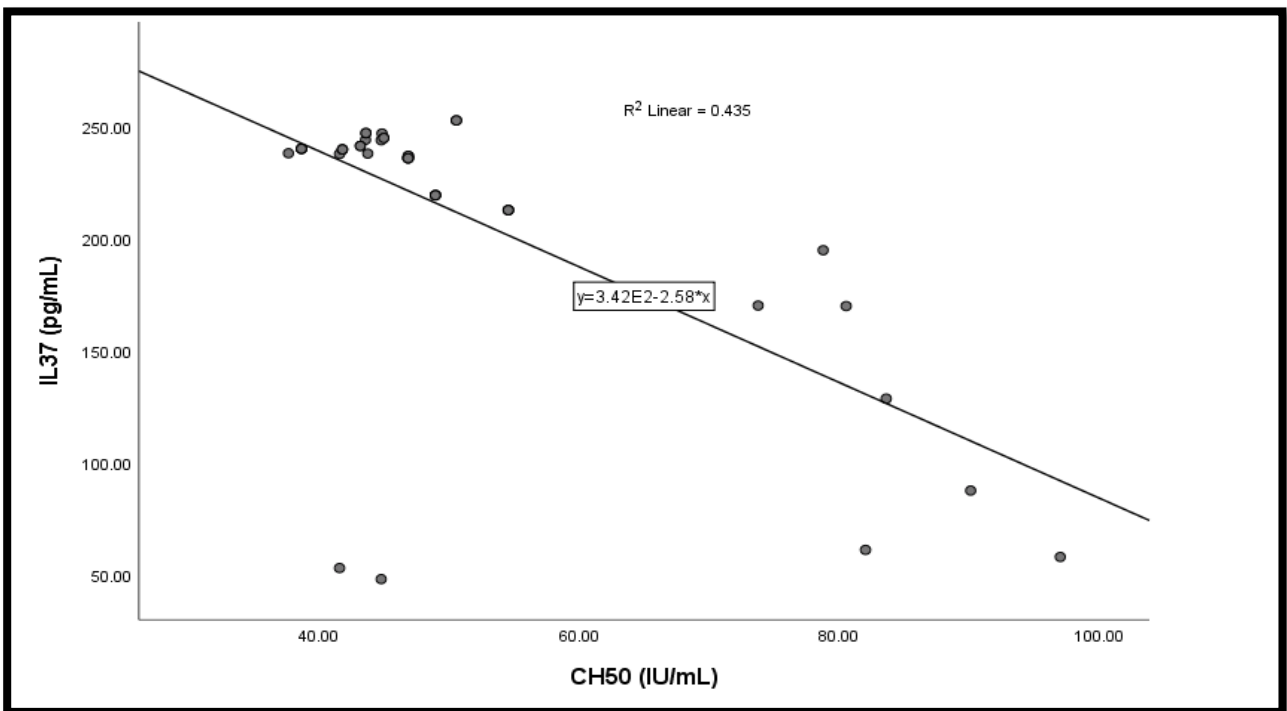
(B)



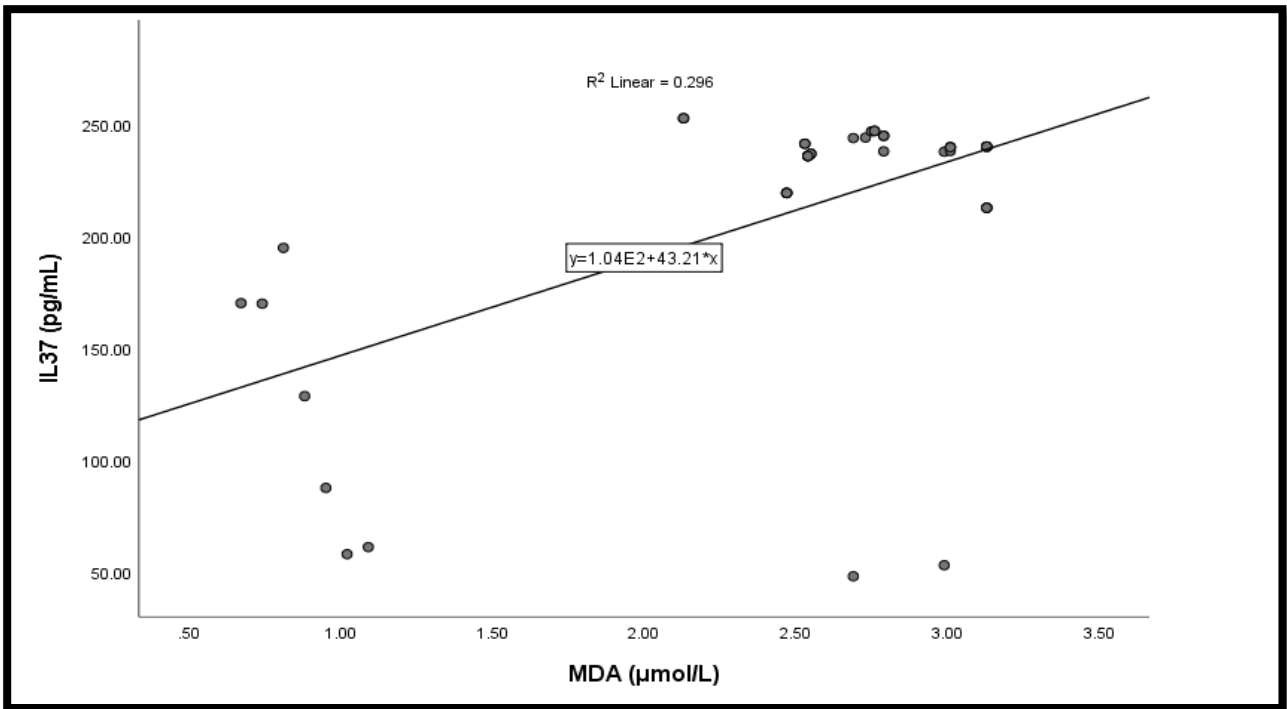
(C)



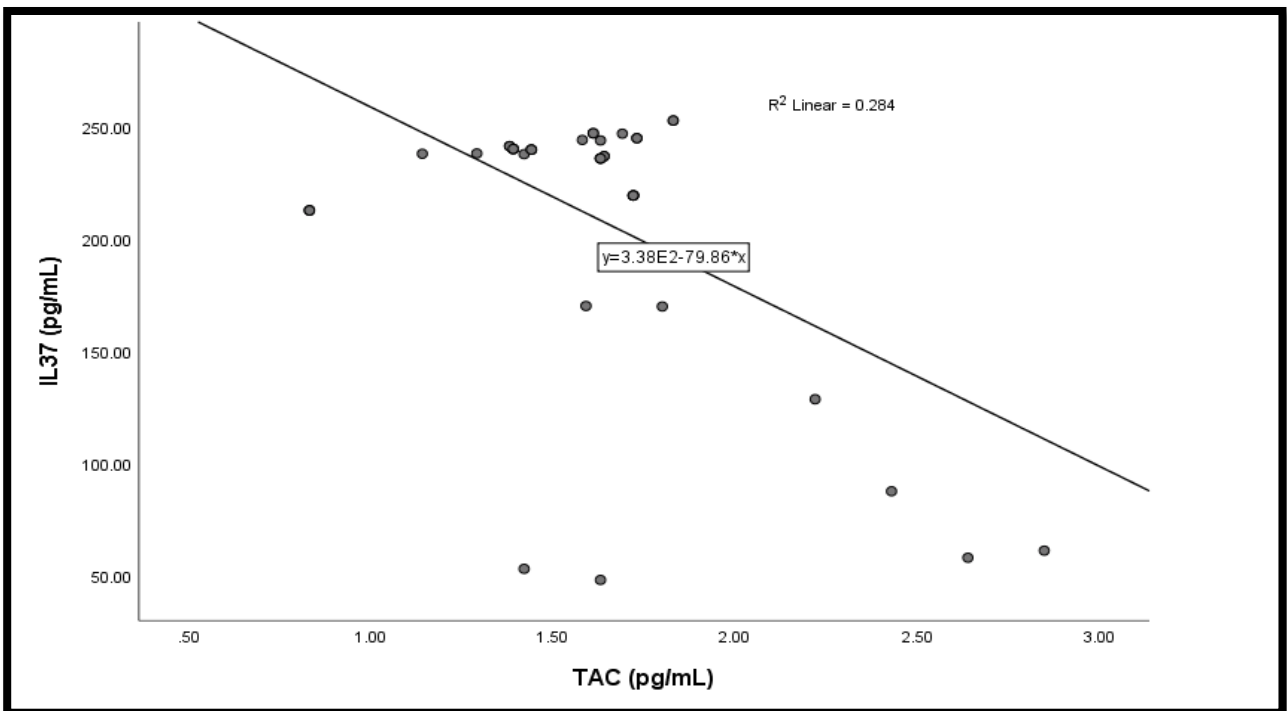
(D)



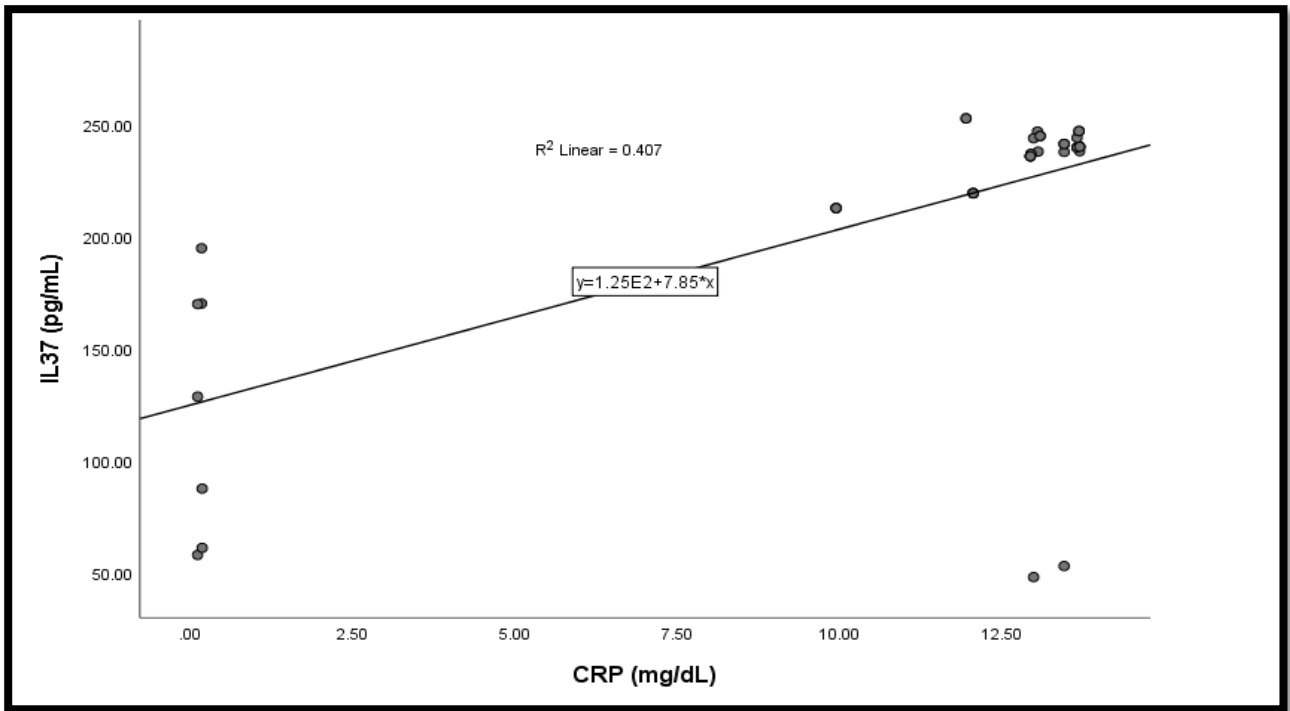
(E)



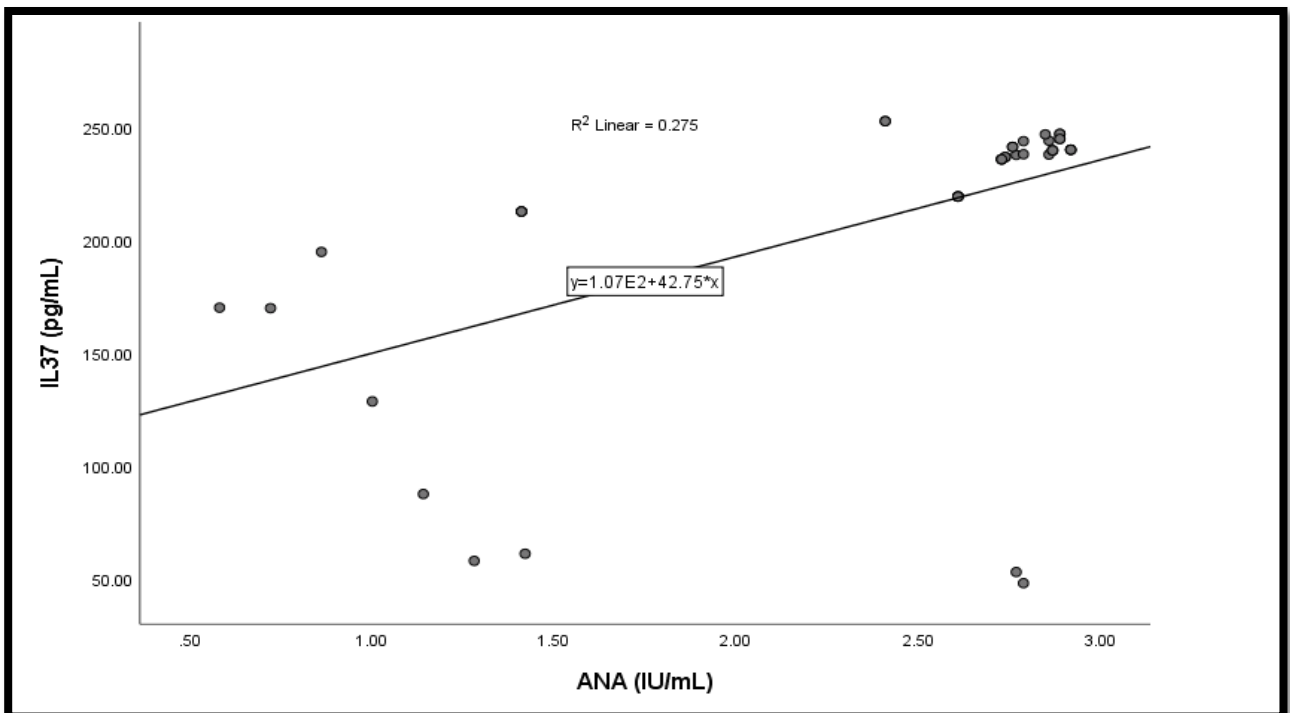
(F)



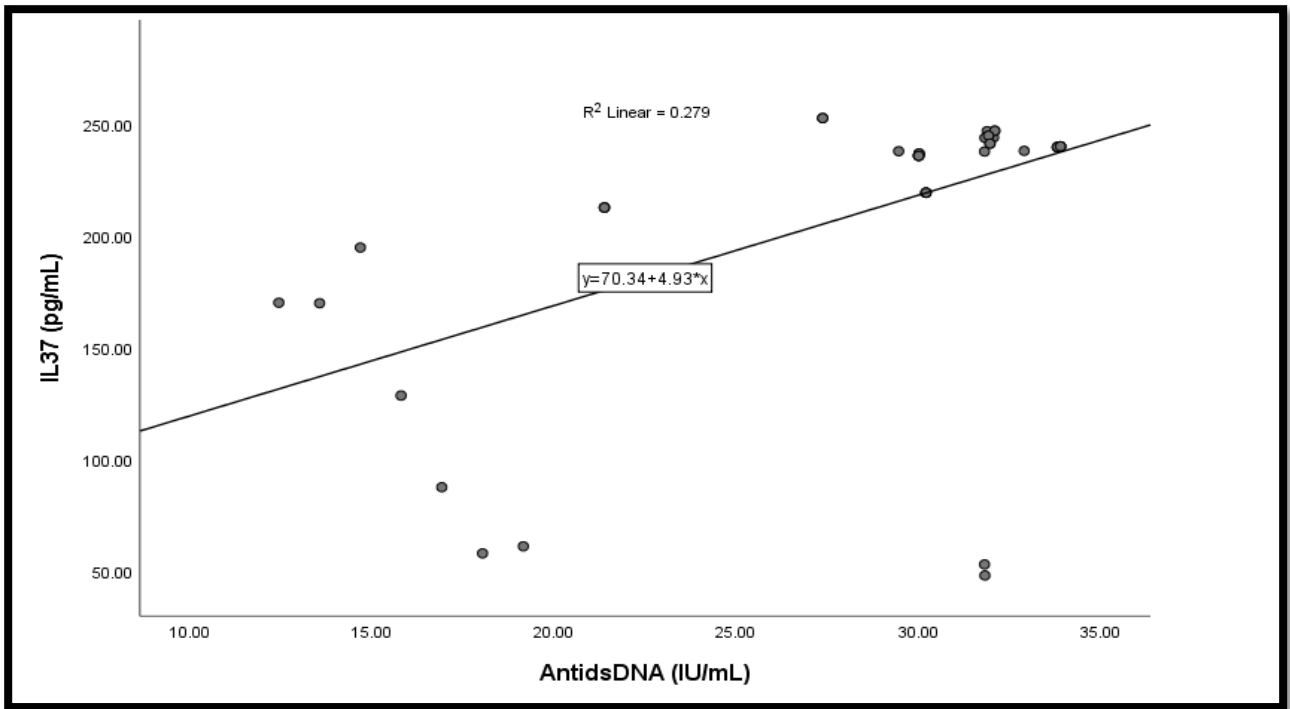
(G)



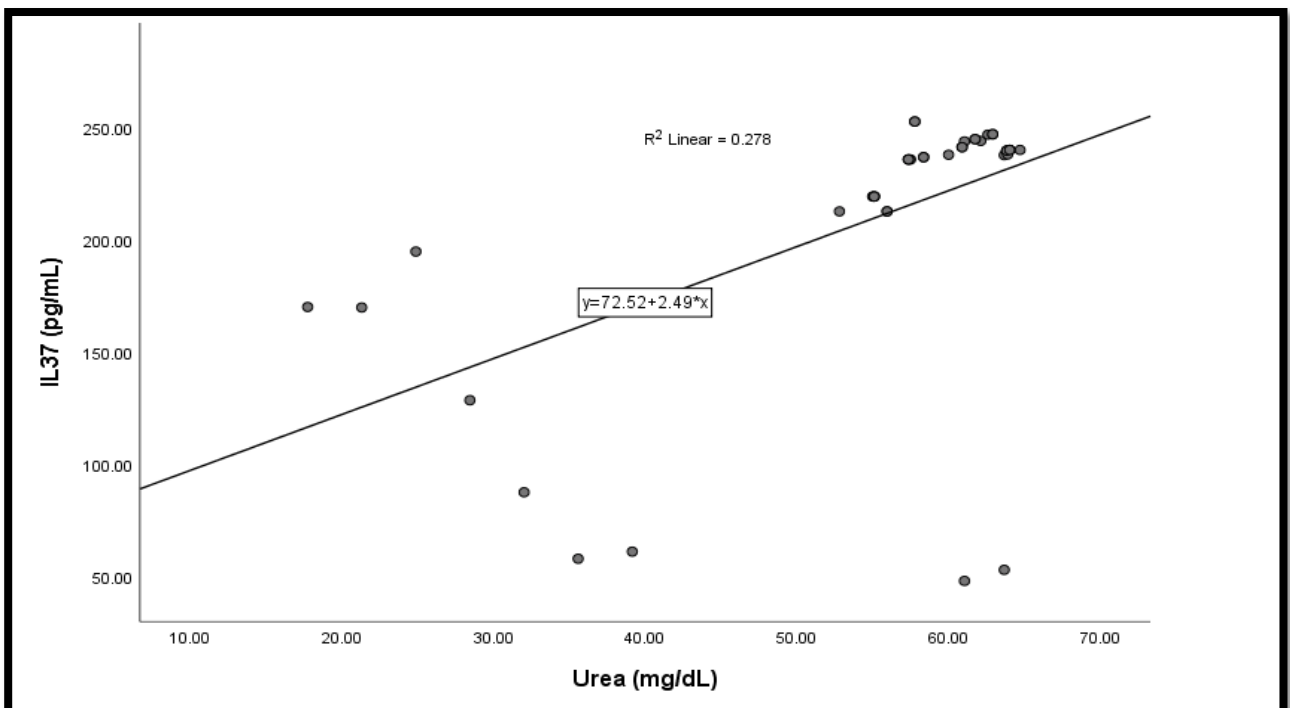
(H)



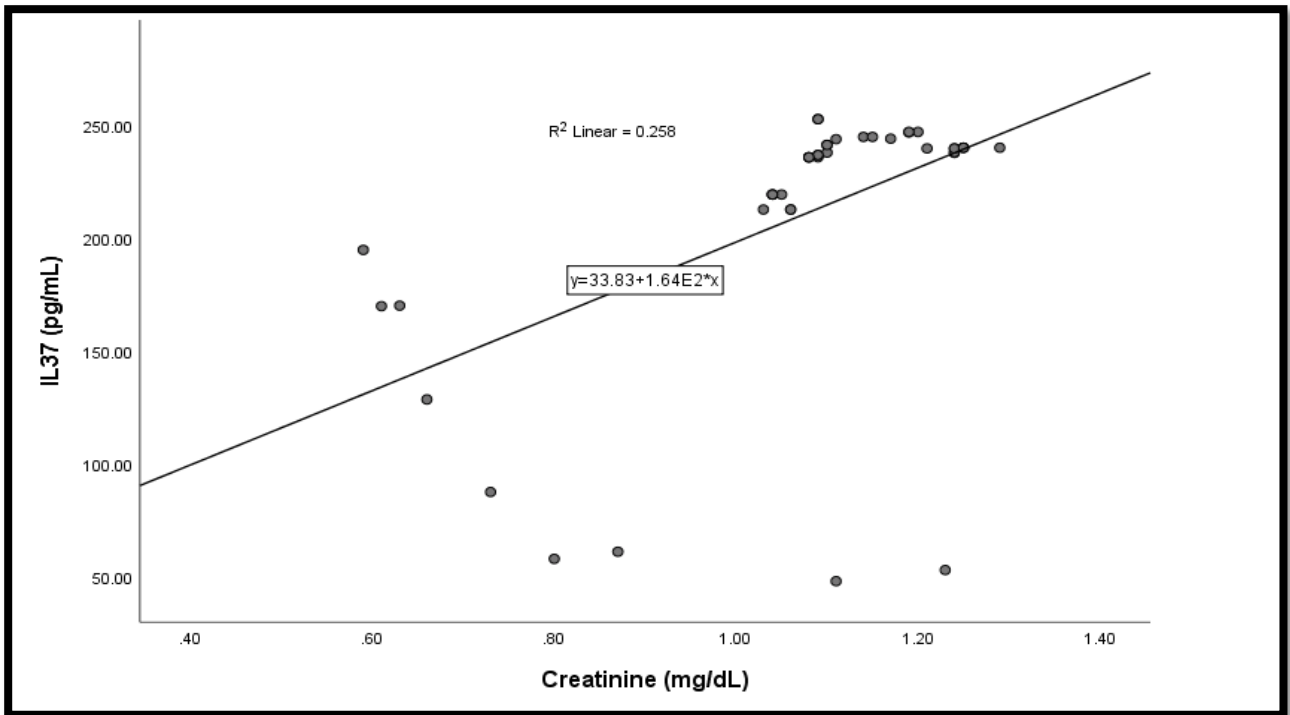
(I)



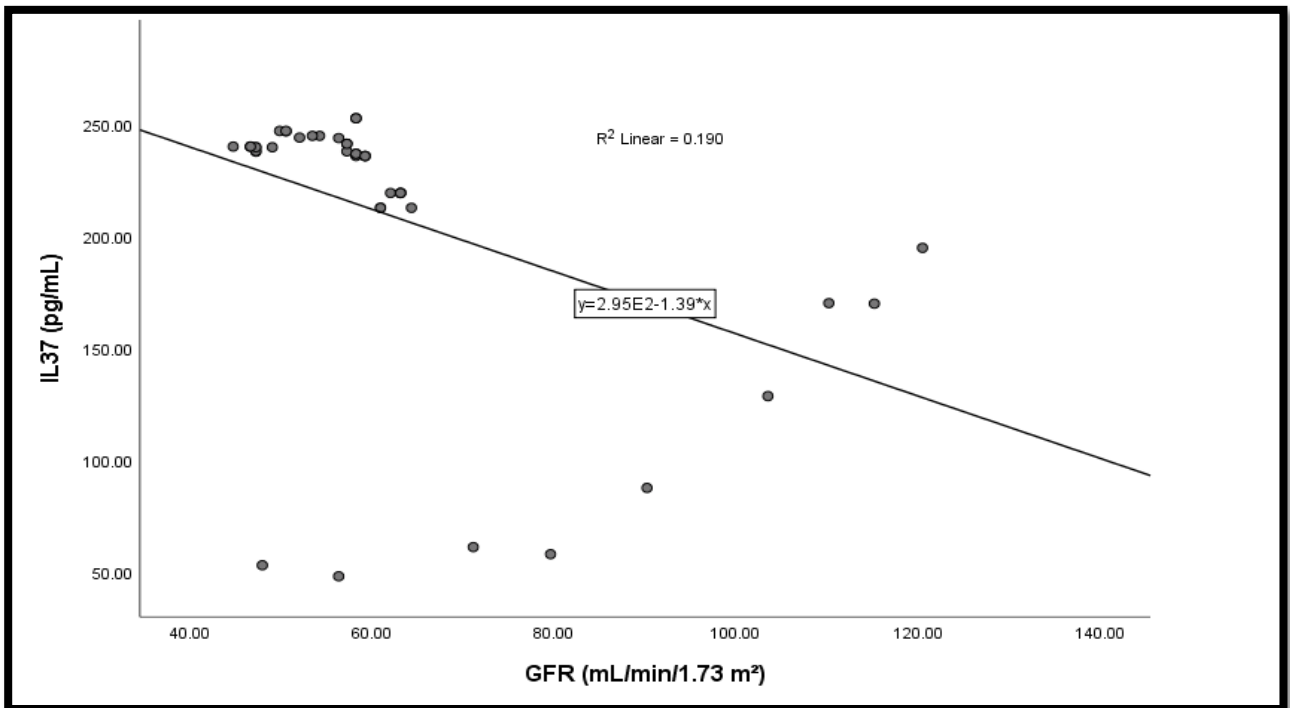
(J)



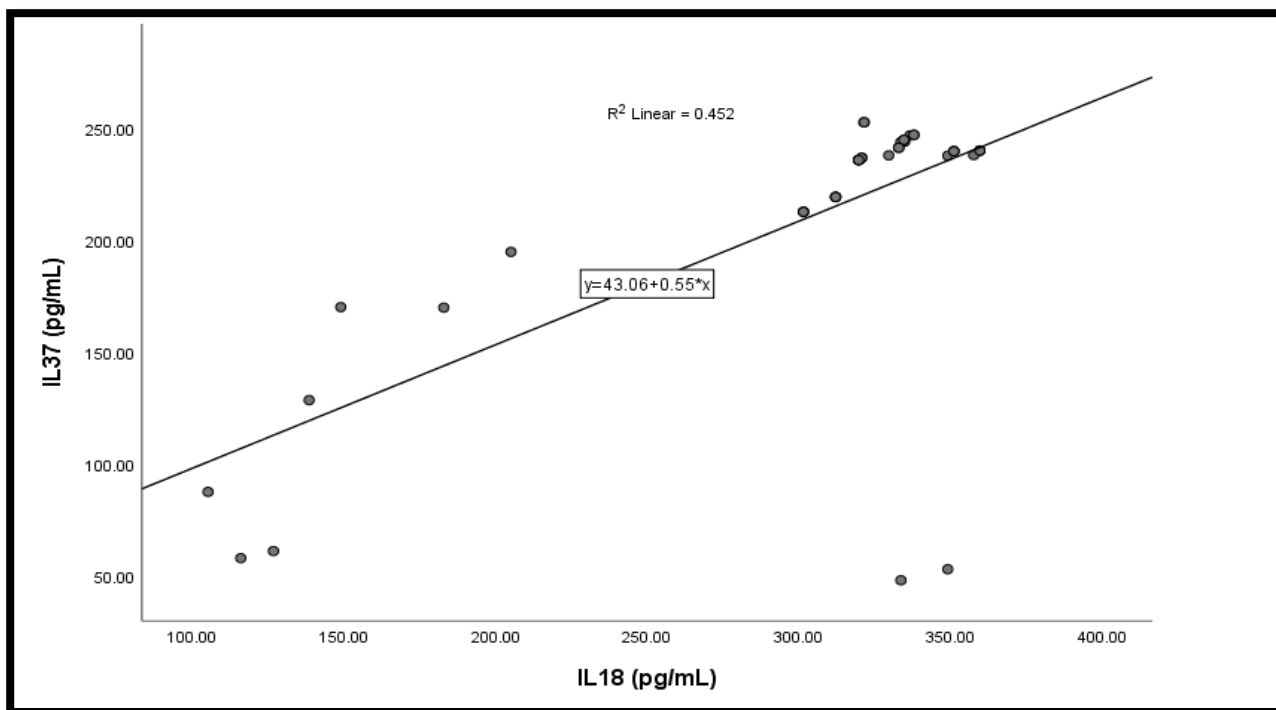
(K)



(L)



(M)



(N)

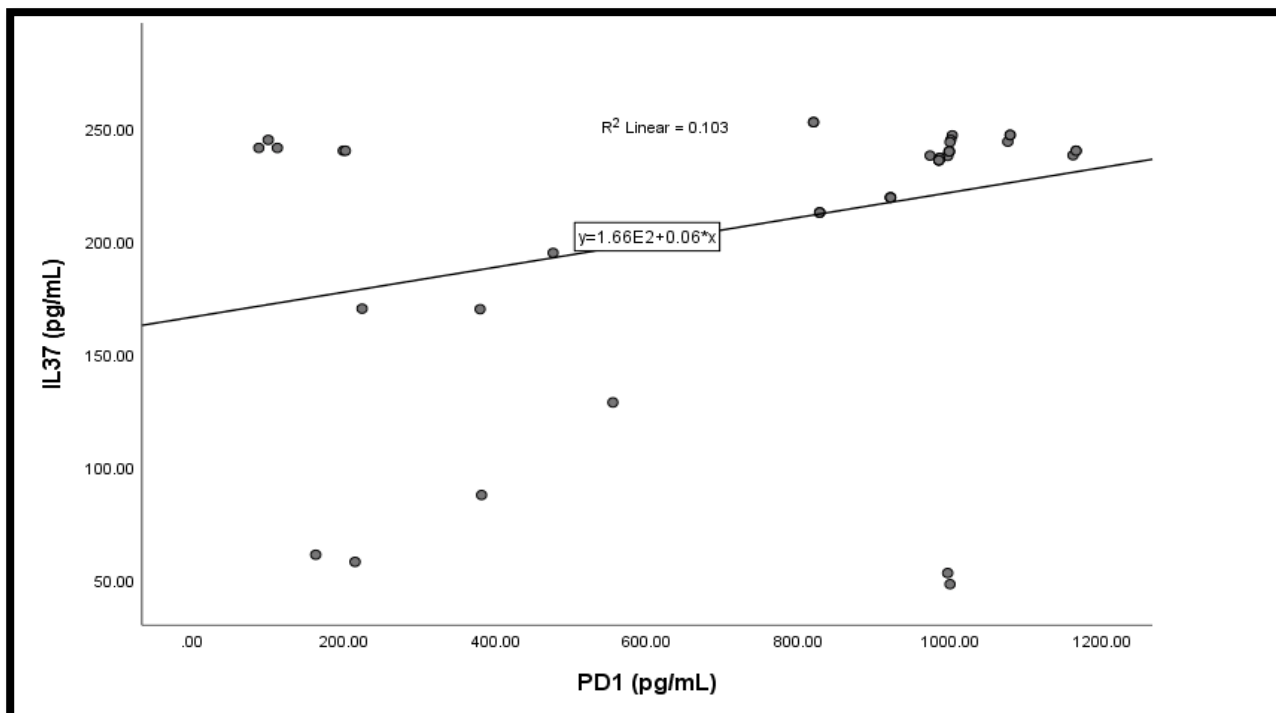


Figure (3.15): Linear regression analysis between serum levels of IL-37 with the following parameters: (A) BMI, (B) C3 (C) C4, (D) CH50, (E) MDA, (F) TAC, (G) CRP, (H) ANA, (I) Anti-dsDNA, (J) Urea, (K) Creatinine, (L) GFR, (M) IL-18, (N) PD-1.

The present investigation demonstrates that complement activation can result in the liberation of pro-inflammatory agents, such as cytokines like IL-18. In SLE, where there is commonly a decrease in complement activity, the body may respond by boosting the production of other cytokines, such as IL-37, as part of an intricate feedback cycle (Chessa *et al.*, 2020). The clearance of ICs, which are produced by the binding of antibodies to self-antigens, involves the participation of C3 and C4. Diminished complement activity can lead to the prolonged presence of ICs, which in turn can cause chronic inflammation and the release of cytokines, including IL-37 (Al-Gahtani, 2021). IL-37 exhibits potent anti-inflammatory characteristics and has the ability to mitigate excessive inflammation. Within the framework of complement insufficiency and chronic inflammation in SLE, the body may generate elevated quantities of IL-37 as a regulatory mechanism in an effort to manage the inflammatory reaction. Complement deficits can contribute to the disruption of immunological regulation, potentially involving IL-37 and its function in controlling immune responses (Wang *et al.*, 2021).

Furthermore, the persistent inflammation and activation of the immune system might result in the generation of ROS and the occurrence of oxidative stress in SLE. Oxidative stress can initiate and intensify inflammation. IL-37, while predominantly acknowledged as an anti-inflammatory cytokine, can be generated in reaction to inflammation and oxidative stress as a component of a feedback loop aimed at regulating excessive inflammation (Nakanishi, 2018). Lower TAC levels indicate a potential decline in the body's capacity to combat oxidative damage. The lack of antioxidants can lead to the accumulation of oxidative damage, which in turn contributes to the release of pro-inflammatory molecules such as IL-37 (Wu *et al.*, 2021). Oxidative stress has the potential to harm several cellular constituents, such as DNA, proteins, and lipids. Lipid peroxidation, resulting in the formation of MDA, indicates cellular membrane damage. Cellular damage has the potential to initiate inflammatory reactions and the secretion of cytokines such as IL-37 (Al-Anazi *et al.*,

2019). IL-37 is recognised for its function in modulating inflammation and immunological reactions. Under conditions of oxidative stress and inflammation, the body may upregulate the production of IL-37 as a means to mitigate exaggerated immune reactions and safeguard against tissue harm (Jaing *et al.*, 2021).

Moreover, increased levels of CRP can function as an indicator of the ongoing inflammatory reaction in patients with SLE. IL-37 plays a role in modulating immunological responses, and its synthesis can be affected by inflammation. During instances of persistent inflammation, the body may generate elevated quantities of IL-37 as a regulatory mechanism to manage exaggerated immune reactions and mitigate inflammation (Ayoub *et al.*, 2019). IL-37 is renowned for its potent anti-inflammatory characteristics. It has the ability to suppress the production of pro-inflammatory cytokines and regulate the responses of immune cells. In SLE, increased concentrations of CRP and other substances that promote inflammation can stimulate the synthesis of IL-37 as a means of regulating the inflammatory response and preventing undue harm to tissues (Al-Fartosy *et al.*, 2017a).

In addition, ANA, specifically anti-dsDNA antibodies, have the ability to create ICs by binding with nuclear antigens and fragments of DNA. Activation of complement and immune cells can be induced by these ICs, leading to an inflammatory response. IL-37 can be generated as a component of the inflammatory cascade triggered by the deposition of ICs (Zhang *et al.*, 2021a). Studies have demonstrated that anti-dsDNA antibodies interact with TLRs on immune cells, specifically TLR-9, which triggers the release of pro-inflammatory cytokines, such as IL-37. The combination between anti-dsDNA antibodies and TLRs can lead to immunological dysregulation and inflammation in SLE (Davaranah *et al.*, 2020; Alaanzy *et al.*, 2020). Increased levels of ANA and anti-dsDNA antibodies may indicate persistent immune system activation and the presence of autoimmunity in SLE. The persistent activation of the immune system might result in the continuous synthesis of pro-inflammatory cytokines such as IL-37 (Sam *et al.*, 2021).

Besides, the immune system mounts an assault on the kidneys, resulting in inflammation and harm in individuals with SLE. This can lead to diminished renal function, as indicated by elevated levels of urea and creatinine in the bloodstream and a decreased GFR (Kholis *et al.*, 2023). The pathophysiology of SLE is primarily driven by immune system activation and inflammation. The occurrence of kidney injury and dysfunction might result in the emission of perilous signals and inflammatory agents, which in turn provoke an immunological response. IL-37, while predominantly acknowledged as an anti-inflammatory cytokine, can be generated in reaction to inflammation (Kono *et al.*, 2021). The kidneys have a role in the metabolic processing and elimination of cytokines, such as IL-37. Renal impairment can disturb the equilibrium of cytokines in the body, perhaps resulting in increased levels of IL-37 as a compensatory approach to counter inflammation. Increased levels of IL-37 may indicate the persistent immunological dysfunction and inflammation in individuals with SLE who have renal impairment (Leonardi *et al.*, 2018). The correlation suggests that the body is using IL-37 to modulate the inflammatory response in response to kidney failure. Nevertheless, the equilibrium between pro-inflammatory and anti-inflammatory mechanisms might be disturbed in SLE, resulting in enduring inflammation and increased levels of IL-37 (Shi *et al.*, 2017).

On the other hand, in SLE, there can be an abnormal regulation of PD-1 expression and signalling on immune cells. Consequently, PD-1 may fail to transmit suppressive signals to T cells and other components of the immune system. Malfunctioning PD-1 signalling can result in heightened activation of immune cells and the release of cytokines, such as IL-37 (Lee and Song, 2020). PD-1 is predominantly found on T cells, and its signalling plays a crucial role in controlling T cell reactions. Malfunctioning PD-1 signalling can lead to T cells becoming excessively active and generating pro-inflammatory cytokines such as IL-37 (El-Sayed *et al.*, 2018). PD-1 and its ligands can also be found on other types of immune cells, including B cells and macrophages. Imbalanced PD-1 signalling can disturb the equilibrium of interactions

among many types of immune cells, resulting in an inflammatory milieu that stimulates the production of IL-37 (Italiani *et al.*, 2018). PD-1 has a role in preserving immunological tolerance and inhibiting autoimmune reactions. Disruption of PD-1 signalling can lead to the failure of immunological tolerance, enabling the immune system to attack self-antigens. This can trigger the release of IL-37 and other cytokines that promote inflammation (Durcan and Petri, 2020).

3.5.3. Correlation between Serum PD-1 Levels with Biochemical Parameters in SLE Patients

Table (3.18) and Figure (3.16) analyse the impact of serum PD-1 on the biochemical investigation of the SLE patients group, assessed using linear regression analysis.

A statistically insignificant positive connection was found between the level of PD-1 and the level of BMI in patients with SLE.

Furthermore, a strong negative association was found between the levels of C3, C4, CH50, TAC, and GFR with the level of PD-1 in the group of individuals with SLE.

On the other hand, a strong positive association was found between the level of PD-1 and the levels of MDA, CRP, ANA, Anti-dsDNA, urea, creatinine, IL-18, and IL-37 in the group of patients with SLE.

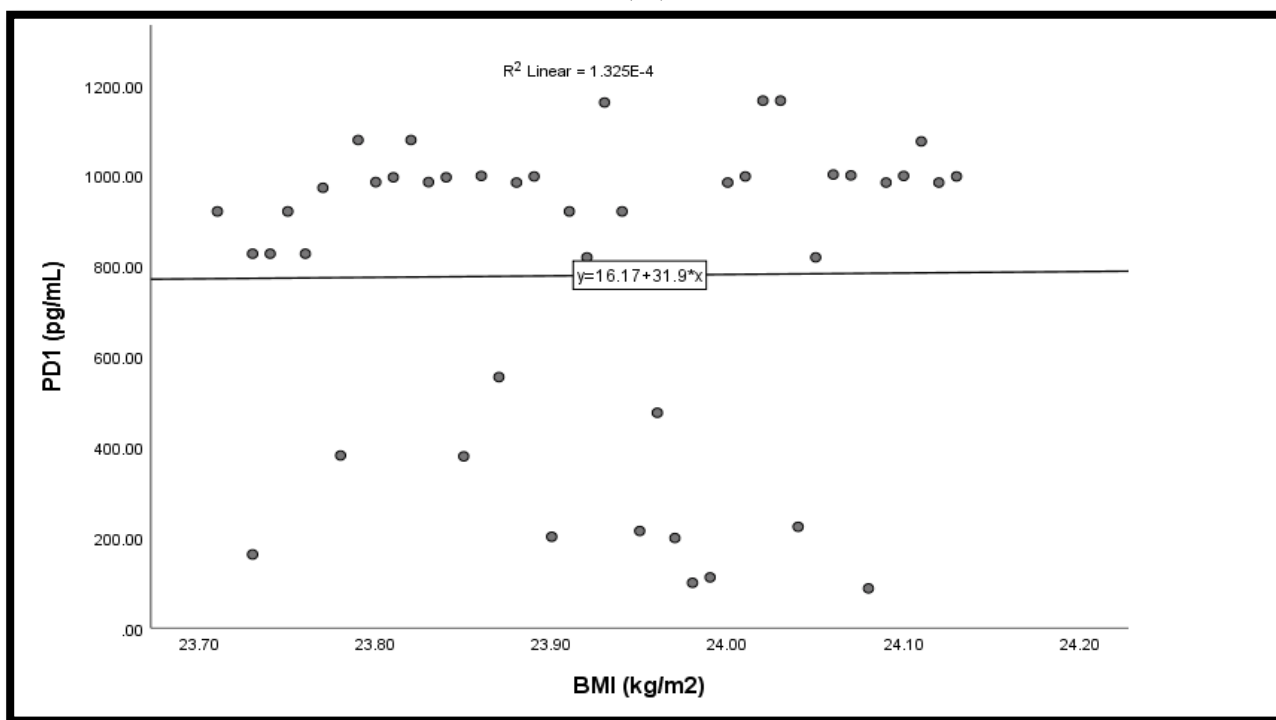
Table (3.18): Correlation between serum PD-1 levels with biochemical parameters in SLE patients group

Parameter	PD-1 (pg/mL)	
	r	P-Value
BMI (kg/m²)	0.012	0.942
C3 (g/L)	-0.500	<0.01
C4 (g/L)	-0.501	<0.01
CH50 (IU/mL)	-0.523	<0.01
MDA (µmol/L)	0.528	<0.01

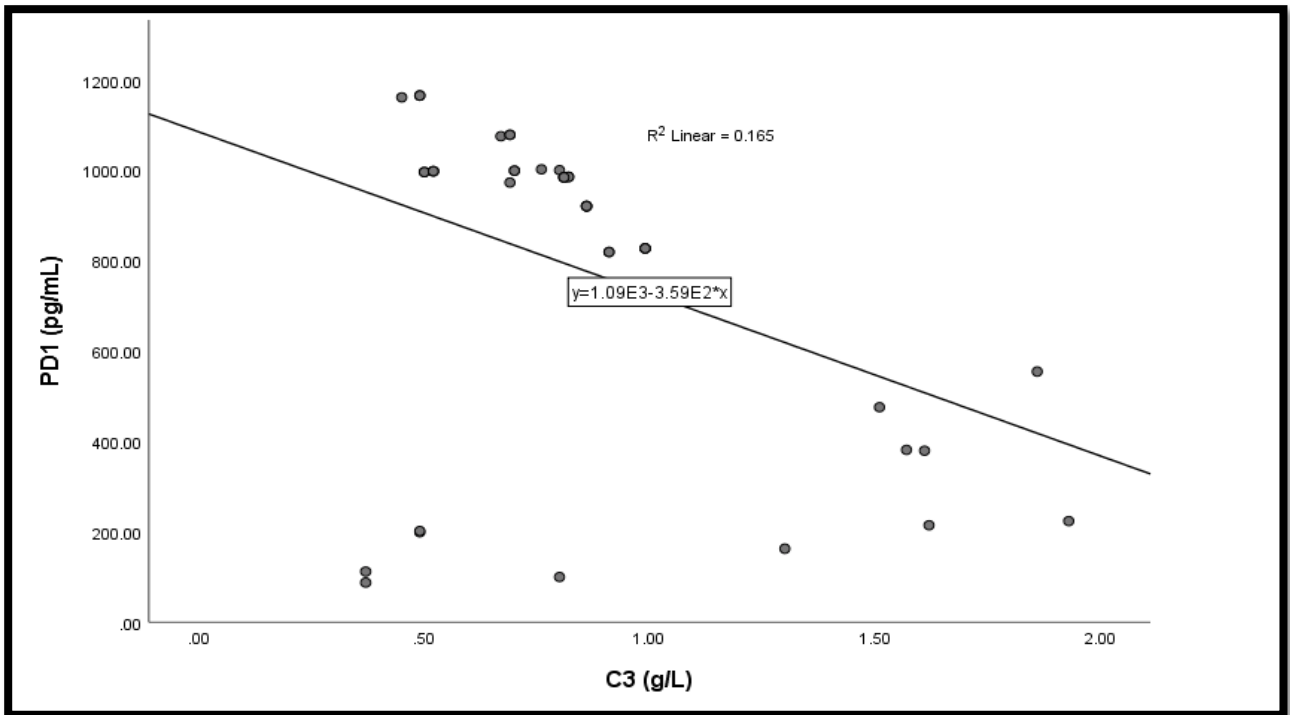
TAC (pg/mL)	-0.504	<0.01
CRP (mg/dL)	0.550	<0.01
ANA (IU/mL)	0.513	<0.01
Anti-dsDNA (IU/mL)	0.509	<0.01
Urea (mg/dL)	0.507	<0.01
Creatinine (mg/dL)	0.532	<0.01
GFR (mL/min/1.73 m ²)	-0.517	<0.01
IL-18 (pg/mL)	0.543	<0.01
IL-37 (pg/mL)	0.502	<0.01

r = Pearson correlation coefficient

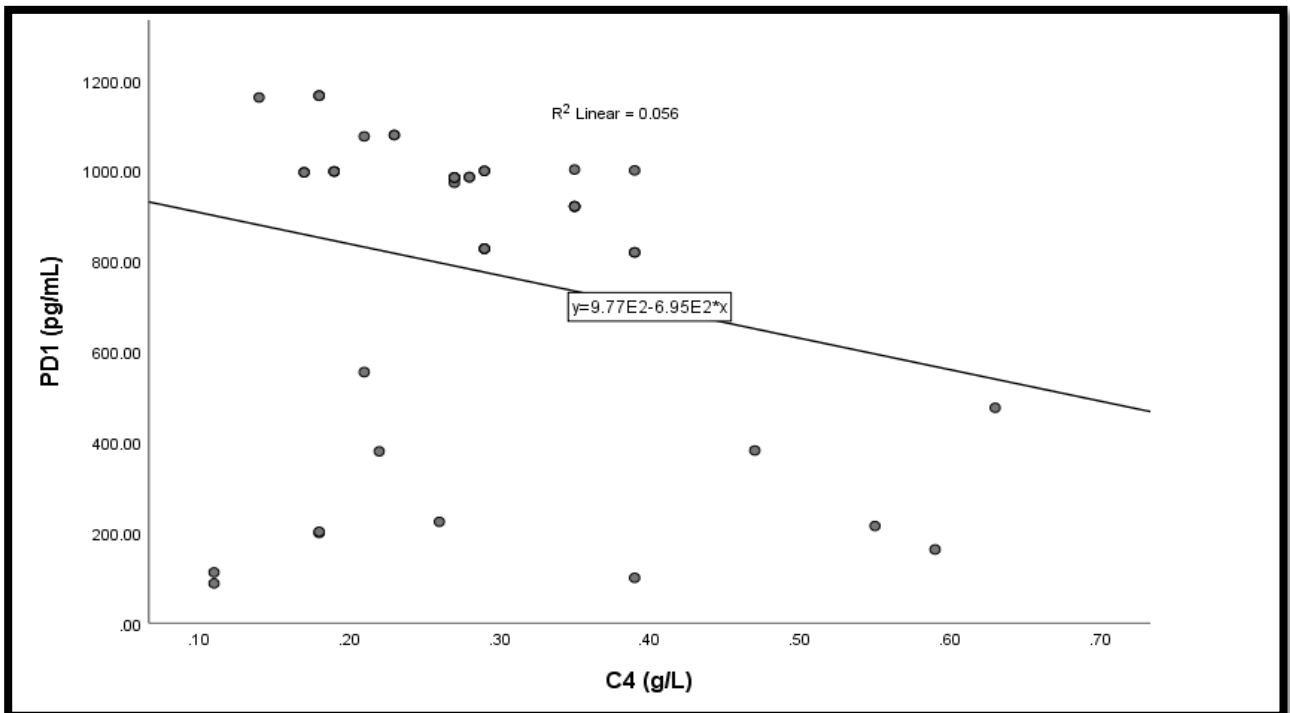
(A)



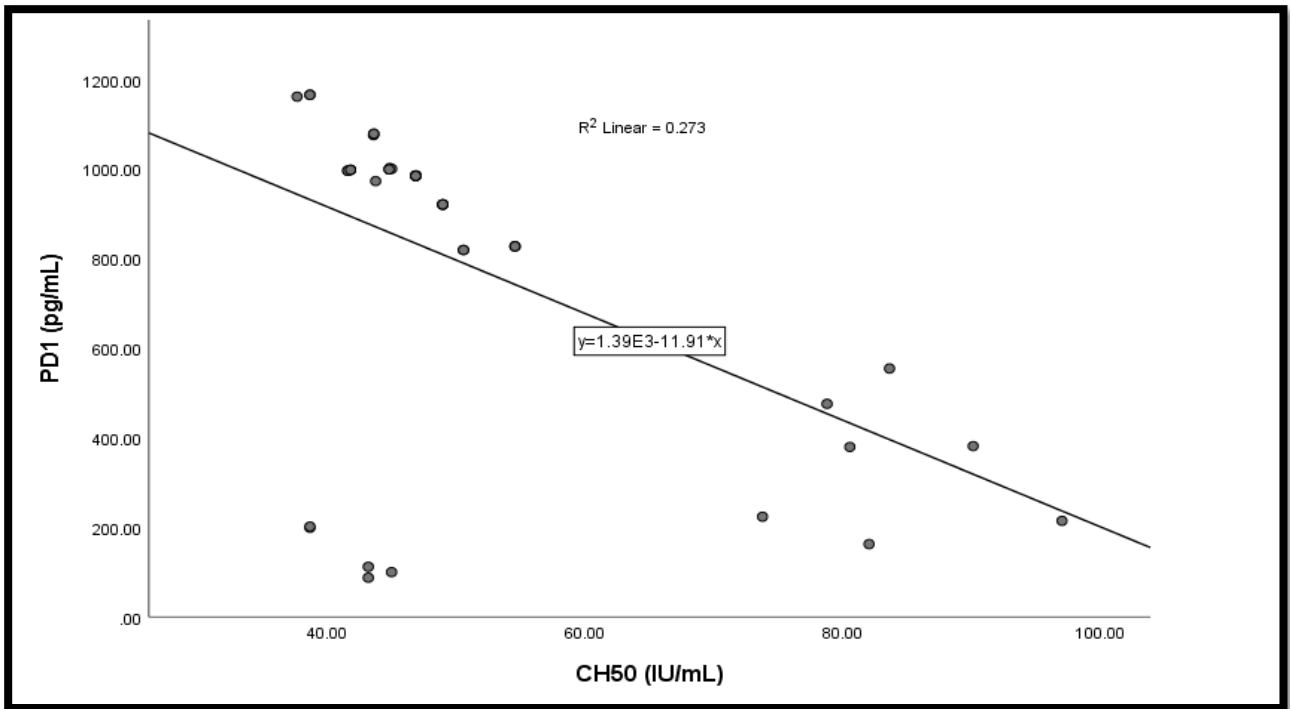
(B)



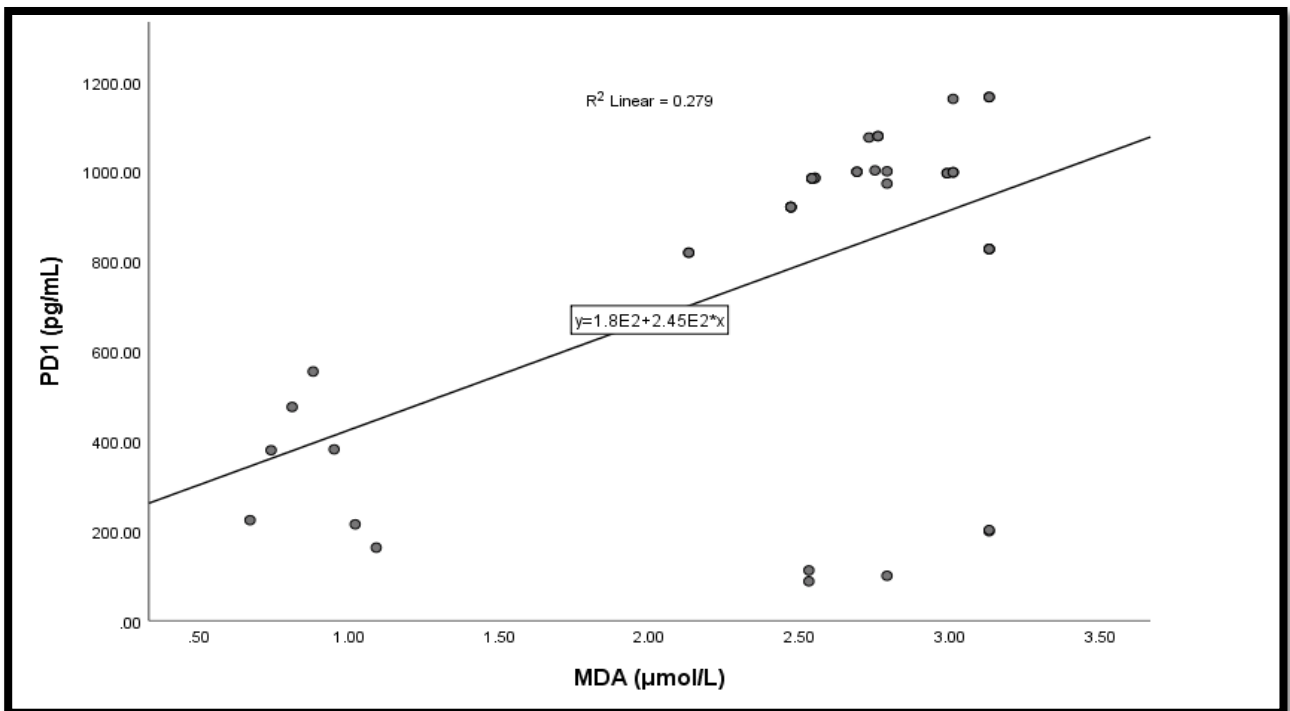
(C)



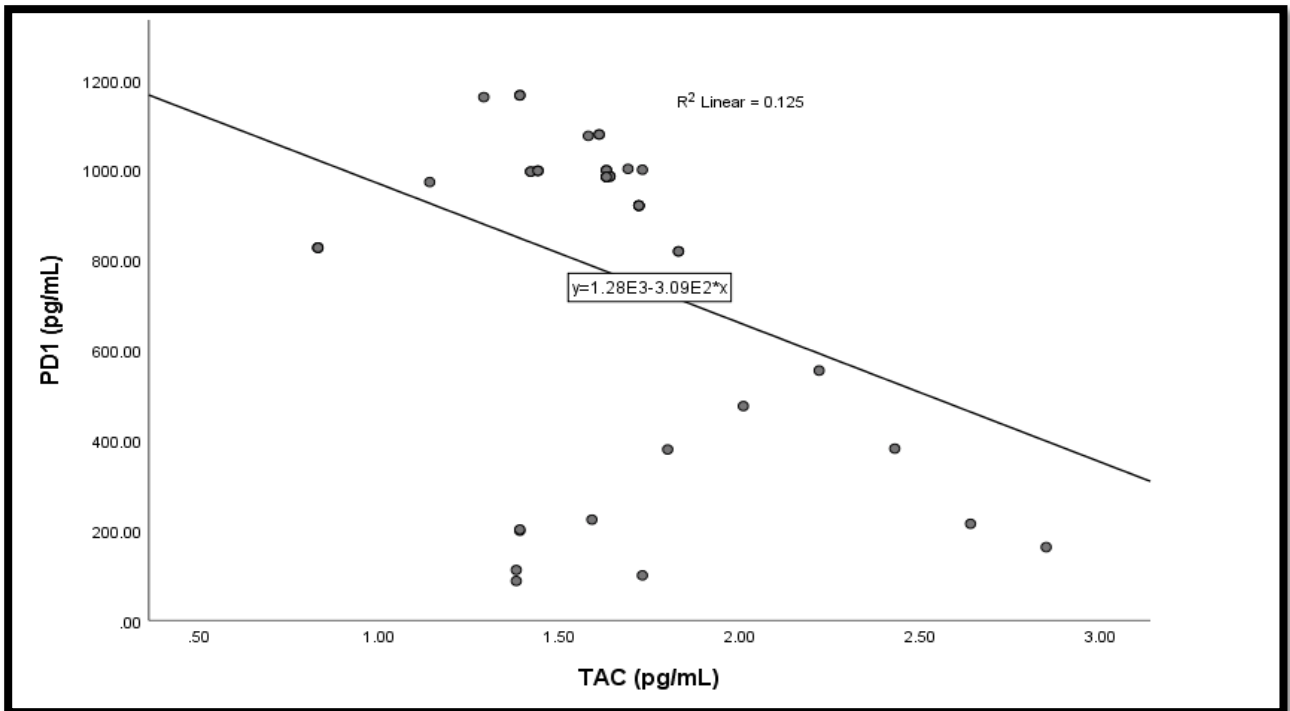
(D)



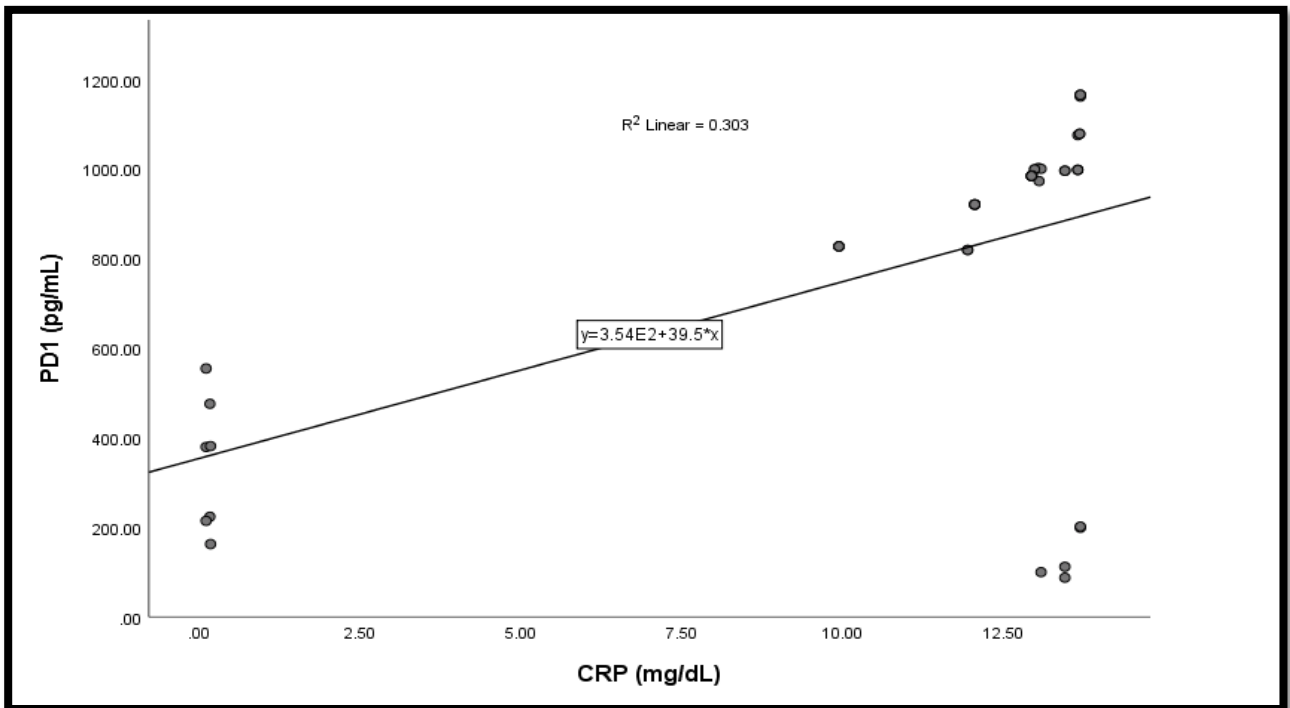
(E)



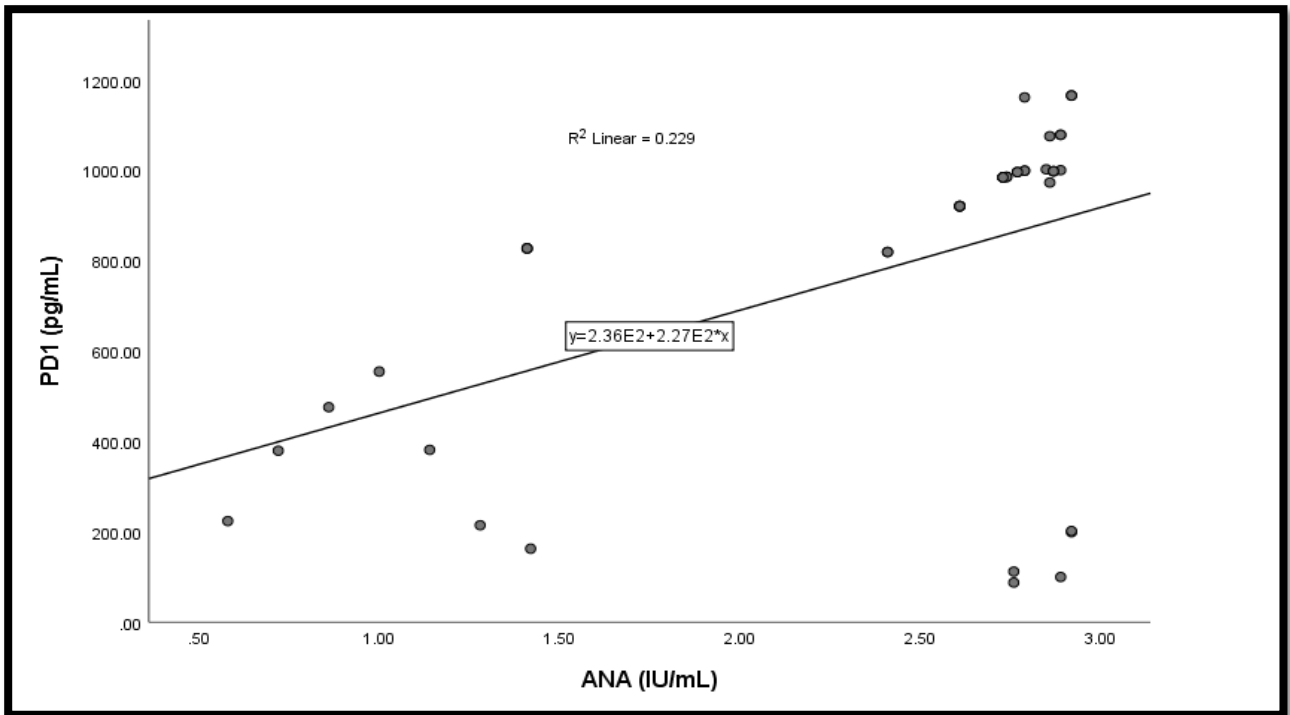
(F)



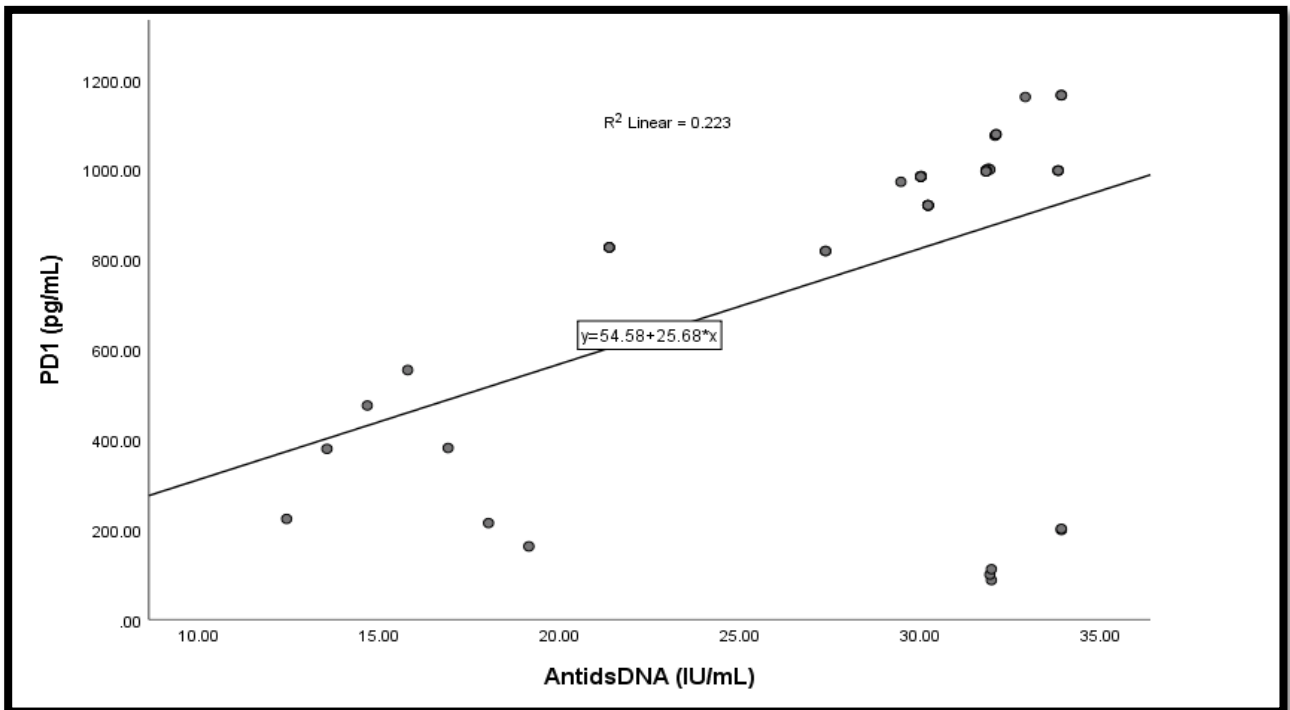
(G)



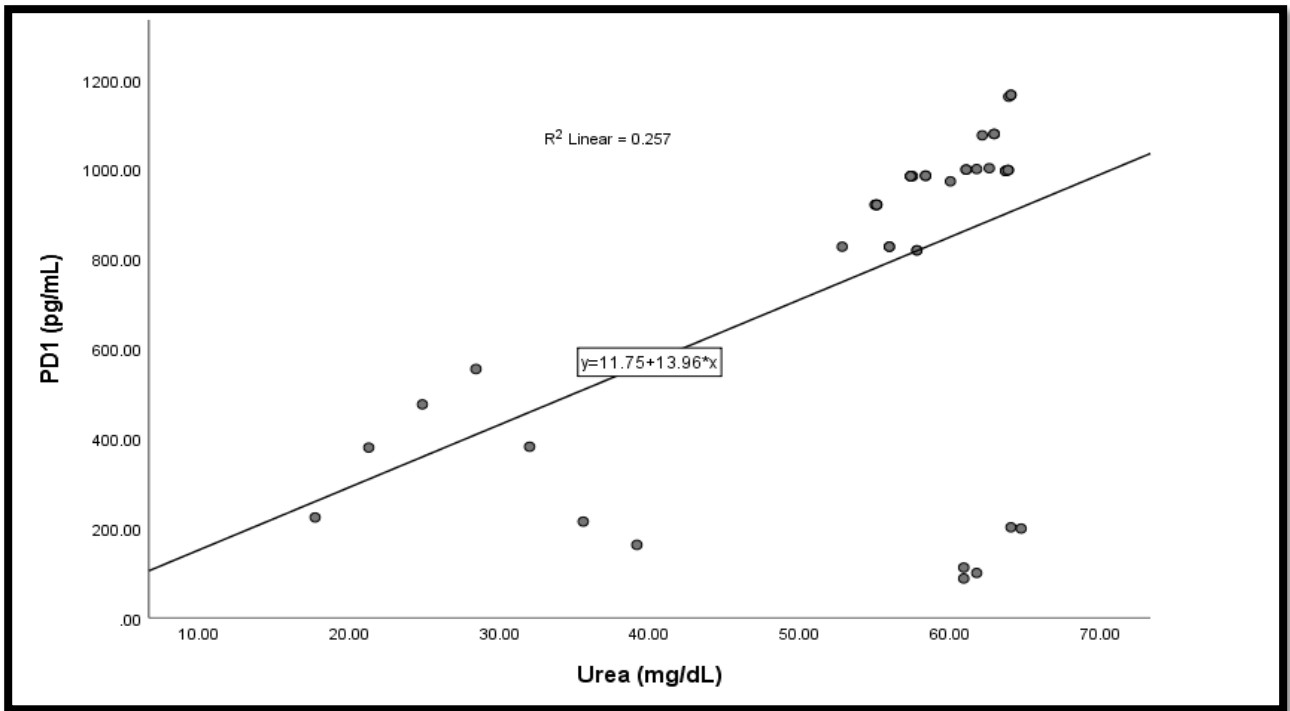
(H)



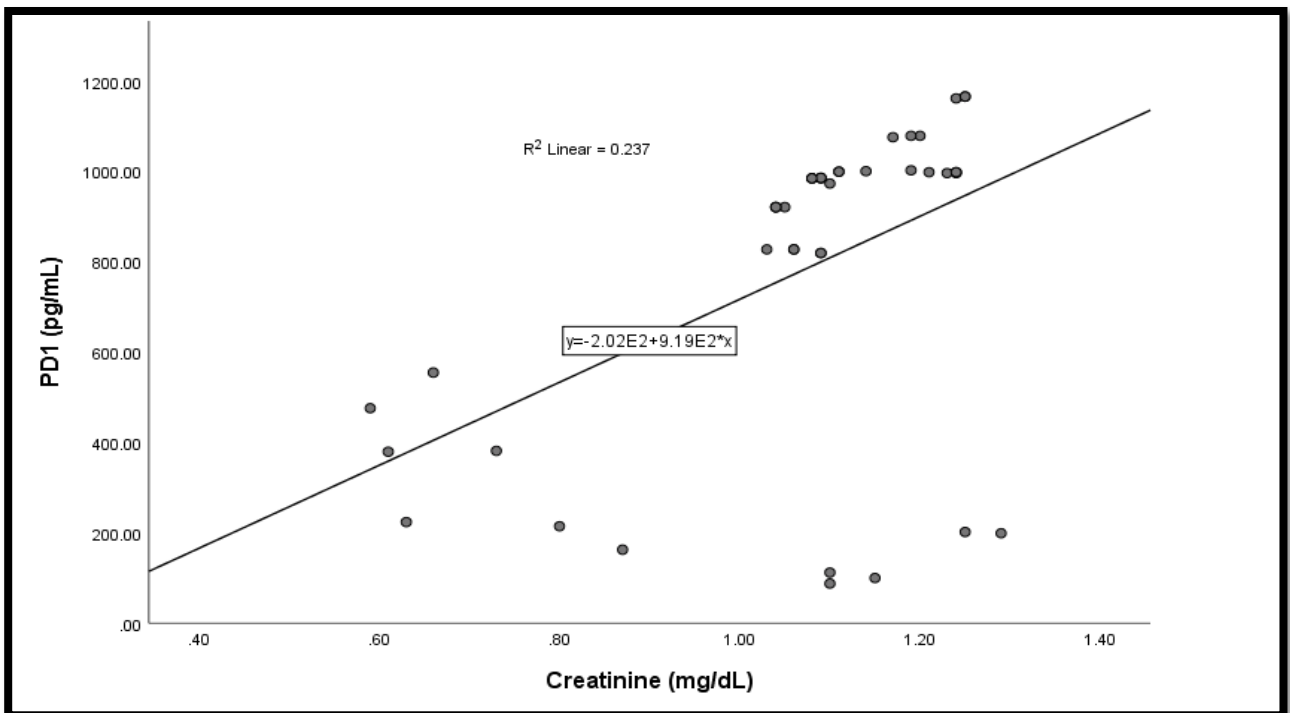
(I)



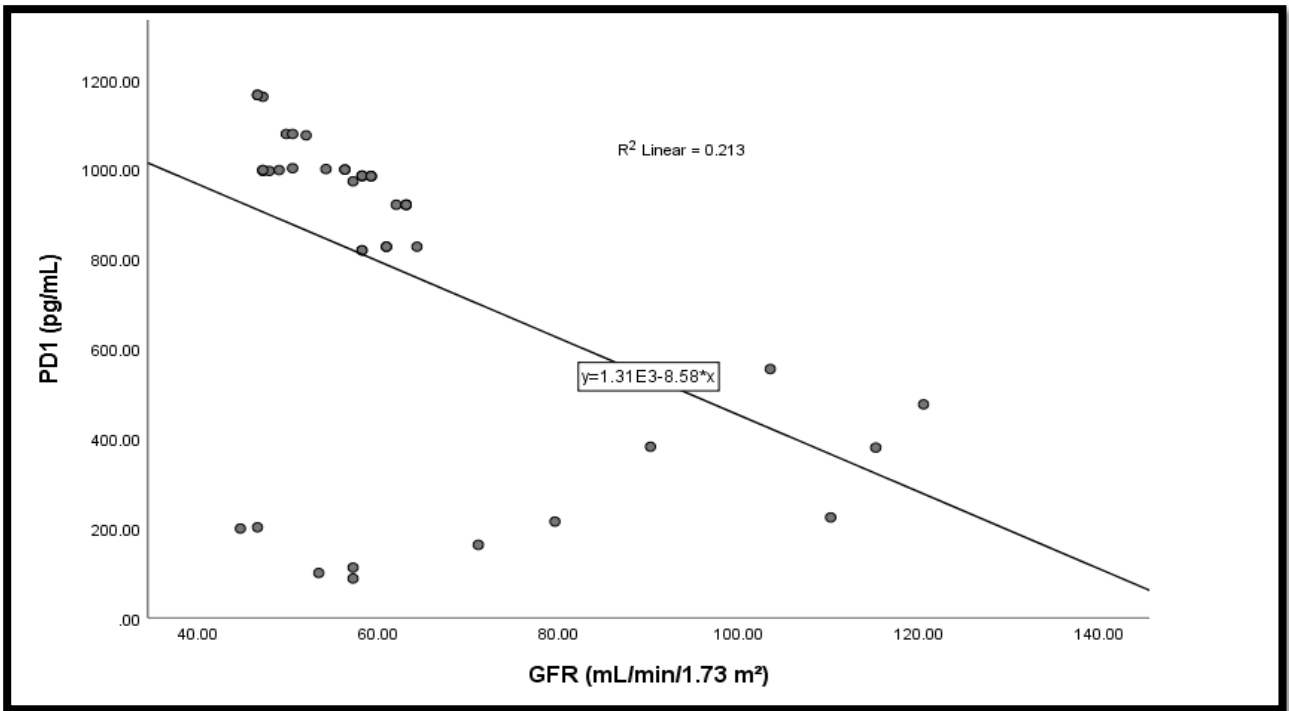
(J)



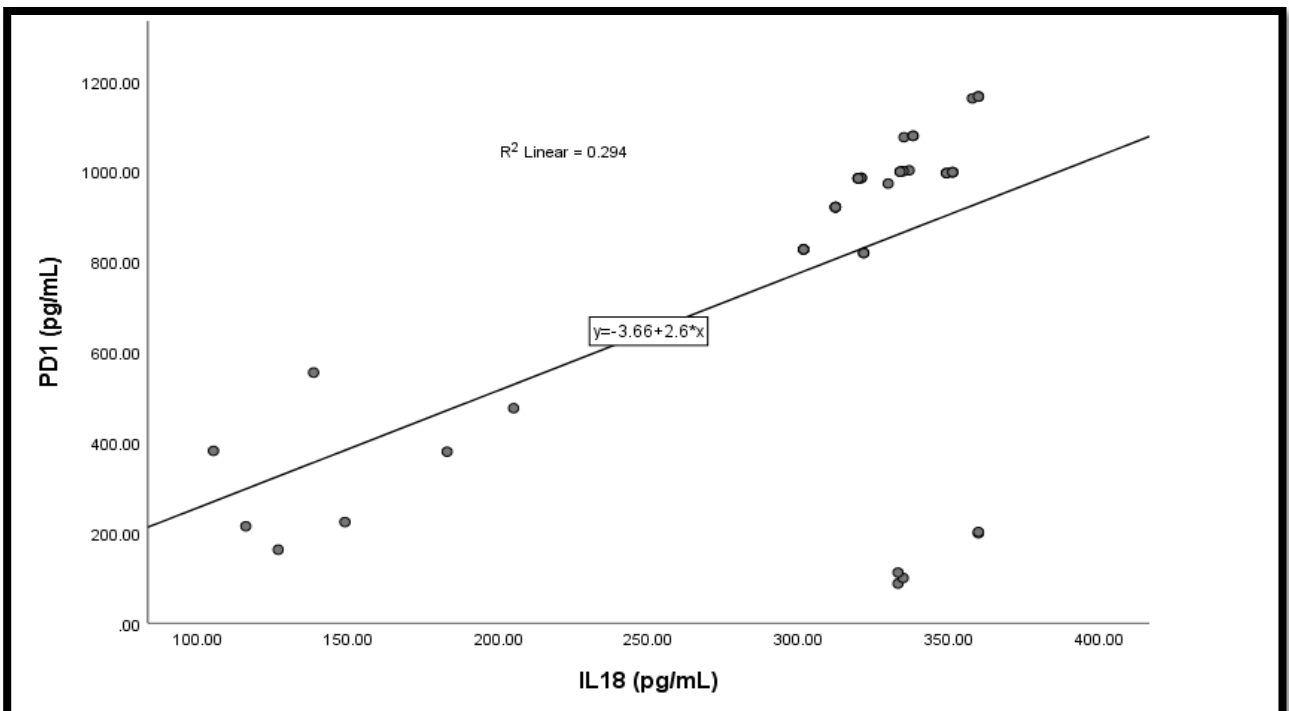
(K)



(L)



(M)



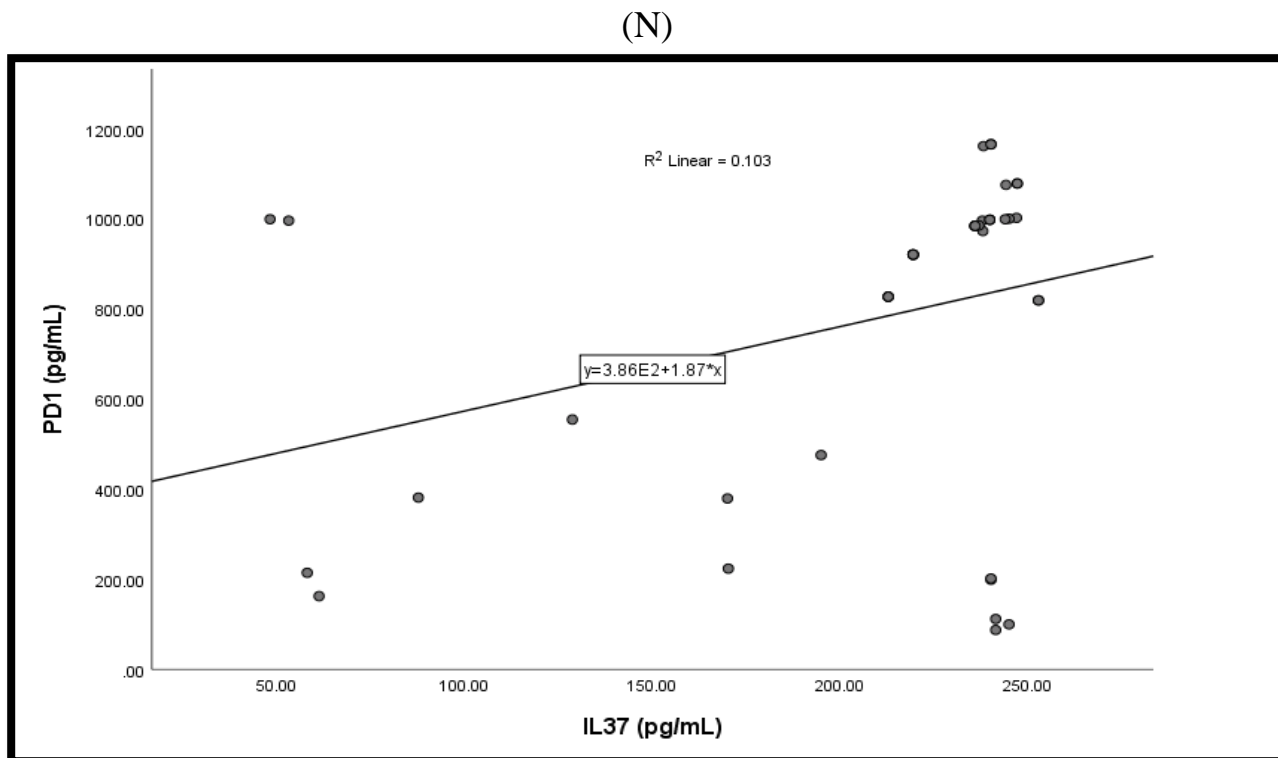


Figure (3.16): Linear regression analysis between serum levels of PD-1 with the following parameters: (A) BMI, (B) C3 (C) C4, (D) CH50, (E) MDA, (F) TAC, (G) CRP, (H) ANA, (I) Anti-dsDNA, (J) Urea, (K) Creatinine, (L) GFR, (M) IL-18, (N) IL-37.

Complement deficits, specifically in C3 and C4, are frequently observed in individuals with SLE in the present investigation. Diminished complement activity can result in the accumulation of ICs, inflammation, and compromised immune responses. The activation of complement can result in the production of pro-inflammatory mediators including cytokines (Al-Fartosy *et al.*, 2019). In SLE, where there is commonly a decrease in complement activity, the body may respond by raising the production of immunological checkpoint molecules such as PD-1. This is done as part of a complicated feedback mechanism to regulate inflammation (Zappulo *et al.*, 2022). The clearance of ICs, which are produced by the binding of antibodies to self-antigens, involves the participation of C3 and C4. The persistence of ICs and the activation of immune checkpoint pathways such as PD-1 might occur due to decreased complement function, resulting in chronic inflammation (Mohammed *et al.*, 2023). PD-1 is an

immune checkpoint molecule that controls and modulates immune responses. Disruption of complement activity can impact the equilibrium of immunological checkpoints such as PD-1, leading to immune dysfunction and inflammation in systemic lupus erythematosus (Zhang *et al.*, 2022).

Moreover, persistent inflammation and activation of the immune system might result in the generation of ROS and the occurrence of oxidative stress. Oxidative stress can initiate and intensify inflammation. Increased levels of MDA and decreased levels of TAC may indicate the presence of persistent oxidative stress and inflammation, which might result in the upregulation of immunological checkpoint molecules such as PD-1 (Han *et al.*, 2019). Lower TAC levels indicate a potential decline in the body's capacity to combat oxidative damage. The lack of antioxidants can lead to the accumulation of oxidative damage, which in turn contributes to the production of pro-inflammatory substances and immunological checkpoint molecules such as PD-1 (Liao *et al.*, 2017). PD-1 plays a role in the regulation of immunological responses. When the body experiences oxidative stress and inflammation, it may increase the production of PD-1 as a regulatory mechanism to manage excessive immune responses and reduce inflammation (Lin *et al.*, 2021).

Additionally, increased levels of CRP can function as an indicator of the continuing inflammatory reaction in patients with SLE. In SLE, persistent inflammation can result in the activation of immune checkpoint molecules such as PD-1. This occurs as a regulatory mechanism to control excessive immunological reactions. PD-1 has a role in controlling immunological responses, and its expression can be affected by inflammation (Al-Fartosy *et al.*, 2020a). During chronic inflammation, the body may increase the production of PD-1 as a regulatory mechanism to manage excessive immune responses and reduce inflammation. PD-1 is recognised for its function in suppressing immunological responses. Increased concentrations of CRP and other pro-inflammatory agents can stimulate the synthesis of PD-1 as a component of a feedback loop to control inflammation and avoid excessive harm to tissues (Smeets *et al.*, 2023).

Besides, ANA, specifically anti-dsDNA antibodies, have the ability to create ICs by binding with nuclear antigens and fragments of DNA. Activation of complement and immune cells can be initiated by these ICs, leading to an inflammatory response. The increase in PD-1 levels could be a result of the inflammatory process triggered by the deposition of ICs (Saha *et al.*, 2021). Studies have demonstrated that anti-dsDNA antibodies interact with TLRs on immune cells, specifically TLR-9. This interaction results in the synthesis of pro-inflammatory cytokines, including those that have the ability to affect the expression of PD-1. The signalling pathway of TLRs and the regulation of immunological checkpoints are interrelated in the context of immune responses (Chen *et al.*, 2018a; Uciechowski and Dempke, 2020). PD-1 plays a role in the regulation of immunological responses. When autoantibodies are present and the immune system is activated, the body may increase the production of PD-1 as a way to regulate overactive immunological responses and reduce inflammation (Al-Fartosy and Mohammed, 2017c).

Furthermore, kidney impairment in LN is linked to immunological stimulation and inflammation occurring within the renal organs. During the immunological response, immune cells that enter the kidney tissue could come into contact with immune checkpoint molecules such as PD-1 and express them (Gao *et al.*, 2017b). PD-1 is predominantly present on T lymphocytes and governs their activation. T cells have a pivotal function in the immunological response occurring in the kidneys during LN. Increased levels of PD-1 may indicate heightened T cell activation and modulation of immunological checkpoints in the renal tissue (Yap *et al.*, 2018). PD-1 plays a role in the regulation of immunological responses. Within the context of renal inflammation and immunological activation, the body may generate elevated amounts of PD-1 as a means of regulating exaggerated immune reactions and safeguarding against more renal harm. In LN, inflammation of the kidneys can cause the release of substances that promote inflammation. These substances can affect the expression of immune checkpoint molecules such as PD-1 (Wasen *et al.*, 2018).

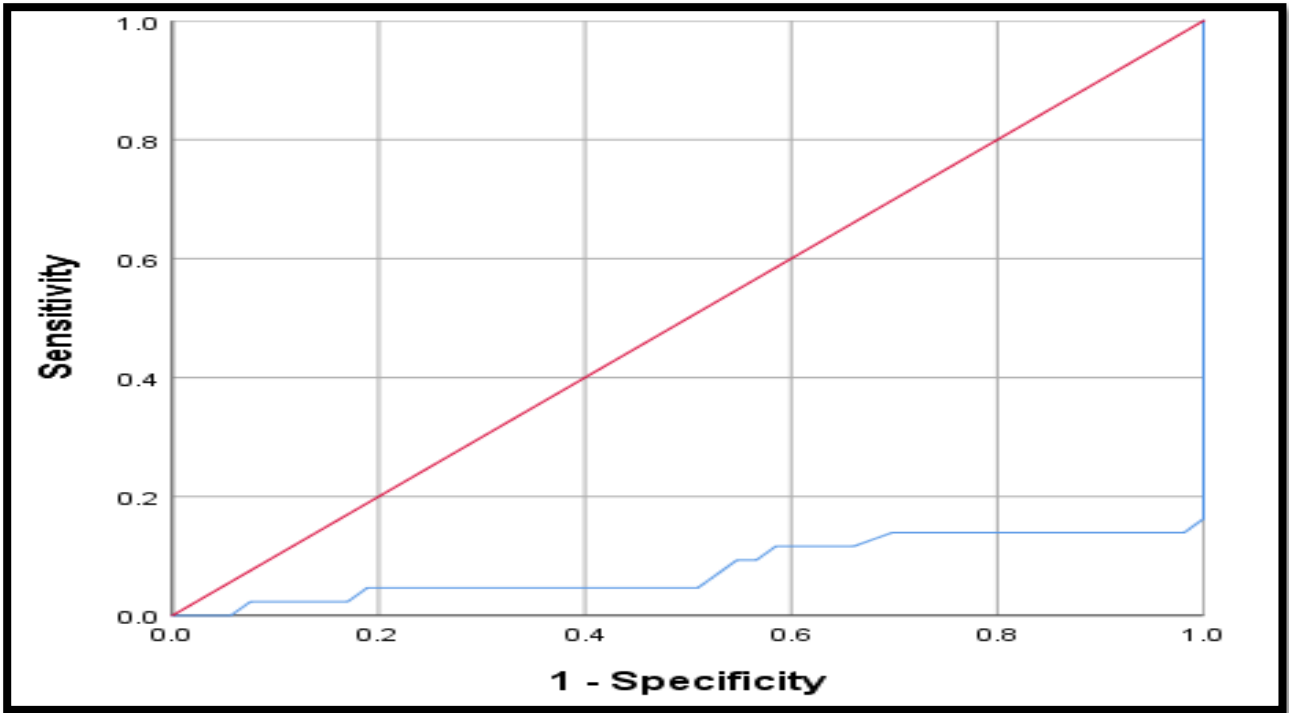
3.6. Receiver Operating Characteristic (ROC) Study

The Receiver Operating Characteristic (ROC) results for the SLE diagnosis details were illustrated in Table (3.19) and Figure (3.17) for C3, C4, CH50, ANA, Anti-dsDNA, IL-18, IL-37 and PD-1. While the ROC results for BMI, MDA, TAC, CRP, Urea, Creatinine and GFR were demonstrated in Figure (3.18).

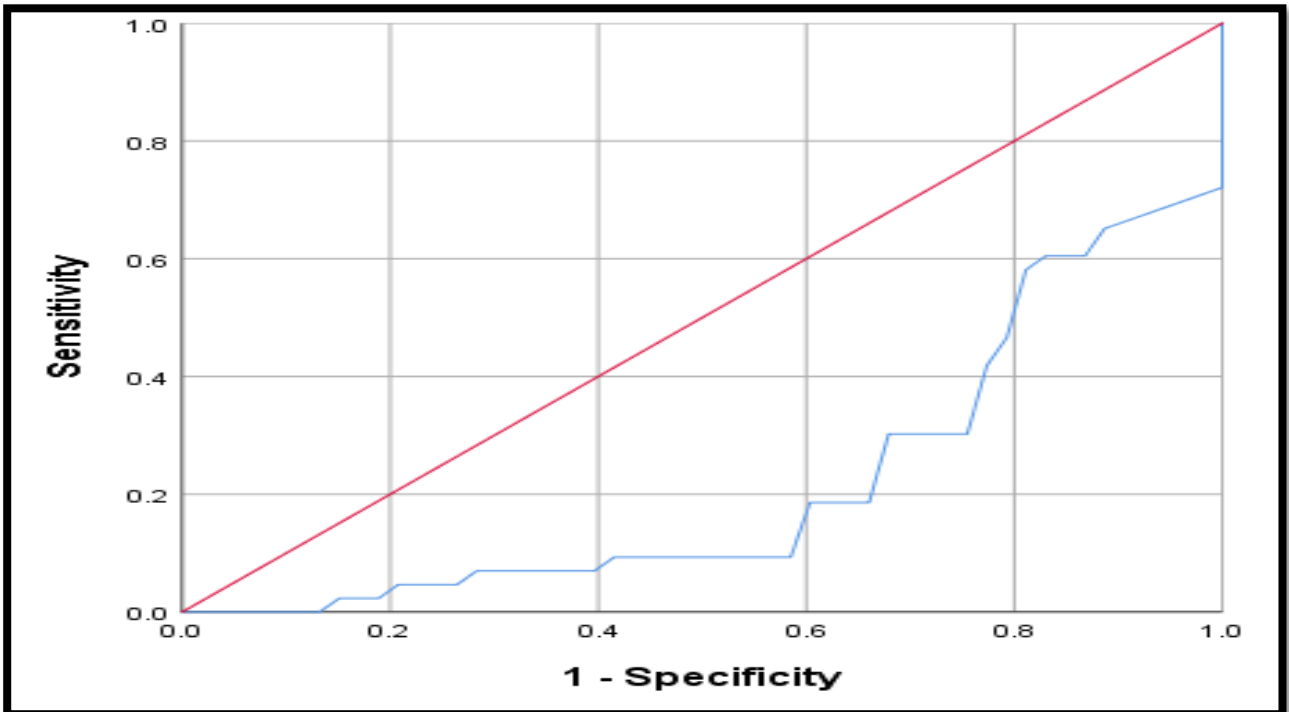
Table (3.19): ROC and AUC analysis of the measured biomarkers for the diagnosis of SLE

Parameter	Cut-off concentration	Sensitivity %	Specificity %	AUC	95% CI of AUC	P-value
C3 (g/L)	≤ 1.30	90.16	89.83	0.080	0.014 – 0.146	<0.01
C4 (g/L)	≤ 0.21	87.29	88.07	0.220	0.128 – 0.312	<0.01
CH50 (IU/mL)	≤ 65.13	92.26	94.13	0.091	0.021 – 0.162	<0.01
ANA (IU/mL)	≥ 1.50	91.72	88.81	0.915	0.851 – 0.979	<0.01
Anti-dsDNA (IU/mL)	≥ 19.79	94.69	91.02	0.922	0.858 – 0.985	<0.01
IL-18 (pg/mL)	≥ 132.87	93.02	94.71	0.985	0.936 – 0.999	<0.01
IL-37 (pg/mL)	≥ 62.98	90.70	89.14	0.968	0.911 – 0.993	<0.01
PD-1 (pg/mL)	≥ 169.02	91.43	88.65	0.940	0.872 – 0.978	<0.01

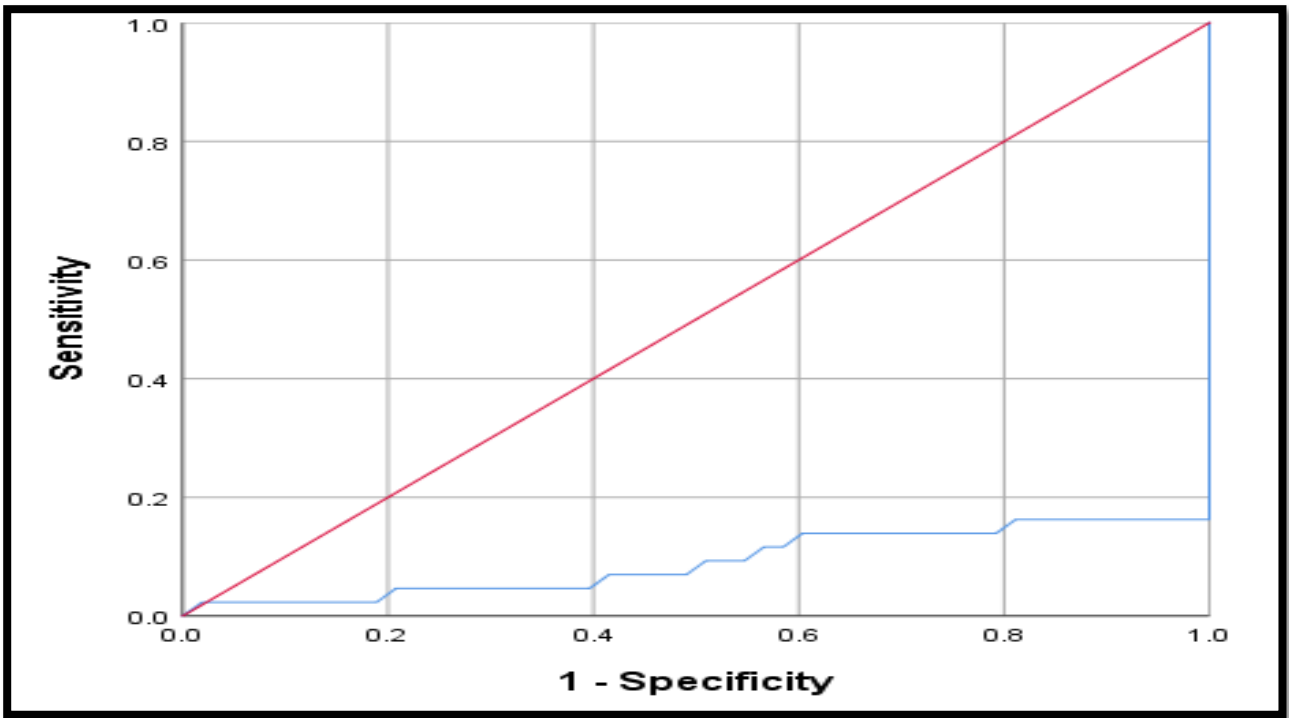
(A)



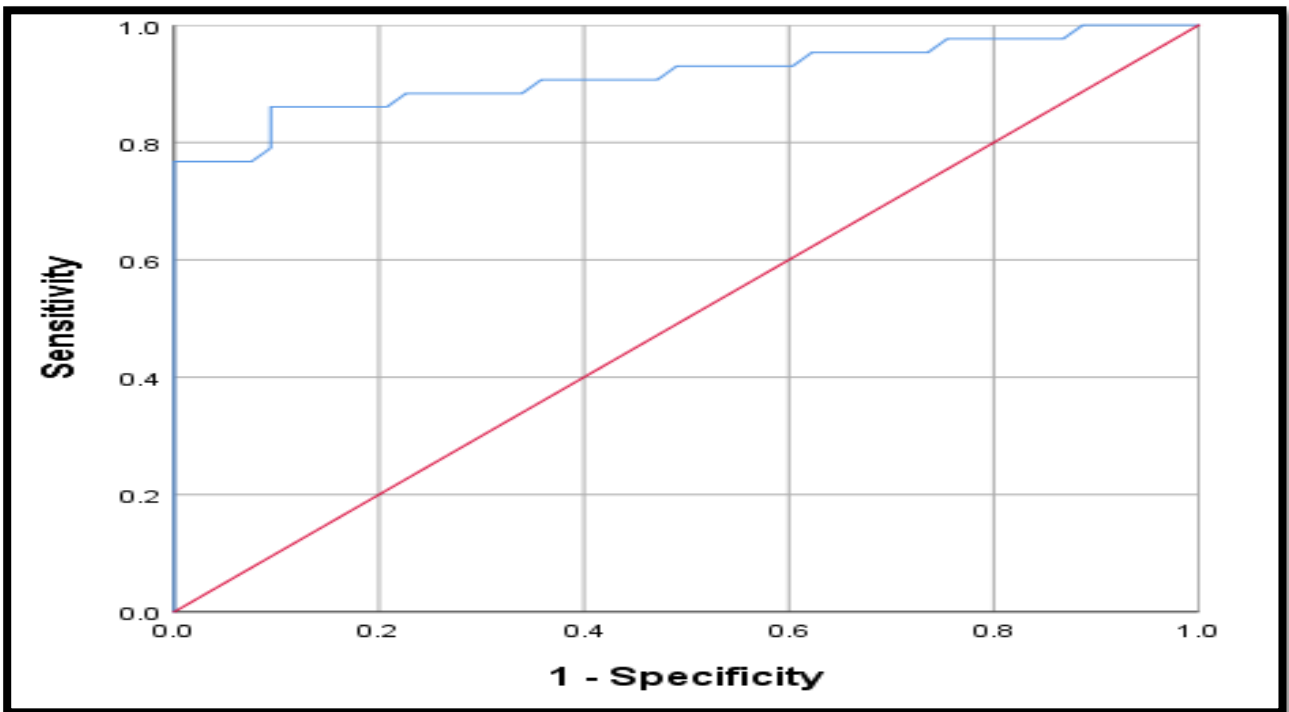
(B)



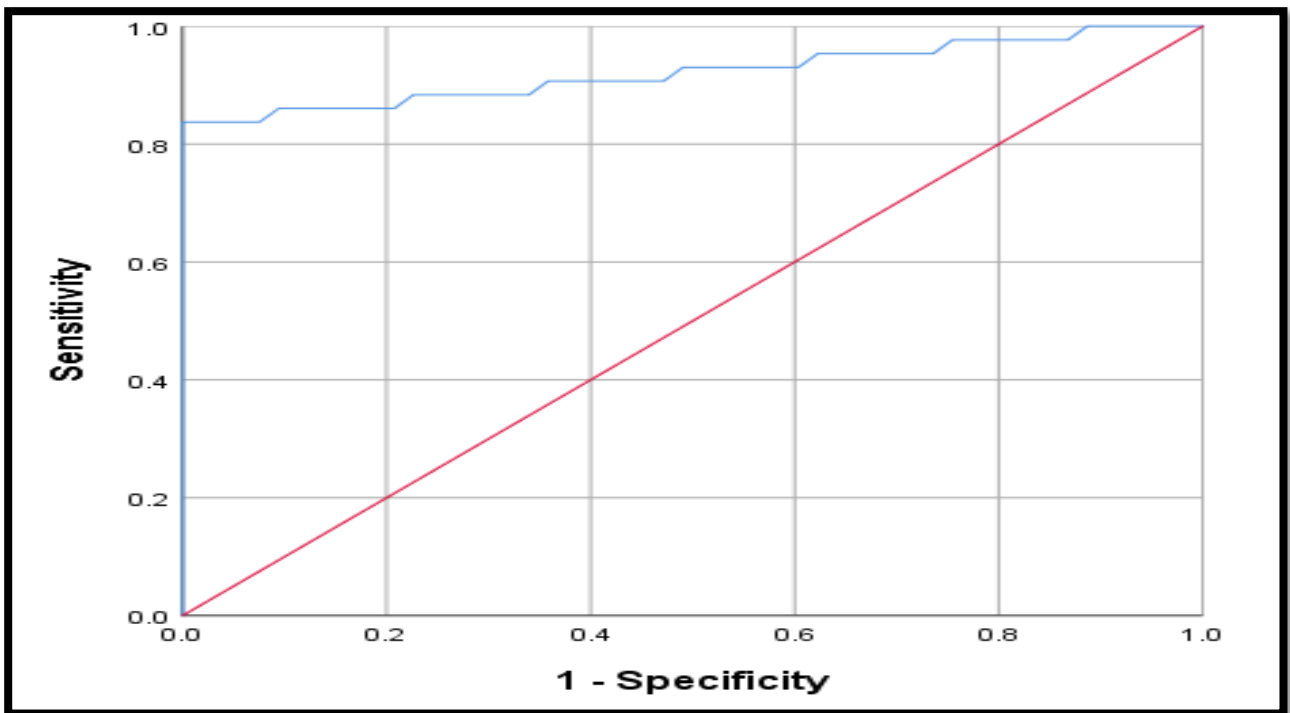
(C)



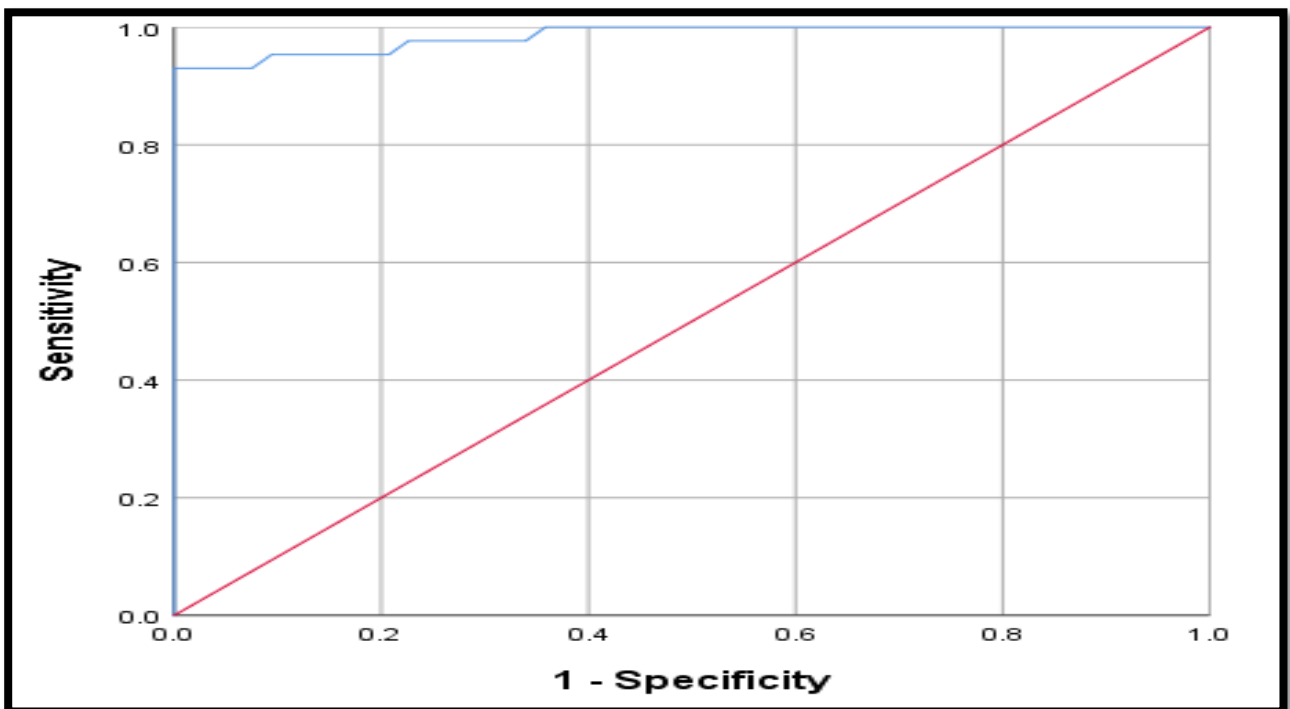
(D)



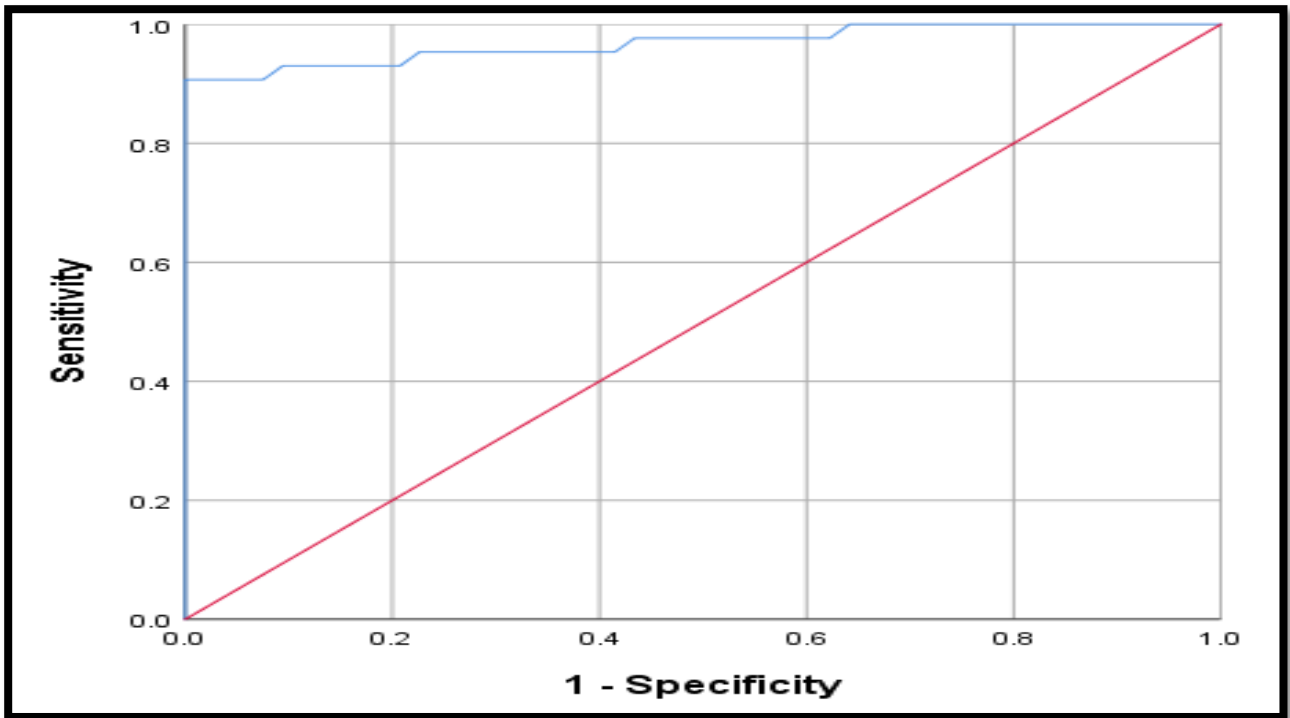
(E)



(F)



(G)



(H)

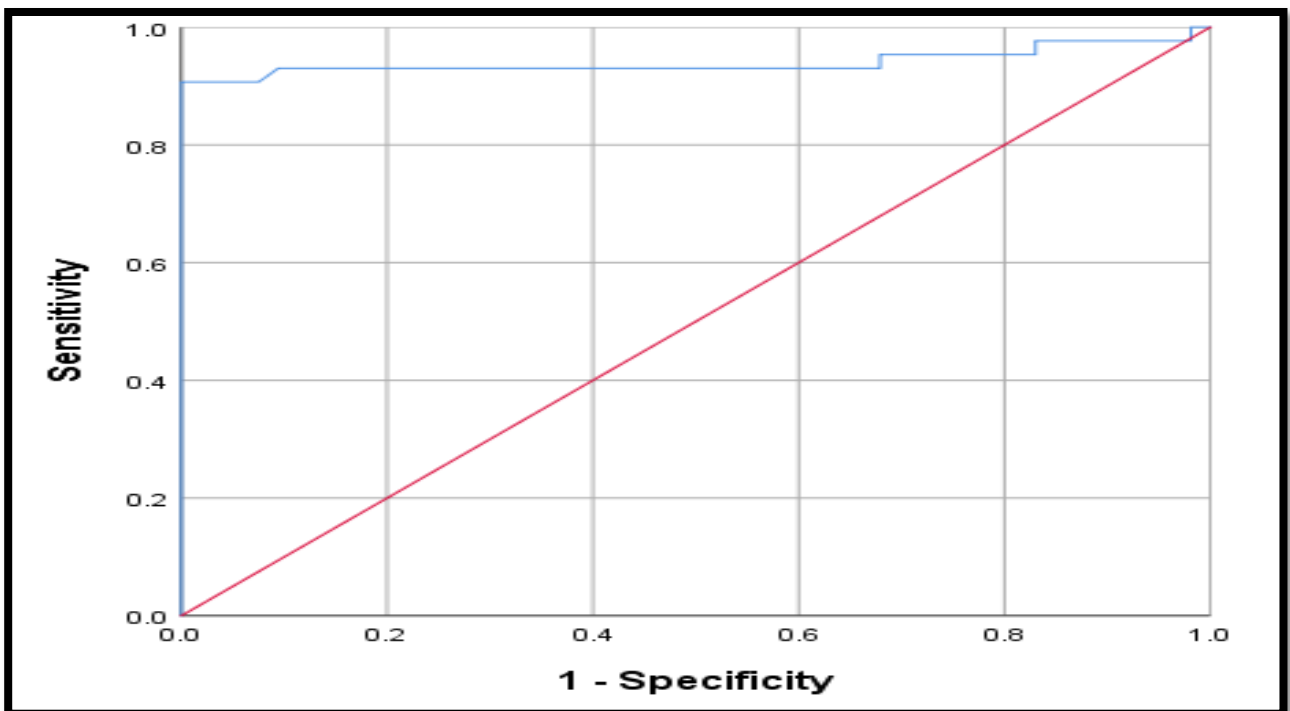
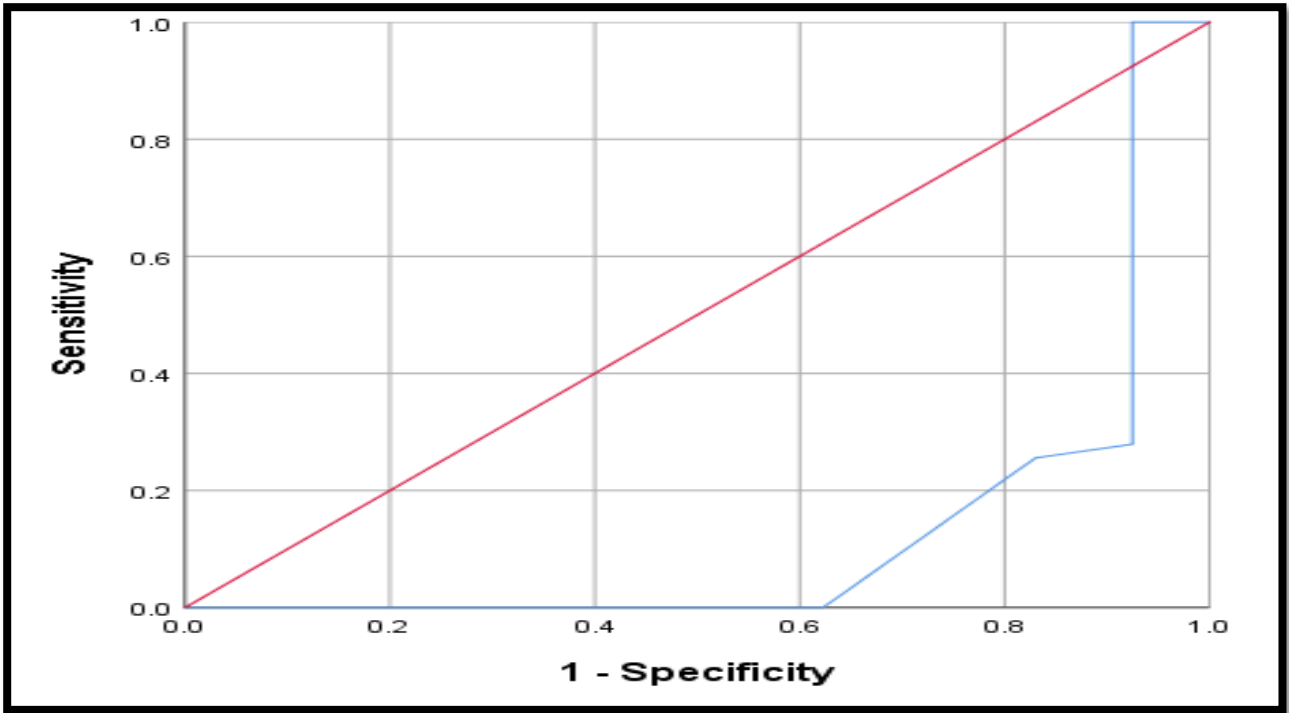
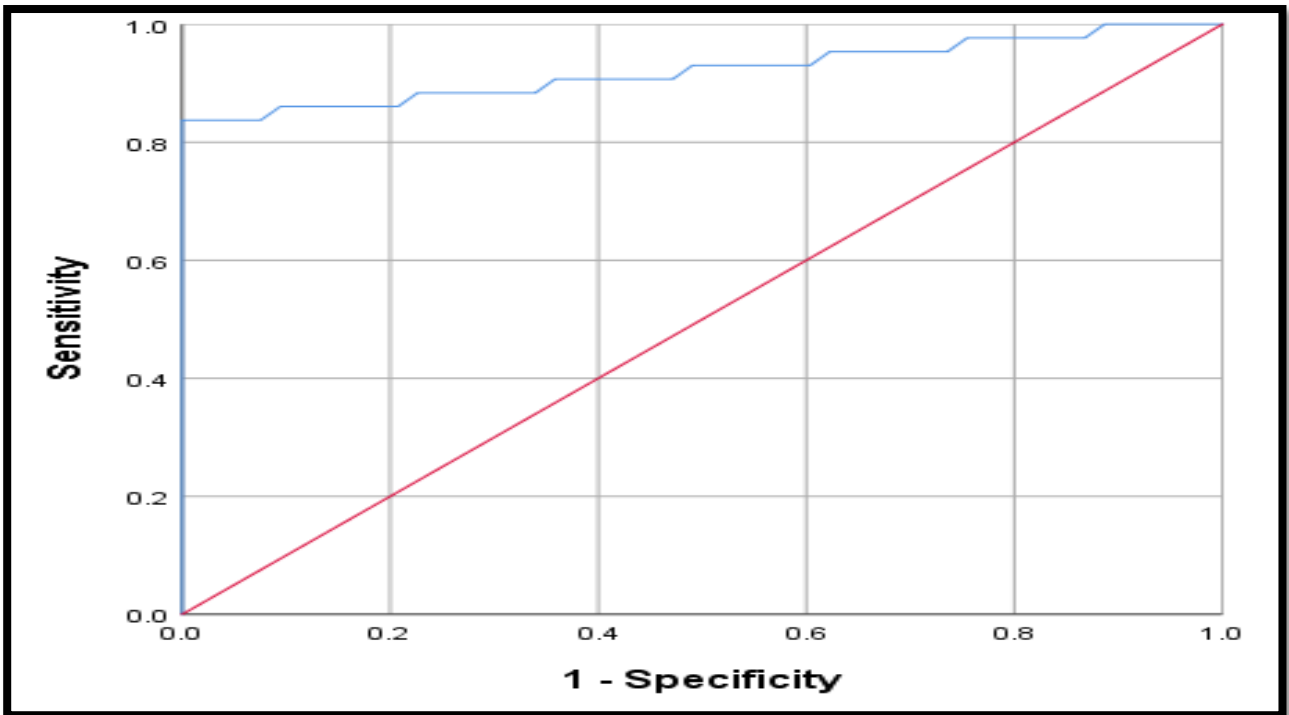


Figure (3.17): ROC curve for (A) C3, (B) C4, (C) CH50, (D) ANA, (E) Anti-dsDNA, (F) IL-18, (G) IL-37, (H) PD-1 in SLE patients and control group.

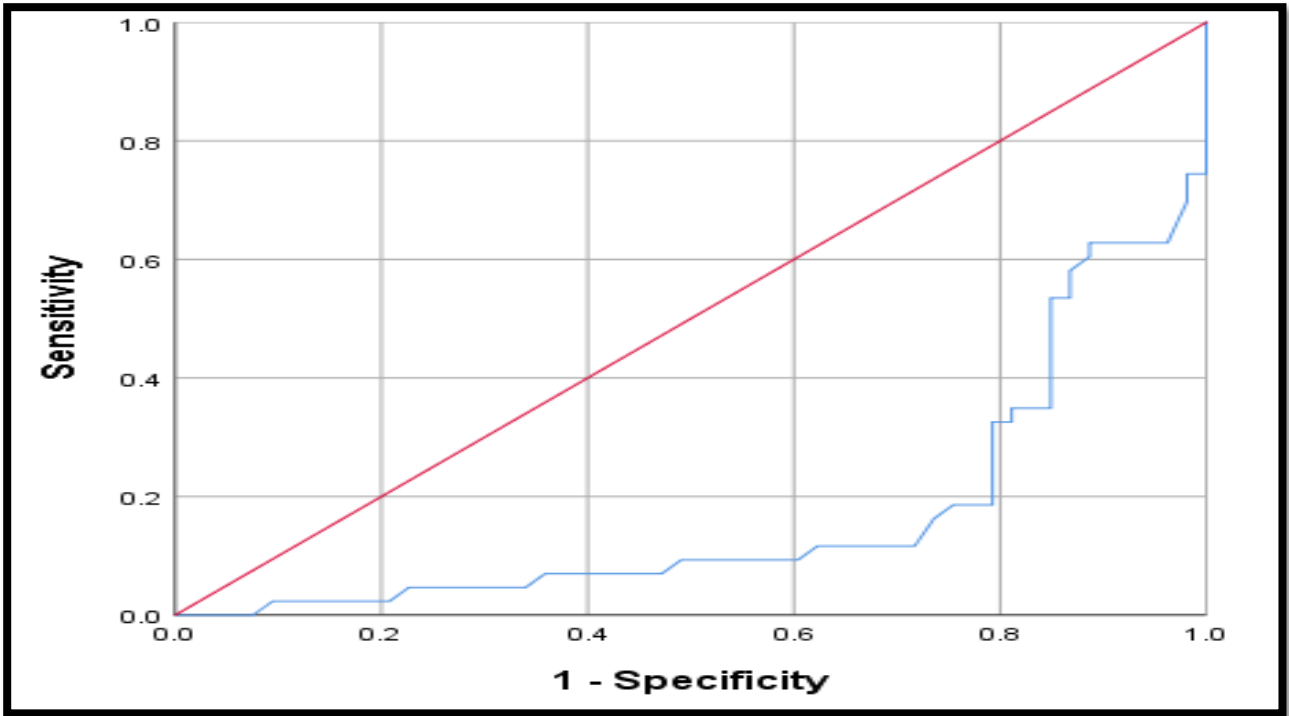
(A)



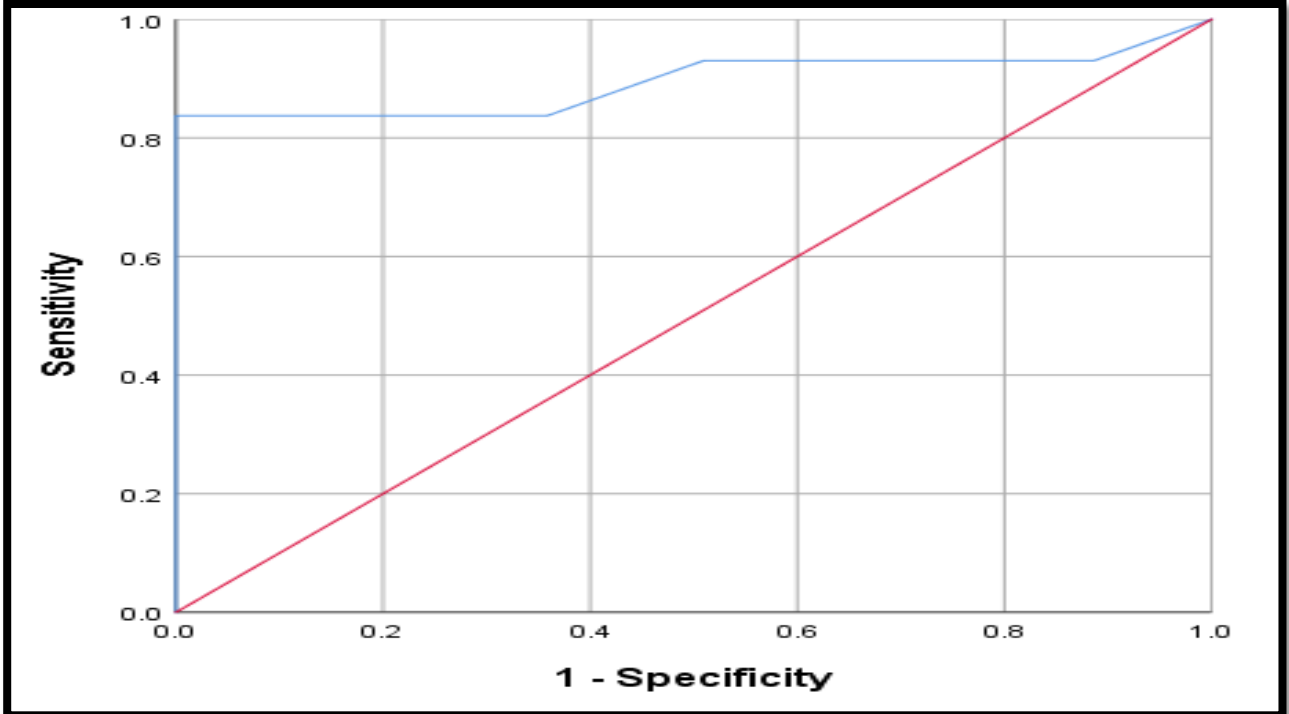
(B)



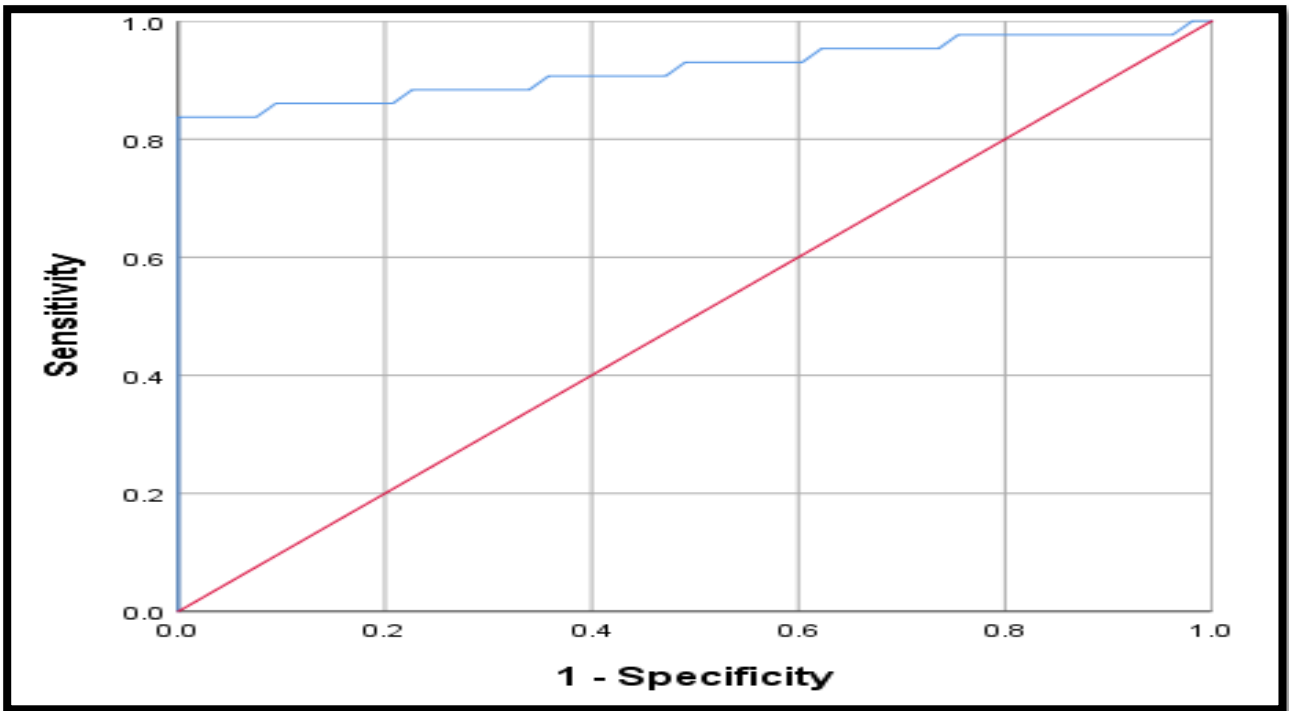
(C)



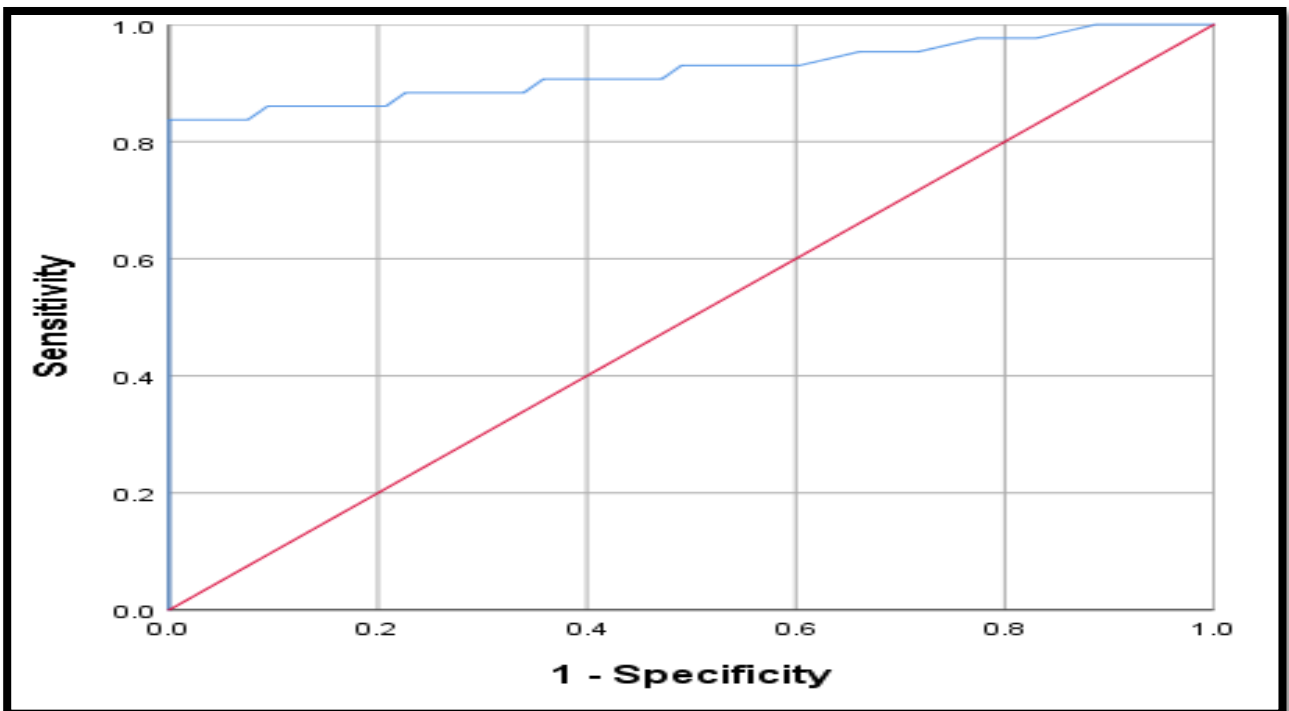
(D)



(E)



(F)



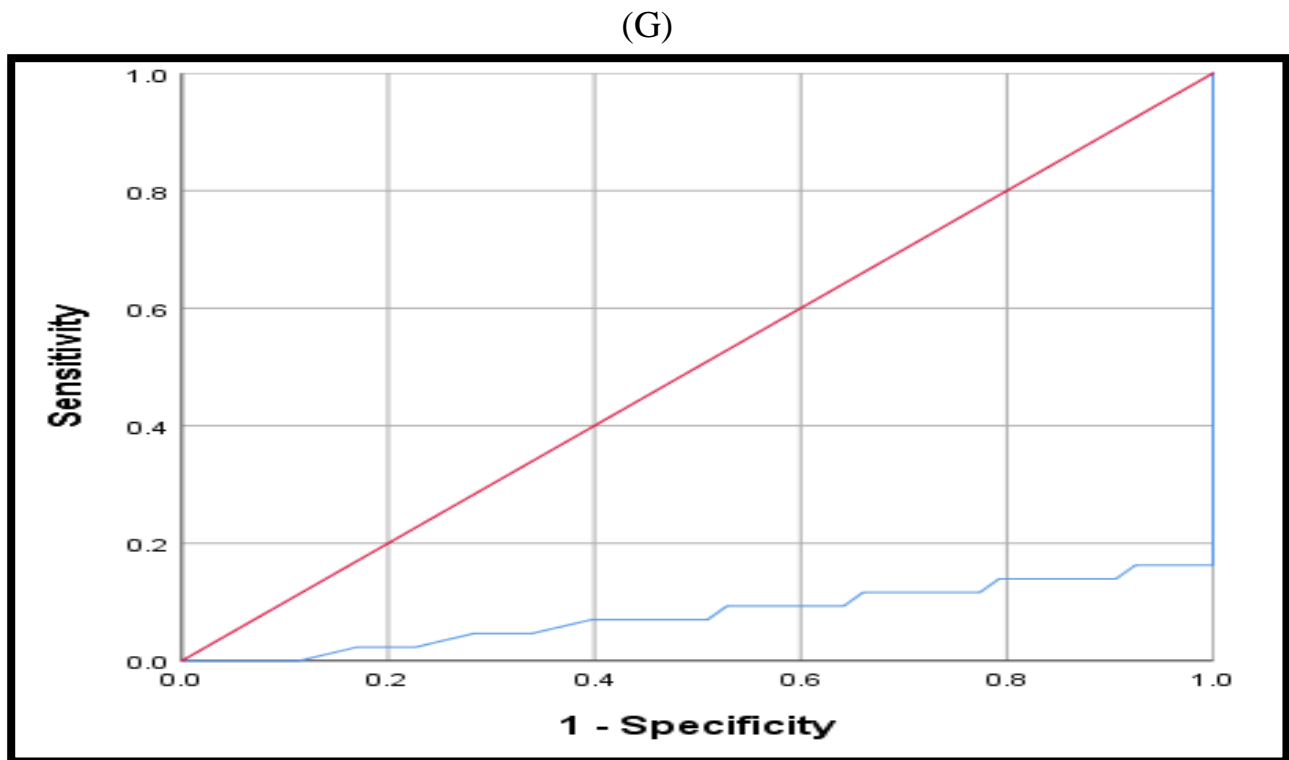


Figure (3.18): ROC curve for (A) BMI, (B) MDA, (C) TAC, (D) CRP, (E) Urea, (F) Creatinine, (G) GFR in SLE patients and control group.

The efficacy of IL-18, IL-37, and PD-1 as biomarkers for predicting the diagnosis of SLE was examined. The ROC analyses conducted on SLE patients and healthy controls revealed that IL-18, IL-37, and PD-1 demonstrated exceptional diagnostic efficacy, as indicated in Table (3.19) and Figure (3.17).

ROC curves are generated by plotting the sensitivity (the fraction of true positives) against the complement of specificity (the fraction of false positives) for various cut-off values of the diagnostic test. Consequently, as the diagnostic test's sensitivity and specificity improve for all possible cut-off values, particularly in terms of its capacity to accurately detect illnesses, the curve will shift towards the upper left corner (Wang *et al.*, 2021). Sensitivity, usually referred to as the 1- "false negative fraction," and specificity, also called the 1- "false positive fraction," are unaffected by the prevalence of the disease in the sample, unlike accuracy (Wu *et al.*, 2021). ROC curve analysis provides an unmodified depiction of disease detectability, independent

of decision threshold effects or disease prevalence. ROC curves are determined by the area under the ROC curve (AURC). The ability to accurately distinguish between individuals who are affected and those who are not is quantified by the AURC (Nakanishi, 2018). Consequently, the optimal diagnostic test would possess an AURC value of 1, while tests with AURCs below 0.5 would lack the ability to differentiate between individuals who are affected and those who are unaffected (Al-Anazi *et al.*, 2019).

During episodes of SLE flares, the immune system may release both inflammatory and anti-inflammatory cytokines as a mechanism to regulate and control inflammation. Therefore, it was shown that the levels of IL-18 and IL-37 were considerably higher in patients with SLE compared to the control group (Jaing *et al.*, 2021). Through study, these cytokines demonstrate a strong ability to differentiate between SLE patients and controls, as evidenced by the ROC curve, which is a commonly used method for summarising classifiers (Bassiouni *et al.*, 2021). A ROC curve is a graphical representation that demonstrates the accuracy and significance of predicting an event. These findings indicate an escalation of inflammation, which is commonly observed in a SLE flares, but are insufficient to effectively control the total inflammation associated with the SLE flares (Ayoub *et al.*, 2019).

Consequently, the immune system becomes deactivated and returns to a state of rest, thus preventing the harm that would otherwise be produced by ongoing immunological responses in the body. The overproduction of cytokines in response to inflammation leads to a rapid and severe systemic inflammatory response called "cytokine storm," which causes damage to multiple organs (Zhang *et al.*, 2021a).

This finding was further corroborated in the current investigation, wherein hospitalised individuals exhibited diminished levels of C3, C4, and CH50, heightened oxidative stress activity (elevated levels of MDA and reduced levels of TAC), elevated levels of other inflammatory markers (CRP), increased levels of autoantibodies (ANA and Anti-dsDNA), and impaired kidney function (elevated levels of urea and creatinine

with reduced levels of GFR). Elevated levels of cytokines in the current study data indicated early detection of organ damage or morbidity-related consequences (Davaranah *et al.*, 2020; Kholis *et al.*, 2023).

3.7. Genetic Study for PD-1 Gene

3.7.1. DNA Extraction and Polymerase Chain Reaction Technique (PCR)

The DNA was isolated from the blood of human volunteers using commercially available kit protocols. The DNA extraction results were validated, with the concentration and purity assessed using a Nanodrop spectrophotometer at a wavelength of 260/280nm, as presented in Table (3.20). The DNA content varied from 139.44 to 671.26 ng/ μ L, while the purity ranged from 1.45 to 2.19 (Sam *et al.*, 2021).

Table (3.20): The purity and concentration of the extracted DNA

Parameter	Mean \pm SD	Range
DNA Concentration (ng/ μ L)	562.34 \pm 78.12	139.44 - 671.26
DNA Purity	1.83 \pm 0.19	1.45 - 2.19

In order to verify the extraction process, the DNA that was separated from the sample was subjected to electrophoresis on a gel made of agarose (0.8% concentration). The resulting DNA bands were then observed using UV light, as depicted in Figure (3.19). These bands correspond to DNA molecules with a large molecular weight (Kono *et al.*, 2021).

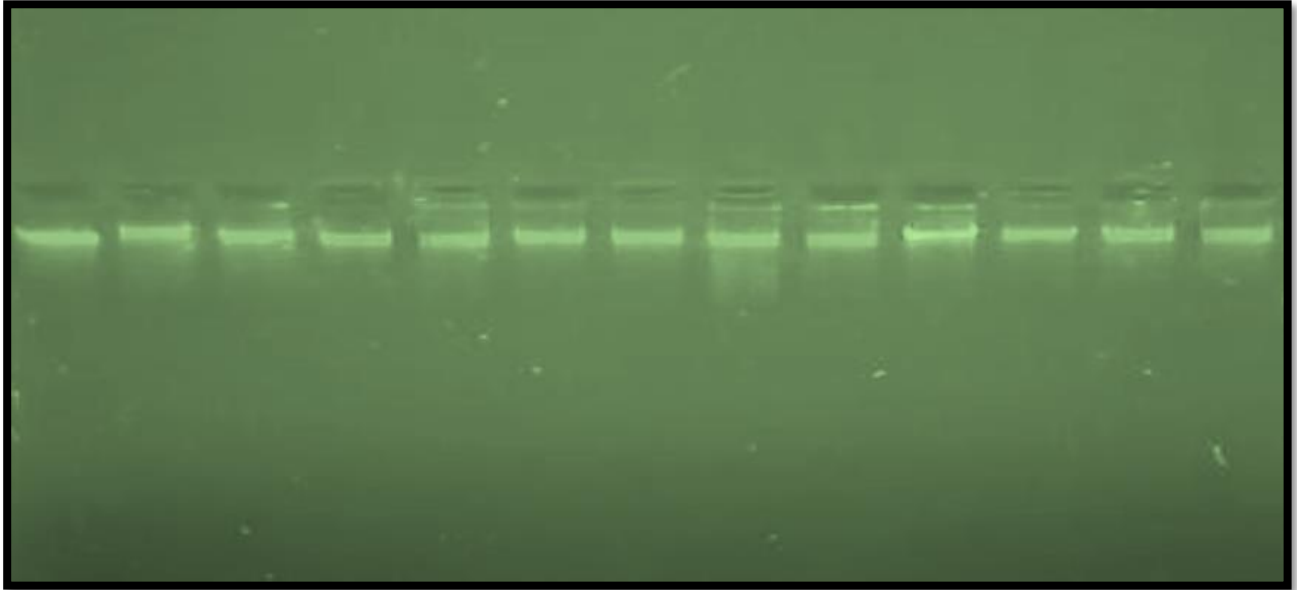


Figure (3.19): Gel electrophoresis of extracted genomic DNA from blood samples and run through 0.8% agarose gel at 5 v/cm² for 1 hour.

The Kit offers a straightforward and efficient method for extracting superior quality DNA from fungus. This kit boasts rapid and effortless processing, resulting in DNA of exceptional quality and purity. This highly adaptable reagent system has the capability to extract genomic DNA from a wide range of materials, including cultivated bacteria. Purified DNA is appropriate for DNA archiving, PCR, AFLP, RFLP/RAPD Southern Blotting, and Real-time PCR (Lee and Song, 2020). A researcher utilised a commercially available kit to extract DNA from blood and tissue samples. The collected DNA was effectively employed for targeted PCR and Random Amplification of Polymorphic DNA (RAPD) PCR study (Durcan and Petri, 2020). PCR procedures, which are used in molecular biological examinations of blood, necessitate the use of pure DNA. The extraction of DNA from a blood sample was expedited in comparison to the DNA extraction using the cetyltrimethylammonium bromide (CTAB) method (Zappulo *et al.*, 2022). Many laboratories prioritise a streamlined and expedient method for acquiring genomic DNA from blood, cell lines, and animal tissues for use in the PCR methodology. The quality and quantity of the sample were adequate for the purpose of polymerase chain reaction amplification and Southern blot analysis (Zhang

et al., 2022). This study utilised a commercial kit DNA extraction technique to isolate high-quality DNA.

3.7.2. Detection for PD-1 Gene in the Studied Group

The interaction was conducted using a PCR kit, following the instructions provided by the company, with a volume of 25 μ L. 12.5 units were extracted from the Master Mix, which contains MgCl₂, dNTPs, and Taq polymerase. This amount was consistently employed for both the samples and the complementary materials, under ideal conditions for the (PD-1) primer (Lin *et al.*, 2021).

The optimal conditions for initial denaturation and annealing were determined after conducting several experiments. The temperature was varied using gradient PCR for all samples in order to select the optimal condition. Additionally, the concentration of the DNA template was adjusted between 1.5-2 μ L. These two factors, temperature and DNA template concentration, are considered important for primer annealing with the complement (Smeets *et al.*, 2023). 1 μ L each of the forward primer (F) and reverse primer (R), each with a concentration of 10 picomole, were added. Additionally, 2 μ L of DNA template was added. In the PCR process, the initial denaturation step was carried out at a temperature of 95 $^{\circ}$ C for a duration of 5 minutes. For the annealing step, a gradient PCR approach was employed, where multiple temperatures were used simultaneously to reduce the overall time. The temperatures used were 55, 57, 59, 61, 63, and 65 $^{\circ}$ C, each for a duration of 30-40 seconds (Uciechowski and Dempke, 2020). Specifically, a temperature of 61 $^{\circ}$ C was used for 40 seconds for a total of 35 cycles. After two hours, the reaction concluded and the results were analyzed electrically. The best outcome was observed at a temperature of 61 $^{\circ}$ C (Saha *et al.*, 2021).

PCR was conducted to detect the presence of the (PD-1) gene in DNA samples collected from both SLE patients and healthy individuals. All tested samples showed positive results for the amplification of the (PD-1) gene. A single band of amplified products with a molecular size of 695 bp was observed, as depicted in Figure (3.20). A PCR negative control was performed in every experiment to detect any contamination.

Due to meticulous implementation of laboratory protocols, all negative controls consistently showed empty gel lanes throughout the optimization studies. Every reaction was performed twice, and only the bands that could be consistently reproduced were taken into account for analysis (Rezaieyazdi *et al.*, 2020).

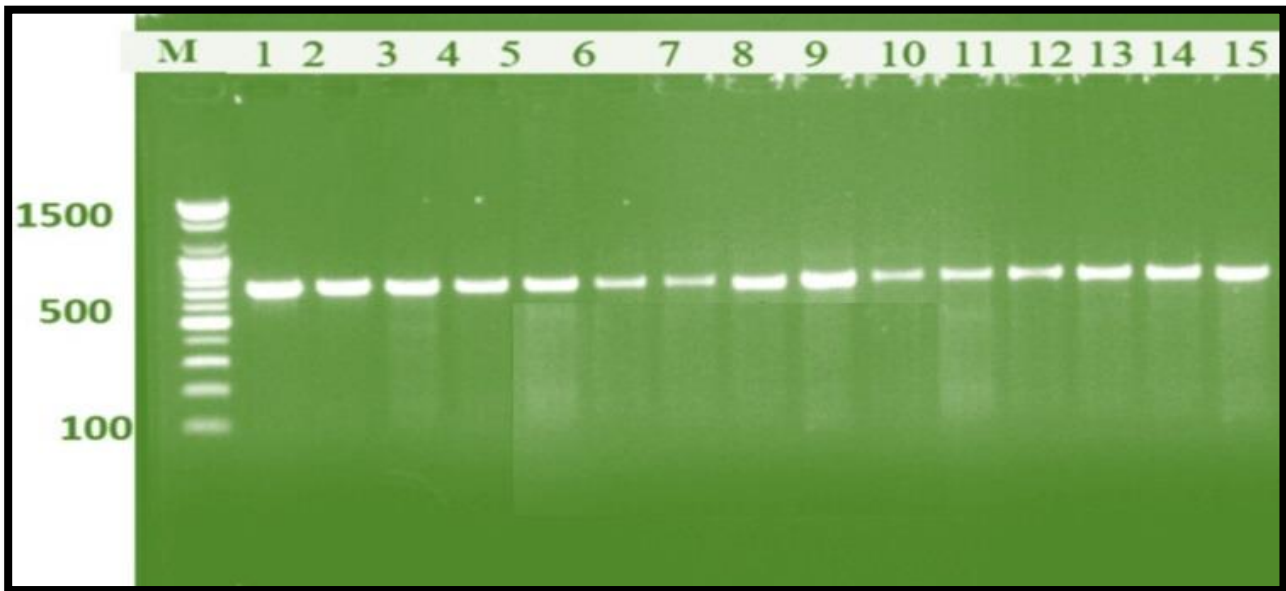


Figure (3.20): Agarose gel electrophoresis of PCR amplification products of PD-1 gene in the samples. 2% agarose, TBE buffer (1X), (5v/cm², 1hr). M: The DNA molecular weight marker (100 bp ladder). Positive amplifications of 695 bp for PD-1 gene.

3.7.3. Purification the Samples from Gel

Following the extraction of DNA from the samples, purification and concentration measurement are conducted. Subsequently, the diagnosis is performed using PCR. Once the results are obtained, they need to be sent for sequencing processing. However, prior to that, purification from the gel after PCR is necessary (Wang *et al.*, 2023). Following electrophoresis, the PCR products were stained and visualized under UV light. Once the bands appeared, they were excised and subjected to the Gel extraction method. After extracting the bands from the gel, the product was measured for purification and concentration using Nanodrop. Subsequently, the extracted samples were sent for sequence analysis (Xu *et al.*, 2021).

3.7.4. Examination of Hardy-Weinberg Equilibrium for PD-1 Gene Polymorphism

3.7.4.1. Genotyping and Allele Frequency of PD-1 SNP +7499

The genotyping frequencies of the PD-1 gene +7499 (G/A) were found to be in accordance with HWE in both the participants with SLE and the healthy control group.

Table (3.21): Genotype frequency and allele frequency of SLE subjects (SNP +7499)

Genotype of SLE (N=43)	HW Expected	H-W Observed	%	X ²	HW P- Value
Dominant Homozygous GG	13	16	37.2	3.23	0.062
Heterozygous GA	20	14	32.6		
Recessive Homozygote AA	10	13	30.2		
Allele Percentage Frequency					
G Allele Frequency %	58				
A Allele Frequency %	42				

The analysis of data from the SLE group Table (3.21) revealed that the frequencies of genotypes for rs6705653 (+7499, G/A) were as follows: 37.2% for homozygous wild type (GG), 32.6% for heterozygous genotype (GA), and 30.2% for homozygous mutant genotypes (AA). The frequency of the G allele is 58%, while the frequency of the A allele is 42%. The table indicates that there is no statistically significant difference between the observed and expected results ($p=0.062$, $X^2 = 3.23$), suggesting that the genotype frequencies were in line with the HWE (Topfer *et al.*, 2022).

Table (3.22): Genotype frequency and allele frequency of control (SNP +7499)

Genotype of Control (N=53)	HW Expected	H-W Observed	%	X ²	HW P-Value
Dominant Homozygous GG	23	26	49.1	4.07	0.29
Heterozygous GA	26	22	41.5		
Recessive Homozygote AA	4	5	9.4		
Allele Percentage Frequency					
G Allele Frequency %	67				
A Allele Frequency %	33				

Table (3.22) displays the frequencies of the rs6705653 (+7499, G/A) genotypes in the healthy control group. The rates of the homozygous wild genotype (GG), heterozygous genotype (GA), and homozygous mutant genotypes (AA) were 49.1%, 41.5%, and 9.4% respectively. The frequency of the G allele is 67%, while the frequency of the A allele is 33%. The data presented in the table demonstrate that there is no statistically significant disparity between the observed and predicted outcomes ($P= 0.29$, $X^2 = 4.07$). This suggests that the frequencies of genotypes are in line with the principles of HWE (Dey *et al.*, 2021).

3.7.4.2. Genotyping and Allele Frequency of PD-1 SNP +7209

The genotyping frequencies of the PD-1 gene +7209 (C/T) were found to be in accordance with Hardy-Weinberg equilibrium (HWE) in both the participants with systemic lupus erythematosus (SLE) and the healthy control group.

Table (3.23): Genotype frequency and allele frequency of SLE subjects (SNP +7209)

Genotype of SLE (N=43)	HW Expected	H-W Observed	%	X²	HW P- Value
Dominant Homozygous CC	28	29	67.4	0.42	0.61
Heterozygous CT	13	11	25.6		
Recessive Homozygote TT	2	3	7		
Allele Percentage Frequency					
C Allele Frequency %	83				
T Allele Frequency %	17				

The analysis of the data from the SLE group Table (3.23) revealed that the frequencies of the rs41386349 (+7209, C/T) genotypes were as follows: 67.4% for homozygous wild type (CC), 25.6% for heterozygous genotype (CT), and 7% for homozygous mutant genotypes (TT). The frequency of the C allele is 83%, while the frequency of the T allele is 17%. The table indicates that there is no statistically significant disparity between the observed and expected outcome ($P=0.61$, $X^2 = 0.42$), suggesting that the genotype frequencies align with the principles of HWE (Morand *et al.*, 2020).

Table (3.24): Genotype frequency and allele frequency of control (SNP +7209)

Genotype of Control (N=53)	HW Expected	H-W Observed	%	X²	HW P- Value
Dominant Homozygous CC	38	40	75.5	1.49	0.27
Heterozygous CT	12	11	20.8		
Recessive Homozygote TT	3	2	3.7		
Allele Percentage Frequency					
C Allele Frequency %	84				
T Allele Frequency %	16				

In Table (3.24), the frequencies of the rs41386349 (+7209, C/T) genotypes in the healthy control group were as follows: 75.5% homozygous wild (CC), 20.8% heterozygous (CT), and 3.7% homozygous mutant (TT). The frequency of the C allele is 84%, while the frequency of the A allele is 16%. The table demonstrates that there is no statistically significant disparity between the observed and expected outcome ($P=0.27$, $X^2=1.49$), indicating that the frequencies of genotypes were in line with the HWE (Xue *et al.*, 2022).

3.7.5. Comparison of Genotype and Allele Frequencies of the Two Polymorphism PD-1 Gene (+7499 and +7209)

The frequencies of genotypes and alleles for the PD-1 gene +7499 SNP in both the SLE and control groups are displayed in Table (3.25). The frequency of the GG genotype for the +7499 (rs6705653) variant was lower in patients with SLE compared to the control group (37.2% vs. 49.1%) using a codominant model. However, this difference was not statistically significant (Jaing *et al.*, 2021). Additionally, we noted that the frequency of the AA genotype for the +7499 (rs6705653) variant was lower in the control group compared to the group of patients with SLE (9.4% vs. 30.2%). This difference was statistically significant, with a p-value of 0.031 and an OR of 3.11 (95% CI: 1.52-5.94) (Zanatta *et al.*, 2020). The dominant genetic model indicated that the homozygous genotype AA, heterozygous genotype GA, and homozygous genotype GG did not exhibit a significant increase in the risk of SLE (OR = 1.68, 95% CI = 1.05-3.19, $P=0.054$) (Al-Shawi and Al-Fartosy, 2022). In addition, the recessive genetic model demonstrated that those with the homozygous genotype AA had a significantly higher risk of developing SLE compared to those with the heterozygous genotype GA and homozygous genotype GG (OR = 2.71, 95% CI = 1.42-4.89, p-value = 0.026). Similarly, the A allele showed a significant association with susceptibility to SLE (OR=1.59, 95% CI = 1.09-2.31, $P=0.043$) (Yan *et al.*, 2021).

Table (3.25): Allelic and genotypic of SNP +7499 G/A polymorphism in SLE and control groups

SNP +7499 G/A Polymorphism	Control N = 53 (%)	SLE N = 43 (%)	OR (95% CI)	P-Value
Codominant				
AA	5 (9.4)	13 (30.2)	3.11 (1.52-5.94)	0.031
GA	22 (41.5)	14 (32.6)	1.29 (0.78-2.64)	0.03
GG (Reference)	26 (49.1)	16 (37.2)	-	-
Dominant Genetic Model				
GA + AA	27 (50.9)	27 (62.79)	1.68 (1.05-3.19)	0.054
GG (Reference)	26 (49.1)	16 (37.2)	-	-
Recessive Genetic Model				
AA	5 (9.4)	13 (30.2)	2.71 (1.42-4.89)	0.026
GA + GG (Reference)	48 (90.6)	30 (69.8)		
Allele Frequency				
G (Wild Allele)	67	58		
A (Mutant Allele)	33	42	1.59 (1.09-2.31)	0.043

On the other hand, Table (3.26) displays the genotypic and allelic frequencies of the PD-1 gene +7209 SNP in both the SLE and control groups. The frequency of the CC genotype (rs41386349) was lower in SLE patients compared to the control group (67.4% vs. 75.5%) under a codominant model, but the difference was not statistically significant (Mertowska *et al.*, 2022). Additionally, we noted that the frequency of the +7209 (rs41386349) TT variant was lower in the control group compared to SLE patients (3.7% vs. 7%), although this difference was not statistically significant (P = 0.58, OR = 1.07, 95% CI = 0.43-3.02) (Wang *et al.*, 2022b). The homozygous genotype TT, heterozygous genotype CT, and homozygous genotype CC did not significantly

increase the risk of SLE. The OR for TT was 1.31 (95% CI = 0.84-2.36, P = 0.27), and the OR for CT was 1.19 (95% CI = 0.42-3.55, P = 0.69). Similarly, there was no significant association between the A allele and susceptibility to SLE (OR = 1.43, 95% CI = 0.68-2.37, p-value = 0.48) (Arab-Zozani *et al.*, 2021).

Table (3.26): Allelic and genotypic of SNP +7209 C/T polymorphism in SLE and control groups

SNP +7209 C/T Polymorphism	Control N = 53 (%)	SLE N = 43 (%)	OR (95% CI)	P-Value
Codominant				
TT	2 (3.7)	3 (7)	1.07 (0.43-3.02)	0.58
CT	11 (20.8)	11 (25.6)	1.21 (0.63-2.03)	0.79
CC (Reference)	40 (75.5)	29 (67.4)		
Dominant Genetic Model				
CT + TT	13 (24.5)	14 (32.6)	1.31 (0.84-2.36)	0.27
CC (Reference)	40 (75.5)	29 (67.4)		
Recessive Genetic Model				
TT	2 (3.7)	3 (7)	1.19 (0.42-3.55)	0.69
CT + CC (Reference)	51 (96.3)	40 (93)		
Allele Frequency				
C (Wild Allele)	84	83		
T (Mutant Allele)	16	17	1.43 (0.68-2.37)	0.48

This study investigated the variations in the PD-1 gene among patients with SLE and persons without the disease. We discovered two distinct locations of genetic variation, namely rs6705653 and rs41386349. The distribution of PD-1 +7499 (G/A) genotypes and allelic frequencies showed that SLE patients had significantly higher frequencies of the AA genotype. Prior study indicates that persons with SLE were more

prone to having the homozygous AA and heterozygous GA genotypes, whereas healthy individuals were more like to have the GG genotype. Consequently, the existence of the A allele and the associated AA genotype at this specific location may be accountable for the heightened susceptibility to SLE (Chao *et al.*, 2021). Furthermore, the presence of the G allele and GG genotype in the +7499 areas of the PD-1 gene may confer protective effects against SLE (Plachouri *et al.*, 2019). This work is the first to investigate the PD-1 +7499 (G/A) SNP in an Iraqi population from Basrah Province and establish its strong correlation with SLE. The absence of experimental data on the link of this locus with SLE makes this finding particularly noteworthy. Further investigation is necessary to underscore the functional importance of SNPs in this specific area. When analysing the allelic frequencies of the PD-1 +7209 (C/T) polymorphism, no noticeable distinction was observed between patients with SLE and individuals who are in good condition (Dini *et al.*, 2017). Prior studies have demonstrated that PD-1 +7209 (C/T) polymorphisms can impact PD-1 expression in individuals with SLE, leading to a worsened prognosis of the disease and decreased effectiveness of the NF-B and RUNX1 transcription factors in binding (Shields *et al.*, 2017; Rashad *et al.*, 2019).

3.7.6. Biochemical Characteristics of SLE and Healthy Control in Relevance to the Distribution of the Genotypes of PD-1 Gene Polymorphism

In order to verify the role of the examined SNPs in influencing the alterations of the pathophysiology in SLE patients, the data were evaluated in relation to the distribution of the genotypes. The genotypes of the PD-1 gene were evaluated. The data was analysed using the analysis of variance (ANOVA) test to compare the different groups. Biochemical features of SLE and healthy controls to the genotypes of PD-1 SNP +7499 polymorphism evaluated under co-dominant model as presented in Tables (1) and (2) correspondingly in the appendix. The biochemical features of individuals

with SLE and healthy individuals were studied in relation to the genotypes of the PD-1 SNP +7209 polymorphism. This analysis was conducted using a co-dominant model, and the results are presented in Tables (3) and (4) in the appendix.

3.7.7. Association of +7499 G/A and +7209 C/T Polymorphism with Serum PD-1 Levels

People with the +7499 GG and +7209 CC genotypes exhibited elevated levels of serum PD-1 compared to people with other genotypes. The levels of PD-1 in patients were markedly elevated compared to those of healthy control subjects, as demonstrated in Figure (3.21). This study found that there was a correlation between high levels of PD-1 in the blood and the presence of the +7499 G/G and +7209 C/C genetic variations. Our observations indicate that the levels of PD-1 in the serum of patients with SLE were markedly greater compared to those of healthy individuals. This suggests the presence of angiogenesis and/or chronic inflammation in SLE patients (Miyake *et al.*, 2018). The serum is the appropriate medium for measuring PD-1, as platelets can potentially contain stored PD-1 (Hinterleitner *et al.*, 2021).

A potential mechanism in the progression of SLE is the involvement of elevated levels of PD-1, which may contribute to the suppression of the activation of the patients' own lymphocytes. Treg cells and Teff cells mutually regulate each other to preserve immunological homeostasis (Hassel *et al.*, 2017). The disruption of homeostatic equilibrium or regulatory T cell (Treg) functionality is linked to the hyper activation of effector T cells (Teff), which mount immune responses against the body's own antigens, resulting in AIDs (Faris *et al.*, 2022a). PD-1, a well-known co-signalling receptor, plays a crucial role in controlling the growth and activation of Teff and Treg cells. Consequently, it is implicated in the progression of AIDs (Mohammed and Al-Fartosy, 2022). Recent investigations have demonstrated the involvement of sPD-1, the soluble version of PD-1, in autoimmune inflammation (Tu *et al.*, 2019; Page *et al.*, 2021). When compared to other negative regulators that do not have antigen-specific properties, the lack of PD-1 can impact the autoimmune response that is unique to antigens. The levels

of PD-1 and sPD-1 expression are strongly linked to the development of SLE, and they can function as autonomous biomarkers and prognostic indicators of disease progression (Lindblom *et al.*, 2022a).

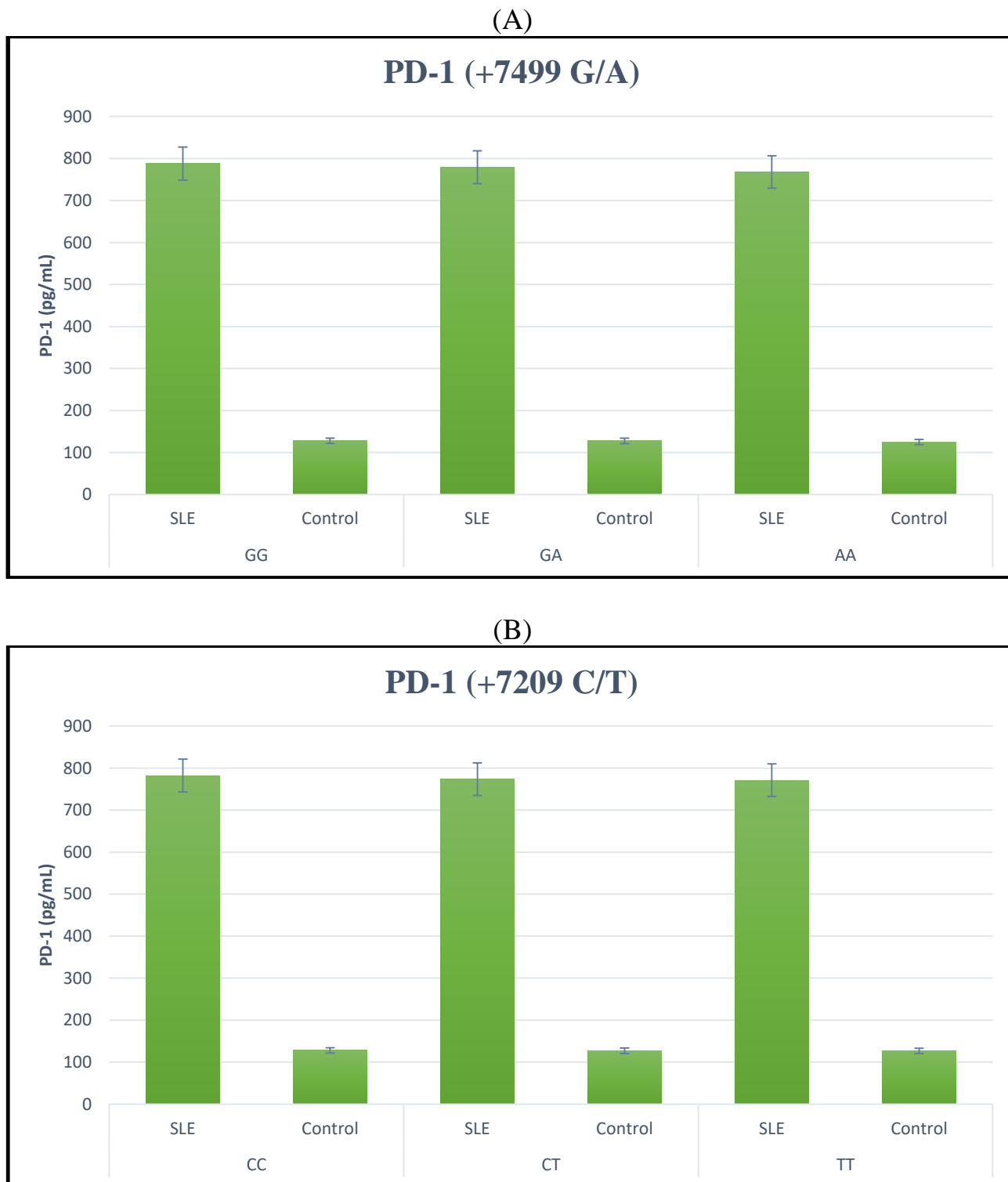


Figure (3.21): Association of the (A) PD-1 +7499 G/A and (B) PD-1 +7209 C/T polymorphism with serum PD-1 levels.

There were certain constraints in our investigation. Initially, all people diagnosed with SLE were examined only at hospitals located in Basrah Province. Hence, this might not accurately reflect the characteristics of the intended demographic. Furthermore, the limited sample size in this investigation could potentially compromise the precision of the current findings. Only two PD-1 SNPs, specifically +7499 G/A and +7209 C/T, were analysed. Hence, it is advisable to conduct thorough investigations to validate the findings and uncover novel outcomes.

Conclusion & Recommendations

Conclusion

Drawing on the preceding findings, the current investigation yields the subsequent deductions:

- 1- There were no statistically significant differences ($p>0.05$) seen in the BMI levels of patients with SLE compared to healthy individuals.
- 2- SLE has been found to be correlated with elevated levels of PD-1, as evidenced by the increased presence of pro-inflammatory cytokines (IL-18) and anti-inflammatory cytokines (IL-37) in the bloodstream.
- 3- The findings of this study suggest that reduced levels of C3, C4, and CH50 may be indicative of a potential risk factor for the development of SLE.
- 4- The assessment of oxidative stress in individuals with SLE can be effectively conducted by examining the reduction in TAC levels and the elevation in MDA levels.
- 5- SLE is linked to elevated levels of ANA, Anti-dsDNA, and CRP in patients, as evidenced by reduced GFR and elevated blood urea and creatinine levels.
- 6- The robust association shown between IL-18, IL-37, and PD-1 with C3, C4, CH50, MDA, TAC, CRP, ANA, anti-dsDNA, urea, creatinine, and GFR indicates that these inflammatory biomarkers potentially exert substantial influence on immune responses and inflammatory mechanisms in SLE.
- 7- The AUC results suggest that C3, C4, CH50, ANA, Anti-dsDNA, IL-18, IL-37, and PD-1 have the potential to be improved predictive biomarkers in SLE patients.
- 8- The sequencing findings of intron-4 in the PD-1 gene demonstrated a noteworthy correlation between the A allele and AA genotypes of PD-1 +7499 (G/A) SNP, which is associated with an increased susceptibility to SLE. The G allele exhibited a higher prevalence among those who were in good health.
- 9- No statistically significant association was found between the PD-1 +7209 (C/T) SNP and SLE.

Recommendations

It is advised that future research endeavours focus on the following investigations:

- 1- Further investigations are necessary to have a comprehensive understanding of the function played by the clinical biomarkers under investigation in the physiology and pathophysiology of SLE development.
- 2- Examine the impact of smoking on inflammation in individuals with SLE.
- 3- There is significant scientific significance in investigating the association between PD-1 and renal impairment as well as oxidative stress.
- 4- SLE exhibits an association with the level of oxidants and antioxidants. So, researches should be undertaken to investigate the potential of dietary supplements in the diagnosis and mitigation of SLE development and associated dangers.
- 5- Investigate the genetic expression of specific proteins and mutations in PD-1 receptors, as well as examine the genetic analysis of several linked antioxidant enzymes in patients with SLE.
- 6- Patients with SLE frequently attend clinics to undergo thorough screening of bodily systems. Ensuring the administration of appropriate medical interventions to the patient and mitigating any problems.
- 7- In order to facilitate the early detection of vascular problems in patients with SLE, it is imperative that the aforementioned clinical and biochemical indicators [complement component 3 (C3), complement component 4 (C4), complement haemolytic 50 (CH50), antinuclear antibody (ANA), anti-double strand DNA (Anti-ds DNA), interleukin-18 (IL-18), interleukin-37 (IL-37), and programmed cell death 1 (PD-1)] be implemented in hospitals and clinics within Basrah Province in the future.



References

References

References

- Aarslev K, Dige A, Greisen SR, Kreutzfeldt M, Jessen N, Vilstrup H, et al. (2017). Soluble programmed death-1 levels are associated with disease activity and treatment response in patients with autoimmune hepatitis. *Scand J Gastroenterol*, 52:93-9.
- Abdalla MA, El Desouky SM, Ahmed AS. (2017). Clinical significance of lipid profile in systemic lupus erythematosus patients: Relation to disease activity and therapeutic potential of drugs. *Egyptian Rheumatologist*, 39(2):93–8.
- Abdualhay RA, Al-Fartosy AJM. (2022). Insulin Resistance and Other Adipokines as Clinical Predictors of Gestational Diabetes Mellitus among Pregnant Women. *Indones Biomed J*, 14(3): 243-51.
- Ahmad S, Ärnlov J, Larsson S. C. (2022). Genetically Predicted Circulating Copper and Risk of Chronic Kidney Disease: A Mendelian Randomization Study. *Nutrients*, 14(3): 509.
- Aibara N, Ichinose K, Baba M, Nakajima H, Satoh K, Atarashi R, et al. (2018). Proteomic approach to profiling immune complex antigens in cerebrospinal fluid samples from patients with central nervous system autoimmune diseases. *Clin. Chim. Acta*, 484: 26–31.
- Alaanzy MT, Alsaffar JMJ, Abdul Bari A. (2020). Evaluate the Correlation Between Antioxidant Capacity and Interferon Γ Level with the Disease Activity of Sle Patients in Iraqi Woman. *Indian Journal of Public Health Research & Development*, 11 (1): 1278-82.
- Al-Anazi MR, Matou-Nasri S, Al-Qahtani AA, Alghamdi J, Abdo AA, Sanai FM et al. (2019). Association between IL-37 gene polymorphisms and risk of HBV-related liver disease in a Saudi Arabian population. *Sci Rep*, 9: 7123.

References

- Al-Fartosy AJM, Ati MH. (2021). A Predictive clinical markers to make prostate cancer and benign prostate hyperplasia easy diagnosis. *Biochem. Cell. Arch*, 21(2): 2939–2947.
- Al-Fartosy AJM, Awad NA, Abdalemam DJ. (2017a). Biochemical study of the effect of insulin resistance on adiponectin, lipid profile and some antioxidants elements with relation to obesity in type 2 diabetic patients/Basrah-Iraq. *Amer J Biochem*, (7): 73-82.
- Al-Fartosy AJM, Awad NA, Alsalimi SA. (2020a). Insulin resistance and specific biomarkers in blood and urine of type 2 diabetic patients with or without nephropathy in Basrah, Iraq. *Afr J Biochem Res*, 14(4): 125-134.
- Al-Fartosy AJM, Awad NA, Alsalimi SA. (2020b). Osteoprotegerin and Some Trace Elements in Type 2 Diabetic Patients with or without Nephropathy: Effect of Insulin Resistance. *International Medical Journal*, 25(4):1771-1784.
- Al-Fartosy AJM, Awad NA, Alsalimi SA. (2021). Clinical markers and some trace elements in patients with type-2 diabetic nephropathy: Impact of insulin resistance. *Journal of Medical Investigation*, 68(12): 76–84.
- Al-Fartosy AJM, Awad NA, Mahmood RA. (2019). A Comparative Study of Leptin, Oxidant/Antioxidant Status and Some Trace Elements in Women of Healthy Control and Unexplained Infertility in Basrah-Iraq. *Indones Biomed J.*,11(3): 327-337.
- Al-Fartosy AJM, Awad NA, Mohammed AH. (2020c). Intelectin-1 and Endocrinological Parameters in Women with Polycystic Ovary Syndrome: Effect of Insulin Resistance. *Ewha Med J*, 43(1): 1-11.
- Al-Fartosy AJM, Awad NA, Mohammed AH. (2023). Evaluating the clinical significance of RBP4, PAI-1, and some trace elements in women with Polycystic Ovary Syndrome. *Revis Bionatura*, 8 (1): 36.

References

- Al-Fartosy AJM, Mohammed IM. (2017a). Biochemical Study of the Effects of Insulin Resistance on Sex Hormones in Men and Women Type-2 Diabetic Patients / Meisan-Iraq. *Advances in Biochemistry*, 5(5): 79-88.
- Al-Fartosy AJM, Mohammed IM. (2017b). Comparison of Insulin Resistance, Prolactin and HbA1c with Relation to Obesity in Men and Women of Healthy Control and Diabetic Patients / Meisan-Iraq. *International Journal of Current Research*, 9(8): 55643-55648.
- Al-Fartosy AJM, Mohammed IM. (2017c). Study the Biochemical Correlation of Insulin Resistance with HbA1c and Sex Hormones in NIDDM Patients/Meisan-Iraq. *Journal of Diabetes Mellitus*, 7, 302-315.
- Al-Fartosy AJM, Shanan SK, Awad NA. (2017b). Biochemical Study of the Effects of Some Heavy Metals on Oxidant / Antioxidant Status in Gasoline Station Workers /Basra-Iraq. *International Journal of Scientific and Research Publications*, (7)2: 83-94.
- Al-Gahtani SN. (2021). A Review of Systemic Lupus Erythematosus (SLE): Symptoms, Risk Factors, Treatment, and Health Related Quality of Life Issues. *Open Journal of Rheumatology and Autoimmune Diseases*, 11: 115-143.
- AL-hameedawi AKJ, Al-Shawi AAA. (2023). Identification of novel mutations in β -thalassemia patients in Maysan Governorate, Iraq. *Molecular Biology Reports*, 50: 3053–3062.
- Ali M, Ejaz A, Iram H, Solangi SA, Junejo AM, Solangi SA. (2021a). Frequency of Intradialytic Complications in Patients of End-Stage Renal Disease on Maintenance Hemodialysis. *Cureus*, 13(1): e12641.
- Ali S, Mumtaz S, Shakir HA, Khan M, Tahir HM, Mumtaz S, et al. (2021b). Current status of beta-thalassemia and its treatment strategies. *Mol Genet Genomic Med*, 9(12):e1788.

References

- Alsalmi SA, Al-Mashkor IMA, Al-Fartosy AJM. (2023). Osteoprotegerin and Interleukin-37 are Correlated with Liver Diseases in Chronic Hepatitis B Virus (HBV)-infected Subjects. *Indones Biomed J*, 15(3): 222-30.
- Al-Shawi HM, Al-Fartosy AJM. (2022). Evaluating the clinical significance of insulin resistance, oxidant/ antioxidant status, some adipokines, and glycoproteins as monitoring indicators in Type 2 diabetic foot syndrome. *Teikyo Medical Journal*, 45(05): 6685-6697.
- Arab-Zozani M, Kheyrandish S, Rastgar A, Miri-Moghaddam E. (2021). A systematic review and meta-analysis of stature growth complications in β -thalassemia major patients. *Ann Glob Health*, 87(1):48.
- Aringer M, Costenbader K, Daikh D, Brinks R, Mosca M, Ramsey-Goldman R, et al. (2019). European League Against Rheumatism/American College of Rheumatology classification criteria for systemic lupus erythematosus. *Ann Rheum Dis*, 78(9):1151-1159.
- Arpaci A, Gul BU, Ozcan O, Ilhan G, El C, Dirican E, et al. (2021) Presentation of two new mutations in the 3' untranslated region of the β -globin gene and evaluating the molecular spectrum of thalassemia mutations in the Mediterranean region of Turkey. *Ann Hematol*, 100(6):1429–1438.
- Ayoub I, Birmingham D, Rovin B, Hebert L. (2019). Commentary on the current guidelines for the diagnosis of lupus nephritis flare. *Curr Rheumatol Rep*, 21:12.
- Bae SC, Lee YH. (2017). Circulating macrophage migration inhibitory factor levels and its polymorphisms in systemic lupus erythematosus: a meta-analysis. *Cell Mol Biol*, 63: 74-9.
- Bassiouni SA, Abdeen HM, Morsi HK, Zaki ME, Abdelsalam M, Gharbia OM. (2021). Programmed death 1 (PD-1) serum level and gene expression in recent onset

References

- systemic lupus erythematosus patients. *The Egyptian Rheumatologist*, 43: 213–218.
- Beberashvili I, Omar MA, Nizri E, Stav K, Efrati S. (2023). Combined use of CRP with neutrophil-to-lymphocyte ratio in differentiating between infectious and noninfectious inflammation in hemodialysis patients. *Scientific reports*, 13(1): 5463.
- Bellan M, Andreoli L, Mele C, Sainaghi PP, Rigamonti C, Piantoni S, et al. (2020). Pathophysiological Role and Therapeutic Implications of Vitamin D in Autoimmunity: Focus on Chronic Autoimmune Diseases. *Nutrients*, 12: 789.
- Belmokhtar I, Lhousni S, Elidrissi Errahhali M, Ghanam A, Elidrissi Errahhali M, Sidqi Z, et al. (2022). Molecular heterogeneity of β -thalassemia variants in the Eastern region of Morocco. *Mol Genet Genomic Med*, 10(8):e1970.
- Bommarito D, Hall C, Taams LS, Corrigall VM. (2017). Inflammatory cytokines compromise programmed cell death-1 (PD-1)-mediated T cell suppression in inflammatory arthritis through upregulation of soluble PD-1. *Clin Exp Immunol*, 188:455-66.
- Brookes EM, Power DA. (2022). Elevated serum urea-to-creatinine ratio is associated with adverse inpatient clinical outcomes in non-end stage chronic kidney disease. *Scientific reports*, 12(1): 20827.
- Cappelli LC, Gutierrez AK, Bingham CO, Shah AA. (2017). Rheumatic and musculoskeletal immune-related adverse events due to immune checkpoint inhibitors: a systematic review of the literature. *Arthritis Care Res (Hoboken)*, 69:1751-63.
- Catalan-Dibene J, McIntyre LL, Zlotnik A. (2018). Interleukin 30 to Interleukin 40. *Journal of interferon & cytokine research: the official journal of the International Society for Interferon and Cytokine Research*, 38(10): 423–439.

References

- Chao CH, Wu CL, Huang WY. (2021). Association between estimated glomerular filtration rate and clinical outcomes in ischemic stroke patients with high-grade carotid artery stenosis. *BMC neurology*, 21(1): 124.
- Chauhan W, Afzal M, Zaka-Ur-Rab Z, Noorani MS. (2021). A Novel Frameshift mutation, deletion of HBB: c.199_202delAAAG [Codon 66/67 (-AAAG)] in β -thalassemia major patients from the Western Region of Uttar Pradesh, India. *Appl Clin Genet*, 14:77–85.
- Chen H, Peng Q, Yang H, Yin L, Shi J, Zhang Y, et al. (2018a). Increased levels of soluble programmed death ligand 1 associate with malignancy in patients with dermatomyositis. *J Rheumatol*, 45:835-40.
- Chen L, Wang Y-F, Liu L, Bielowka A, Ahmed R, Zhang H, et al. (2020). Genome-wide assessment of genetic risk for systemic lupus erythematosus and disease severity. *Human Molecular Genetics*, 29(10): 1745–1756.
- Chen M, Chen X, Wan Q. (2018b). Altered frequency of Th17 and Treg cells in new-onset systemic lupus erythematosus patients. *Eur. J. Clin. Investig*, 48: e13012.
- Chessa E, Piga M, Floris A, Devilliers H, Cauli A, Arnaud L. (2020). Use of Physician Global Assessment in Systemic Lupus Erythematosus: A Systematic Review of Its Psychometric Properties. *Rheumatology*, 59: 3622-3632.
- Chisavu F, Gafencu M, Stroescu R, Motofelea A, Chisavu L, Schiller A. (2023). Acute kidney injury in children: incidence, awareness and outcome—a retrospective cohort study. *Sci Rep* 13: 15778.
- Coronel-Restrepo N, Posso-Osorio I, Naranjo-Escobar J, Toboń GJ. (2017). Autoimmune diseases and their relation with immunological, neurological and endocrinological axes. *Autoimmun Rev*, 16:684-92.

References

- Dai C, Kuo S-J, Zhao J, Jin L, Kang L, Wang L, et al. (2019). Correlation between genetic polymorphism of angiotensin-converting enzyme 2 gene and clinical aspects of rheumatoid arthritis. *Int. J. Med. Sci*, 16(2): 331-336.
- Dall'Ara F, Cutolo M, Andreoli L, Tincani A, Paolino S. (2018). Vitamin D and systemic lupus erythematosus: A review of immunological and clinical aspects. *Clin. Exp. Rheumatol*, 36: 153–162.
- Davarpanah E, Jafarzadeh A, Nemati M, Bassagh A, Abasi MH, Khosravimashizi A, et al. (2020). Circulating concentration of interleukin-37 in Helicobacter pylori-infected patients with peptic ulcer: its association with IL-37 related gene polymorphisms and bacterial virulence factor CagA. *Cytokine*, 126: 154928.
- Demir S, Erten G, Artım-Esen B, Şahinkaya Y, Pehlivan Ö, Alpay-Kantitez N, et al. (2018). Increased serum leptin levels are associated with metabolic syndrome and carotid intima media thickness in premenopausal systemic lupus erythematosus patients without clinical atherosclerotic vascular events. *Lupus*, 27(9): 1509-1516.
- Deng Y, Tsao BP. (2017). Updates in Lupus Genetics. *Curr. Rheumatol. Rep*, 19: 68.
- Dey M, Parodis I, Nikiphorou E. (2021). Fatigue in Systemic Lupus Erythematosus and Rheumatoid Arthritis: A Comparison of Mechanisms, Measures and Management. *J. Clin. Med*, 10: 3566.
- Diaz-Rizo V, Bonilla-Lara D, Gonzalez-Lopez L, Sanchez-Mosco D, Fajardo-Robledo NS, Perez-Guerrero EE, et al. (2017). Serum levels of adiponectin and leptin as biomarkers of proteinuria in lupus nephritis. *PLoS One*, 12:e0184056.
- Dini AA, Wang P, Ye DQ. (2017). Serum adiponectin levels in patients with systemic lupus erythematosus: a meta-analysis. *J Clin Rheumatol*, 23: 361–367.
- Du W, Shen T, Li H, Liu Y, He L, Tan L, et al. (2017). Low apolipoprotein M serum levels correlate with Systemic lupus erythematosus disease activity and

References

- apolipoprotein M gene polymorphisms with Lupus. *Lipids in Health and Disease*, 16: 88.
- Durcan L, Petri M. (2020). The clinical and serological associations of hypocomplementemia in a longitudinal SLE cohort. *Semin Arthritis Rheum*, 50:1081–86.
- El-Sayed EH, Saleh MH, Al-Shahaly MH, Toraih EA, Fathy A. (2018). IL-37 gene variant (rs3811047): a marker of disease activity in rheumatoid arthritis: a pilot study. *Autoimmunity*, 51:378–85.
- Engel S, Boedecker S, Marczyński P, Bittner S, Steffen F, Weinmann A, et al. (2021). Association of serum neurofilament light chain levels and neuropsychiatric manifestations in systemic lupus erythematosus. *Ther. Adv. Neurol. Disord*, 14: 17562864211051497.
- Fanouriakis A, Kostopoulou M, Alunno A, Aringer M, Bajema I, Boletis JN, et al. (2019). 2019 update of the EULAR recommendations for the management of systemic lupus erythematosus. *Ann. Rheum. Dis*, 78: 736–745.
- Faris ST, Al-Fartosy AJM, Al-Fregi AA. (2022a). Interleukin-37 and Interleukin-18 as Prognostic Biomarkers for End-Stage Renal Disease. *Azerbaijan Medical Journal*, 62(4): 1429- 1439.
- Faris ST, Al-Fartosy AJM, Al-Fregi AA. (2022b). Genetic Polymorphism of Vascular Endothelial Growth Factor (VEGF) Associated with Hypothyroid in Hemodialysis Patients. *ECB*, 11(11): 1-9.
- Fava A, Petri M. (2019). Systemic Lupus Erythematosus: Diagnosis and Clinical Management. *J Autoimmun*, 96: 1–13.
- Fike AJ, Elcheva I, Rahman ZSM. (2019). The post-GWAS era: how to validate the contribution of gene variants in lupus. *Curr. Rheumatol. Rep*, 21: 3.

References

- Fujita Y. (2017). Leptin and autoimmune disease. *Nihon Rinsho Meneki Gakkai Kaishi*, 40: 155–159.
- Fukasawa T, Yoshizaki A, Ebata S, Nakamura K, Saigusa R, Miura S, et al. (2017). Contribution of soluble forms of programmed death 1 and programmed death ligand 2 to disease severity and progression in systemic sclerosis. *Arthritis Rheum*, 69:1879-90.
- Furie AR, Morand EF, Bruce IN, Manzi S, Kalunian KC, Vital EM, et al. (2019). Type I interferon inhibitor anifrolumab in active systemic lupus erythematosus (TULIP-1): A randomised, controlled, phase 3 trial. *Lancet Rheumatol*, 1: e208–e219.
- Galli E, Hartmann F, Schreiner B, Ingelfinger F, Arvaniti E, Diebold M, et al. (2019). GM-CSF and CXCR4 define a T helper cell signature in multiple sclerosis. *Nat. Med*, 25: 1290–1300.
- Gao J, Gai N, Wang L, Liu K, Liu XH, Wei LT, et al. (2017a). Meta-analysis of programmed cell death 1 polymorphisms with systemic lupus erythematosus risk. *Oncotarget*, 8:36885-97.
- Gao L, Bird AK, Meednu N, Dauenhauer K, Liesveld J, Anolik J, et al. (2017b). Bone Marrow–Derived Mesenchymal Stem Cells From Patients With Systemic Lupus Erythematosus Have a Senescence-Associated Secretory Phenotype Mediated by a Mitochondrial Antiviral Signaling Protein–Interferon- β Feedback Loop. *Arthritis & Rheumatology*, 69: 1623-1635.
- Gergianaki I, Bortoluzzi A, Bertsias G. (2018). Update on the epidemiology, risk factors, and disease outcomes of systemic lupus erythematosus. *Best. Pract. Res. Clin. Rheumatol*, 32: 188–205.

References

- Han L, Yang X, Yu Y, Wan W, Lv L, Zou H. (2019). Associations of circulating CXCR3(-)PD-1(+)CD4(+)T cells with disease activity of systemic lupus erythematosus. *Mod Rheumatol*, 29:461-9.
- Hanna Kazazian N, Wang Y, Roussel-Queval A, Marcadet L, Chasson L, Laprie C, et al. (2019). Lupus Autoimmunity and Metabolic Parameters Are Exacerbated Upon High Fat Diet-Induced Obesity Due to TLR7 Signaling. *Front. Immunol*, 10: 2015.
- Hassel JC, Heinzerling L, Aberle J, Baˆhr O, Eigentler TK, Grimm MO, et al. (2017). Combined immune checkpoint blockade (anti-PD-1/anti-CTLA-4): evaluation and management of adverse drug reactions. *Canc Treat Rev*, 57:36-49.
- He J, Zhang R, Shao M, Zhao X, Miao M, Chen J, et al. (2020). Efficacy and safety of low-dose IL-2 in the treatment of systemic lupus erythematosus: A randomised, double-blind, placebo-controlled trial. *Ann. Rheum. Dis*, 79: 141–149.
- Hinterleitner C, Strahle J, Malenke E, Hinterleitner M, Henning M, Seehawer M, et al. (2021). Platelet PD-L1 reflects collective intratumoral PD-L1 expression and predicts immunotherapy response in non-small cell lung cancer. *Nat Commun*, 12(1):7005.
- Hu G-N, Wang Y, Tang C-H, Jin L-L, Huang B-F, Wang Q. (2022). The impact of Angiopoietin-2 genetic polymorphisms on susceptibility for malignant breast neoplasms. *Scientific Reports*, 12:14522.
- Huang Q, Shen S, Qu H, Huang Y, Wu D, Jiang H, et al. (2020). Expression of HMGB1 and TLR4 in neuropsychiatric systemic lupus erythematosus patients with seizure disorders. *Ann. Transl. Med*, 8: 9.
- Ichinose K, Ohyama K, Furukawa K, Higuchi O, Mukaino A, Satoh K, et al. (2018). Novel anti-suprabasin antibodies may contribute to the pathogenesis of neuropsychiatric systemic lupus erythematosus. *Clin.Immunol*, 193: 123–130.

References

- Islam MA, Khandker SS, Alam SS, Kotyla P, Hassan R. (2019). Vitamin D status in patients with systemic lupus erythematosus (SLE): A systematic review and meta-analysis. *Autoimmun. Rev*, 18: 102392.
- Islam MA, Khandker SS, Kotyla PJ, Hassan R. (2020). Immunomodulatory Effects of Diet and Nutrients in Systemic Lupus Erythematosus (SLE): A Systematic Review. *Front. Immunol*, 11: 1477.
- Italiani P, Manca ML, Angelotti F, Melillo D, Pratesi F, Puxeddu I, et al. (2018). IL-1 family cytokines and soluble receptors in systemic lupus erythematosus. *Arthritis Res Ther*, 20:27.
- Jaing TH, Chang TY, Chen SH, Lin CW, Wen YC, Chiu CC. (2021). Molecular genetics of β -thalassemia: a narrative review. *Medicine (Baltimore)*, 100(45):e27522.
- Jiang F, Lyu GZ, Zhang VW, Li DZ. (2021). Identification of thalassemia gene cluster deletion by long-read whole-genome sequencing (LR-WGS). *Int J Lab Hematol* 43(4):859–865.
- Khan S, Dar SA, Mandal RK, Jawed A, Wahid M, Panda AK, et al. (2018). Angiotensin-Converting Enzyme Gene I/D Polymorphism Is Associated With Systemic Lupus Erythematosus Susceptibility: An Updated Meta-Analysis and Trial Sequential Analysis. *Front. Physiol*, 9:1793.
- Khanjari Y, Oladnabi M, Abdollahi N, Heidari A, Mohammadi S, Tabarraei A. (2020). Variants in Intron 4 of PD-1 Gene are Associated with the Susceptibility to SLE in an Iranian Population. *Iran J Immunol*, 17(3):204-214.
- Kholis FN, Farhanah N, Limantoro C, Widyastiti NS, Sobirin MA. (2023). Increased Levels of IFN- γ , PAI-1, and NT-proBNP are Associated with the Occurrence of Hypoxemia in COVID-19. *Indones Biomed J*, 15(5): 341-50.

References

- Kitagori K, Yoshifuji H, Oku T, Ayaki T, Kuzuya A, Nakajima T, et al. (2019). Utility of osteopontin in cerebrospinal fluid as a diagnostic marker for neuropsychiatric systemic lupus erythematosus. *Lupus*, 28: 414–422.
- Klein A, Selter RC, Hapfelmeier A, Berthele A, Müller-Myhsok B, Pongratz V, et al. (2019). CSF parameters associated with early MRI activity in patients with MS. *Neurol. Neuroimmunol. Neuroinflammation*, 6: e573.
- Kono M, Nagafuchi Y, Shoda H, Fujio K. (2021). The Impact of Obesity and a High-Fat Diet on Clinical and Immunological Features in Systemic Lupus Erythematosus. *Nutrients*, 13: 504.
- Kubick N, Klimovich P, Flournoy PH, Bieńkowska I, Łazarczyk M, Sacharczuk M, et al. (2021). Interleukins and Interleukin Receptors Evolutionary History and Origin in Relation to CD4+ T Cell Evolution. *Genes*, 12(6), 813.
- Kuo C-Y, Tsai T-Y, Huang Y-C. (2020). Insulin resistance and serum levels of adipokines in patients with systemic lupus erythematosus: a systematic review and meta-analysis. *Lupus*, 0(0): 1–7.
- Kwon YC, Chun S, Kim K, Mak A. (2019). Update on the genetics of systemic lupus erythematosus: genome-wide association studies and beyond. *Cells*, 8:1180.
- Lambring CB, Siraj S, Patel K, Sankpal UT, Mathew S, Basha R. (2019). Impact of the Microbiome on the Immune System. *Crit. Rev. Immunol*, 39: 313–328.
- Laurent L, Le Fur A, Le Bloas R, Néel M, Mary C, Moreau A, et al. (2017). Prevention of lupus nephritis development in NZB/NZW mice by selective blockade of CD28. *Eur J Immunol*, 47: 1368-76.
- Lee WF, Wu CY, Yang HY, Lee WI, Chen LC, Ou LS, et al. (2019). Biomarkers associating endothelial Dysregulation in pediatric-onset systemic lupus erythematosus. *Pediatr Rheumatol Online J*, 7(1):69.

References

- Lee YH, Song GG. (2018). Association between circulating leptin levels and systemic lupus erythematosus: an updated meta-analysis. *Lupus*, 27: 428–435.
- Lee YH, Song GG. (2020). Circulating Interleukin-18 Level in Systemic Lupus Erythematosus. *J Rheum Dis*, 27, (2): 110-115.
- Leonardi GC, Gainor JF, Altan M, Kravets S, Dahlberg SE, Gedmintas L, et al. (2018). Safety of programmed death-1 pathway inhibitors among patients with nonsmall-cell lung cancer and preexisting autoimmune disorders. *J ClinOncol*, 36(19): 1905–12.
- Liao W, Zheng H, Wu S, Zhang Y, Wang W, Zhang Z, et al. (2017). The systemic activation of programmed death 1-PD-L1 axis protects systemic lupus erythematosus model from nephritis. *Am J Nephrol*, 46:371-9.
- Lin W, Zhang Q, Shen Z, Qu X, Wang Q, Wei L, et al. (2021). Molecular and phenotype characterization of an elongated β -globin variant produced by BB:C.313delA. *Int J Lab Hematol*, 43(6):1620–1627.
- Lin XY, Guo XJ, He YZ, Hou SF, Zhu HB, Cheng Y, et al. (2018). Association between interleukin 37 (rs3811047) polymorphism and multiple autoimmune diseases in a Chinese population: a PRISMA-compliant meta-analysis. *Medicine (Baltimore)*, 97:e0386.
- Lindblom J, Mohan C, Parodis I. (2022a). Biomarkers in Neuropsychiatric Systemic Lupus Erythematosus: A Systematic Literature Review of the Last Decade. *Brain Sci*, 12: 192.
- Lindblom J, Mohan C, Parodis I. (2022b). Diagnostic, predictive and prognostic biomarkers in systemic lupus erythematosus: Current insights. *Curr. Opin. Rheumatol*, 34: 139–149.

References

- Lu L, Kong W, Zhou K, Chen J, Hou Y, Dou H, et al. (2021a). Association of lipoproteins and thyroid hormones with cognitive dysfunction in patients with systemic lupus erythematosus. *BMC Rheumatol*, 5: 18.
- Lu X, Chen X, Forney C, Donmez O, Miller D, Parameswaran S, et al. (2021b). Global Discovery of Lupus Genetic Risk Variant Allelic Enhancer Activity. *Nature Communications*, 12: 1611.
- Mende R, Vincent FB, Kandane-Rathnayake R, Koelmeyer R, Lin E, Chang J, et al. (2018). Analysis of serum interleukin (il)-1 β and il-18 in systemic lupus erythematosus. *Front Immunol*, 9:1250.
- Mertowska P, Mertowski S, Smarz-Widelska I, Grywalska E. (2022). Biological Role, Mechanism of Action and the Importance of Interleukins in Kidney Diseases. *International journal of molecular sciences*, 23(2), 647.
- Mike EV, Makinde HM, Gulinello M, Vanarsa K, Herlitz L, Gadhvi G, et al. (2019). Lipocalin-2 is a pathogenic determinant and biomarker of neuropsychiatric lupus. *J. Autoimmun*, 96: 59–73.
- Mitratza M, Klijs B, Hak AE, Kardaun JWPF, Kunst AE. (2021). Systemic autoimmune disease as a cause of death: Mortality burden and comorbidities. *Rheumatology*, 60: 1321–1330.
- Miyake CNH, Gualano B, Dantas WS, Pereira RT, Neves W, Zambelli VO, et al. (2018). Increased Insulin Resistance and Glucagon Levels in Mild/Inactive Systemic Lupus Erythematosus Patients Despite Normal Glucose Tolerance. *Arthritis Care Res (Hoboken)*, 70(1):114-124.
- Mohamed AAA, Hammam N, El Zohri MH, Gheita TA. (2019). Cardiac manifestations in systemic lupus erythematosus: clinical correlates of subclinical echocardiographic features. *Biomed Res Int*, 2019:2437105.

References

- Mohammed IM, Al-Fartosy AJM. (2022). Evaluating the clinical significance of Osteoprotegerin Serum Levels as a Predictive Marker in Rheumatoid Arthritis. *Azerbaijan Medical Journal*, 62(6): 1461- 1468.
- Mohammed IM, Alsalimi SA, Al-Fartosy AJM. (2023). Trace Elements and Oxidant/Antioxidant Status in Beta-Thalassemia Patients. *Bahrain Medical Bulletin*, 45(4): 1772-78.
- Mohammed SF, Abdalla MA, Ismaeil WM, Sheta MM. (2018). Serum leptin in systemic lupus erythematosus patients: Its correlation with disease activity and some disease parameters. *Egyptian Rheumatologist*, 40(1):23–7.
- Mok CC. (2019). Metabolic syndrome and systemic lupus erythematosus: the connection. *Expert Rev Clin Immunol*, 15: 765–775.
- Moon J, Kim D, Kim EK, Lee SY, Na HS, Kim GN, et al. (2020). Brown adipose tissue ameliorates autoimmune arthritis via inhibition of Th17 cells. *Sci. Rep*, 10: 12374.
- Morand EF, Furie R, Tanaka Y, Bruce IN, Askanase AD, Richez C, et al. (2020). Trial of Anifrolumab in Active Systemic Lupus Erythematosus. *N. Engl. J. Med*, 382: 211–221.
- Nagafuchi Y, Shoda H, Fujio K. (2019). Immune Profiling and Precision Medicine in Systemic Lupus Erythematosus. *Cells*, 8: 140.
- Nakanishi K. (2018). Unique action of interleukin-18 on T cells and other immune cells. *Front Immunol*, 9: 763.
- Narani A. (2019). Systemic Lupus Erythematosus (SLE) - A Review of clinical approach for diagnosis and current treatment strategies. *Jaffna Medical Journal*, 31(2): 9-13.

References

- Noris-García E, Arce S, Nardin P, Lanigan EM, Acuña V, Gutierrez F, et al. (2018). Peripheral levels of brain-derived neurotrophic factor and S100B in neuropsychiatric systemic lupus erythematosus. *Lupus*, 27: 2041–2049.
- Page MJ, McKenzie JE, Bossuyt PM, Boutron I, Hoffmann TC, Mulrow CD, et al. (2021). The PRISMA 2020 statement: An updated guideline for reporting systematic reviews. *BMJ*, 372: 71.
- Pan Y, Wen X, Hao D, Wang Y, Wang L, He G, et al. (2020). The role of IL-37 in skin and connective tissue diseases. *Biomed Pharmacother*, 122:109705.
- Plachouri KM, Vryzaki E, Georgiou S. (2019). Cutaneous adverse events of immune checkpoint inhibitors: a summarized overview. *Curr. Drug Saf*, 14 (1): 14–20.
- Postal M, Vivaldo JF, Fernandez-Ruiz R, Paredes JL, Appenzeller S, Niewold TB. (2020). Type I interferon in the pathogenesis of systemic lupus erythematosus. *Curr. Opin. Immunol*, 67: 87–94.
- Qi S, Chen Q, Xu D, Xie N, Dai Y. (2018). Clinical application of protein biomarkers in lupus erythematosus and lupus nephritis. *Lupus*, 27: 1582–1590.
- Qi Y-Y, Cui Y, Lang H, Zhai Y-L, Zhang X-X, Wang X-Y, et al. (2021). The ZNF76 rs10947540 polymorphism associated with systemic lupus erythematosus risk in Chinese populations. *Scientific Reports*, 11:5186.
- Ramirez GA, Coletto LA, Bozzolo EP, Citterio L, Carpini SD, Zagato L, et al. (2018). The TRPC6 intronic polymorphism, associated with the risk of neurological disorders in systemic lupus erythematosus, influences immune cell function. *J. Neuroimmunol*, 325: 43–53.
- Rashad NM, Allam RM, Said D, Ali AE, Mohy NM, Abomandour HG. (2019). Influence of +299G>A and +62G>A resistin gene promoter variants on cardiovascular risk in Egyptian women with systemic lupus erythematosus. *Egypt Rheumatol*, 41: 215–220.

References

- Rees F, Doherty M, Grainge MJ, Lanyon P, Zhang W. (2017). The worldwide incidence and prevalence of systemic lupus erythematosus: a systematic review of epidemiological studies. *Rheumatology (Oxford)*, 56: 1945–1961.
- Reid S, Alexsson A, Frodlund M, Morris D, Sandling JK, Bolin K, et al. (2020). High genetic risk score is associated with early disease onset, damage accrual and decreased survival in systemic lupus erythematosus. *Ann Rheum Dis*, 79:363–69.
- Rezaieyazdi Z, Mirfeizi Z, Mohammad RH, Gholami G, Sedighy S, Esmaily H, et al. (2020). The association between adipokines and stigmata of atherosclerosis in patients with systemic lupus erythematosus. *The Egyptian Rheumatologist*, 42: 195-99.
- Saha J, Panja A, Nayek K. (2021). The prevalence of HBB mutations among the transfusion-dependent and non-transfusion dependent Hb E/ β -thalassemia children in a Tertiary Center of West Bengal, India. *Hemoglobin*, 45(3):157–162.
- Sam NB, Guan S-Y, Wang P, Li X-M, Wang D-G, Pan H-F, et al. (2021). Levels of the macrophage migration inhibitory factor and polymorphisms in systemic lupus erythematosus: a meta-analysis. *Arch Med Sci*, 17 (5): 1232–1240.
- Samuels H, Malov M, Saha Detroja T, Ben Zaken K, Bloch N, Gal-Tanamy M, et al. (2022). Autoimmune Disease Classification Based on PubMed Text Mining. *J. Clin. Med*, 11: 4345.
- Sánchez-Pérez H, Tejera-Segura B, de Vera-González A, González-Delgado A, Olmos JM, Hernández JL, et al. (2017). Insulin resistance in systemic lupus erythematosus patients: contributing factors and relationship with subclinical atherosclerosis. *Clin Exp Rheumatol*, 35(6):885-892.

References

- Schell R, Hale JJ, Mullis MN, Matsui T, Foree R, Ehrenreich IM. (2022). Genetic basis of a spontaneous mutation's expressivity. *Genetics*, 220(3):iyac013.
- Schwartz N, Stock AD, Putterman C. (2019). Neuropsychiatric lupus: New mechanistic insights and future treatment directions. *Nat.Rev. Rheumatol*, 15: 137–152.
- Shahrokhi SZ, Nezhad SRK, Ahmadi SB, Akhoond MR. (2017). Association Study of the PTPN22 Gene Polymorphisms with Systemic Lupus Erythematosus in Lorestan Province of Iran. *Gene Cell Tissue*, 4(3): e12023.
- Sharaf-Eldin W, Kishk N, Sakr B, El-Hariri H, Refeat M, ElBagoury N, et al. (2020). Potential Value of miR-23a for Discriminating Neuromyelitis Optica Spectrum Disorder from Multiple Sclerosis. *Arch. Iran. Med*, 23: 678–687.
- Shi H, Ye J, Teng J, Yin Y, Hu Q, Wu X, et al. (2017). Elevated serum autoantibodies against co-inhibitory PD-1 facilitate T cell proliferation and correlate with disease activity in new-onset systemic lupus mcmc erythematosus patients. *Arthritis Res Ther*, 19(52): 1–10.
- Shields KJ, El Khoudary SR, Ahearn JM, Manzi S. (2017). Association of aortic perivascular adipose tissue density with aortic calcification in women with systemic lupus erythematosus. *Atherosclerosis*, 262: 55–61.
- Shruthi S, Thabah MM, Zachariah B, Negi VS. (2021). Association of Oxidative Stress with Disease Activity and Damage in Systemic Lupus Erythematosus: A Cross Sectional Study from a Tertiary Care Centre in Southern India. *Ind J Clin Biochem*, 36(2): 185–193.
- Silverman GJ. (2019). The microbiome in SLE pathogenesis. *Nat. Rev. Rheumatol*, 15: 72–74.
- Singla S, Wenderfer SE, Muscal E, Sagcal-Gironella ACP, Orange JS, Makedonas G. (2017). Changes in frequency and activation status of major CD4(+) T-cell

References

- subsets after initiation of immunosuppressive therapy in a patient with new diagnosis childhood-onset systemic lupus erythematosus. *Front Pediatr*, 5:1-8.
- Smeets NJL, Teunissen EMM, van der Velden K, van der Burgh MJP, Linders DE, Teesselink E, et al. (2023). Glomerular filtration rate in critically ill neonates and children: creatinine-based estimations versus iohexol-based measurements. *Pediatric nephrology (Berlin, Germany)*, 38(4), 1087–1097.
- Sun C, Qin W, Zhang YH, Wu Y, Li Q, Liu M, et al. (2017). Prevalence and risk of metabolic syndrome in patients with systemic lupus erythematosus: A meta-analysis. *Int J Rheum Dis*, 20(8): 917-928.
- Sun J, Li X, Zhou H, Liu X, Jia J, Xie Q, et al. (2019). Anti-GAPDH Autoantibody Is Associated with Increased Disease Activity and Intracranial Pressure in Systemic Lupus Erythematosus. *J. Immunol. Res*, 2019: 7430780.
- Takehima Y, Iwasaki Y, Fujio K, Yamamoto K. (2019). Metabolism as a key regulator in the pathogenesis of systemic lupus erythematosus. *Semin. Arthritis Rheum*, 48: 1142–1145.
- Tarr T, Papp G, Nagy N, Cserep E, Zeher M. (2017). Chronic high-dose glucocorticoid therapy triggers the development of chronic organ damage and worsens disease outcome in systemic lupus erythematosus. *Clin. Rheumatol*, 36: 327–333.
- Teh P, Zakhary B, Sandhu VK. (2019). The impact of obesity on SLE disease activity: Findings from the Southern California Lupus Registry (SCOLR). *Clin. Rheumatol*, 38: 597–600.
- Topfer SK, Feng R, Huang P, Ly LC, Martyn GE, Blobel GA, et al. (2022). Disrupting the adult globin promoter alleviates promoter competition and reactivates fetal globin gene expression. *Blood*, 139(14):2107–2118.

References

- Tu Y, Guo R, Li J, Wang S, Leng L, Deng J, et al. (2019). MiRNA regulation of MIF in SLE and attenuation of murine lupus nephritis with miR-654. *Front Immunol*, 10:2229.
- Uciechowski P, Dempke WCM. (2020). Interleukin-6: A Masterplayer in the Cytokine Network. *Oncology*, 98(3), 131–137.
- van der Meulen TA, Harmsen HJM, Vila AV, Kurilshikov A, Liefers SC, Zhernakova A, et al. (2019). Shared gut, but distinct oral microbiota composition in primary Sjogren’s syndrome and systemic lupus erythematosus. *J. Autoimmun*, 97: 77–87.
- Vincent FB, Slavin L, Hoi AY, Kitching AR, Mackay F, Harris J, et al. (2018). Analysis of urinary macrophage migration inhibitory factor in systemic lupus erythematosus. *Lupus Sci Med*, 5:e000277.
- Wang C, Kong L, Kim S, Lee S, Oh S, Jo S, et al. (2022a). The Role of IL-7 and IL-7R in Cancer Pathophysiology and Immunotherapy. *International journal of molecular sciences*, 23(18), 10412.
- Wang J-M, Xu W-D, Yuan Z-C, Wu Q, Zhou J, Huang A-F. (2021). Serum levels and gene polymorphisms of angiopoietin 2 in systemic lupus erythematosus patients. *Scientific Reports*, 11:10.
- Wang M, Hsu HC, Yu MC, Wang IK, Huang CC, Chan MJ, et al. (2022b). Impact of kidney size on the outcome of diabetic patients receiving hemodialysis. *PloS one*, 17(3), e0266231.
- Wang P, Wang S, Huang B, Liu Y, Liu Y, Chen H, et al. (2023). Clinicopathological features and prognosis of idiopathic membranous nephropathy with thyroid dysfunction. *Frontiers in endocrinology*, 14: 1133521.

References

- Wasen C, Erlandsson MC, Bossios A, Ekerljung L, Malmhall C, Toyra Silfversward S, et al. (2018). Smoking is associated with low levels of soluble PD-L1 in rheumatoid arthritis. *Front Immunol*, 9:1677.
- Wu Q, Zhou J, Yuan Z-C, Lan Y-Y, Xu W-D, Huang A-F. (2021). Association between IL-37 and Systemic Lupus Erythematosus Risk. *Immunological Investigations*, 51(4): 727-738.
- Xu Y, Li L, Evans M, Xu H, Lindholm B, Carrero JJ. (2021). Burden and causes of hospital admissions and readmissions in patients undergoing hemodialysis and peritoneal dialysis: a nationwide study. *Journal of nephrology*, 34(6): 1949–1959.
- Xue, D., Moon, B., Liao, J., Guo, J., Zou, Z., Han, Y., Cao, S., Wang, Y., Fu, Y. X., & Peng, H. (2022). A tumor-specific pro-IL-12 activates preexisting cytotoxic T cells to control established tumors. *Science immunology*, 7(67), eabi6899.
- Yan M, Yang Y, Zhou Y, Yu C, Li R, Gong W, et al (2021). Interleukin-7 aggravates myocardial ischaemia/reperfusion injury by regulating macrophage infiltration and polarization. *Journal of cellular and molecular medicine*, 25(21): 9939–9952.
- Yang F, Zhai Z, Luo X, Luo G, Zhuang L, Zhang Y, et al. (2020). Bioinformatics identification of key candidate genes and pathways associated with systemic lupus erythematosus. *Clin Rheumatol*, 39: 425–434.
- Yap HY, Tee S, Wong M, Chow SK, Peh SC, Teow SY. (2018). Pathogenic role of immune cells in rheumatoid arthritis: implications in clinical treatment and biomarker development. *Cells*, 7:161.
- Yin X, Kim K, Suetsugu H, Bang SY, Wen L, Koido M, et al. (2020). Meta-analysis of 208370 East Asians identifies 113 susceptibility loci for systemic lupus erythematosus. *Ann. Rheum. Dis*, 2020.

References

- Yuan Z-C, Xu W-D, Wang J-M, Wu Q, Zhou J, Huang A-F. (2020). Gene polymorphisms and serum levels of sVEGFR-1 in patients with systemic lupus erythematosus. *Scientific Reports*, 10:15031.
- Zanatta E, Ferrazzi B, Michelotto A, Cozzi F, Frigo AC, Alaibac M. (2020). PD-1 gene rs2227981 (PD-1.5) polymorphism analysis in patients with systemic sclerosis. *Gene Reports*, 20: 100776.
- Zappulo F, Cappuccilli M, Cingolani A, Scrivo A, Chiocchin ALC, Nunzio MD, et al. (2022). Vitamin D and the Kidney: Two Players, One Console. *International journal of molecular sciences*, 23(16), 9135.
- Zhang L, Wu Y, Nie Y, Lv W, Li Y, Zhu B, et al. (2022). The serum free triiodothyronine to free thyroxine ratio as a potential prognostic biomarker of chronic kidney disease in patients with glomerular crescents: A retrospective study. *Frontiers in endocrinology*, 13, 977355.
- Zhang S, Feng G, Kang F, Guo Y, Ti H, Hao L, et al. (2020). Hypothyroidism and Adverse Endpoints in Diabetic Patients: A Systematic Review and Meta-Analysis. *Frontiers in endocrinology*, 10, 889.
- Zhang S, Li M, Zhang L, Wang Z, Wang Q, You H. (2021a). Clinical Features and Outcomes of Neuropsychiatric Systemic Lupus Erythematosus in China. *J. Immunol. Res*, 2021: 1–10.
- Zhang S, Wang L, Li M, Zhang F, Zeng X. (2021b). The PD-1/PD-L pathway in rheumatic diseases. *J Formos Med Assoc*, 120 (1): 48–59.



Appendix

Appendices

Appendices

1- Appendix 1: Biochemical Characteristics of SLE and Healthy Control in Relevance to the Distribution of the Genotypes of PD-1 Gene Polymorphism

Table 1: Biochemical characteristic of SLE in relevance to the genotypes of PD-1 gene polymorphism (SNP +7499) analyzed under codominant model (N=43)

Parameter	GG (N=16) Mean±SD	GA (N=14) Mean±SD	AA (N=13) Mean±SD	P-Value
Age (Years)	35.44 ± 5.42	35.18 ± 5.74	35.35 ± 6.09	0.992
SLE Duration (Years)	1.09 ± 0.37	0.96 ± 0.05	0.90 ± 0.06	0.091
SLEDAI-2K	2.98 ± 1.36	2.69 ± 0.86	2.52 ± 1.40	0.60
BMI (Kg/m ²)	23.97 ± 0.15	23.88 ± 0.09	23.90 ± 0.11	0.092
C3 (g/L)	0.91 ± 0.49	0.81 ± 0.26	0.83 ± 0.40	0.770
C4 (g/L)	0.29 ± 0.11	0.28 ± 0.09	0.28 ± 0.15	0.937
CH50 (IU/mL)	52.07 ± 13.27	51.46 ± 15.61	50.71 ± 18.09	0.973
MDA (µmol/L)	2.51 ± 0.68	2.40 ± 0.88	2.43 ± 0.74	0.925
TAC (pg/mL)	1.67 ± 0.35	1.60 ± 0.42	1.57 ± 0.45	0.787
CRP (mg/dL)	10.80 ± 4.30	10.75 ± 5.74	10.75 ± 4.79	0.999
ANA (IU/mL)	2.43 ± 0.78	2.39 ± 0.70	2.34 ± 0.75	0.959
Anti-dsDNA (IU/mL)	28.29 ± 6.55	28.23 ± 7.50	28.12 ± 5.28	0.998
Urea (mg/dL)	55.09 ± 14.22	55.02 ± 14.66	54.80 ± 8.34	0.998
Creatinine (mg/dL)	1.08 ± 0.19	1.06 ± 0.23	1.05 ± 0.11	0.905
GFR (mL/min/1.73 m ²)	62.18 ± 20.66	61.66 ± 22.56	61.77 ± 11.57	0.997
IL-18 (pg/mL)	306.67 ± 57.56	301.21 ± 85.57	295.81 ± 79.12	0.926
IL-37 (pg/mL)	213.57 ± 51.21	207.94 ± 64.41	205.90 ± 67.65	0.939
PD-1 (pg/mL)	787.95 ± 314.09	779.36 ± 306.89	768.06 ± 442.26	0.989

Appendices

Table 2: Biochemical characteristic of healthy control in relevance to the genotypes of PD-1 gene polymorphism (SNP +7499) analyzed under codominant model (N=53)

Parameter	GG (N=26) Mean±SD	GA (N=22) Mean±SD	AA (N=5) Mean±SD	P-Value
Age (Years)	34.44 ± 5.97	34.23 ± 4.11	33.80 ± 6.64	0.967
BMI (Kg/m ²)	24.04 ± 0.63	23.98 ± 0.94	23.79 ± 1.51	0.832
C3 (g/L)	1.67 ± 0.21	1.59 ± 0.19	1.58 ± 0.21	0.322
C4 (g/L)	0.46 ± 0.18	0.43 ± 0.15	0.38 ± 0.17	0.539
CH50 (IU/mL)	82.04 ± 9.74	81.39 ± 8.39	81.18 ± 9.41	0.963
MDA (µmol/L)	0.91 ± 0.16	0.84 ± 0.12	0.83 ± 0.25	0.241
TAC (pg/mL)	2.23 ± 0.46	2.16 ± 0.41	2.09 ± 0.72	0.793
CRP (mg/dL)	0.17 ± 0.04	0.16 ± 0.04	0.16 ± 0.04	0.834
ANA (IU/mL)	1.01 ± 0.34	0.96 ± 0.24	0.89 ± 0.46	0.683
Anti-dsDNA (IU/mL)	15.79 ± 2.78	15.46 ± 2.10	15.57 ± 2.73	0.898
Urea (mg/dL)	28.40 ± 8.03	28.16 ± 6.17	28.03 ± 10.41	0.991
Creatinine (mg/dL)	0.71 ± 0.12	0.69 ± 0.08	0.64 ± 0.13	0.370
GFR (mL/min/1.73 m ²)	99.73 ± 16.48	99.50 ± 20.43	98.56 ± 26.22	0.992
IL-18 (pg/mL)	93.13 ± 21.81	92.69 ± 24.65	91.91 ± 34.46	0.994
IL-37 (pg/mL)	51.63 ± 7.02	50.99 ± 6.27	50.74 ± 10.55	0.938
PD-1 (pg/mL)	128.05 ± 21.77	127.82 ± 25.17	125.14 ± 39.23	0.971

Appendices

Table 3: Biochemical characteristic of SLE in relevance to the genotypes of PD-1 gene polymorphism (SNP +7209) analyzed under codominant model (N=43)

Parameter	CC (N=29) Mean±SD	CT (N=11) Mean±SD	TT (N=3) Mean±SD	P-Value
Age (Years)	35.62 ± 5.53	34.55 ± 5.66	35.33 ± 8.02	0.869
SLE Duration (Years)	1.03 ± 0.28	0.92 ± 0.06	0.87 ± 0.06	0.27
SLEDAI-2K	2.81 ± 1.14	2.61 ± 1.58	2.70 ± 0.61	0.902
BMI (Kg/m ²)	23.93 ± 0.13	23.91 ± 0.09	23.83 ± 0.16	0.367
C3 (g/L)	0.88 ± 0.41	0.81 ± 0.39	0.76 ± 0.25	0.816
C4 (g/L)	0.29 ± 0.10	0.27 ± 0.14	0.25 ± 0.19	0.809
CH50 (IU/mL)	51.53 ± 13.60	51.29 ± 19.53	51.39 ± 19.45	0.999
MDA (µmol/L)	2.51 ± 0.72	2.35 ± 0.80	2.23 ± 1.04	0.737
TAC (pg/mL)	1.62 ± 0.37	1.60 ± 0.52	1.60 ± 0.14	0.982
CRP (mg/dL)	10.84 ± 5.03	10.62 ± 5.19	10.64 ± 1.22	0.991
ANA (IU/mL)	2.43 ± 0.73	2.31 ± 0.77	2.28 ± 0.86	0.860
Anti-dsDNA (IU/mL)	28.30 ± 6.51	28.10 ± 6.76	27.86 ± 5.68	0.992
Urea (mg/dL)	55.21 ± 13.03	54.57 ± 12.51	54.23 ± 13.06	0.985
Creatinine (mg/dL)	1.08 ± 0.20	1.05 ± 0.15	1.03 ± 0.14	0.818
GFR (mL/min/1.73 m ²)	62.05 ± 21.54	61.75 ± 10.28	60.83 ± 16.96	0.994
IL-18 (pg/mL)	303.15 ± 63.39	298.90 ± 94.17	296.61 ± 98.56	0.980
IL-37 (pg/mL)	211.06 ± 59.28	206.86 ± 69.55	202.96 ± 28.41	0.964
PD-1 (pg/mL)	782.06 ± 309.62	773.62 ± 423.94	771.17 ± 534.71	0.997

Appendices

Table 4: Biochemical characteristic of healthy control in relevance to the genotypes of PD-1 gene polymorphism (SNP +7209) analyzed under codominant model (N=53)

Parameter	CC (N=40) Mean±SD	CT (N=11) Mean±SD	TT (N=2) Mean±SD	P-Value
Age (Years)	34.40 ± 5.14	33.82 ± 5.59	34.75 ± 8.84	0.943
BMI (Kg/m ²)	24.05 ± 0.71	23.77 ± 1.34	24.02 ± 0.01	0.644
C3 (g/L)	1.64 ± 0.20	1.59 ± 0.22	1.59 ± 0.16	0.743
C4 (g/L)	0.45 ± 0.16	0.42 ± 0.17	0.41 ± 0.23	0.868
CH50 (IU/mL)	82.01 ± 9.08	80.73 ± 9.88	80.58 ± 2.06	0.905
MDA (µmol/L)	0.88 ± 0.14	0.85 ± 0.20	0.82 ± 0.20	0.818
TAC (pg/mL)	2.21 ± 0.42	2.14 ± 0.60	2.07 ± 0.81	0.845
CRP (mg/dL)	0.17 ± 0.04	0.16 ± 0.04	0.17 ± 0.08	0.856
ANA (IU/mL)	1.00 ± 0.30	0.91 ± 0.33	0.95 ± 0.52	0.697
Anti-dsDNA (IU/mL)	15.73 ± 2.46	15.37 ± 2.51	14.99 ± 4.07	0.853
Urea (mg/dL)	28.35 ± 6.57	28.07 ± 10.40	27.68 ± 9.01	0.988
Creatinine (mg/dL)	0.71 ± 0.10	0.66 ± 0.11	0.67 ± 0.14	0.436
GFR (mL/min/1.73 m ²)	100.08 ± 17.27	97.76 ± 23.74	98.15 ± 31.61	0.934
IL-18 (pg/mL)	93.18 ± 23.39	91.85 ± 27.69	91.29 ± 19.60	0.983
IL-37 (pg/mL)	51.47 ± 6.49	50.75 ± 8.47	50.38 ± 12.09	0.940
PD-1 (pg/mL)	127.92 ± 23.08	126.96 ± 32.50	126.88 ± 24.56	0.993

Appendices

2- Appendix 2: Books facilitating the task (Ethical Approval)

العدد: ١٠٦٨
التاريخ: ١٠/١٠/٢٠٢٢

جمهورية العراق
وزارة الصحة
دائرة صحة البصرة
مكتب المدير العام
مركز التدريب والتنمية البشرية
شعبة ادارة المعرفة/البحوث

الى / م. الفحاء
م. الموائى
م. الصدر التعليمي
م. البصرة التعليمي
م/ تسهيل مهمة

دائرة صحة البصرة
مكتب المدير العام
مركز التدريب والتنمية البشرية
تحية طيبة... قسم التدريب والتنمية البشرية

درست لجنة البحوث في دائرة صحة البصرة مشروع البحث ذي الرقم (٦٣٥) المعنون:
دراسة تعدد الأشكال لجين موت الخلايا المبرمج ١ وبعض المتنبئات الصحيحة لمرضى الذئبة الحمامية الجهازية
في محافظة البصرة - العراق) والمقدم من قبل الباحث
(سعدون عباس عيدان) طالب دراسات عليا دكتوراه في كلية العلوم / قسم الكيمياء / جامعة البصرة
بتاريخ ١٧/١٠/٢٠٢٢ وقررت:

"الموافقة على تنفيذ مشروع البحث بصيغته المقدمة ولا مانع من تنفيذه في مؤسسات الدائرة."

لتفضلكم بالاطلاع وتسهيل مهمة الباحث لاجراء بحثه مع التقدير....

المرفقات:
قرار لجنة البحوث المرقم ٢٠٢٢/٢٦٥

د. عبد كاظم شاكر
الطبيبه الاختصاص
د. رجاء احمد محمود
مديرة مركز التدريب والتنمية البشرية
١٧ / ١٠ / ٢٠٢٢

دائرة صحة البصرة
مكتب المدير العام
مركز التدريب والتنمية البشرية

نسخة منه الى/
مركز التدريب والتنمية البشرية / مع الاوليات.



وزارة الصحة
دائرة صحة البصرة
مركز التدريب والتنمية البشرية
لجنة البحوث



رقم القرار ٢٠٢٢/٢٦٥

تاريخ القرار ٢٠٢٢/١٠/١٧

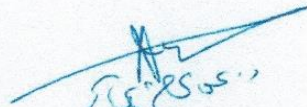
قرار لجنة البحوث

درست لجنة البحوث في دائرة صحة البصرة مشروع البحث ذي الرقم (٦٣٥) المعنون:
(دراسة تعدد الأشكال لجين موت الخلايا المبرمج ١ وبعض المتنبئات الصحيحة لمرضى الذئبة الحمامية الجهازية في
محافظة البصرة - العراق) والمقدم من قبل الباحث

(سعدون عباس عيدان) طالب دراسات عليا دكتوراه في كلية العلوم / قسم الكيمياء / جامعة البصرة

بتاريخ ٢٠٢٢/١٠/١٧ وقررت:

"الموافقة على تنفيذ مشروع البحث بصيغته المقدمة ولأمانع من تنفيذه في مؤسسات الدائرة."


الطبيب الاختصاص

د. علي كاظم قاسم

مقرر لجنة البحوث / دائرة صحة البصرة

٢٠٢٢/١٠/١٧



المرفقات:
لا يوجد

الملاحظات:

- تم تحويل رئيس لجنة البحوث او مقرر اللجنة للتوقيع على هذا القرار استنادا الى النظام الداخلي للجنة البحوث.
- الموافقة تعني ان مشروع البحث قد استوفى المعايير الأخلاقية والعلمية لإجراء بحث والمعتمدة في وزارة الصحة. اما التنفيذ فيعتمد على التزام الباحث بتعليمات المؤسسة الصحية التي سينفذ فيها البحث. وعلى الباحث التواصل مع مسئول البحوث في المؤسسة الصحية التي يجري بها البحث واطلاعه على مجريات البحث بشكل دوري ولحين انتهاء البحث.

3- Appendix 3: Published Researches

RESEARCH

O&G Forum 2024; 34-3s: 1610-1621

INFLAMMATORY CYTOKINES AND PROGRAMMED DEATH-1 CORRELATION IN SUBJECTS DIAGNOSED WITH SYSTEMIC LUPUS ERYTHEMATOSUS IN THE PROVINCE OF BASRA / IRAQ

Sadoun Abbas Alsalimi^{1,2*} Adnan Jassim Mohammed Al-Fartosy¹

¹Department of Chemistry, College of Science, University of Basrah, Qarmat Ali Complex, Basra, Iraq

²Department of Basic Sciences, College of Nursing, University of Basrah, Baghdad Street, Basra, Iraq
sadoun.alsalimi@uobasrah.edu.iq

Abstract

Background: Several biological indicators have been suggested as potential predictors of subclinical occurrences in SLE. We aimed to examine the correlation between certain inflammatory cytokines and PD-1 in SLE subjects.

Methods: This study had 43 SLE and 53 healthy subjects. Blood samples were collected and subjected to biochemical analysis. Furthermore, the subjects underwent medical history assessments using standardized self-administered questionnaires.

Results: Statistically significant increases ($p < 0.01$) were observed in MDA, CRP, ANA, Anti-dsDNA, urea, creatinine, IL-18, IL-37, and PD-1, conversely, statistically significant decreases ($p < 0.01$) were observed in C3, C4, CH50, TAC, and GFR in serum levels of SLE subjects compared to controls. This study revealed a positive correlation between IL-18, IL-37, and PD-1, which exhibited significantly positive correlations with MDA, CRP, ANA, anti-dsDNA, urea, and creatinine, and significantly negative correlations with C3, C4, CH50, TAC, and GFR. Moreover, the AUC of ROC curve for IL-18, IL-37, and PD-1 was calculated (0.985, 0.968, and 0.940, respectively).

Conclusion: The potential inflammatory biomarkers for the early development of SLE subjects may include IL-18 and IL-37, which exhibit a positive correlation with PD-1. Additionally, the high positive value of the AUC for IL-18, IL-37, and PD-1 further supports their potential as biomarkers in this context.

Key Words: interleukin-18; interleukin-37; programmed death-1; systemic lupus erythematosus; inflammation; autoimmune disease

Introduction

Systemic lupus erythematosus (SLE) is a combinatorial autoimmune disease of complicated nature, characterized by an overproduction of diverse autoantibodies (1). Dysregulated T-cell-dependent production of autoreactive B-cells is regarded to have an essential part in the progression of SLE. The presence of these autoantibodies is responsible for inducing damage to tissues in multiple organs, such as the joints, kidneys, skin, and central nervous system (CNS) (2).

Interleukin-18 (IL-18) is a multifunctional cytokine that is synthesized by a variety of cells, such as endothelial cells, macrophages, and hematopoietic cells. It plays a crucial role in the controlling of both innate and acquired immunity (3). In more elaboration, IL-18 is an extremely potent stimulator of interferon-gamma (IFN- γ) synthesis, exerting this effect on both natural killer (NK) cells and T-helper 1 (Th1) lymphocytes. Consequently, IL-18 is implicated in the development and progression of autoimmune disorders. The available body of research has provided clarification that IL-18 may possess a significant association with the symptoms of SLE and may contribute to its underlying mechanisms (4).

Interleukin-37 (IL-37), a novel constituent of the IL-1 family, has been acknowledged as an endogenous suppressor of immunological reactions. The amount of IL-37 production

exhibits a notable increase in various cell types, including dendritic cells (DCs), peripheral blood mononuclear cells (PBMCs), macrophages, T-cells, and epithelial cells, upon activation by pro-inflammatory cytokines (5). However, it is important to note that IL-37 is not expressed continuously in normal human tissue. The up-regulation of inflammatory cytokine production, including IL-1 β , IL-6, and tumor necrosis factor (TNF- α), can be observed when human peripheral blood mononuclear cells (PBMCs) from healthy persons undergo therapy with neutralizing monoclonal anti-IL-37 (6).

Programmed death-1 (PD-1), a constituent of the CD28 family, was initially discovered to play a role in the programmed cell death pathway. Nevertheless, it functions as a negative costimulatory molecular structure and has been observed to be present on the surface of various cell types, including, T cells, activated monocytes, NK cells, myeloid cells, and B cells (7). The programmed cell death protein 1 (PD-1) receptor engages with its ligands, namely PD-L1 and PD-L2, to exert immunosuppressive effects. This interaction leads to the inhibition of lymphocyte activation and the subsequent reduction in cytokine output (8).

Given the available information regarding the different modulatory and inflammatory activities of IL-18, IL-37, and PD-1, as well as their altered levels observed during the early

OBSTETRICS & GYNAECOLOGY FORUM 2024 | ISSUE 3s | 1610



الجامعة الإسلامية العالمية ماليزيا
INTERNATIONAL ISLAMIC UNIVERSITY MALAYSIA
بِسْمِ اللَّهِ الرَّحْمَنِ الرَّحِيمِ
Garden of Knowledge and Virtue

LEADING THE WAY

KHALIFAH - AMANAH - IGHRA' - RAHMATAN UL-ALAMIN

SUSTAINABILITY INSTITUTION OF THE YEAR

Our Ref : IIUM/305/14/1/1

Date : 29th April 2024

Dr. Sadoun Abbas Alsalimi
Department of Chemistry,
College of Science, University of Basrah,
Qarmat Ali Campus, Basra, Iraq

Dear Dr. Sadoun Abbas Alsalimi,

ACCEPTANCE OF MANUSCRIPT FOR PUBLICATION IN IIUM MEDICAL JOURNAL OF MALAYSIA (IMJM)

The above matter is kindly referred.

This is to inform you that your manuscript titled 'Study of Programmed Cell Death 1 Gene Polymorphism and Some Valid Predictors of Systemic Lupus Erythematosus Patients in Basra Province - Iraq' with reference no. OJS 2478 has been accepted for publication in the IIUM Medical Journal Malaysia (IMJM).

Thank you and Wassalam.

Sincerely,

PROF. DR. NASSER MUHAMMAD AMJAD
Chief Editor, IMJM
Kulliyah of Medicine



Green Growth Awards
WINNER
2020 SUSTAINABILITY
INSTITUTION OF THE YEAR



GreenTree Growth
WINNER
2020 SUSTAINABILITY
INSTITUTION OF THE YEAR



Record of Al-Khawalizmi
EDUCATION AWARD 2020



Premier
Digital Tech
University

KULLIYAH OF MEDICINE (KOM)

International Islamic University Malaysia, Jalan Sultan Ahmad Shah, Bandar Indera Mahkota, 25200 Kuantan, Pahang Darul Makmur
(Company No. 101067-P)

Tel: +609 570 4000 Fax: +609 571 6770 Email: medicine@iiu.edu.my
<https://www.iiu.edu.my/kulliyah/kom>



الخلاصة

الذئبة الإحمرارية الجهازية (SLE) هي مرض مناعي ذاتي اندماجي ذو طبيعة معقدة، يتميز بتوليد أجسام مضادة ذاتية متنوعة. من المسلم به على نطاق واسع أن خلل تنظيم الآليات المعتمدة على الخلايا التائية التي تحفز الخلايا البائية ذاتية التفاعل هو عامل محوري في التسبب في مرض الذئبة الحمراء. وقد لوحظ أن وجود هذه الأجسام المضادة الذاتية يؤدي إلى تلف الأنسجة في أعضاء متعددة، مثل الجلد والكلى والجهاز العصبي المركزي (CNS) والمفاصل. ومن ثم، فإن الهدف من هذه الدراسة هو دراسة محتوى وخصائص التغيير في مستويات موت الخلايا المبرمج 1 (PD-1) كعلامة لمرضى الذئبة الحمراء في سكان محافظة البصرة (جنوب العراق). في هذه الدراسة، شارك 43 مريضاً من مرضى الذئبة الحمراء (إناث) وتمت متابعة 53 من الأشخاص الذين يبدون انهم اصحاء (إناث) لمدة 11 شهراً حتى نهاية الدراسة.

تمت مطابقة المجموعتين لعدد من المؤشرات الحيوية مثل مؤشر كتلة الجسم BMI، C3، C4، CH50، MDA، TAC، CRP، ANA، Anti-dsDNA، اليوريا، الكرياتينين، GFR، IL-18، IL-37، و PD-1. بالمقارنة مع الاصحاء، أشارت النتائج إلى أن مرضى الذئبة الحمراء لديهم زيادة كبيرة ($P < 0.01$) في مستويات MDA، CRP، ANA، Anti-dsDNA، اليوريا، الكرياتينين، IL-18، IL-37، و PD-1. من ناحية أخرى، ذكرت بياناتنا أن C3، C4، CH50، TAC، و GFR انخفضت بشكل ملحوظ ($P < 0.01$) في مرضى الذئبة الحمراء مقارنة مع مجموعة الاصحاء. علاوة على ذلك، أشارت النتائج التي تم الحصول عليها إلى عدم وجود فرق معنوي ($P > 0.05$) في مستوى BMI لدى مرضى الذئبة الحمراء مقارنة بمجموعة الاصحاء.

علاوة على ذلك، أشارت المنطقة الواقعة تحت منحنى (AUC) خصائص تشغيل المستقبل (ROC) إلى أن C3، C4، CH50، MDA، TAC، CRP، ANA، Anti-dsDNA، اليوريا، الكرياتينين، GFR، IL-18، و PD-1 يمكن أن يكونا بمثابة مؤشرات حيوية تنبؤية أكثر دقة في الأشخاص الذين يعانون من مرض الذئبة الحمراء (AUC = 0.08، 0.22، 0.091، 0.922، 0.07، 0.894، 0.915، 0.922، 0.919، 0.922، 0.06، 0.985، 0.968، و 0.940) على التوالي.

كشفت البيانات المقدمة في الدراسة عن وجود علاقة إيجابية بين IL-18 و IL-37 مع PD-1. بالإضافة إلى ذلك، أظهرت IL-18 و IL-37 و PD-1 ارتباطات إيجابية بشكل ملحوظ مع ANA، CRP، MDA، و Anti-dsDNA، اليوريا، والكرياتينين. على العكس من ذلك، كان لدى IL-18، IL-37، و PD-1 ارتباطات سلبية بشكل ملحوظ مع C3، C4، CH50، TAC، و GFR.

في هذه الدراسة، تمت دراسة تعدد الأشكال الجيني PD-1 الموجود داخل الإنترون-4 بين الأشخاص المصابين بمرض الذئبة الحمراء ومجموعة الأصحاء في بعض مستشفيات البصرة التعليمية، كما قمنا بدراسة تأثيره على مستوى

المصل. تم تحديد المواقع متعددة الأشكال لـ PD-1 من خلال استخدام تفاعل البلمرة المتسلسل PCR، مما أدى إلى التعرف على موقعين مختلفين، وهما rs6705653 و rs41386349. فيما يتعلق بالترددات الأليلية وتوزيعات النمط الجيني لـ (G/A) +7499 PD-1، فقد تبين أن النمط الجيني AA أظهر زيادة ذات دلالة إحصائية بين الأشخاص الذين يعانون من مرض الذئبة الحمراء. تماشيًا مع الأبحاث السابقة، أظهرت الأنماط الجينية المتماثلة الزيغوت AA والمتغايرة الزيغوت GA تكرارًا أعلى بين الأشخاص المصابين بمرض الذئبة الحمراء، بينما لوحظ النمط الجيني GG بشكل أكثر شيوعًا بين الأفراد غير المصابين بالمرض. لذلك، يمكن أن يكون ارتفاع خطر الإصابة بمرض الذئبة الحمراء مرتبطًا بوجود الأليل A، وبالتالي النمط الجيني AA في هذا الموقع. بالإضافة إلى ذلك، فقد لوحظ أن وجود أليل G والنمط الجيني GG في المنطقة +7499 PD-1 قد يمنح تأثيرات وقائية ضد مرض الذئبة الحمراء. كشف فحص الترددات الأليلية لأشكال (C/T) +7209 PD-1 لدى الأفراد المصابين بمرض الذئبة الحمراء مقارنة بالأفراد الذين لا يعانون من هذه الحالة عن عدم وجود تباين ذي دلالة إحصائية. تشير نتائج التحقيق الحالي إلى أن الأليل T يمكن اعتباره أليل خطر محتمل لمرض الذئبة الحمراء، في حين أن الأليل C قد يكون له تأثير وقائي. وجد أن تعدد الأشكال لترددات الأنماط الجينية يتوافق مع توازن هاردي-واينبرغ.



جامعة البصرة
كلية العلوم
قسم الكيمياء



دراسة تعدد الأشكال لجين موت الخلايا المبرمج ١
وبعض المتنبئات الصحيحة للنساء المصابات
بمرض الذئبة الإحمرارية الجهازية في محافظة
البصرة – العراق

أطروحة

مقدمة الى مجلس كلية العلوم – جامعة البصرة
كجزء من متطلبات نيل درجة الدكتوراه فلسفة في
علوم الكيمياء – الكيمياء الحياتية السريرية

من قبل

سعدون عباس عيدان السالمي

بكالوريوس ٢٠١١

ماجستير ٢٠٢٠

أ.د. عدنان جاسم محمد الفرطوسي
المشرف

٢٠٢٤ م

١٤٤٥ هـ